THE

The American Journal of ANATOMY

VOLUME 109

JULY SEPTEMBER, NOVEMBER 1961

PUBLISHED BY

THE WISTAR INSTITUTE OF ANATOMY AND BIOLOGY

PHILADELPHIA PA

CONTENTS

No. 1 JULY 1961

No. 2 SEPTEMBER 1961

CONTENTS

No 3 NOVEMBER 1961

The Morphology of Tylotrich Follicles in the Skin of the Rabbit

WILLIAM E. STRAILE
Department of Zoology Birkbeck College Uni ersity I London E gland

Although several types of encapsulated nerve endings have been described in the glabrous skin of mammals (cf Weddell et al '55) similar structures are apparently not present in mammalian skin containing hairs. Sensory innervation of hairy skin is primarily made up of naked nerve endings terminating in the dermis and hair follicles. All hair follicles therefore are effective tactile units but some such as the well known vibrissa follicles show a high degree of adaptation for sensory function. This publication describes another type of hair follicle that contains highly specialized sensory and erectile tissues (fig 1) These large follicles which were preliminarily described by Straile ('58) are sparsely scattered throughout the skin of the rabbit single follicles appearing at intervals of approximately ½ to 1 cm in adult animals. The term *tylotrich follicle* is suggested for this tactile organelle

Recent observations indicate that tylotrich follicles are present in the skin of many mammals (Straile '60) These highly specialized follicles have a similar distribution and structure in the rabbit, mouse rat, guinea pig and chinchilla. In each of these animals the tylotrich follicle is associated with a richly innervated and vascularized region of epidermis called the *Haarscheibe* which was extensively described in the human by Pinkus ('05) and Tamponi ('39) Pinkus also reported that *Haarscheiben* occur widely in mammals (monotremes, insectivores rodents and primates) The present study shows that the *Haarscheibe* of the rabbit is not a separate sensory structure but is an important part of the tylotrich follicle.

MATERIALS AND METHODS

Twenty adult male and three adult female Dutch rabbits were used for this study A total of 60 quiescent and 36 growing tylotrich follicles were removed from the skin of these animals. For the study of general histological detail, the tylotrich follicles with some surrounding tissue were appropriately processed and serially sectioned for the following techniques van Gieson s picro-acid fuchsin stain with alum hematoxylin Ehrlich s hematoxylin with eosin B and Weigert s iron hematoxylin with safranin Gold chloride and chloral hydrate methods were used for demonstrating nerve endings (cf Conn and Darrow '46)

OBSERVATIONS AND COMMENTS

Except for the two highly specialized regions described below (the annular complex and the *Haarscheibe* with its associated structures) the morphology of the rabbit tylotrich follicle closely parallels that of the common guard-hair follicle (fig 1) The following descriptions are of tylotrich follicles in the quiescent phase of the hair growth cycle unless specific reference is made to follicles in the growing phase For a discussion of the hair growth cycle see Chase ('54)

The an ular complex

The annular complex is composed of three concentric structures that encircle the external root sheath of the quiescent tylotrich follicle just above the hair club. The most prominent part of this complex is the large outer component, called the *annulus* which is made up of coarse connective tissue enclosing numerous capillaries and nerve fibers (fig. 1 and fig. 2)

United States Public Health Service Post doctoral Research Fellow of the National Cancer Institute.

Present address Biological Station, Roswell Park Memorial Institute, Springville, New York, U S A.

Although most of this structure lies deeper within the skin its upper part surrounds the small sebaceous gland (fig 1) The large connective tissue fibers of the annulus are easily recognized because they wrap around the capillaries in a circular arrangement. This pattern contrasts strongly with the more random orientation of the smaller connective tissue fibers adjacent to the annulus (fig 2) In gold chloride preparations the annulus is deeply stained and many fine fibers, which may be nerve endings can be seen within it (fig. 3) The border of the annulus also *stains* with gold chloride and is called the *annulus sheath* (fig 1 and fig. 3)

When skin containing quiescent hair follicles is rubbed or stimulated by plucking out the club hairs the capillary network within the annulus dilates and becomes visible to the eye as a small red mark. Dilation may persist for a few minutes; and if these tylotrich follicles are quickly removed and placed in 10% neutral formalin, they can be fixed in the dilated state Longitudinal sections of such follicles demonstrate well the extreme size of the dilated capillaries. Actually capillary diameter may at times exceed that of the tylotrich follicle itself (fig. 4) These observations suggest that the annulus is an erectile organelle possibly controlling the sensitivity of the tylotrich follicle [illegible]

The central component of the annular [illegible]

Tangential sections of these cells show that they contain very long nuclei (fig 5) and cross sections of tylotrich follicles show that the nuclei are regularly aligned along the sides of the follicle (fig. 6) These elongate cells resemble smooth muscle cells but they are not typical because their nuclei are longer and less wrinkled than the nuclei of smooth muscle cells In addition their cytoplasm is less fibrous and does not stain as darkly in hematoxylin and eosin preparations For l ck of a better term these elongate cells will be called *smooth muscle-like cell*

The *inner component of the annular* complex is a bilaminar arrangement of nerve fibers and it is closely associated with the band of smooth muscle-like cells (fig 1 and fig. 6) The orientation of these nerve fibers is very precise the inner fibers running vertical to the follicle and the outer fibers encircling the follicle. When both layers are superimposed in a tangentially cut section they have the appearance of a grid (fig. 7) Similar arrangements of nerve fibers are also found in the smaller types of rabbit hair follicles but the fibers are sparse and are irregularly spaced Additionally the literature contains numerous descriptions of nerve networks surrounding hair follicles in other mammals (cf Weddell et al '55)

The Haarscheibe and its associated structures

Acentrically surrounding the orifice of each rabbit tylotrich follicle is a thick area of epidermis called the *Haarscheibe* The bulk of this structure is posterior to the hair follicle or on the side where the follicle forms an obtuse angle with the surface of the skin (fig 1 and fig. 2). There is a gradual change in epidermal thickness *along the anterior and posterior borders* of the *Haarscheibe* (fig. 2) but along the lateral borders there is an abrupt transition (fig 8) Just above the sebaceous gland of the tylotrich follicle the external root sheath also has great depth and this thick area of epithelium is continuous with the *Haarscheibe* (fig 1 and fig 2). Both of these specialized epithelial areas have more layers of cells than the adjacent unspecialized epithelium This could be a result of a high proliferative rate or a greater retention of cells within these specialized regions. There is much morphological diversity in the population of cells forming the *basal cell layer of the Haarscheibe There* are two predominant types of columnar epithelial cells. The nuclei of one cell type occupy the upper part of the cells while the nuclei of the other type lie near the basement membrane in a very precise alignment. These two distinct layers of nuclei give the basal cell layer a pseudostratified appearance (fig 9) Cells of a third type are also seen in the basal layer of the *Haarscheibe* These elongate cells are

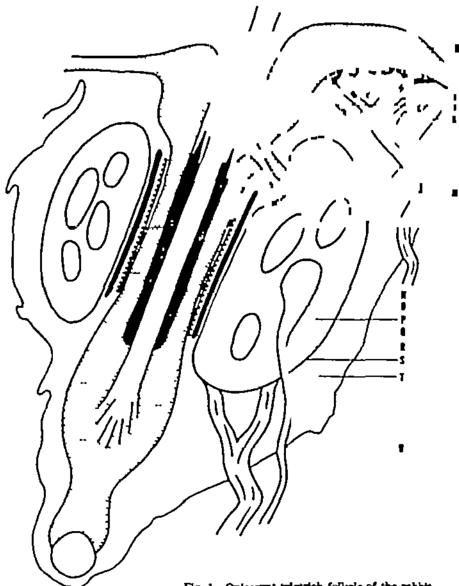


Fig. 1 Quiescent tylotrich follicle of the rabbit.

A, epidermis
B internal root sheath
C, external root sheath
D hair
E, hair club
F germ of follicle
G, dermal papilla
H, *Haarscheibe*
I, capillary within specialized region of dermis
J thickened area of external root sheath
K, specialized region of dermis below *Haarscheibe*
L, branch of large nerve innervating *Haarscheibe* and specialized region of dermis
M, sebaceous gland
N bilaminar arrangement of nerve fibers
O, band of smooth muscle-like cells
P annulus
Q capillary within annulus
R, capillary supplying or draining vessels within annulus
S, annulus sheath
T connective tissue capsule
U large nerve innervating annular complex, *Haarscheibe* and specialized region of dermis

fails to produce of similar response. One does not know whether this physiological change is concomitantly associated with changes in sensory function, but it is associated with rather extensive alterations in the morphology of the annulus and *Haarscheibe* These structures appear to be mechanically compressed during the growth phase During the quiescent phase of the hair growth cycle the skin is very flaccid. In contrast, growing skin is turgid and has great resilience. This change may be largely due to the increase in size of the follicles and the hairs. In fact, distortion or compression of the annulus and *Haarscheibe* during the growing phase can be closely correlated with the width of the hair shaft passing through the tylotrich follicle To understand this one must first examine the size and shape of the tylotrich The part of the tylotrich embedded in the quiescent follicle (dorsum of adult animal) is approximately 45 μ wide Hair width increases to about 60 μ at the center of the shaft. Midway between the center and the tip the tylotrich reaches a maximum width of approximately 120 μ and then gradually tapers off to a point. During the growth phase the sensory and erectile parts of the tylotrich follicle make considerable structural adjustments in order to accommodate this constantly changing hair shaft. How much this compression affects the neural physiology of to follicle is unknown but its effect on the morphology of the annulus and *Haarscheibe* is considerable

SUMMARY

Tylotrich follicles which contain highly specialized sensory and erectile tissues are sparsely scattered throughout the skin of the rabbit In adult animals single tylotrich follicles occur at intervals of approximately ½ to 1 cm These follicles are slightly larger than common guard hair follicles and they produce longer and straighter hairs

The most prominent sensory portion of the tylotrich follicle is called the *annular complex* It i composed of three structures that concentrically encircle the external root sheath of the follicle just below the sebaceous gland The largest of these structures the annulus is a ring of connective tissue enclosing a network of capillaries which is capable of great dilation in response to stimulation. The central component of the annular complex is a thin band of smooth muscle-like cells. The inner component is a bilaminal arrangement of nerve fibers composed of inner fibers that run vertical to the follicle and outer fibers that encircle it.

The *Haarscheibe* which acentrically surrounds the orifice of the tylotrich follicle, is another sensory component. It is a thick, richly innervated area of epidermis covering a highly vascularized region of dermal connective tissue Most of the *Haarscheibe* is located at the posterior side of the tylotrich follicle.

ACKNOWLEDGMENTS

I should like to thank Professor William S Bullough for generously supplying laboratory facilities for this research at Birkbeck College University of London. For their good advice I am indebted to both Professor Bullough and Dr I Griffiths. I also wish to thank Professor Herman B Chase Professor William Montagna, and Dr Stanley J Mann all of Brown University for many helpful suggestions.

LITERATURE CITED

Chase H. B 1954 Growth of the hair Physiol. Rev 34 113–126.

Conn, H. J and M. A. Darrow 1946 Staining Procedures Used by the Biological Stain Commission. Biotech Pub., Geneva N Y pp IC-23, 29.

Dry F W 1926 The coat coloration of the mouse (*Mus musculus*) nd the rat (*M norvegicus*) J Genet., 20 131–144

Fitzgerald, O 1940 Discharges from the sensory org ns f the at' vibrissae nd the modification in their activity by ions. J Physiol., 98 163–178

Messenger J F 1900 The vibrissae of certain mammals. J Comp. Neur 10 399–40?

Mont gna, W and R A Elli 1958 The vascularity and innerv tion of human h i folli les In The Biology of Hair Growth W Mont and R. A. Elli ed Academic Pres Inc New York, N Y pp 219–227

Pink F 1903 Über H utainnesorgane be dem menschlichen H (Haarscheiben) u ihre vergleichend an tomische Bedeutung Arch. mikr An t. 65 121–170

Straile W E. 19.8 Atypical guard hair f licles in the kin of the bbit. N ture 181 1604–1605.

——— 1960 Sensory hair follicles in mammalian skin the tylotrich follicle. Am. J Anat., 106 133–145.

Tamponi, M. 1939 Nuovo contributo alla conoscenza del disco del pelo" (Haarscheibe di Pinkus) con particolare riguardo alla sua iconografia macroscopica Arch Ita Sifilogr Venereol., 15 3[illegible]–3 4

Wed[illegible], G., E. Palmer a d [illegible] Nerve endings in mamma[illegible] [illegible] 3 159–19

PLATE 1

EXPLAN TION FIGURES

All f these photomicrographs are of q lescent follicles.

2 Longitudinal histological section of tylotrich follicle st ined with an Gieson picro-acid fuchsin tai with l m hematoxylin. The lower rrow point t the center of the annulus. Notice the circula arrangement of connective tissue fibers surrounding the large capillaries in the nnulus. The upper arrow point to th *Haarscheibe* Notice the gradual tra sition in thickness between the *H arscheibe* nd the surround g epidermi t the terior and posterior sides of the follicle The middle rrow marks the thick rea of the ternal root she th above the sebaceou gl nd. A group f small down hair follicles l typically positioned at the posterior edge of the *H rscheibe* (left side of the photomicrograph) The hair had been pl ked from thi q lesce t follicle j t before fixation. 100

3 Tylotrich follicl stained with gold chloride The lower arrow poi ts t the lus she th which encloses th darkly tained annulus. The specialized region of dermis, which lies between the *Haarscheibe* and the ul is marked with the upper rrow 210

4 Cros section of tylotrich follicl The arrow marks capillary i the nnul s. This essel is lmost as wide the follicle it rrounds. Notice the smooth nd fl ened shape f the endothelial lining f thi pill ry Section stained with Dela field' hematoxyl w th eosi × 100

5 H stological section pa sing ta gentially through the band f smooth m scle-like cell (arrow) Obser he elongat hape f their uclei Section tained with Weigert iron hematoxylin with safra in. 415

6 Longitudinal section of tylotrich follicle tai ed with W igert iron hem toxylin w h safranin. Notice the precise alignmen of the uclei of the mooth muscle-like cell on both sides of the f llicle The upper rrow poi t t these cell on the posterior side of the follicle The lower rrow ma k the area occupied by the bilamina rrangement of nerve fibers 210

7 Sec ion pa si g tangentially through the bilaminar rr gement of nerv fibers These w uperimposed l yers ha the appearance f very regula network. Section ned w th gold hloride × 415


2


3


4


5


6


7

PLATE 2

EXPLAN TION OF FIGURES

All of these photomicrographs are of quiescent follicles.

8 Cross section of *Haarscheibe* showing the abrupt transition in epidermal depth along its lateral borders. Notice the papilla of the *Haarscheibe* which is marked by the arrow Section stained with Delafield' hematoxylin with eosin. × 100

9 Section stained with an Gieson picro-acid-fuchsin stain with lum hematoxylin howing highly magnified *H rscheibe* Observe the two distinct rows of nuclei *the basal cell layer (arrows) × 210*

10 Each arrow points to the spindle-shaped nucleus of cell i the *Haarscheibe* Section stained with an Gieson picro-acid fuchsin stain with alum hematoxylin. × 415.

11 Gold chloride tained section showing nerve branching within the specialized region of dermis nd giving off fibers which form the network below the *Haarscheibe* The arrow marks this network. × 210.

12 Section howing branching pill ry marked with the rrow within the specialized region of dermis under the *H ackeibe* Tissue tained with an Gieson picro-acid-fuchsin stain with al m hematoxylin 210

13 Cross section of the precapillary arteriole (lower rrow) venule (middle rrow) and nerv (pper rrow) which supply the tylotrich follicle Section stained with van *Gieson picro-acid fuchsin stain with alum hematoxylin. × 415*








PLATE 3

EX LANATION FIG

All of these photomicrographs re f q lescent follicles except th one in figure 19

14 The arrow poi t t the l rge pillary supplyi g blood to or draining blood from the ascular network within the ann l s. Section tained with van Gieson picro-acid fuchsi stain with al m hem toxylin. × 100.

15 Gold hloride t ined section bowing the large nerve marked with the arrow givi g off branches t the lar compl (right branch) d to the *Haarsch ibe* (l ft branch) × 100

16 Sil er t ined section demonstr ting the network f fine nerv fibers below the *Haa scheibe* The rrow m rk tw expanded nerve endings that termin te nea or on peci lized basal cell th type that h uclei positioned nea the basement mem brane 415

17 Sil er tained section showing the redistribution of nerve fibers t form the bil mina rra geme t (arrow) that surrounds the follicle j t below the sebaceous gland. × 210.

18 The rrow ma k some nerv fibers within the ulus f the tylotrich follicle Section t ined with gold hloride 100

19 Compressed *H rscheibe* f growi g tylotrich follicle t ined with Gieson picro-acid fuchsin stain with l m hematoxylin 210

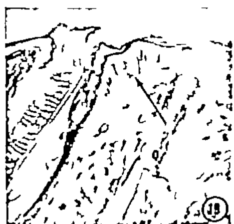

14


15


16


17


18


19

Liver Glycogen Zonation in the Mouse Following Fructose and Glucose Injection[1]

LEWIS M NEPORENT[2] AND ARVIN S. GLICKSMAN
Department of Medicine and Section on Radiobiology
Memorial Sloan-Kettering Cancer Center N Y

Glycogen is often found to be localized in certain zones of mammalian liver lobules. Many investigators have reported regular cyclic changes in the locus of the stored glycogen in relation to the absorptive and post-absorptive states of the animals studied. Glycogen has been reported to be deposited first around the central veins of the hepatic lobules (Noel '23; Kater '33) It is now generally agreed however that the initial deposition of glycogen occurs peripherally i.e., around the hepatic portal venous and arterial branches, gradually filling the central areas of the lobules (Smith, '31 Deane 44 Deane et al. 46 Ekman and Holmgren, 49) It is thought that glycogen is first localized peripherally since the peripheral cells first come in contact with the sugar rich blood entering the liver lobules (Deane 44)

Ekman and Holmgren (49) reported that glycogen mobilization begins peripherally in mice a central deposit of glycogen being indicative of glycogenolysis. A peripheral type of liver glycogen distribution however was sometimes found in the fasted animals.

Gluconeogenesis arising from protein and fat mobilization tends to maintain normal blood sugar levels in fasting animals and increases in liver glycogen have been reported to occur during the diurnal cycle of rats (Agren et al. '31) in spite of prolonged inanition. The varying degrees of gluconeogenesis in the liver superimposed on a pattern of glycogen mobilization may account for many of the differences in distribution of glycogen in fasted animals observed by several investigators (Deane 44 Ekman and Holmgren 49)

In the present experiments a series of animals were adrenalectomized in order to rule out, to a large extent the mechanisms of gluconeogenesis which might tend to obfuscate the pattern of glycogen deposition.

Fructose was used in our experiments because of several properties of this sugar which merit special consideration: Fructose unlike glucose is not dependent on insulin for transport into cells and subsequent phosphorylation (Cori and Cori, '29 Gameltoft et al 44) Park et al. ('56) however have shown that fructose transport into cells could be accelerated by insulin The specific kinase reactions in the liver glucokinase and fructokinase appear to be rate limiting in glycogen synthesis (Cahill et al. '59) and the activity of fructokinase has been shown to be 10 times that of glucokinase in rat liver homogenates (Vestling et al. '50) It is therefore logical to expect a more rapid liver glycogen deposition from fructose than from glucose.

It is the purpose of this paper to report the histological patterns of glycogen deposition after both fructose and glucose administration in adrenalectomized mice

MATERIALS AND METHODS

For these studies female Swiss albino mice of the I.C.R. strain, two to three months old and weighing from 23 to 35 gm were used The mice were bilaterally adrenalectomized and were used in these experiments one week after the removal of the adrenals. The animals were fed "Big Red G.L.F dog pellets oats and given 1%

[1] Portions of the text were submitted by Dr Neporent to the faculty of Cornell University in partial fulfillment of the degree of Master of Arts

[2] Present address Montefiore Hospital, Bronx N Y

salt solution as drinking water to correct for their imbalance in mineral metabolism

The mice were injected intravenously via a tail vein with either 10% glucose or fructose in water in a dose of 0 6 gm of sugar per kilogram of body weight.

The intravenous concentration of sugar was calculated to raise the blood sugar level about 200 mg %

At varying periods after injection the mice were killed by cervical dislocation The large right median lobe of the liver was quickly excised small pieces of liver were fixed in ice-cold Rossman s fluid for approximately 24 hours The tissues were then dehydrated in absolute alcohol and cleared in toluene After embedding in "Tissuemat the tissues were sectioned routinely at 5 μ

The stain used was McManus periodic acid Schiff method for the demonstration of *glycogen and other polysaccharide com* plexes Occasionally saliva digest control sections were processed simultaneously with the undigested slides

The various patterns of glycogen zona tion were classified as follows (1) peripheral deposition as occurring primarily around the hepatic portal venous radicles with little or no deposition in the centrolobular areas (2) central deposition as occurring primarily around the central veins with little or no glycogen peripherally (3) spotty deposition as only scattered cells having no definite pattern of glycogen deposition in the lobule and (4) generalized as having nearly total or diffuse glycogen deposition throughout the liver lobule The total amount of stainable liver glycogen was estimated by noting the depth and extent of the color reaction ranging from 1+ for slight to 6+ for a very heavy glycogen distribution

RESULTS

Control

Sixty-eight and four tenths per cent of the starved controls had littl or no stainable liver glycogen (fig 1 When glycogen was present it was u ll y sparse but in a few cases moder t concentrations of glycogen were seen t bles 1 and 3)

Fructose infusion

The glycogen deposition in the livers ex amined 10 minutes after intravenous injection of fructose followed no clearly defined pattern Of 15 anim ls sacrificed 10 minutes after injection of the sugar 7 had appreciably stainable deposits of glycogen. Five had a spotty or generalized type of deposit and one each a peripheral or central deposit (table 1)



Fig 1 The absence of liver glycogen in 24-hour starved control animal McM us periodic acid leucofuchsin tai hematoxylin counter tain 210

TABLE 1

Fructose i t avenou i jectio —types of glycogen deposition

	Control	10′	30′
Neg or sc t ered	13	8	
Spotty	4	1	3
Generalized	3	4	8
Peripheral	—	1	12
Cen al	1	1	2
Tot l	19	15	25

By 20 minutes glycogen deposition frequently appeared in the periphery of the liver lobules. The areas surrounding the central veins were often conspicuously devoid of histologically demonstrable glycogen (table 1 and fig. 2). Approximately one-third of the animals however demonstrated a generalized type of deposit at 20 minutes with no zonation present (table 1 and fig. 3).

Central deposits were occasionally noted in both the starved control group (one animal) and in the infused group (table 1). Such a pattern probably represents residual glycogen not mobilized during the fast.

TABLE 2

Glucose intravenous injection—type of glycogen deposition

	20'	60'
Neg. or scattered	8	4
Spotty		3
Generalized	—	5
Peripheral	4	—
Central	—	—
Total	14	12



Fig. 2. The distribution of glycogen in the liver of an animal 20 minutes after an intravenous injection of fructose. There is well localized peripheral deposit of glycogen; the cells surrounding the central veins are devoid of glycogen. McManus periodic acid leucofuchsin stain hematoxylin counterstain. × 210.

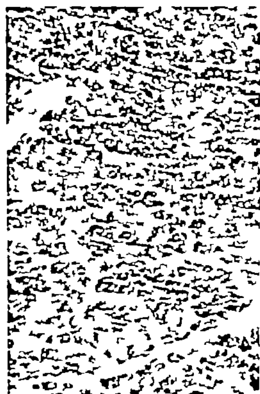


Fig. 3. The distribution of glycogen in the liver of an animal 20 minutes after an intravenous injection of fructose. There is heavy generalized glycogen deposition. McManus periodic acid leucofuchsin stain hematoxylin counterstain. × 210.

TABLE 3

Fructose intravenous injections—estimated glycogen content of livers

	Controls	10'	20'
0±	13	8	2
1	4	1	4
2	2	1	3
3	—	4	4
4	—	1	4
5	—	—	1
6	—	—	1
Total	19	15	24

Glucose infusion

The intravenous injection of glucose in 14 animals sacrificed 20 minutes post injection showed demonstrable glycogen in only 6 animals (tables 3 and 4) There was a spotty distribution in two (fig 4) and 4 animals had well localized peripheral deposits Previous unpublished experiments have shown that there is no significant deposition of glycogen 10 minutes after intravenous glucose injection

TABLE 4

Glucose intra enou injection —estimated glycogen content f livers

	20'	60'
0 =	8	4
1	5	5
2	1	2
3	—	1
4	—	—
5	—	—
6	—	—
Total	14	12



F g 4 The dis ribution f gl oge in the liver of imal 20 min es fte enous injection of glucose The distribu on of a potty non loc lized haracter M M periodic acid leucofuchsin in hema oxylin counterst in. 310



Fig. 6 The bsence of glycogen in the metaphase of the division f hepatic cell. Glycogen i present in the urrounding interkinetic cells. McMan periodic acid leucofuchsin stain; hematoxylin counterstain. × 850.

Of 12 animals injected with glucose sacrificed one hour after the injection, none had peripheral types of deposits three animals had spotty deposits 5 generalized and 4 negligible glycogen deposits It is noted from table 4 that the apparent total glycogen deposits did not increase significantly after more than 20 minutes post injection One-third of the animals had only negligible amounts of liver glycogen at the end of one hour

Occasional mitotic figures were found in the microscopic sections of the liver samples All stages of mitosis were encountered in which the cells were devoid of glycogen (figs 5 and 6) Many cells in prophase and metaphase were noted how ever in which a peripheral ring of glycogen urrounded a clear cytoplasmic area



Fig. 6 The absence of glycogen in the telophase of the division of an hepatic cell McManus periodic acid leucofuchsin stain hematoxylin counterstain. × 850.

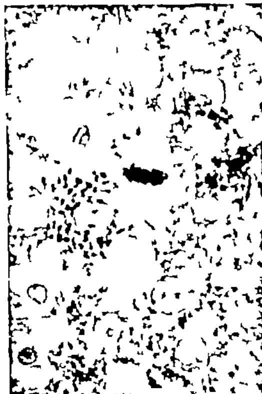


Fig. 7 The presence of thin peripheral ring of glycogen surrounding clear cytoplasmic area in the metaphase of liver cell McManus periodic acid leucofuchsin stain hematoxylin counterstain. × 850

(fig. 7). No anaphases contained glycogen, and the cytoplasm of cells in telephase occasionally contained small amounts of stainable glycogen.

DISCUSSION

These data suggest that there may be initial glycogen deposition from infused fructose as early as 10 minutes post injection, although no clear pattern of deposition is evident

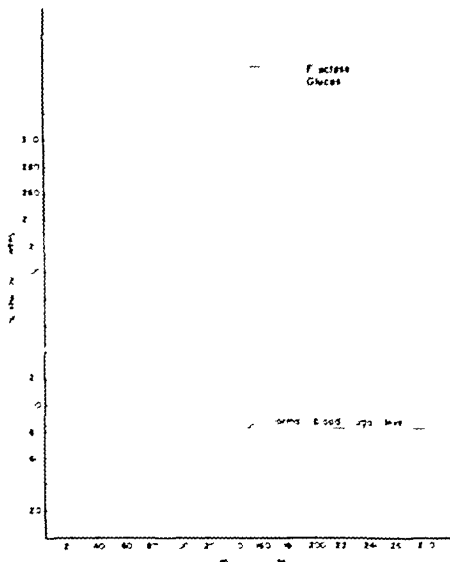
Contrasted with the 20-minute fructose injection experiment, it is apparent that glycogen deposition is slower and the glycogen deposition is less following glucose infusion than after giving fructose (tables 3 and 4) In both groups of animals the peripheral-type of glycogen zonation is apparent at 20 minutes, although it occurred more frequently after fructose than after glucose injection. It is noteworthy that the peripheral pattern of glycogen zonation was not found in the starved control series. Since a significant number of the 24-hour starved control animals had residual glycogen (tables 1 and 3) it is possible that a peripheral deposition of glycogen in some of the fructose and glucose injected animals was superimposed on this residual pattern to give the picture of a generalized deposition. On the other hand, it is probable that in some animals glycogen was initially deposited in a generalized pattern.

In the absence of the adrenals, liver glycogen should quickly be depleted due to an inability of the starved animal to mobilize fat and protein for gluconeogenesis (Soskin and Levine '52) It was found that after a 24-hour fast, in female adrenalectomized animals the liver usually is depleted of histologically demonstrable glycogen.

Hepatic tissues of adrenalectomized animals have been shown to oxidize glucose

and fructose or store them as glycogen at a normal rate (Ashmore et al. '58, Renold et al. '53). Cori and Cori ('27) have reported that the carbohydrate utilization of adrenalectomized rats is normal, while Ingle and Nezamis ('48) have shown that eviscerated adrenalectomized rats utilize infused glucose at a moderately higher rate than non-adrenalectomized eviscerates.

From an inspection of typical mammalian fructose and glucose tolerance curves (fig. 8) it is seen that the disappearance of fructose from the blood is much faster than for glucose at high sugar concentrations. The disappearance of the sugars from the blood reflects the rates of sugar uptake by both the liver and extrahepatic tissues. The extrahepatic uptake of glucose, however, at normal blood sugar concentrations, has been shown to be three times as rapid as it is for fructose (Levine and Huddlestun '47).



F 8 F u ose and glucose ... ves f d ... fter in ravenou injection of ... tolerance ... urv ... slightl modified from d ... f Smith et al. ('38). ... courtes ... J. J. O'Toole Dep rtment f Physiology Cornell Uni ... School.

Fructose is largely utilized independent of the action of insulin High levels of glucose in the blood stimulate the secretion of insulin by the pancreatic islet tissue (Soskin and Levine '52) An elevated level of insulin in the blood has been found to increase the extrahepatic utilization of glucose beyond that found at normal blood sugar levels (Cori and Cori '27 Bridge '38 Wick et al '51) and to decrease hepatic glycogen formation (Cori, '26) Recent experiments have suggested that insulin may decrease the hepatic output of glucose (Madison et al. '59 and De Bodo et al. '59) As yet, however this mechanism is controversial (Cahill et al. '59)

It therefore becomes apparent that a greater percentage of sugar should be deposited in the liver after injection of animals with fructose than with equal amounts of glucose

On intravenous injection of fructose into an animal the blood fructose level rises *to high levels. At such high levels the fruc*tose uptake is rapid and with the greatest proportion presumed to be taken up by the liver Levine and Huddlestun ('47) found that the liver utilizes about 85% of injected fructose The peripheral cells of the liver lobule coming into contact first with the sugar rich blood, might conceivably withdraw so much of the fructose that the blood draining centrally would contain a very low level of the injected sugar At low fructose concentrations the uptake of the sugar which is in reality a reflection of the fructokinase reaction, is relatively slow This can readily be seen by an inspection of the fructose tolerance curve (fig. 8) Microscopically this situation might be characterized by an initial peripheral type of glycogen deposition.

The same principles should hold true for glucose deposition as for fructose deposition in the liver The initial high blood glucose levels might concomitantly stimulate a rapid hepatic and extrahepatic glucose uptake as well as stimulate insulin output by the pancreas While initially there might be an appreciable glucose gradient from the periphery to the center of the hepatic lobule as the blood glucose *level falls the centrally located lobule cells* should have access to concentrations of glucose nearer to those of the peripheral cells and soon (one hour post injection) more evenly distributed types of deposits *might* be expected.

According to the variable peripheral utilization of glucose coexistent with hepatic glycogen deposition the histologically demonstrable glycogen distribution patterns might vary thus at one hour it may be presumed that significant glycogenolysis *may have occurred in order to satisfy pe*ripheral glucose demands thus altering any pure deposition pattern of glycogen. The large percentage of animals with little or no histologically demonstrable liver glycogen is to be noted at 20 minutes and one hour for glucose

Gerold ('51) in a study of regenerating mouse livers studied the glycogen changes of mitotic cells. He has noted that cells undergoing mitosis gradually lose their glycogen stores. According to his description of events prophasic cells may contain large amounts of glycogen the glycogen *content gradually diminishing during the* mitotic process until anaphase in which stage all cells are devoid of glycogen Glycogen, he reports, gradually reappears in the cells during telophase

From an examination of the mitotic cells found in the glycogen-stained liver sec*tions the above description of events ap*pears to be in the main substantiated Whereas many cells entering prophase contained large stores of glycogen all stages of mitosis were encountered in which the cells were devoid of glycogen (figs 5 and 6) The presence of glycogen in some but not all cells early in mitosis may be dependent on the presence or absence of glycogen in the cells just prior to the mitotic process No cells in anaphase contained glycogen and the cytoplasm of cells in telophase occasionally contained small amounts of stainable glycogen

Glycogen is probably utilized by the cell during the process of cell division and this may account for the disappearance of glycogen during mitosis Bullough and Eisa ('50) studying the mitotic activity in the skin of albino mice found the glycogen concentration of the skin to be intimately related to the frequency of mitosis A high mitotic rat was found in the skin containing a low concentration of glycogen.

Thus it was concluded that glucose deposited from the blood is the critical factor in determining the mitotic rate. Liver cells would then seem to reside in an environment extremely favorable for mitotic activity; its cellular elements normally have access to large amounts of both intracellular glycogen and an extracellular blood-borne glucose supply.

An alternate explanation may be that dividing hepatic cells lose their functional capacity to store glycogen and regain this capacity when cell division is complete.

SUMMARY

1. The pattern of liver glycogen zonation after intravenous administration of glucose and fructose in adrenalectomized mice was investigated.

2. In 20 minutes glycogen was frequently localized peripherally after intravenous injection of fructose; the shortest period for histochemically visualizing glycogen from intravenously injected fructose may be between 10 and 20 minutes.

3. Intravenous injection of glucose resulted in negligible liver glycogen deposition in over half the animals at 20 minutes and in one-third of the animals at 60 minutes, and the peripheral glycogen distribution was less frequent than for fructose. It is believed that the stimulation of insulin by injected glucose, effecting a greater peripheral tissue utilization of glucose, may be responsible for this result.

4. Dividing cells were found to lose glycogen during the mitotic process.

LITERATURE CITED

Agren, G., O. Wilander and E. Jorpes 1931 Cyclic changes in glycogen content of liver and muscles of rats and mice; their bearing upon sensitivity of animal to insulin and their influence on urinary output of nitrogen. Biochem. J. ... 783

Ashmore, J., C. F. Cahill, J. ... B. Hastings and A. E. Renold 1955 Adrenal ... hepatic ... Endocrinology ... 21

[illegible]

Cori, C. F. 1926 The rate of glycogen formation in the liver during glucose absorption. Proc. Soc. Exp. Biol. Med., 23: ...86–...89.

Cori, C. F., and G. T. Cori 1927 The fate of sugar in the animal body. VII. The carbohydrate metabolism of adrenalectomized rats and mice. J. Biol. Chem., 74: 473–494.

——— 1929 Fate of glucose and other sugars in the eviscerated animal. Proc. Soc. Exp. Biol. Med., 26: 432.

Deane, H. W. 1944 A cytological study of the diurnal cycle of the liver of the mouse in relation to storage and secretion. Anat. Rec., 88: 39–65.

Deane, H. W., F. B. Nesbitt and A. B. Hastings 1946 Improved fixation for histological demonstration of glycogen and comparison with chemical determination in the liver. Proc. Soc. Exp. Biol. Med., 63: 401–406.

De Bodo, R. C., R. Steele, N. Altszuler, A. Dunn, D. T. Armstrong and J. S. Bishop 1959 Further studies on the mechanism of action of insulin. Metabolism, 8: 520–530.

Ekman, C. A., and H. Holmgren 1949 The effect of alimentary factors on liver glycogen rhythm and the distribution of glycogen in the liver lobule. Anat. Rec., 104: 189–216.

Gammeltoft, A., P. Kruhøffer and E. Lundsgaard 1944 Insulin and the assimilation of fructose. Acta Physiol. Skand., 8: 162–172.

Gerold, N. J. 1931 Histochemical and cytological observations on the regenerating liver of the partially hepatectomized albino mouse. Thesis (Ph.D.), Cornell University.

Ingle, D. J., and J. E. Nezamis 1948 Effect of adrenalectomy upon the tolerance of the eviscerated rat for intravenously administered glucose. Am. J. Physiol., 152: 598–602.

Kater, J. McA. 1933 Comparative and experimental studies on the cytology of the liver. Ztschr. Zellforsch. Mikr. Anat., 1... 21 ... 16

Levine, R., and B. Huddlestun 1947 The comparative action of insulin on the disposal of intravenous fructose and glucose. Fed. Proc., 6: 151–15...

Madison, L. L., B. Combes, W. Strickland, R. Unger and R. Adams 19... Evidence for direct effect of insulin on hepatic glucose output. Metabolism, 8: 469–4...

Noel, R. 1923 Recherches histo-physiologiques sur la cellule hépatique des mammifères. Arch. Anat. Micr., 19: 1–158.

Park, C. R., R. L. Post, C. F. Kalman, J. H. Wright, J. L. H. Johnson and H. E. Morgan 1956 Ciba Foundation Colloquia on Endocrinology. Internal Secretion of the Pancreas. The transport of glucose and other sugars across cell membranes and the effect of insulin. Little, Brown and Co., Boston, pp. 13–2...

... A. F. ... C. T. Teng, F. B. ... and A. B. H... Studies on carbohydrate ... L... II. The effect of ... and of hormonal deficiencies. J. Biol. ... 13...

Smith, D. 1931 The deposition and withdrawal of glycogen of the liver in the rat. Anat. Rec., 51 (Suppl.) 74.

Soskin, S., and R. Levine 1952 Carbohydrate Metabolism. University of Chicago Press, Chicago.

Vestling, C. S. A. K. Mylroie, U. Irish and N. H. Grant 1950 Rat liver fructokinase. J. Biol. Chem., 185 789-801.

Wick, A. N. D. R. Drury H. W. Bancroft and E. M. MacKay 1951 Action of insulin on the extrahepatic tissues. Ibid., 188 241-249.

A Quantitative Study of the Lethal and Teratogenic Effects of Hypoxia on the Three-Day Chick Embryo[1]

CASIMER T GRABOWSKI[2]
Department of Anatomy School of Medicine University of Pittsburgh Pittsburgh, Pennsylvania

A previous study (Grabowski and Paar '58) has shown that the effects of hypoxia on the chick embryo—both lethal and teratogenic—can be studied in a quantitative manner The degree of exposure can be carefully regulated and graded and a proportional response recorded. For a given age of embryo (between one and 4 days) and time period of exposure (6 hours) as one progressively reduces the oxygen concentration the following relationships can be observed:

1 No effects of hypoxia are noted between 15–20% oxygen which constitutes a *latent range*

2. The incidence of embryos with malformations increases in an exponential fashion below approximately 15% oxygen, which is the teratogenic range.

3 The severity of the malformations and number of symptoms per embryo also increases as conditions become more severe.

4. Death rates also increase in an exponential manner

5 The incidence of abnormal development drops rapidly as the death rates rise rapidly towards the 100% level, forming a *lethal range*

6 A progressively increasing sensitivity to both the lethal and teratogenic effects of hypoxia was apparent with increasing age.

In this experiment only two variables were studied, namely the age of the embryo and oxygen levels during exposure to hypoxia. The duration of exposure was held constant at 6 hours.

The purpose of the present investigation was to explore further the quantitative relationships between degrees of hypoxia and teratogenic and lethal effects by studying an additional variable, time The degree of hypoxia was therefore controlled by varying not only oxygen levels between 0 to 21% but also the duration of exposure to oxygen deficient atmospheres between three to 24 hours. The age of the embryo was held constant at three days. Again regular quantitative relationships were observed between oxygen level and duration of exposure on one hand and death and abnormal development on the other Qualitative differences were also observed since different degrees of hypoxia induced different kinds of anomalies. This indicates that there may be more than one mode of action of hypoxia on developing organs.

MATERIALS AND METHODS

A mixture of nitrogen and air at normal pressures was used to provide the oxygen deficient atmospheres for this study This method provided greater flexibility and a finer degree of control over the experimental environment than the partial vacuum used earlier (Grabowski and Paar '58) The differences in results from the two methods are slight and are discussed in some detail on pages 32–33.

The air-nitrogen mixtures were prepared from compressed gases by the displacement of water from 5-gallon carboys (fig. 1A) Thirteen-gallon carboys were used for the long-term experiments. The oxygen concentration was measured with a Beck

[1] This study was aided by grant from the Easter Seal Research Foundation. The author wishes to acknowledge the capable technical assistance of Mr Ted Lakawa and Miss Sally Grant in the pursuit of these experiments.

[2] Present address Department of Zoology University of Miami, Coral Gables 46, Florida.

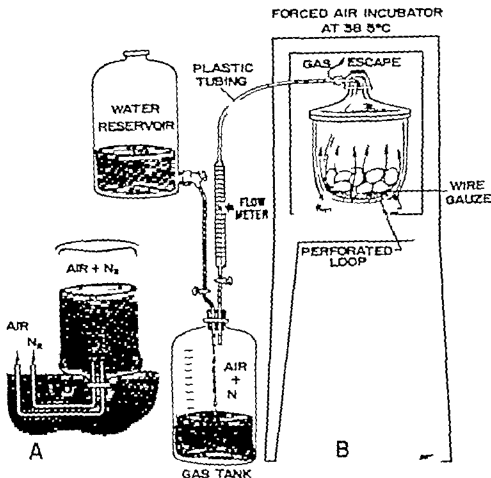


Fig. 1 Equipment used to produce oxygen deficient atmosphere. See text for explanation.

man Oxygen Meter accurate to within $\pm 0.25\%$ O_2. Adjustments were made, when necessary to bring the oxygen concentration to a predetermined level. The gas mixture was also delivered to the eggs by water displacement, as illustrated in figure 1B From 20 to 25 eggs were loosely arranged on a wire gauze support in a vacuum desiccator over a loop of perforated plastic tubing. This loop was connected, through the arm of the desiccator with a long length of plastic tubing which in turn was connected with the gas tank. Water dripping into the gas tank displaced the experimental gas from the tank, through a flow meter and the plastic tube, over the eggs and out through the arm of the desiccator At the start of the experiment, 15 liters of gas were passed through the system at a rate of 1000 cm per minute. This served to flush the desiccator whose volume was 3000 cm^3 rapidly and completely The rate of flow was then reduced to 50 cm^3 per minute. This *latter rate provided a slow and steady* movement of gas over the eggs, as demonstrated by the addition of cigarette smoke to the stream. This rate of flow also assured a constant environment for the eggs since 24 three-day embryos would consume only 0 10 cm^3 of oxygen per minute under optimum conditions (Romanoff 41).

The eggs for these experiments were obtained from a commercial poultry farm and were from Darby chickens, a strain of White Leghorn. Incubation was always begun within 5 days after laying. The experiments were performed exclusively on three-day embryos. They were exposed to oxygen concentrations of 0 to 21% for

periods of from three to 24 hours. At the end of the treatment they were returned to a regular egg incubator The dead embryos were examined as soon as death was detected survivors on the 7th day after treatment. At the time of autopsy the embryos were checked for externally visible malformations Then they were weighed, and the crown-rump length and diameters of both eyes measured. Internal autopsies were not performed because the previous study indicated that visceral anomalies were relatively infrequent at this stage. Altogether over 2000 eggs were used in this study

RESULTS

All of the results of this survey are summarized in table 1 The teratological data are plotted in figure 2. Again, as in the previous study a series of bell-shaped curves were obtained. For each time period of exposure, as the oxygen concentration is progressively reduced a latent range is first apparent in which there is no observable effect upon development. Beyond the latent range the initial rise in abnormal development is exponential The drop in abnormal development at lower oxygen concentrations is due to a very rapid increase in the number of embryos dying during or immediately after the treatment. It is further apparent from the study of figure 2 that (1) a significant degree of abnormal development occurs only at oxygen concentrations of 13% or less regardless of duration of exposure- (2) the peak frequencies of abnormal de-

TABLE 1

Summary of results

Hours	Oxygen	Total number	Normal	Immediate dead	Delayed dead	Anomalous
	%		%	%	%	%
3	0.0	50	2	74	18	18
3	1.1	54	9	61	17	24
3	2.1	43	65	26	2	9
3	4.2	44	73	9	18	9
3	6.3	46	82	2	10	7
3	8.4	53	87	9	0	4
3	10.5	50	94	4	4	4
6	2.1	22	0	91	5	9
6	4.2	71	18	24	17	40
6	6.3	46	35	15	9	41
6	8.4	49	66	8	10	25
6	10.5	49	67	8	13	14
6	12.6	43	84	4	3	9
6	14.7	45	80	0	10	10
6	16.8	23	92	0	8	4
12	2.1	28	3	90	7	0
12	4.2	43	0	58	40	35
12	6.3	43	16	35	28	23
12	8.4	30	33	28	26	26
12	10.5	45	69	9	8	15
12	12.6	63	68	10	8	16
12	14.7	60	93	7	2	2
12	16.8	95	96	2	2	0
24	4.2	26	0	100	0	0
24	6.3	70	0	90	10	2
24	8.4	47	43	18	30	11
24	10.5	67	82	7	6	4
24	12.6	63	90	0	6	6
24	14.7	59	84	0	13	3
24	16.8	58	82	0	16	2
24	21.0	24	92	4	4	0
—	—	303	84.2	—	12.5	5.6

Control series.

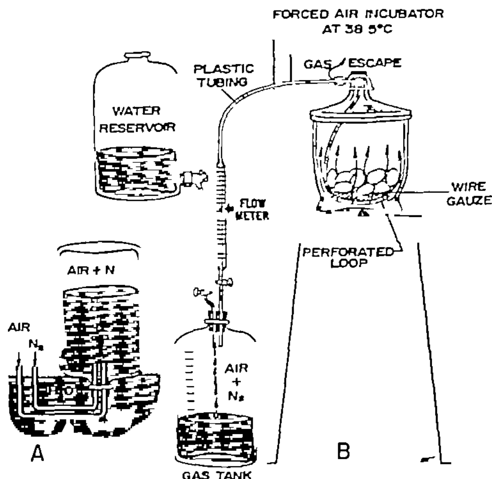


Fig. 1 Equipment used to produce oxygen deficient atmosphere. See text for explanation.

man Oxygen Meter accurate to within ± 0.25% O_2. Adjustments were made when necessary to bring the oxygen concentration to a predetermined level. The gas mixture was also delivered to the eggs by water displacement, as illustrated in figure 1B From 20 to 25 eggs were loosely arranged on a wire gauze support in a vacuum desiccator over a loop of perforated plastic tubing This loop was connected, through the arm of the desiccator with a long length of plastic tubing which in turn was connected with the gas tank. Water dripping into the gas tank displaced the experimental gas from the tank, through a flow meter and the plastic tube, over the eggs and out through the arm of the desiccator At the start of the experiment, 15 liters of gas were passed through the system at a rate of 1000 cm^3 per minute. This served to flush the desiccator whose volume was 3000 cm^3 rapidly and completely The rate of flow was then reduced to 50 cm^3 per minute. This latter rate provided a slow and steady movement of gas over the eggs as demonstrated by the addition of cigarette smoke to the stream. This rate of flow also assured a constant environment for the eggs since 24 three-day embryos would consume only 0 10 cm^3 of oxygen per minute under optimum conditions (Romanoff 41).

The eggs for these experiments were obtained from a commercial poultry farm and were from Darby chickens, a strain of White Leghorn. Incubation was always begun within 5 days after laying. The experiments were performed exclusively on three-day embryos. They were exposed to oxygen concentrations of 0 to 21% for

periods of from three to 24 hours. At the end of the treatment they were returned to a regular egg incubator. The dead embryos were examined as soon as death was detected, survivors on the 7th day after treatment. At the time of autopsy the embryos were checked for externally visible malformations. Then they were weighed and the crown-rump length and diameters of both eyes measured. Internal autopsies were not performed because the previous study indicated that visceral anomalies were relatively infrequent at this stage. Altogether over 2000 eggs were used in this study.

RESULTS

All of the results of this survey are summarized in table 1. The teratological data are plotted in figure 2. Again as in the previous study a series of bell-shaped curves were obtained. For each time period of exposure, as the oxygen concentration is progressively reduced, a latent range is first apparent in which there is no observable effect upon development. Beyond the latent range the initial rise in abnormal development is exponential. The drop in abnormal development at lower oxygen concentrations is due to a very rapid increase in the number of embryos dying during or immediately after the treatment. It is further apparent from the study of figure 2 that (1) a significant degree of abnormal development occurs only at oxygen concentrations of 13% or less regardless of duration of exposure; (2) the peak frequencies of abnormal de-

TABLE 1
Summary of results

Hours	Oxygen	Total number	Normal	Immediate dead	Delayed dead	Anomalous
	%		%	%	%	%
3	0.0	50	2	74	18	18
3	1.1	54	9	61	17	24
3	2.1	43	65	28	2	9
3	4.2	44	73	9	18	9
3	6.3	46	82	2	10	7
3	8.4	53	87	9	0	4
3	10.5	50	94	4	4	4
6	2.1	22	0	81	5	8
6	4.2	71	28	24	17	40
6	6.3	46	35	15	9	41
6	8.4	49	66	8	10	25
6	10.5	49	67	8	13	14
6	12.6	43	84	4	3	9
6	14.7	45	80	0	10	10
6	16.8	23	92	0	8	4
12	2.1	28	3	89	7	0
12	4.2	43	0	58	40	35
12	6.3	43	10	35	28	23
12	8.4	39	23	28	26	28
12	10.5	45	69	0	9	15
12	12.6	63	68	10	8	18
12	14.7	60	97	7	2	2
12	16.8	65	96	2	2	0
24	4.2	20	0	100	0	0
24	6.3	70	0	90	10	2
24	8.4	47	43	10	30	11
24	10.5	67	83	7	0	4
24	12.6	63	90	0	5	6
24	14.7	60	84	0	13	3
24	16.8	68	82	0	16	2
24	21.0	94	92	4	4	0
—	—	301	84.3	—	12.5	5.6

Control series.

velopment occurred at progressively lower oxygen concentrations as the time of exposure is decreased; (3) the highest incidence of abnormal development was obtained at oxygen concentrations of 4 to 6% for 6 to 12 hours (4) an exposure time of three hours is not teratogenic unless the oxygen concentration is 4% or less (5) exposure to hypoxia for 24 hours does not result in much abnormal development This last item is partly explained by the fact that high death rates are obtained before the oxygen concentration is reduced to teratogenic levels. However there are also indications that some kind of adaptation occurs at the longer time periods of exposure.

The data on death rates are represented in figures 3 and 4 The first of these figure 3 is for the total death rate that is,

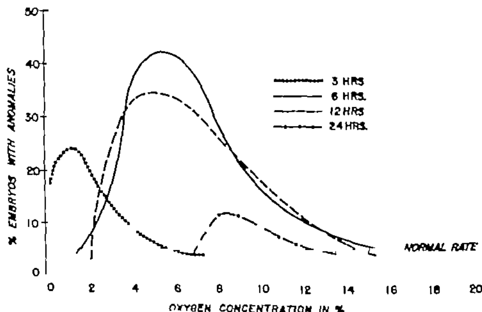


Fig. 2 The frequencies with which embryos with anomalies were obtained after various exposure conditions.

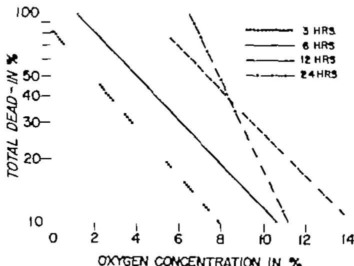


Fig. 3 Total death rates. Semi-log plot. Slopes of lines calculated by method of least squares.

the total number of embryos dying between the time the experiment was started and the time it was finished one week later In figure 4 are plotted the data for immediate deaths, that is the embryos that die during the treatment or within 24 hours afterwards. It can be seen that in both figures the lines are fairly regularly displaced to the right as the treatment time is increased between three to 12 hours with but slight changes in the slopes of the lines. Again, however the lines for the 24-hour experiments are different, suggesting some degree of adaptation. But despite the exception at 24 hours, the death rate data show considerably more regularity than do those for abnormal development (fig 2) For instance the initial rise in the curves for abnormal development after exposures of 6 12 and 24 hours are virtually the same but separate at lower oxygen concentrations. The three-hour curve is quite different. These data suggest that although the relationship of hypoxia to death may be relatively simple, several different factors may be operating with respect to abnormal development.

Comparing the curves in a different way the data show that the requirements for abnormal development are rather critical since teratogenic doses are also lethal doses. This close relationship of death to abnormal development under conditions of hypoxia is illustrated by the following correlations. The peaks for abnormal development at all time periods of exposure occur when the total death rates are between 50 to 65% and the immediate death rates are between 35 to 50% (table 1) Both death rate and maldevelopment start to increase at approximately the same oxygen level. For example for all experimental conditions a death rate of 20% closely corresponds to an incidence of abnormal development in 10% of the embryos (both of these values were chosen because they are twice normal) This correspondence between death and maldevelopment was also found in chick embryos at other ages by Grabowski and Paar ('58) The optimum incidence of malformations was obtained in embryos between one and 4 days old when the total death rate was 50% and the immediate death rate was 35%

The relative sensitivity of different structures of three-day embryos to different degrees of hypoxia

The degree to which embryos are exposed to hypoxia can be controlled by manipulating both oxygen concentration

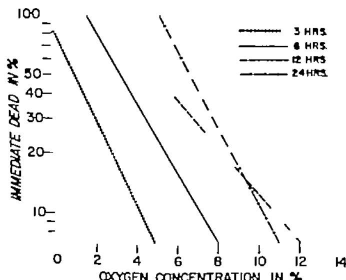


Fig. 4 Immediate death rates. Semi log plot. Slopes calculated by method of least squares.

and duration of exposure. As these conditions are varied, one obtains not only the quantitative differences in degree of abnormal development mentioned in the above section but also qualitative differences. For instance, an incidence of 15% malformed embryos can be obtained after treating the embryos (1) for three hours with no oxygen or with 2% oxygen, (2) for 6 hours with 3% or 9% oxygen; and (3) for 12 hours with 2½% or 9% oxygen (fig. 2) Quantitatively these conditions are equivalent, but qualitatively they are not, since the kinds of anomalies obtained under these various conditions are quite different. This feature of these experiments can be examined in some detail.

Different conditions of hypoxia have been arranged into what seemed natural groupings ranging from very severe through moderate to mild conditions (table 2) The incidence with which various structures were affected after the indicated treatments is shown along with the incidence in control embryos. The chief anomalies found in the experimental embryos are as follows:

1 *Completely malformed head.* An undersized head containing multiple anomalies of the brain eyes and beak, obtained almost exclusively after exposure to anoxia or severe hypoxia for three hours.

2 *Brain.* A variety of anomalies such as hydrocephaly microcephaly cranioschisis exocephaly and folded midbrains fairly common after severe or moderate conditions.

3 *Beak.* Cleft beak and palate crossbeak and short upper common after severe conditions for three hours and moderate hypoxia for 6 hours, but not after 12.

4 *Eyes* Mostly microphthalmos, common after severe and moderate conditions sometimes after mild hypoxia for 6 hours

5 *Extremities* Absent or malformed fair incidence after exposure to severe or moderate conditions.

6 *Rumplessness* Fair incidence (3%) in control series, significant increase above that in the controls was obtained after exposure to moderate or mild conditions.

The frequencies which are significantly above the normal have been underlined in table 2, consequently the solid lines indi-

TABLE 2

Relative frequencies of anomalous organs obtained after exposure of three-day embryos to different conditions of hypoxia

	Controls	3 hours 0–2% O_2 (severe)	6 hours 2–9% O_2 (moderate)	12 hours 2–9% O_2 (moderate)	6 hours 10–15% O_2 (mild)	12 hours 10–15% O_2 (mild)	24 hours 8–15% (mild)
Total no. embryos	303	147	167	153	163	160	236
Number anomalous	17	26	62	43	21	15	13
Structure							
Entire head	0	8.8	0.5	0.6	0.6	0	0
Brain	1.6	11.6	4.3	7.2	2.5	1.3	0.4
Beak	1.3	10.2	7.0	1.3	2.5	1.3	0.4
Eyes	2.3	18.2	16.5	7.2	4.3	1.3	0.4
Extremities	0.7	3.4	6.4	7.2	1.2	1.9	0.8
Rump	3.0	4.8	11.2	15.0	8.6	6.3	3.0

The figures in the columns represent the incidence in per cent with which the structure was affected. Underlined figures indicate the ranges over which given structure is most likely to be affected (see text)

cate the ranges over which a given structure is most likely to be affected. It is apparent that although completely malformed heads are obtained only after exposure to severe conditions of hypoxia, the individual structures of the head are generally affected by hypoxia of moderate degree. The extremities are likely to be affected by moderate or mild conditions. At the other extreme of sensitivity is the tail. A significant increase in rumplessness is not obtained after exposure to severe hypoxia. Moderate hypoxia induces rumplessness to a considerable extent. It is also clear from table 2 that rumplessness is by far the most common anomaly obtained after prolonged mild exposure to hypoxia. The data show that the relative frequencies of head, trunk, and tail anomalies can vary after exposure to different conditions of hypoxia even though the age of the embryo at the time of treatment is held constant. The data also suggest that since severe moderate and mild hypoxia affect the embryo in different ways hypoxia can affect the embryo in more than one manner. Other studies (Grabowski '59 '60) support this conclusion.

It is also apparent from the study of table 2 that exposure to hypoxia for 12 hours is milder than exposure to the same concentration of oxygen for 6 hours. That is 12 hour exposures are less teratogenic than those of 6 hours duration. Comparable oxygen levels for exposures of 24 hours are virtually non-teratogenic. These data suggest that there is some kind of adaptation at the longer time periods of exposure to oxygen deficiency The nature of this possible adaptation is not known.

Effects of hypoxia on quantitatively varying characters

In the above discussions the effects of hypoxia were measured in terms of discrete characters namely death and malformed tissues. Also studied was the effect of hypoxia on quantitatively varying characters such as crown-rump length, body weight and the diameters of the left and right eyes The latter were chosen because the eye was often affected by hypoxia especially the left one. Initially an attempt was made to get weights and measurements of all embryos regardless of the time of death but this did not prove practical. Postmortem maceration and

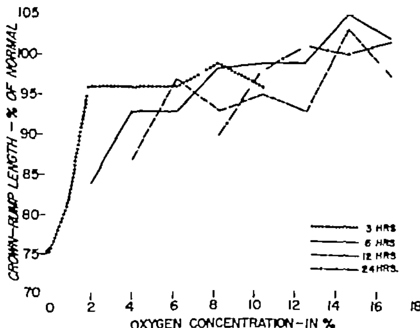


Fig. 5 Effect of various conditions of hypoxia on body size.

swelling rendered the data on embryos dead for more than one day meaningless. Since it was difficult to detect promptly the death of the younger embryos almost all of these were automatically eliminated. In effect the data below are limited to embryos which survived the treatment for at least 5 days. To facilitate comparison between embryos of different stages, all data are expressed as per cent of normal. Norms were established from control embryos at each stage between stages 28 to 38 (Hamburger and Hamilton, '51). To eliminate the effect of seasonal fluctuations new norms were calculated every three months.

The results were surprisingly uniform for all categories and all periods of treatment. Hypoxia had very little or no effect on average size or weight except at the most severe conditions for given exposure time. That is the only conditions in which hypoxia had any significant effect on weight or organ or body size are those which are virtually incompatible with any continued life. This is illustrated in figure 5 in which data for crown-rump length are plotted. A significant decrease in size was recorded only for the one or two low points at which survivors were first recorded. Precisely the same pattern was obtained for body weight and eye diameters. The size of the left eye lagged behind that of the right eye between 2 to 5% at the most, or not at all, and this was due to a sporadic severe effect on a few embryos and not to some effect on all embryos of the group.

There was a very slight decrease in average size for oxygen concentrations of less than 12% oxygen as against the size of embryos exposed to oxygen concentration of more than 12% (fig. 5). A closer examination of the data again shows that any decrease from the normal is not due to a slight effect on all embryos but the presence within the group of embryos affected to a considerable extent by the treatment. This can be seen in table 3 in which data is given on the diameter of the right eye of embryos treated with hypoxia for three hours. Examination of the column which gives the range of values for a given experiment shows that the highest figure in each case is always a little over 100% of normal but the low values may range from 0 to 89%. Again this pattern was consistent for all categories and conditions studied.

TABLE 3

Effect of hypoxia on the diameter of the right eye

O_2 conc.	No. of cases	Diameter	Range
0.0	5	33	101–0
1.1	12	79	107–0
2.1	32	100	109–83
4.2	42	96	103–75
6.3	43	98	103–69
8.4	46	101	110–89
10.5	48	99	111–86

Three-day embryos exposed to oxygen-deficient atmosphere for three hours. Eye diameter expressed as per cent of normal.

The conclusion is clear. Exposure to oxygen deficient atmospheres for as much as 24 hours has very little effect on body weight, on body size or organ size of the majority of the embryos so treated. Any decrease of the average value from normal is due to a few afflicted embryos, usually very badly malformed ones.

Comparison of vacuum and air nitrogen mixtures as a source of oxygen deficient atmospheres

In the present study two changes were made from the previous one (Grabowski and Paar '58). First the strain of White Leghorn was changed from Mount Hope to Darby. Secondly air nitrogen mixtures were used rather than partial vacuum to obtain oxygen deficient atmospheres. Extensive comparisons of both variables were made to see how the two experiments compare. Among the control embryos the kinds of malformations observed did not differ between the two strains except for a higher incidence of spontaneous rumplessness in the Darby strain of 3%. This anomaly alone accounted for the somewhat higher total incidence of spontaneous malformations in the Darby strain of 5.6% as against 2.5% in the Mount Hope White Leghorns. To compare the data on air-nitrogen mixtures at normal pressures with the previous studies in which a partial vacuum was used, 136 embryos of the Darby strain were also subjected to partial vacuum and the results compared with the Mount Hope data (see table 4). It

TABLE 4

Comparison of vacuum and air-nitrogen mixtures as sources of oxygen-deficient atmospheres

Oxygen	Total dead		Anomalies	
	Vacuum	Air/N	Vacuum	Air/N
%	%	%	%	%
3.4	70	60	28	21
6.3	50	32	30	35
9.3	21	12	1	23
12.2	17	10	9	10
15.3	8	10	13	5

All embryos exposed to hypoxia for 6 hours at three days. Vacuum data is an average of from 23 to 43 embryos per point. Data from air-nitrogen mixtures taken from figures 2 and 3.

can be readily seen that although the death rates in the vacuum experiments are somewhat higher the incidence of maldevelopment was comparable in the two experiments. The kinds of anomalies obtained in the two series also did not significantly differ except for rumplessness in the Darby strain. It was concluded therefore that the teratogenic effects of hypoxia induced by partial vacuum do not significantly differ from the teratogenic effects of hypoxia induced by air nitrogen mixtures at normal pressures.

DISCUSSION

There have been many studies which have clearly demonstrated that periods of fairly severe oxygen deficiency can affect the development of vertebrate embryos (see Grabowski and Paar '58 pp 313 to 315 for review) But there has been little quantitative comparison of the effects of graded degrees of hypoxia on embryos. The primary aim of this as well as the previous investigation was to explore many conditions of hypoxia and to determine those which can precipitate abnormal development and embryonic death. The earlier study explored the effects of oxygen concentration and age of embryo The results are briefly summarized in the introduction to this paper The present study extended these observations by introducing a third variable—time—by varying the duration of exposure to hypoxia as well as the oxygen level during the treatment. It was found again that regular relationships exist between the duration of exposure and oxygen level during treatment on one hand and death and abnormal development on the other These relationships can also be considered as patterns of response to varying conditions of hypoxia.

The basic pattern for any given age of embryo and time period of exposure can be summarized as follows. As oxygen is progressively restricted latent teratogenic and lethal ranges can be recognized Beyond the latent range both death rate and the incidence of maldevelopment rise exponentially The incidence of malformed embryos starts to decrease as the number of immediate dead rises rapidly above the 35% level. This basic pattern is affected by several factors. First sensitivity to hypoxia increases markedly with increasing age. Secondly the duration of exposure to hypoxia has the expected effect, namely increased exposure results in increased sensitivity However the effect of time is not always predictable, especially for long exposures because of what seems to be an adaptive phenomenon Furthermore it must be realized that qualitative differences can be superimposed over the above generalizations on the quantitative level. At least as far as the three-day embryo is concerned different degrees of hypoxia induce different kinds of malformations. Other studies now in progress indicate that this is true for other ages as well.

In short, it is clear that the effects of hypoxia on embryos are complex. An adequate picture can only be obtained by studying many different conditions rather than just a few It is also clear that all of the characteristics of the patterns of response that have been obtained must eventually be explained by any notions of

the mechanism of action of hypoxia on embryos.

The basic effects of hypoxia

When any two of the variables of these experiments namely age of embryo, oxygen concentration and duration of exposure are held constant the degree of hypoxia can be expressed quantitatively with respect to the remaining one. However when two are changed simultaneously different levels of hypoxia can only be subjectively compared as acute moderate or mild. It would be desirable to relate the data on death rates and abnormal development to some absolute measure of dosage of hypoxia comparable to roentgen unit of radiologists, which is independent of time Such a unit is not yet available. Test calculations based on the regularity of death rates between three to 12 hours show that there is some equivalence some basis for interchangeability between the two factors of oxygen concentration and time But this relationship is not simple and is not described in any detail here because its significance does not, as yet warrant the space. It will suffice to say at the moment that these calculations indicate that the rate of induction of hypoxia is important.

What is induced in embryos exposed to hypoxia is a toxic physiological state which in turn precipitates death and/or abnormal development. (See Grabowski and Paar '58 pp. 336 to 337) If the basis for this toxic state can be determined it may serve as a basis for an absolute measure of hypoxia. Studies of tissue oxygen levels during exposure to hypoxia and chemical changes in body fluids after exposure to hypoxia are in progress with this aim in mind The data described in this paper are serving as a guide for these studies since this toxic state must in some manner be related to the different death rates and kinds of abnormal development obtained after different exposures to hypoxia. The possibility that several different modes of action of hypoxia exist is also recognized in these further studies.

SUMMARY AND CONCLUSIONS

1 Over 2000 chick embryos, three days of age were exposed to atmospheres at normal pressures containing from 0 to 21% oxygen for periods of from three to 24 hours. Death rates and the incidence of abnormal development as well as measurements of body size and weight were recorded.

2. For each time period of exposure, as the oxygen concentration was progressively reduced, latent, teratogenic, and lethal ranges were observed. For exposures of 6 to 12 hours abnormal development was initially obtained at an oxygen level of 13% optimum maldevelopment (in up to 40% of the embryos) at about 5% oxygen, dropping to nothing at 2% oxygen because of the high death rate. For exposures to hypoxia of three hours duration abnormal development was obtained only at oxygen concentrations of 4% or less. Very little abnormal development was obtained after exposures of 24 hours. This is partly due to a high death rate at relatively high oxygen levels, partly to what appears to be a form of adaptation.

3. The rise in death rate is exponential as oxygen concentration is reduced. The curves are regularly arranged as exposure time is changed.

4. Quantitatively varying characters such as crown-rump length, body weight and eye diameter are not generally affected after hypoxia except after severe conditions of exposure.

5. Qualitatively different kinds of anomalies were obtained after different kinds of exposure to hypoxia. For instance short acute exposures induced complete malformation of the head moderate exposures predominantly affected individual structures of the head and trunk, but prolonged exposure to mild hypoxia induced mostly rumplessness. Since all of these different kinds of anomalies were obtained after exposure on the third day of incubation, the data suggest that different degrees of hypoxia can affect the embryo of a given age in different ways.

6. It is apparent that the effects of hypoxia upon embryos are complex. They can best be studied by examining many different conditions rather than just a few All of the characteristics of the patterns of response of embryos to hypoxia that have been obtained must eventually be ex

plained by theories of the modes of action of hypoxia on embryos. The survey data obtained also serves as a guide for such studies on the analysis of the mechanisms of action of hypoxia.

LITERATURE CITED

Grabowski, C. T 1959 Further studies of the teratogenic effects of graded doses of hypoxia on the chick embryo. Anat. Rec 133 281

——— 1960 Teratogenic significance of ocular difficulties induced by hypoxia in the hick embryo. Ibid., 136 200.

Grabowski, C. T and J. Paar 1958 The teratogenic effects of graded doses of hypoxia on the hick embryo. Am. J Anat., 103 313–346.

Hamburger V and H. Hamilton 1951 A series f normal stages in the development of the chick embryo. J Morph., 88 49–92.

Romanoff A. L. 1941 The study of the respiratory behavior of individual chicken embryos. J Cell. and Comp. Physiol., 18 199–214.

Visceral and Vascular Transposition in Fishes and a Comparison with Similar Anomalies in Man[1]

K. FRANCE BAKER-COHEN[2]
Genetics Laboratory New York Zoological Society and the Albert Einstein College of Medicine New York, N Y

Situs inversus viscerum is one of the anatomical anomalies that in man has attracted the greatest attention. The medical literature on this subject is immense. In animals the condition first was described by Aristotle (Linebeck, '20) but it has not received as much attention as in the human. Most of the animal examples reported have been found in double monsters and conjoined twins of natural or experimental origin

In fish, situs inversus has been described in single embryos, twins and double monsters from the same batches of eggs, of trout and salmon (Bovet, '31 Komai, '38 Lynn 46) and in double monsters of trout (Morrill, '19 Stockard '21 Swett, '21; Cropek, '50) Conjoined twins have been reported occasionally in live-bearing tropical aquarium fishes (e.g., Innes '33; Walker 48) but the internal anatomy was not examined.

In this report a high incidence of situs inversus in normal single individuals of a domesticated strain of the viviparous teleost, *Xiphophorus maculatus* the common platyfish, is described. Comparative figures on several other strains of platyfish are presented, as well as on two species of the swordtail—*X. montezumae* and *X. helleri*. Evidence with respect to the relation between situs inversus and twinning in platyfish is given. In addition, an inversion of the normal asymmetry of the vascular system is described and its incidence in the same strains of fish is compared with and related to that of situs inversus viscerum The genetic implications of the frequencies of both anatomical variations within the strains of fish are discussed.

MATERIALS AND METHODS

The origins of the strains of platyfish which figure in this report were given by Baker et al. ('55) and of the Montezumae swordtails by Baker ('59) The majority of the specimens were retained as serial sections from previous studies (Baker '58a, b; '59; Baker-Cohen, 60 '61) and these have been reexamined with respect to the anatomical features discussed here.

Platyfish

Fury strain. Forty-seven specimens (25 females and 22 males) were examined in serial sections. Their ages ranged from 22 days to over two years. These fish included normal young animals radioiodine treated young and adult fish potassium iodide-treated individuals with thyroid tumors in their kidneys, and fish with untreated renal thyroid tumors. In addition to these histologically prepared specimens 78 female and 107 male fish which had been preserved entire were grossly dissected for determination of visceral orientation. Eight of these females contained embryos in the ovary these were removed, freed of membranes and examined for evidence of twinning. Embryos from 6 females were in late stages of development the yolk of these was dissected away to reveal the viscera and thus demonstrate the asymmetry of the liver and gut.

BH strain. Serial sections of 303 specimens ranging in age from 30 days to over two years were examined. These included normal fish from the breeding stock, experimentally treated fish and their normal controls and animals with renal thyroid

---

[1] Supported by grant C-297 to Dr Myron Gordon from the National Cancer Institute of the U S. Public Health Service and by research fellowship CF-6184 to the author from the National Cancer Institute.

[2] Present address Department of Anatomy, Albert Einstein College of Medicine Bronx 61, New York.

tumors. Experimental fish had been treated with potassium iodide, thiourea, radioiodine or radiophosphorus.

30 strain. Sixteen fish were examined in serial sections. Five of these were radioiodine-treated young; the remainder were normal fish of various ages.

163 strain. Serial sections of 27 adult fish were examined. These included radioiodine-injected individuals and their normal broodmate controls and 5 specimens with thyroid tumors in their kidneys 20 females and 7 males made up the group.

Hp strain (Rio Hondo) Four wild-caught adult fish were examined in serial sections.

30 × *BH* hybrids. Ten fish were examined in serial sections—all had renal thyroid tumors.

30 × *Fury* hybrids. Thirty-two young mature fish (16 male, 16 female) from a single brood were grossly dissected for determination of visceral asymmetry

Swordtails

Montezuma swordtails (*X. montezumae*). Nineteen fish of various ages, including two embryos and 17 adults, were examined in serial sections. These all were untreated—some had cystic kidneys and many were goitrous.

Green swordtails (*X. helleri*) Twenty-four normal adult fish derived from three different wild populations were examined in serial sections. These groups were as follows: 3B—6 males, two females; *Cd*—4 males, 4 females; *Bx*—8 males. The wild ancestors of the *3B* and *Cd* lines were collected from the Arroyo Zacatispan and the Rio Papaloapan respectively Oaxaca, Mexico by Dr Myron Gordon, in 1939 The *Bx* line was derived from wild fish

TABLE 1

Visceral and venous asymmetry in laboratory platyfish and swordtails

Species and strain	Liver on left (normal)	Liver on right (inverted)	Per cent inverted	Inf. jug. v on left (inverted)	Inf. jug. v on right (normal)	Per cent of "minor variants"*
Platyfish						
BH	303	0	0	29	262	9 7
Fury	20	—		2	18	10.0
	—	18		13	5	27 7
	124	68		unknown		
Total	144	86	37 4			
163	25	—		2	20	16 0
	—	1		1	—	
	—	1		—	1	
Total	25	2	7 4			
30	13	—		2	13	20.0
	—	1		—	1	
Total	15	1	6.3			
Hp	4	0	0	0	4	
30 × Fury	32	0	0	unknown		
30 × BH	10	0	0	2	8	20.0
Swordtails						
Montezuma	19	0	0	2	14	12.5
Green						
3B	8	0	0	1	7	12 5
Cd	8	0	0	0	8	0
Bx	8	0	0	1	7	

*"Minor variants" include fish with normal visceral situs and inverted asymme the inferior jugular vein, and fish with situs inversus viscerum and normal asymme the vein (see text)

It is possible that this fish with situs inversus and a broodmate with the exception opposite asymmetry were rare pair of mirror image twins (see text)

caught in the Belize River British Honduras, in 1949 by Dr Gordon.

RESULTS

Situs inversus viscerum

The usual arrangement of the viscera in laboratory platyfish and swordtails is such that the liver lies to the fish s left side as viewed from the dorsum, with the intestinal coil to the right, the gall bladder between these and the air-bladder dorsocaudad to the viscera in the median plane (see fig 1 in Baker '58a) The liver position thus is opposite to that normally found in trout and salmon (Morrill, '19; Swett '21; Komai, '38; Lynn, 46) and in man.

As seen in table 1 the left-sided liver position, exclusively was found in speci mens of two strains of platyfish and of two species of swordtails. A single individual with the liver on the right side occurred in a third strain of platyfish, and two fish with right-sided livers were found in a 4th strain. It was, therefore, of considerable interest to find that in many individuals of the Fury strain of platyfish

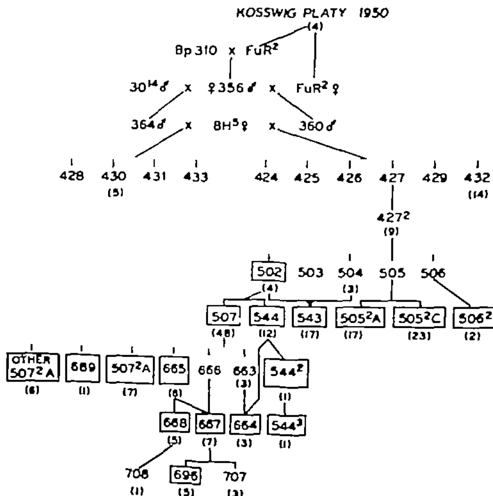


Fig 1 Pedigree chart, showing the occurrence of visceral inversion in the Fury strain of platyfish. The number of individuals examined is shown in parentheses under each mating number Matings in which situs inversus was found are enclosed in blocks. Unbranched lines of descent represent progenies of sibling matings.

the viscera were reversed from the normal pattern (figs. 5 6) Examination was made of 230 fish of this strain: 37% *of the specimens proved to have situs inversus viscerum* (table 1)

Pedigree and brood records were analyzed and the 230 fish arranged accordingly (fig 1 table 2) The pedigree chart shows that situs inversus first appeared in the third generation after an outcross to the *BH* strain of platyfish and thereafter it was found in nearly all matings. At first glance the differences in incidence *of the peculiarity between male and female* offspring of several matings suggested some form of sex-linkage. The known facts regarding sex determination and sex linkage in this strain may be summarized *briefly as follows (fig. 2) The sex chromosomal* constitution of the *Fury* strain was postulated to be WY = female and YY = male. The prominent black pigment pattern (fuliginosus) characterizing the strain (figs. 5 9) was known from crosses to be due to a single dominant gene, *Fu*, which was linked to the Y chromosome (Kosswig, '38 Gordon, '57) In our stock, females of two types were produced in *equal numbers, Fu and + (wild-type lack* ing strong black pigment) while the

TABLE 2

Situs inversus viscerum (S.I.V.) in the Fury strain of platyfish[1]

Mating number	Females examined	Males examined	Females with S.I.V	Males with S.I.V	Per cent with situs inversus	
					Females	Males
Kosswig platy	3	1	0	0		
430	—	5	—	0		
432	—	14	—	0		0
437^{3}	6	3	0	0		
502	1	3	0	3		
504	0	3	—	0		
505^{2} ( )	2	1	1	0		
*505^{2}A	16	1	3	0	21	
505^{2}C	15	8	7	0	50	0
506^{2}	0	2	—	2		
543 (502 × 504)	8	9	2	1	25	11
502^{4}	0	2	—	2		
544 (502^{1})	4	8	2	3		38
544	0	1	—	1		
544^{1}	0	1	—	1		
507 (502^{1})	22	28	9	19	41	68
507^{4}A	11	6	3	1	27	
507^{4}C	0	2	—	0		
663 (507^{6})	0	3	—	1		
665 (507^{6})	0	6	—	5		
669 (507^{6})	0	1	—	1		
507^{1}	1	3	1	1		
664 (544 × 663)	0	3	—	2		
668 (665^{1})	2	3	2	2		
708 (668^{1})	1	0	0	—		
667 (668 × 665)	1	6	1	5^{3}		
696 (667^{1})	0	5	—	2		
707 (667^{1})	2	1	0	0		
696, 707 708	4	0	3	—		
Pedigree unknown	2	0	1	—		
Total	101	129	35	51	35	40
Sexes combined	230		86		37	

[1] Incidence of situs inversus is given as per cent only for groups of 8 or more fish. Those matings which are starred ( ) are known to have been made up of single pair of fish; in matings 544 507^{4}A and 665 there were two female parents and one male, and in mating 543 there was one female and three males. In the remainder of the matings no records of the number of parents are available. Hence only in the starred matings are the ratios genetically meaningful.

[2] From the label on the vial containing these fish, it was impossible to tell whether they were 505^{2} or parents of 505^{2} mating. No date or brood number was attached.

[3] The male fish with normal situ here was a parent of mating 696.

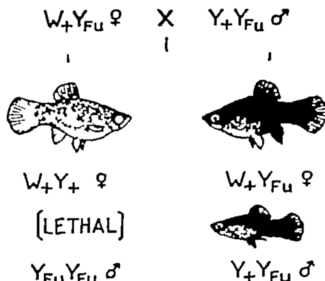


FIG. 2 Diagram showing the inheritance of the dominant sex-linked gene *Fu*, in strain *Fury* platyfish. In the heterozygous state the gene produced sooty black (or fuliginosus) coloration. In the homozygous state, it appeared to be neo-natal lethal (see text)

males were exclusively *Fu* and their numbers equaled only one-half of the total females. The + females routinely were discarded and all matings used in maintaining the strain were made up with *Fu* fish exclusively These and other observations led Gordon and Baker ('55) to hypothesize that the *Fu* gene was lethal in homozygotes and that only heterozygous males (Y Y) survived to maturity Females would be of the genotypes W Y or W Y_{Fu}.

Examination of the 35 *Fury* strain female fish with situs inversus revealed no evidence for association between the sex-linked color pattern and the visceral pattern (see figs. 2, 5) Eighteen of these females were of the + type, and 15 of the *Fu* with color unrecorded in two fish. Examination of all preserved females for color and visceral asymmetry led to similar results. Of the 47 *Fu* females 32% had situs inversus, and of the 47 + females 38% had situs inversus. The color of 7 females was unrecorded. When the entire group of strain *Fury* platyfish is considered the proportion of males and females with situs inversus compared with those with normal situs (situs solitus) was similar (females 35% males 40%)

As situs inversus has been associated with twinning by several authors (see Discussion) examination of embryos found in gravid females of the *Fury* strain was made. Ninety-six embryos at optic cup and later stages, were surveyed, and no sign of twins was found. The position of the liver and gut was determined by dissection of 55 of the oldest embryos and the relation to the direction of curling of the embryos on the yolk sac analyzed in 38 of these. The curling of the embryos was found to be equal in either direction (53% to the right) and no relation to visceral position appeared.

In table 3 the visceral asymmetry of 55 embryos is compared with that of their mothers. It may be seen that normality or reversal of asymmetry in the mother is not positively correlated with a similar asymmetry in her offspring The male parents of these embryos were broodmates of the mothers but were not individually identified. For this reason, visceral asymmetry in the father could not be investigated.

The specimens with situs inversus viscerum found in the *163* strain were both males, while the sex of the single exceptional fish of strain *30* was not known.

TABLE 2

Sinus inversus viscerum (S.I.V.) in Fury strain platyfish embryos and their mothers

	Pedigree of mother	Sinus of mother	Number of embryos	S.I.V. embryos Number	Per cent
1	507 brood 19	S.I.V.	28	16	57
2	507 brood 11	normal	10	7	70
3	505°C, brood 37 no. 1	S.I.V.	5	2	40
4	505°C, brood 37 no. 2	normal	3	1	33
5	505°C, brood 37 no. 3	S.I.V.	5	1	20
6	505°C, brood 37 no. 4	S.I.V.	4	1	25
	Total		55	28	51

Normal females 8/13 of embryos had S.I.V. (62%)
S.I.V. females 20/42 of embryos had S.I.V. (48%)

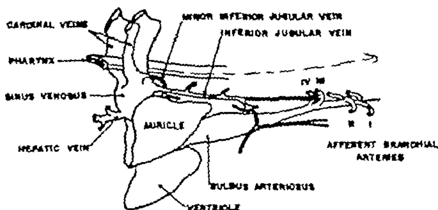


Fig. 3 Diagrammatic representation of some major blood vessels in the pharyngeal area of the platyfish. A minor inferior jugular vein is shown, as described in footnote 3. Ordinarily the inferior jugular was unpaired, and ppeared on the fishes right side as shown (redrawn after Baker '58a)

Venous asymmetry

As in other teleost fishes (Silvester '04) a normal asymmetry occurs in the venous drainage of the head region of platyfish and swordtails. Instead of a pair of veins a single inferior jugular vein is found which in most cases enters the right cardinal vein (figs. 3 7 8) It was noted by Baker ('58a) that in some specimens (7 out of 57 or 12.3%) of the BH strain of platyfish the inferior jugular vein entered the *left* cardinal. These observations now have been amplified and extended to other strains of platyfish and to two species of swordtails (table 1) It was found that, in most of the groups of fish examined between 10 and 20% of the individuals exhibited reversed asymmetry with respect to this feature The exceptions were Rio Hondo platyfish of which only sentatives were examined, and green swordtails, of which 8 fish were examined. The latter may represent random deviation from a ratio similar to that found in the other swordtails.

In some fish, there appeared to be two inferior jugular veins of unequal size. When the smaller vein was traced anteriorly in serial sections of several fish, it was found (1) to dwindle rapidly to a very minute vessel which could not be followed further; (2) to pass ventrally along the pericardium immediately anterior to the cardinal juncture and split into two small vessels in the lining of the pericardium and gill chamber (see fig. 3); or (3) to pass in dorsal direction into the pharyngeal musculature very little anterior to the cardinal juncture. Thus, this second vein never was found to be ... with the true inferior jugular veir ... ed large and extended far ... subpharyngeal area (fig. 3) The ... nt represent a vestigial remnant ... symmetry ... seen in lower fis ... shark— ... '30)

Among fish with situs inversus viscerum, the asymmetry of the inferior jugular vein usually also was reversed, so that, in most of these individuals it entered the left cardinal vein. Thus most of the fish with reversal of the abdominal viscera appeared to be complete mirror images of their normal fellows. As in normal fish however a smaller proportion of individuals showed (doubly) reversed asymmetry with respect to the inferior jugular vein (i.e., it entered the right cardinal vein, as in *normal* fish) Both of these lesser types of reversed asymmetry are henceforth called minor variants for convenience in this paper Minor variants were seen to be somewhat more common among fish with situs inversus viscerum than among fish with normal visceral situs (28% as compared with 10%)

Among young fish of one brood of the *30* strain were two individuals which might have been mirror image twins. One of these had normal visceral situs and reversal of the inferior jugular vein the other had situs inversus and normal asymmetry of the vein. The latter was the only case of situs inversus found in fish of the strain, and it seems doubly unusual that it should have been both a minor variant and a case of situs inversus. Unfortunately the young fish were not serially sectioned far enough caudally to include the gonads, so that identity of sex in the two fish could not be demonstrated. Three broodmates were normal with respect to both visceral and venous asymmetry as were 9 other fish of the strain.

Of the two fish with situs inversus in the *163* strain, one had normal asymmetry of the inferior jugular vein, and was thus a minor variant, while the other was fully reversed in asymmetry

Examination of the pedigrees of the 8 Fury strain fish with minor variant asymmetry showed little of interest. Two of these, both + females, from the same brood (mating 543) could have been mirror-image twins. Another pair of mirror imaging broodmates (mating 544) could not have been twins for although the same color they were of opposite sex. The other minor variant fish were from matings 507 507' and 696 707 708-pooled (see table 2). There were altogether 5 females and three males in the variant group

A pedigree chart for the *BH* strain, showing the distribution of minor variants is given in figure 4 The sex ratio among the 27 exceptional fish was 19 males to 8 females; only in three closely related matings were reversed females found In one line of descent the frequency of the anomaly dropped much lower than was seen in the parental generation and in two collateral lines. Among the latter groups the frequency varied from about one in 5 to one in 10 animals In the former group the frequency fell to about one in 40 animals. The higher frequencies are of the same order of magnitude as those found for minor variants in the other strains of platyfish and in the Montezuma, *3B* and *Bx* green swordtails (table 1)

DISCUSSION

Considerations on the mode of inheritance of situs inversus viscerum in Fury strain platyfish

Cytoplasmic (maternal) inheritance The lack of a positive correlation between the incidence of situs inversus in embryos and the visceral situs of the mother appears to exclude this possibility

Sex-linked inheritance Sex linkage is ruled out chiefly by the observation of equality in incidence of situs inversus viscerum between the two color types of females carrying, or lacking, the dominant sex linked marker Fu. It is also ruled out by the ratios seen in the two sexes when the data are compared with theoretical results of various simple genetic schemes as follows. In the first case the chromosomal pattern is assumed to be WY = female, and YY = male (as indicated by breeding tests) with no crossing-over between the W and Y chromosomes If then, the situs inversus gene (or genes) were on the W chromosome, whether recessive or dominant, all daughters would receive it, but no sons. If the gene were on the Y chromosome of the father and he were heterozygous, all daughters of one color type would receive it and none of the other type or if the father were homozygous 100% of the daughters would re-

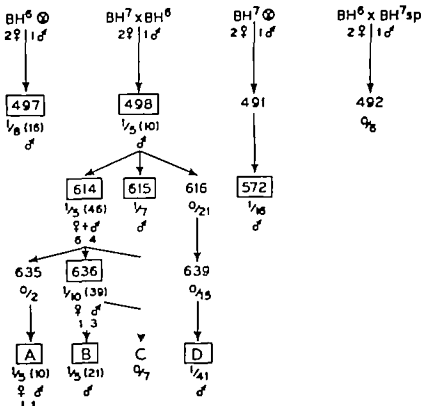


Fig. 4 Pedigree chart showing the appearance of inverted asymmetry of the inferior jugular vein ("minor variants") in strain *BH* platyfish. Matings in which the anomaly was found are enclosed in blocks. All progenies are from one sibling pair of parents unless otherwise noted on the chart. Fractional frequencies shown for each mating are reduced to a numerator of 1 over the nearest integral denominator. The full number of fish examined is given in parentheses where it differs from the latter Sex distribution is shown by ♀ ♂ ratios; ♂ equals all males.

ceive it. This also would be true whether the gene were dominant or recessive If the gene were on the mother's Y chromosome and dominant, 100% of the sons would show the trait but daughters would vary depending on the father; if recessive both daughters and sons could vary from 0 to 100% incidence depending on the father's constitution. In either case, the daughters could show incidences of only 0 100 or 50% with color linkage in the latter case. None of these hypothetical patterns was observed. In one mating no males were found with the character but the females did not approach 100% in incidence. Therefore the lack of males may have been fortuitous (only 8 of them were examined)

In the second case, if crossing-over between the W and Y chromosomes were assumed to have occurred partial sex-linkage would be found. However the ratios seen in most of the larger progenies, and that seen in the females speak against this also

The sex differences in the ratios of situs inversus to situs solitus which were seen in some matings therefore must have been due to factors other than sex-linkage. Among these factors variation in hormonal, growth or survival patterns or other genetic modifiers, perhaps some with sex linkage, might have been present. The latter was possible, as the strain was only partially inbred at the time. Similar ratios in the two sexes which occurred in several matings further support the probability of autosomal inheritance.

Autosomal inheritance No simple genetic scheme appears to fit the ratios seen

in the larger brood groups which were known to be from a single pair It seems significant, however that there was no evidence for the occurrence of any matings doubly homozygous for the situs inversus genes Nine matings (of which 4 definitely were known to have had a single pair of parents) in which 5 or more off spring were examined, showed none to have produced either 100% or 0% reversed offspring Of all 24 matings, 14 showed progeny of both types, 5 had only normal and 5 had only inverted offspring. But in the latter two categories, at most three progeny were examined per mating When the frequencies of the trait in the 6 sets of embryos (table 3) were considered for which the phenotype of the female parent was known hypothetical schemes for either single dominant or single recessive gene action showed that the only types of matings which could *not* have led to either 0% or 100% inverted offspring would be as follows:

A. Dominant single gene action
Ss ♀ (s.i.v.) × Ss or ss ♂
ss ♀ (normal) × Ss ♂

B Recessive single gene action:
ss ♀ (s.i.v.) × Ss ♂
Ss ♀ (normal) × Ss or ss ♂

Thus all dominant homozygotes would be excluded from the parentage

These two sets of observations suggested the occurrence of lethal activity of a dominant gene as was shown by the *Fu* gene in the strain. If lethality *were* involved, this would require dominance of the factor for situs inversus for if it were recessive, this would lead to the paradox of dominant homozygous lethality of the normal allele. An alternative possibility might be that reversed fish for an unknown reason, always chose normal fish to mate with although where single pairs were mated there was no choice offered. However wrongly mated pairs might have produced few or no young—many matings in this strain of platyfish were discarded for this reason.

The occurrence of modifying genes or differences in penetrance of the factor(s) for inversion may have led to the ratios which seemed to exclude homozygous dominance. Partial expression in heterozygotes or homozygotes for a single dominant gene could be fitted to the ratios of reversed embryos and the phenotypes of their mothers. Using this scheme parental homozygous dominance could have occurred. However the fact that no broods included more than 70% or especially less than 20% inverted individuals still seems difficult to reconcile with this type of genetic scheme.

Thus, the inheritance of visceral inversion in these fish seems by no means simple Without complete knowledge of the phenotypes of both parents and examination of a large number of offspring in a series of matings, the true manner of inheritance of the character will remain obscure It is to be regretted that since the fish included in this report were collected, the strain as a closed breeding population has been discontinued, and only the *Fu* gene survives in outcrossed descendants. It is unlikely that the factor(s) for situs inversus could easily be recovered, particularly if more than one gene were involved

The inheritance of venous asymmetry inversion in platyfish

Although features found in the pedigree analysis of the *BII* strain of platyfish suggested that genetic factors were operating in the production of the variant individuals rather than merely random environmental variations during development, the data are insufficient to permit the formulation of an hypothesis of the nature of such factors or their manner of action. Since the strain was true-breeding and its known dominant sex linked color pattern was shared by both sexes, it was of no utility to a genetic analysis of crosses within the strain, for a solution of the asymmetry problem. The differential between male and female incidence of minor variants, therefore, could not be simply resolved on such a basis. Without knowledge of the individual asymmetries of both parents in a series of crosses there is little hope of a solution to the problem

Unfortunately for this retrospective analysis, matings were often made up with two or occasionally even three sisters, and brother or cousin. Unless regular monthly broods, t different times of the month, occurred, the offspring of two or more females could not be distinguished.

of the inheritance of this anatomical peculiarity

Situs inversus viscerum — general considerations

Situs inversus has been associated with twinning since Förster (1861) upon consideration of the frequent visceral inversions seen in one member of human double monster pairs theorized that when inversion occurred in single individuals, the individual was in reality a member of a twin pair of which the normal member had been destroyed *in utero* In 1894 Bateson enunciated his theory that "homologous twins and double monsters, were derived from total or partial separation of the early blastomeres of a single fertilized egg and that for this reason the composite body might be expected to show an over-all bilateral symmetry These two authors have been credited with creation of the mirror image hypothesis in explanation of the origin of situs inversus viscerum. According to Aird ('54) 73% of human double monsters exhibit this kind of symmetry and Bovet ('31) gave almost exactly the same ratio for double fishes. The mirror image hypothesis gained support from embryological experiments of Spemann and his students ('19; '22) on the amphibian *Triton*. These investigators found that twins artificially induced by constriction of the early embryo often exhibited situs inversus viscerum in the right-hand member This and other evidence led many authors to reaffirm Förster's "lost twin" theory in which the missing member of the pair might have been resorbed or included as a possibly minute, teratomatous structure within its twin (Koller 1899 McMurrich, '13; Boeminghaus, '20 Stockard, '21)

This idea, although esthetically satisfying has little foundation in fact. Bateson (1894) from the outset noted that situs inversus was not ordinarily found in members of separate human twin pairs, and cited the fact that in Kuchenmeister's (1883) collection of 152 cases of situs inversus only one was a twin. He concluded that the loss of a twin could not be held responsible for cases of reversal of asymmetry In man, only 13 pairs of separate, probably monozygotic twins in which situs inversus viscerum occurred have accumulated in the literature since 1825 (table 4) In 9 of these pairs one member was inverted and in 5 pairs both members were; the latter pairs thus were not mirror images of each other Situs inversus viscerum was seen concordantly in one pair of dizygotic like-sexed twins (Torgersen, 48) and in one member each of two pairs of like-sexed twins of which the other member had died young — consequently neither visceral symmetry nor zygosity was established (Torgersen, 50) Isolated car

TABLE 4

Human twin pairs in which situs inversus totalis was reported

All pairs were like-sexed but good criteria for monozygosity were not always presented, particularly in the older reports.

	Author( )	Date	Sex of twins
	A. Discordant for situs inversus viscerum (mirror images)		
1	Baron	1828	Males
2.	Miller	1893	Unrecorded
3.	Dubreuil-Chambardel	1927	Males
4.	Araki	1935	Males
5	Cockayne	1939	Females
6.	Helweg-Larsen	1947	Males
7	Jeune and Confavreux	1948	Males
8.	Lowe and McKeown	1954	Males
	B. Concordant for situs inversus viscerum		
9	Reinhardt	1912	Males
10.	Pezzi and Carugati	1924	Males
11	Boccia and Maglione	1927	Males
12.	Cockayne	1938	Males
13.	Keen	1942	Females

diac inversion was reported discordantly in two pairs of dizygotic unlike-sexed twins by Doolittle ('07) The frequency of situs inversus viscerum was far below the normal incidence of twinning in large human populations, and the frequency of twins among established cases of situs inversus was no more than would be expected on the basis of chance association — 1 7% compared with a general twin frequency of 2.3–2.8% (Torgersen '50) In the identical quadruplets of the Texas armadillo *Dasypus novemcinctus* situs inversus does not occur (Newman, '16) In the platyfish described here there was no evidence for monozygotic twinning, either equal or with a deficient member Teratomatous included twins could not be excluded, but in histological examination of serial sections from head to tail of many fish no oddity which might have represented such an occurrence was seen.

Incidences of situs inversus viscerum in man, reported from many sources have ranged from 0 003 to 0 07% (table 5). The average frequency seems to be about 0 01% (or one in 10,000) This is very low when compared with the data available on fish (table 6) In normal single trout and salmon, and in single fish of two strains of platyfish, the incidence of situs inversus was about 5–8% although in one strain of platyfish the frequency was unknown as no inversions were found among 303 specimens (table 1) In the case of the hatchery fish (trout salmon) the high incidences occurred under environmental conditions which led to an outburst of double monstrosities. The frequency of situs inversus was markedly increased in deformed individuals in smaller members of twin pairs and in triplets. These figures point to a cause common to all the abnormalities, including double monsters. However the frequencies in normal single fish and normal twins still may have been due to inherent factors in the fish in view of the agreement with some of the platyfish figures. No data are available on situs inversus in adult trout or salmon of either hatchery fish or wild origin. Variation in the frequency of situs inversus in human populations was suggested by the data of Francisco and Ongpin ('36) They found incidences of one in 2500–3500 and suggested that special (unknown) factors might have been acting on embryological processes in the Philippine population to bring about much higher frequencies of situs inversus than those generally reported in European or North American populations. It indeed may be seen in table 5 that their percentages rank among the highest when referred radiographic examinations are omitted, and are 3–4 times as high as the over-all average Variation in the incidence of situs inversus in human populations also was discussed by Günther ('23) He quoted autopsy figures which suggested that the frequencies in Northern and Southern Germany differed with an almost complete absence of the anomaly in one area. More recently Torgersen ('49) noted a significant difference (0 02 and 0 007%) between the incidences of situs inversus in two counties of Norway based on mass radiography Additional variations in frequency between areas of Norway were recorded in a later paper (Torgersen '50)

In man situs inversus viscerum was suggested to be dependent on a single recessive gene by Feldman ('25 41) Dessylla and Monticelli ('31) further supported this hypothesis, and Cockayne ('38) amassed considerable evidence in favor of a single recessive mechanism in the inheritance of the anomaly This view was challenged by Torgersen ('49) after a more extensive investigation of a very large population Torgersen gave no explicit alternative but felt that full expression of a single recessive gene was incompatible with his data. In the mouse situs inversus was found to occur as a single recessive genetic trait, although a deficiency of 50% was noted in the offspring of doubly heterozygous matings (Tihen et al., 48) The latter was attributed to either prenatal mortality or to incomplete external expression of the character at birth (association with hydrocephalus, small and sickly appearance) In platyfish, the data are insufficient to derive an hypothesis as to the type of inheritance of situs inversus. It can only be stated that it appears to be autosomal, and that the factor (or factors) causing it, in all likelihood are not always fully expressed.

TABLE 5

The incidence of situs inversus totalis in man

Year	Author(s)	Source of figures	Reported incidence	Per cent
1905	Benda (in Kehr et al.)	Autopsies	2 in 10,000	0.02
?	Blodgett[3]	German army phys. exam.	2 in 20,000	0.01
1922	Sherk	*Mayo Clinic admissions from 1910*[3]	10 in 347,000	0.0029
1923	Günther	Clinical	5 in 63,377	0.0079
		Autopsies[4]	3 in 22,402	0.013
		Autopsies[4]	9 in 61,453	0.015
1925	LeWald	X-ray referrals[4]	29 in 40,000	0.072
		U.S. Army phys. exam.	1 in 35,000	0.0029
		Autopsies	1 in 5,000	0.02
		Dissecting room	1 in 10,000	0.01
1925	Willis	Hospital admissions	3 in 10,000	0.03
?	Bland-Sutton[3]	Abdominal operations	1 in 3,000	0.033
1926	Cleveland	Dissecting room	1 in 10,000	0.01
1926	Le Goff	X-ray examinations[4,5]	3 in 60,000	0.005
1928	Mandelstamm and Reinberg	X-ray examinations[4]	26 in 39,000	0.067
?	Verfasser[10]	Unknown	3 in 12,000	0.025
1936	Francisco and Ongpin	Mass radiography	32 in 126,858	0.025
		Autopsies	4 in 10,000	0.04
1937	Adams and Churchill	Hospital admissions (Mass. General from 1868)	23 in 232,112	0.0099
		Autopsies	1 in 8,000	0.013
1937	Sleur and Clenet	X-ray examinations[4]	30 in 280,000	0.011
1938	Cockayne	Clinical examination	20 in 476,402	0.004
		Mass radiography school children	5 in 97,877	0.005
		German autopsies[11]	14 in 124,830	0.011
1944	Prescott and Zollinger	Hospital admissions	3 in 15,374	0.0195
		X-ray examinations[4]	1 in 7,072	0.014
1945	Gould	Mass radiography[12]	40 in 442,253	0.009
1945	Parson	Private patients	2 in 15,000	0.013
1946	Caplan	U. S. Navy phys. exam.[13]	12 in 100,000	0.012
1949	Torgersen	Mass radiography[14]	195 in 1,500,000	0.013
1949	Blegen	Clinical examination	3 in 63,000	0.0048
		X-ray examinations[4]	5 in 50,000	0.01
		Mayo Clinic admissions	3 in 10,000	0.03
1949	Bell (in Blegen)	Autopsies	3 in 30,000	0.01
1950	Torgersen	Mass radiography	200 in 1,800,000	0.011
1951	Tanner-Cain and Crump	U. S. Army phys. exam.	1 in 35,000	0.003
		Hospital admissions	3 in 51,246	0.0059
1954	Lowe and McKeown	Mass radiography	13 in 95,362	0.014
Total			443 in 3,764,933	0.012
Total less x-ray examinations[4]			349 in 3,238,861	0.011

A few figures on the sex distribution of situs inversus viscerum in man showed rather striking differences between male and female. Kuchenmeister (1883) collected 152 cases of situs inversus from the literature. Of these 54% were male, 29% female and 17% of unknown sex. Francisco and Ongpin ('36) gave the sexes of 32 cases collected in a mass radiographic survey 21 of these were males, or 66% Of the human twin pairs of known sex in which situs inversus was found in one or both members 10 out of 12 were male pairs (table 4) These data appeared to suggest that situs inversus is more common in males, but figures collected by Torgersen ('49) did not indicate a sex difference. He found 90 males and 78 females among 168 cases of situs inversus (or 54 and 46% respectively) and stated that, as the chance of detecting the anomaly was somewhat greater in males, that the ratio was probably 1 1 In the *Fury* strain of platyfish, some brood ratios showed an excess of females with situs inversus one showed an excess of males and the remainder showed approximately equal sex distributions of the character As discussed above there was no evidence for sex linkage other possible conditions which might have been responsible for sex differences were not identified.

Situs inversus, as seen in platyfish bore one striking dissimilarity to the character as seen in man and mouse. There was no evidence for any association with other anatomical abnormalities in any of the fish showing this trait. In the mouse, as mentioned, hydrocephalus was characteristically associated, and the homozygous recessive animals did not live long. In man situs inversus often has been associated with bronchiectasis (Kartagener '33 '35 Adams and Churchill, '37) malformations of the heart (Leininger and Gibson, '50) and minor afflictions of the nasal tract (Kartagener '33) The first two associated anomalies often were lethal, although not necessarily before reproductive age. In man, situs inversus has also been related to reduced fertility (Arge '60) The latter is suggestive in relation to the platyfish results, for lack of fertility might help to explain the phenotypic ratios that suggested absence of doubly homozygous matings.

Table 5 footnotes

A complete tabulation is presented here, as the references to situs inversus incidence in man have been spotty and confused. The authors have regularly misquoted one another, and the selections of material cited have been hit or miss. It is hoped that this table will be complete and accurate synopsis of the material to date.

Given by Doolittle ('07) with no reference.

By hurried search of the records. This figure was quoted as from Counsellor by Troutt ('33) and thence by Francisco and Ongpin ('36) Neither gave a bibliographic citation.

These figures were quoted by Rösler with no reference to Günther They have since then been credited to Rösler by several authors.

Tabulated from 6 earlier (named) authors.

Since, as LaWald stated, many of the x-ray examinations were made on patients for confirmation of clinical diagnosis of situs inversus, and thus were biased sample, all x-ray examination figures other than for mass radiography are deducted from the definitive total. As may be seen, in the long run, this correction made little difference.

These two sets of figures may be the same, as LaWald did not mention the data in his text with his other personal figures, but inserted it in his table without comment. The closeness of publication years and the geographical proximity of the two authors suggests possible communication. One set of figures is therefore omitted from the total.

These figures were given by Bettman and Binswanger ('35) with no reference.

Referred to as de Goff" by Rösler and several other authors.

[10] This citation was given by Rösler with no reference

[11] Cockayne' clinical figure is omitted from the total because the terminal digits "402" are too suggestive of Günther's figures, although these data were on autopsies. Cockayne gave no source for this figure. For the latter reason, Cockayne figures on "German autopsies also is omitted from the total.

[12] These were cases of dextrocardia. Gould thought about half" had visceral transposition. The figures are omitted from the total, as isolated dextrocardia is not included here.

[13] These cases were found by 35 mm radiography Eight were further confirmed by more detailed radiography and 4 were not further studied.

[14] This figure is omitted from the total in favor of Torgersen's later total (1950)

TABLE 6

Situs inversus viscerum in single fish

Author date	Type of individual	Total fish	S I V I Number	S I V I Per cent	S I V P Number	S I V P Per cent	Per cent total S I V
Komai, '38	Normal singles	200	13	6.5	0	0	6.5
	Deformed singles	420	55	13.1	33	7.9	21.0
	Equal separate twin	350	15	4.3	10	2.9	7.2
	Unequal separate twins	152	11	7.3	4	2.7	10.0
	Total for twins	502	26	5.2	14	2.8	8.0
Lynn 46	Normal singles	510	11	2.2	13	2.5	4 7
	Spirally twisted singles	600	77	12 8	90	15.0	27.8
	Normal separate twins	231	7	3 0	13	5.6	8.6
	Unequal separate twins	130	12	9.2	25	19.2	28.4
	Total for twins	361	19	5.2	38	10.4	15.6
Lynn and Peadon, 49	Three separate triplets	15			4		26.7
Jo	Separate twins	34			13		38.2
	Strain 30 normal singles	16			1	6.3	0.3
	Strain 163 normal singles	27			2	7 4	7 4
	Strain Fury normal singles	230			86	37 4	37 4

us viscerum is designated as situs inversus imperfecti (S.I.V.I.) when incomplete and as situs inversus viscerum perfecti en complete.

a n — In twin viscera the total number of individuals, as in singles is given here and not total pairs as tabul ted by the origi al

I — ynn (46) as a st te in which the liver wa medio-ventral the gut straight and medial and the air bladder

not specified.

A number of investigators have concluded that there may be two types of situs inversus viscerum, a genetic and a rarer mirror image type (Cockayne, '39 Helweg Larsen, 47) The former would not be associated with twinning and would include dizygotic and probably most concordant monozygotic twin pairs; the latter discordant type would be exclusively a monozygotic twin phenomenon and a further stage in the type of doubling seen in symmetrical double monsters. The amount of mirror imaging would depend upon the embryological mechanics of the species and on the extent and timing of the doubling process (Helweg-Larsen, 47) Presumably the causes of this doubling would be environmental and accidental, and would more often be associated with other abnormalities. In the armadillo identical quadruplets, although no situs inversus occurs, external integumentary features show mirror imaging. Newman ('16) attributed this to the initiation of twinning in the ectoderm, with passive involvement of the endoderm at a later period, when new axes of symmetry had been established; the original bilateral symmetry of the blastodermic vesicle thus would be preserved only in ectodermal derivatives. In the platyfish described here, there is some evidence to suggest that the two types of situs inversus may have occurred. The rarer type resulting from the twinning process, may have appeared in the two broodmates of the 30 strain which showed complete mirror imaging with respect to one another The two inverted individuals found in the *163* strain might also have been so derived. These two strains had similar frequencies of the anomaly But in the *Fury* strain with its extremely high incidence of the anomaly and lack of evidence for associated twinning, there seems no question that the inversions were genetically determined, although the mode of inheritance appeared to be complex.

Reversed venous asymmetry — general considerations

As the heart of the platyfish is three-chambered and not grossly asymmetrical, dextrocardia, as seen in man (Caplan 46; Lowe and McKeown, '54) was not detected. However the asymmetry of the inferior jugular vein might have been taken to reveal that an analogous situation can occur in platyfish Using terms applied to man, specimens showing normal situs of the viscera and reversed asymmetry of the inferior jugular might have been classed as cases of "isolated dextrocardia, and those showing situs inversus viscerum and normal venous asymmetry might have been classified as having situs inversus imperfectus, or "isolated laevocardia."

This analogy must not be forced too far however for the appearance of the venous anomaly in the platyfish was found in relatively high frequencies in nearly all groups, including those with few or no cases of visceral inversion. On the other hand, in man both isolated dextrocardia and isolated laevocardia are far more rare than is total visceral inversion. Reinberg and Mandelstamm ('28) stressed the rarity of isolated dextrocardia, and Torgersen ('50) estimated a frequency of about 0 0001% for the anomaly Torgersen also expressed belief that isolated transposition of the viscera was probably as rare as isolated dextrocardia.

Cockayne ('38) suggested that partial transpositions in man might be inherited as alleles of the single recessive gene which he postulated as responsible for total situs inversus. Torgersen ('50) although disagreeing about the allelic and single gene nature of the hereditary factors felt that familial occurrences of both partial and complete inversions indicated their dependence upon the same factors, with prenatal selection as partly responsible for the rarity of partial inversions.

Not only is isolated dextrocardia more rare in man than total visceral transposition, but it frequently is characterized by gross anomalies of the heart, which cause death shortly after birth (Caplan, 46)

In view of these facts and since venous inversion occurred so frequently in normal platyfish and swordtails, it does not appear proper that a parallel be drawn between man and fish in this instance, either with respect to the genetic relationship to total visceral inversion or with respect to the anatomical relationship between the symmetries of the heart and greater vessels (i.e there is no evidence that the heart in

fish with venous inversion is *intrinsically* reversed) Visceral and venous inversion also appear to be independently inherited.

Isolated dextrocardia or analogous anomalies have not been reported in other animal species as far as the author is aware.

SUMMARY

1 Situs inversus viscerum, an anomaly which occurs in about one out of 10,000 human beings, was found in 37% of specimens of an inbred line of the domesticated *Fury* strain of the platyfish, *Xiphophorus maculatus* In 4 other strains of platyfish and in two species of the closely related swordtail, this anomaly proved to be infrequent or was not found.

2. Examination of unborn embryos of the *Fury* strain revealed no evidence for twinning in association with situs inversus or for a positive correlation between visceral situs of mother and offspring

3. The asymmetry of the unpaired inferior jugular vein, which occurs in fishes of the genus Xiphophorus, was found to be inverted in 10–20% of fish of nearly all strains of platyfish and swordtails examined. In fish with situs inversus viscerum, associated inversion of the venous asymmetry was found in most specimens (which thus were mirror images of their normal fellows in both respects) Again as in fish with normal visceral situs, about 10–20% showed relative inversion of the vein (or a double inversion—thus producing normal venous asymmetry)

4 Investigation of pedigrees led to the conclusion that both types of inversion were independently genetically determined, but in neither instance could a simple hypothesis for the mechanism of inheritance be fitted to the available data. Situs inversus viscerum in the *Fury* strain of platyfish, in which it chiefly appeared, was not sex-linked, nor was it maternally influenced. The indications were that it was due to autosomal gene(s) lacking full expression.

ACKNOWLEDGMENTS

The author wishes to thank Professor Ernst Scharrer and Dr L. J Smith Department of Anatomy Albert Einstein College of Medicine and Dr James W Atz, New York Zoological Society for critical reading of the manuscript.

Profound appreciation is due the Library Staff of Albert Einstein College of Medicine in particular Mrs. Florence Sturtz, whose diligent inter-library searches made it possible for the author personally to examine all references, a privilege denied to many earlier writers on the phenomenon of situs inversus.

Gratitude is expressed to Dr Goro Kikuchi, Tohoku University School of Medicine Sendai, Japan who supplied microfilms of the Araki paper and examined the journal source for the elimination of faulty references.

LITERATURE CITED

Adams, R., and E. D. Churchill 1937 Situs inversus, sinusitis, bronchiectasis. J Thoracic Surg., 7 206–217

Aird, I. 1954 The conjoined twins of Kano. Brit. Med. J., 1 831–837

Araki, R. 1935 Situs inversus viscerum totalis in monozygotic twins. Nagasaki Igakkai Zasshi, *13* 1691–1700 (in Japanese, with German summary).

Arge, E. 1960 Transposition of the viscera and sterility in men. The Lancet, I. 412–414.

Baker K. F 1958a Heterotopic thyroid tissues in fishes. I. The origin and development of heterotopic thyroid tissue in platyfish. J Morph., 103: 91–134

——— 1958b Heterotopic thyroid tissues in fishes. II. The effect of iodine and thiourea upon the development of heterotopic thyroid tissue in platyfish. J Exp. Zool., 138: 329–334.

——— 1959 Heterotopic thyroid tissues in fishes. III. Extrapharyngeal thyroid tissue in Montezuma swordtails, guppy and cherry barb. Zoologica, 44: 133–140.

Baker K. F O. Berg, A. Gorbman, R. F Nigrelli and M. Gordon 1955 Functional thyroid tumors in the kidneys of platyfish. Cancer Res., *15* 118–123.

Baker-Cohen, K. F 1960 Observations on the role of the thyroid in the development of platyfish Anat. Rec., 137 338 (abstract).

Baron (no init.) 1826 Transposition complète des viscères abdominaux et thorachiques. Arch. Gén. Med., *10* 131

——— 1828 Transposition complète des viscères abdominaux et thorachiques. Bull. Sci. Méd., *8* 132.

Bateson, W 1894 Materials for the Study of Variation. MacMillan Co., London.

Bettman, R. B., and H. F Binswanger 1926 Cholecystitis associated with situs transversus Am. J Med. Sci., 172 570–573.

Blegen, H. M. 1949 Surgery in situs inversus. Ann. Surg., *129* 244–259.

Boccia, D and R. Maglione 1927 Dos casos de situs inversus viscerum. Rev Sud-Amer Endocrinol., Buenos Aires, *10* 705–715.

Boenninghaus, H. 1920 Ueber Dickdarmanomalie bei Situs Inversus. Deutsche Ztschr. Chir., 155 174–189.
Bovet, D 1931 L orientation des viscères chez les truites doubles. Bull. Biol. France Belg., 65 216–233.
Caplan, S. M. 1946 Dextrocardia with situs inversus. Report of eight cases with a review of the literature on dextrocardia. Nav Med. Bull., Wash., 46 1011–1016.
Cleveland, M. 1926 Situs inversus viscerum. An anatomic study Arch. Surg., 13 343–368.
Cockayne, E. A. 1938 The genetics of transposition of the viscera. Quart. J Med., 31 479–493.
——— 1939 Transposition of the viscera and other reversals of symmetry in monozygotic twins. Biometrika, 31 287–294.
Czopek, J 1960 The structure of the compound monsters in the embryos of the Dunajec sea trout *Salmo trutta* L. and brown-trout *Salmo trutta f fario* L. Bull. Acad. Polonaise Sci. Lett., Ser. B II 1–11.
Desylla, C., and M. Monticelli 1931 Cardiopatie congenite in casi di destrocardia congenita con senza sterotassi. Riv Radiol. Fis. Med., 3 667–728.
Doolittle, W F 1907 Congenital dextrocardia. Boston Med. Surg. J 157 662–663.
Dubreuil-Chambardel, L. 1927 La dextrocardie chez les jumeaux. Presse Med 35 1157
Feldman, W M. 1925 Transposition of viscera behaving as Mendelian recessive character with congenital absence of the appendix. Proc Roy Soc. Med., 28 753–758.
——— 1941 The inheritance of congenital transposition of the viscera. Proc. 7th Int. Cong. Genet., Edinburgh, pp. 119–120.
Förster, A. 1861 Die Missbildungen des Menschen. Friedrich Mauke Jena (2nd ed., 1865 was seen, obtained from library of Columbia U College of Physicians and Surgeons)
Francisco, E. A., and C. Ongpin 1935 Situs inversus totalis case discovered by x-ray among Filipinos. J Philippine Islands Med. Assoc., 15 633–640
Gall, E. A., and V F Woolf 1934 Situs inversus viscerum totalis in siblings. Case reports. Ann. Int. Med., 7 1370–1375.
Gordon, M. 1957 Physiological genetics of fishes. In The Physiology of Fishes. M. E. Peters, ed. Academic Press, Inc., N Y vol. 2, pp. 431–501.
Gordon, M., and K F Baker 1955 Post-natal lethal gene in the platyfish *Xiphophorus maculatus*. Anat. Rec., 122 436–437
Gould, D. M. 1945 Non-tuberculous lesions found in mass x-ray surveys. J Am. Med. Assoc., 127 753–756.
Günther, H. 1923 Die biologische Bedeutung der Inversionen. Biol. Zbl., 43 175–213.
Helweg-Larsen, H. F 1947 Situs inversus in one monozygotic twin. Ann. Eugen 14 1–8
Innes, W T 1933 A case of twins. The Aquarium, 1 310.
Jeune, M., and J Contavreux 1948 Une paire de jumeaux monoamniotiques en miroir Arch. Franc. Pédiat., 5 250–256.
Kartagener M. 1933 Zur Pathogenese der Bronchiektasien. I. Bronchiektasien bei Situs viscerum inversus. Beitr. Klin. Tuberk., 83: 489–501.
Kartagener M., and A. Horlacher 1935 Zur Pathogenese der Bronchiektasien. V Situs viscerum inversus und Polyposis nasi in einem Falle familiärer Bronchiektasien. Ibid., 84 331–333.
Kehr H., H. Liebold and Neuling 1908 Drei Jahre Gallensteinchirurgie. J F Lehmanns, Munich, p. 332.
Koller, A. 1899 Ein Fall von Situs viscerum inversus und seine Deutung. Virchow's Arch., 156 116–150.
Komai, T 1938 Problem of situs inversus viscerum, as studied on single and duplicate salmon embryos. Mem. Coll. Sci. Kyoto Imp. Univ Ser B., 14 155–170.
Kosswig, C. 1938 Ueber einen neuen Farbcharakter des *Platypoecilus maculatus*. Istanbul Universitesi Fen Fakultesi Mecmuasi, 3 1–8.
Kuchenmeister F 1883 Die angeborne vollständige seitliche Verlagerung der Eingeweide des Menschen. J A. Barth, Leipzig (obtained from Yale Medical Library).
Leininger C. R., and S. Gibson 1950 Transposition of viscera in siblings. J Pediat. 37 195–200.
Le Goff (no init.) 1926 Présentation d'un cliché d'inversion totale des organes. Bull. Mém. Soc. Radiol. Méd. France, 14 21 22.
LeWald, L. T 1925 Complete transposition of the viscera. A report of 29 cases, with remarks on etiology J Am. Med. Assoc., 84 261 268.
Lineback, P E. 1920 An extraordinary case of situs inversus totalis. Ibid., 75 1775–1778.
Lowe C. R., and T McKeown 1954 An investigation of dextrocardia with and without transposition of abdominal viscera, with a report of case in one monozygotic twin. Ann. Eugen., 18 267–277
Lynn, W G. 1946 Situs inversus viscerum in conjoined twins of the brook trout. J Morph., 79 1–35.
Lynn, W G., and A. M. Pendon 1949 Situs inversus viscerum in conjoined triplets of the Brook trout. Ibid., 84: 411–426.
Mandelstamm, M., and S. Reinberg 1928 Die Dextrocardie. Ergebn. Inn. Med. Kinderheilk., 34 154–200.
McMurrich, J P 1913 The Development of the Human Body 4th ed. Blakiston Co., Philadelphia, p. 46.
Miller, N 1893 Ueber homologe Zwillinge Jb. Kinderheilk., 36. 333–343.
Morrill, C. V 1919 Symmetry reversal and mirror imaging in monstrous trout and comparison with similar conditions in human double monsters. Anat. Rec., 16 265–291
Newman, H. H. 1916 Heredity and organic symmetry in armadillo quadruplets. II. Mode of inheritance of double scutes and discussion of organic symmetry Biol. Bull., 30 173–209.

Parson, G. W 1945 Dextrocardia with situs inversus complicated by chronic rheumatic aortic and mitral endocarditis. Ann. Int. Med., 23 102–107

Pezzi, C., and L. Carugati 1934 Destrocardia transposizione viscerale (situs inversus) in due gemelli. Cuore e Circulazione, Rome, 8 361–368.

Prescott, M. U., and R. W Zollinger 1944 Appendicitis in situs inversus totalis. Am. J Surg., 64 288–290.

Quiring, D P 1950 Functional Anatomy of the Vertebrates. McGraw-Hill Book Co., New York.

Rainberg, S A., and M. E. Mandelstam 1926 On the various types of dextrocardia and their diagnostics. Radiology 11 240–249

Rainhardt (no init.) 1912 Ein Fall von Situs viscerum inversus totalis bei Zwillingen (Bakruten) Deutsche Militärärztl. Ztschr., 41 932–934

Rösler H. 1930 Beiträge zur Lehre von den angeborenen Herzfehlern. VI. Über die angeborene isolierte Rechslage des Herzens. Wiener Arch. Inn. Med., 19: 505–510.

Ruud, G., and H. Spemann 1922 Die Entwicklung isolierter dorsaler und lateraler Gastrulahälften von Triton taeniatus und alpestris ihre Regulation und Postgeneration. Arch. Entwmech. Org. 52 95–166.

Sherk, H. H. 1922 Total transposition of the viscera. Surg. Gyn. Obst., 35 53–57

Sleur, M., and E. Clauet 1937 Un cas exceptionnel d'hétérotaxie thoraco-abdominale J Radiol. Electrol., 21 313–314

Silvester C. F 1904 The blood-vascular system of the tilefish Lopholatilus chamaeleonticeps. Bull. Bur Fish., 24 87–114

Spemann, H., and H. Falkenberg 1919 Über asymmetrische Entwicklung und situs inversus Viscerum bei Zwillingen und Doppelbildungen. Arch. Entwmech. Org., 45 371–422.

Stockard, C. R. 1921 Developmental rate and structural expression an experimental study of twins, double monsters" and single deformities, and the interaction among embryonic organs during their origin and development. Am. J Anat., 28 115–277

Swett, F H. 1921 Situs inversus viscerum in double trout. Anat. Rec., 22: 183–199.

Tanner-Cain, N and E. P Crump 1951 Situs inversus. Report of three cases and a review of the literature. J Pediat., 38 199–207

Tihen, J A., D R. Charles and T O Sippel 1948 Inherited visceral inversion in mice. J Hered., 39 29–31.

Torgersen, J 1948 Concordant situs inversus in dizygotic twins. Ibid., 39 293–294

——— 1949 Genic factors in asymmetry and in the development and pathological changes of lungs, heart and abdominal organs. Arch. Path., 47 566–593.

——— 1950 Situs inversus, asymmetry and twinning. Am. J Human Genet., 2: 361–370.

Troutt, J M. 1933 Situs transversus viscerum. Report of case with cholelithiasis. Ann. Surg., 98 1109–1113.

Walker B. W 1948 Swordtail twins. The Aquarium J 19: 18–19

Willis, B C. 1925 Appendicitis and transposition of the viscera. Ann. Surg., 82: 256–259.

PLATE 1

EXPLANATION OF FIGURES

5 Four platyfish of the Fury strain, grossly dissected to show mirror imaging in the positions of the gut coil and liver Above are two Fu females, with the normal fish on the left below are two + females with the normal fish on the right. × 2.

6 Photomicrographs of cross sections of two sibling groups of platyfish of the Fury strain, showing variation in asymmetry of the liver and gut. These specimens were selected at random from larger groups preserved en masse and were embedded in paraffin blocks as groups. Sections were cut so that the fish are facing the observer Inverted specimens are marked by arrows. 6a Four males. × 6; 6b; Four females, × 7 Photos in figures 5 and 6 by Jay Walker, Albert Einstein College of Medicine.

7 Photomicrograph showing the inferior jugular vein (arrow) as it pproaches the cardinal vein in the pericardial lining. In this platyfish, the vein is surrounded by hypertrophied thyroid tissue The uricle of the heart shows at the bottom right of the photograph. In this specimen, the normal asymmetry of the inferior jugular vein occurs. × 140.

8 *Photomicrograph showing an unusual vascular variation in pl tyfish. In this speci*men, no distinct inferior jugular vein occurred, but network of small veins appeared in its place. Part of the uricle shows t the lower right. Much connective tissue appears around the small veins, which may be recognized by the nucleated red blood cells massed in them. × 100.

9 Male (above) and female (below) fish of the Fury strain of platyfish. × 1 Photo by Sam Dunton, New York Zoological Society


5
6a
6b
7
8
9

The Localization of Alkaline Phosphatase in Tissues of Mice Using the Electron Microscope[1]

SAM L. CLARK, Jr.
Department of Anatomy Washington University School of Medicine Saint Louis, Missouri

Alkaline phosphatase a widely distributed enzyme is concentrated in certain sites in animal cells where it may be demonstrated with the histochemical technique introduced simultaneously by Gomori and Takamatsu in 1939 (see the review by Roche '50) The relationships of substrate and pH to the cytological localization of the enzyme have received comprehensive study (for instance Dempsey and Deane 46 Neumann, 49) but it remains uncertain whether alkaline phosphatase is a single non-specific enzyme which will split a variety of phosphate esters, or several enzymes with individual avidities for substrates. There is general agreement that enzymatic activity is concentrated in brush borders, endothelia, and certain other places but sites of weaker reactions, such as nuclei, have a more doubtful significance (Chèvremont and Firket, '53) The histochemical localization of enzymatic activity depends upon two premises first, that under the conditions of the experiment, enzymatic activity is the only source of the observed product, and second, that neither the enzyme nor its reaction product has moved from the original site of the enzyme. These premises have been well-founded, in the case of Gomori's technique, by the careful experiments of Danielli (46) Gomori ('50) Leduc and Dempsey ('51) and others who have shown that the method localizes sites of strong activity accurately at the level of resolution of the light microscope.

The electron microscope offers the opportunity for greater resolution in histochemical localization, and with it, reactions attributed to alkaline phosphatase have been demonstrated by Brandes Zetterqvist and Sheldon ('56) and by Mölbert, Duspiva and von Deimling ('60) The former investigators reported a reaction in the brush border of the small intestine and the latter group studying the kidney described a reaction in the cell membranes of tubular glomerular and endothelial cells. The strong reaction characteristic of the brush border in proximal tubular cells was shown to lie in the cell membranes covering the microvilli, and thus to be comparable to the reaction found in other cell membranes. Both groups of workers used modifications of Gomori's technique in which blocks of tissue after brief fixation, were incubated with substrate in a buffered solution containing calcium or lead ions to precipitate with the phosphate ions released by enzymatic activity Subsequently the tissue was fixed again, embedded and sectioned for electron microscopy In both these studies the reaction was attributed to the action of alkaline phosphatase because it did not appear in tissues incubated without substrate. As additional evidence Brandes et al. ('56) stated that the reaction could be prevented by adding cyanide to the incubation medium. Neither group tested the accuracy of localization. In the experiments to be described, the technique of Mölbert et al. ('60) was applied to several tissues and variations in the technique were introduced to explore the questions of specificity and accuracy in localization of the enzyme.

MATERIALS AND METHODS

Tissues from 34 Swiss albino mice, varying in age from two days to 6 months, were cut into blocks one or two millimeters

[1] This work was supported in part by grants BG-3784 and RG-7176(C1) from the National Institutes of Health, United States Public Health Service

This work was performed during the tenure of Senior Fellowship of the National Institutes of Health, United States Public Health Service.

on a slide and fixed at 0 C in W C. Bauer's mixture (personal communication '60) of a 1% solution of osmium tetroxide buffered to pH 7 4 in a balanced salt solution designed for tissue culture (White '54) This solution contained all the ingredients specified by White except ferric nitrate. Following fixation for a period varying from three to 60 minutes the tissue was washed 5 or 10 minutes at room temperature in 0 05 molar tris (2 amino-2-(hydroxymethyl)-1,3-propanediol) buffer at pH 7 6 and shaken gently at room temperature for two to 60 minutes in a modification of the incubation medium used by Mölbert et al. ('60) In this medium the potassium sodium tartrate was increased to 2.7 gm of the hydrated salt per 45 ml of buffer in *order to keep the lead more completely* in solution. The mixture was made immediately before use from the specified quantities of the following stock solutions:

2.7 gm of potassium sodium tartrate (4 H_2O);
45.0 ml of 0.05 M tris buffer pH 7.6;
5.0 ml of 0.04 M substrate solution;
1.0 ml each of 2% solutions of manganese chloride and magnesium chloride, calculated as the anhydrous salts;
2.5 ml of 0.1 M lead nitrate added last of all, dropwise.

Three substrates were used: disodium phenyl phosphate disodium para-nitrophenyl phosphate, and sodium β-glycerophosphate. Following incubation, the tissues were fixed for another hour either at 0 or at room temperature dehydrated rapidly in a graded series of ethanol-water mixtures, embedded in a mixture of methyl and n-butyl methacrylate polymerized by heat after the addition of benzoyl peroxide sectioned with a Porter Blum microtome (Servall) using glass knives and examined both by phase contrast microscopy and in an RCA EMU 2E electron microscope. Control preparations consisted of companion blocks of tissue treated in exactly the same way except for the omission of substrate from the incubation medium. Using disodium para-nitrophenyl phosphate as substrate the release of nitrophenol into the medium during incubation was measured by the technique of Bessey Lowry and Brock (46) as an indication of phosphatase activity

RESULTS

Granular deposits similar to those described by Mölbert et al. ('60) were seen in electron micrographs of all the tissues studied, including small intestine trachea, diaphragm, and the fimbria of the oviduct. Deposits were found only in tissues incubated with a substrate whereas companion tissues treated identically except for the omission of substrate from the incubation medium had none (figs. 1 2) If tissues were transferred directly from fixative to control incubation medium without washing first, weak reactions did develop but with the standard procedure there were no reactions attributable to a direct interaction of the tissue with lead. By phase contrast microscopy a reaction to incubation with substrate could be detected only in the brush border of the small intestine but in electron micrographs deposits were seen regularly in cell membranes in membranes bounding some cytoplasmic vesicles in the sarcoplasmic reticulum of skeletal muscle and in centrioles basal bodies and cilia. Reactions were most intense at the surfaces of blocks of tissue and could not be detected more than about 100 μ beneath the surface. Diffuse deposits were found in both nuclei and cytoplasm of most cells in this peripheral region of intense reaction, but deeper in the tissue deposits were confined to the discrete localizations listed above.

The manner of fixation prior to incubation was not critical within certain limits. Fixation at 0 C in osmium tetroxide dissolved in veronal-acetate buffer (Palade, '52) or in 0 4 to 4 0% formaldehyde in White's balanced salt solution ('54) both allowed reactions to be obtained similar to those already described although the reaction seemed less intense after formaldehyde fixation. Fixation in osmium tetroxide in balanced salt solution at 0 C for as little as three minutes or as long as an hour produced comparable results, except that the longer fixation led to a more coarsely granular reaction which extended farther into the tissue and very short fixation allowed some leaching and disintegration of cells near the surface of the block.

Two fundamental questions of interpretation arise anew at the level of resolution of the electron microscope and attempts

have been made to answer them. The first question, that of whether the reaction is solely the product of enzymatic activity can be affirmed with reasonable certainty from the following considerations and observations. First, the reaction is most intense in the brush border of the small intestine where alkaline phosphatase is known to reside. Second the reaction was produced equally well by each of the three substrates, but was absent from control preparations indicating that the deposits were not produced by the interaction of tissue directly with lead salts. Third, the intensity of the reaction was roughly proportional to the duration of incubation, as one would expect an enzymatic reaction to be Fourth, varying the pH of the incubating medium between 7.3 and 9.0 did not alter the intensity or localization of the reaction although signs of cellular disintegration were observed in tissues incubated at pH 8.5 or 9 0 Finally using disodium para-nitrophenyl phosphate as substrate the release of nitrophenol into the medium during incubation of tissue was demonstrated and the quantity of nitrophenol released was found to be roughly proportional to the duration of incubation. Prolongation of pre-fixation to an hour reduced the amount of nitrophenol released to approximately one-third of that released by tissue fixed for three minutes but it did not abolish either the release of nitrophenol or the histochemical reaction. Placing the tissue in boiling water for one minute prior to incubation did abolish the release of nitrophenol and prevented the development of a reaction visible in the electron microscope, although the structure of the tissue was still recognizable (fig. 5) The addition of potassium cyanide to the incubation medium in concentrations as high as 0.1 M partially inhibited the release of nitrophenol and likewise diminished but did not alter the localization of the histochemical reaction. However such high concentrations probably form complexes with lead salts, so that inhibition of the precipitation of lead phosphate may have been responsible for the reduction in the histochemical reaction. Nevertheless, taken altogether this evidence seems sufficient to assert that the reactions observed were the result of the activity of a phosphatase capable of acting at an alkaline pH.

The second question, whether the location of the deposits represents an accurate localization of the enzyme or merely preferential sites for the precipitation of lead phosphate is not so easy to answer In an attempt to precipitate lead phosphate by non-enzymatic means tissues were soaked 5 minutes in 0 02 M disodium phosphate prior to incubation in medium lacking substrate. A precipitate appeared on the surface of the tissue but none could be detected in relation to any cellular structures. This negative evidence fails to answer the question, and the most that can be said is that the reproducibility and sharp localization of the reaction make it seem likely that the enzyme is not far away

Discrete reactions were found in two classes of structures, namely membranes and centriolar derivatives. Here is a more detailed description of them

The reaction in the brush border of the small intestine was located in the cell membrane covering the microvilli, and in the intervening extracellular space but the extracellular deposits were confined to regions of intense reaction near the surface of the block (figs 3 4 6, 7) The reaction in the membrane consisting often of a single row of granules, extended around the entire circumference of the cell and along small tubular invaginations of the apical cell membrane into the subcuticular region (figs. 4 6 7 8 9) The exact position of the row of granules in relation to the osmiophilic components of the cell membrane was not determined. A similar reaction was found in the cell membrane of every cell observed in regions where a reaction was present at all, including all of the types of epithelial cells in the small intestine (figs. 3, 4 8 9 10) tracheal epithelial cells (fig. 20) oviductal epithelium, erythrocytes (fig. 12) blood vascular and lymphatic endothelial cells (figs. 12, 13) smooth and skeletal muscle cells (figs. 12, 14 15 16) mesothelium (fig. 15) neurons in myenteric ganglia, Schwann cells (fig 12) and several varieties of connective tissue cells.

Small cytoplasmic vesicles with reactive bounding membranes were observed

in a wide variety of cellular types but particularly in the subcuticular region of intestinal absorptive cells (figs. 6 7) just beneath the cell membranes of smooth muscle (figs. 12, 14 15) in mesothelial cells (fig. 15) and in endothelial cells (figs. 12, 15)

The characteristic reaction in the Golgi region of intestinal absorptive cells stained by Gomori's technique was not found in the present study The elements of the Golgi complex were consistently free of reaction, even though nearby cell membranes reacted strongly (fig. 8) Occasionally small dense reactive bodies were found in the supranuclear region, but not with enough frequency to account for the reaction produced by Gomori's technique.

In striated muscle of the diaphragm, a reaction was found in the region between myofibrils occupied by the sarcoplasmic reticulum and was particularly heavy at the level of the I band where the specialized triad of the sarcoplasmic reticulum lies (fig. 16) (Porter and Palade, '57)

A reaction was observed in the centrioles of eosinophils in the small intestine (figs. 17 18 19) and in the basal bodies and cilia of tracheal and oviductal epithelium (figs. 20 21 22). In all of these structures the deposits were found in the region of the internal filaments, although an exact relationship was not established.

Of the diffuse cytoplasmic and nuclear reactions found near the surface of the tissue, that in the cytoplasm of smooth muscle was most intense and was found at a greater depth in the block than other diffuse reactions. The subcuticular region of intestinal absorptive cells likewise reacted more intensely than neighboring cytoplasm (figs. 4 6) The significance of these reactions is difficult to assess, because the diffuse nature of the deposits may be only the result of the diffusion of enzyme or reaction product, or it may truly represent a dispersed arrangement of the enzyme

DISCUSSION

The reaction seen in electron micrographs is reproducible both in these experiments and in comparison with the experience of Mölbert et al. ('60) It is absent from control preparations incubated without substrate, and is thus attributable to the action of a phosphatase. It will be discussed in terms of three ideas the identity of the enzyme the significance of the histochemical localization, and the functional roles of phosphatases in cells.

The phosphatase studied here resembles in several ways the alkaline phosphomonoesterase (non-specific alkaline phosphatase) studied so extensively with Gomori's technique. It appears to lack specificity in that it reacted similarly with each of the three substrates. It reacted well at pH values ranging from 7.3 to 9.0 but the participation of acid phosphatase in the reaction has not been ruled out by incubating tissues in acid media. The enzyme also resembles alkaline phosphatase in its tolerance to prolonged fixation (Danielli, 46). Heavy reactions in brush borders and endothelia are characteristic of alkaline phosphatase, but the failure of the Golgi apparatus of intestinal absorptive cells to react is not. This difference may be only quantitative however because the reaction in the Golgi region takes longer to appear using Gomori's technique, than does that in the brush border (Dempsey and Deane, 46)

The cytological localizations of the other phosphatases which have been studied also bear some resemblance to those reported here. Acid phosphatase has been localized to the brush border of the intestine (Sheldon, Zetterqvist and Brandes, '55) and to small bodies perhaps pinocytosis vacuoles, near the surface membrane of an ameba (Birns, '60) Glucose-1-phosphatase activity has been demonstrated in cell membranes, as well as in mitochondria and some small dense bodies in cardiac muscle (von Deimling, Mölbert and Duspiva, '60) and 5-nucleotidase activity has been found in the cell membranes of hepatic parenchymal cells (Essner Novikoff and Masek, '58) Reactions attributed to adenosinetriphosphatase have been observed in cell membranes of both renal and hepatic cells (Spater Novikoff and Masek, '59 Kaplan and Novikoff '59 Essner Novikoff and Masek, '58) and have also been found within cilia (Gersh '59 Lansing and Lamy '61) Therefore some of the reactions observed in the present study may have been the result of the splitting of

simple phosphate esters by one of the more specific enzymes cited above or contrariwise, reactions reported by previous investigators may be attributable to a non-specific alkaline phosphatase acting on the substrates they used. Indeed Tosteson has observed that alkaline phosphatase isolated from hog intestine possesses adenosinetriphosphatase activity in proportion to its phosphomonoesterase activity (J. C. Tosteson, personal communication). However observations in this field are still too fragmentary for final conclusions to be drawn concerning the identity of the enzyme or enzymes active in the present experiments.

There is no direct evidence that the submicroscopic localization of alkaline phosphatase indicated by these experiments is accurate nor is it possible to state whether the diffuse deposits observed near the surface of the tissue represent dispersed sites of relatively weak reaction or artifacts of diffusion. Until experiments are designed to settle these uncertainties—and this would appear to require identification of the enzyme in situ with a fastidiousness different in magnitude from that used to establish the accuracy of Gomori's technique—it should be profitable to proceed on the assumption that the discrete sites of reaction described above accurately locate the enzyme. In this way other tissues may be explored, but the most interesting information should come from observing situations in which phosphatase activity is known to change dramatically in response to physiological or pathological influences. Such an instance was examined as a corollary to the present study. In mice, the alkaline phosphatase of the small intestine increases from low to adult levels of activity during the third week after birth (Moog, '58). Coincidentally the absorptive cells lose the ability to ingest proteins and colloids (Clark, '59). However a reaction attributable to phosphatase, though less intense than that in adult animals, was found in the same locations in the intestines of mice varying in age from two to 12 days as it was in adults (figs. 3, 6, 9, 10, 17, 19). One of the chief limitations of this histochemical technique in such problems, as pointed out by Mölbert et al. ('60), is the crudeness with which quantitative estimations of activity must be made. Nevertheless, it offers such high spatial resolution as to make it a promising adjunct to other methods.

With the foregoing qualifications, it appears that alkaline phosphatase activity may be a general property of cell membranes, some cytoplasmic membranes, and centrioles and their derivatives. Here is a speculative attempt to relate these findings to the function of the enzyme in cells. First, each of the sites of discrete reaction has been implicated directly or indirectly in movement. Cell membranes and cilia have been observed in action. Centrioles participate in mitosis. It is suspected that the small vesicles seen near the surfaces of cells are the product of pinocytosis, and the small vesicles in endothelial cells have been implicated in the movement of materials across vessel walls (Palade, '56). The sarcoplasmic reticulum of striated muscle has been suggested as the agent which conducts the action potential from the surface of the muscle cell to the region of the myofibrils, thus initiating movement (Porter and Palade, '57). Second, the splitting of adenosinetriphosphate by a phosphatase has been implicated as a means of transducing energy for movement in striated muscle (Mommaerts, '51), in cilia (Brokaw, '61) and in the movement of ions across the membrane of the erythrocyte (Post, Merritt, Kinsolving and Albright, '60; Tosteson, Moulton and Blaustein, '60). Perhaps, then, alkaline phosphatase functions in some comparable way in the transduction of energy for movement. For instance it might serve in transphosphorylations involved in the mutability of membranes which contain phospholipids.

SUMMARY

A reaction attributable to the action of alkaline phosphatase has been observed by electron microscopy in a variety of tissues from mice. It is localized in the cell membranes of all types of cells studied, in small vesicles near the surfaces of some cells such as intestinal absorptive cells, smooth muscle cells and endothelial cells, in the sarcoplasmic reticulum of skeletal muscle and in centrioles, basal bodies and cilia. Evidence is brought forward to

support the contention that the reaction is due to the activity of a phosphatase acting at an alkaline pH, and the problem of determining the accuracy with which the localization of the reaction represents the actual site of the enzyme is discussed

LITERATURE CITED

Bessey O A., O. H. Lowry and M. J Brock 1946 A method for the rapid determination of alkaline phosphatase with 5 cubic millimeters of serum. J Biol. Chem., *164* 321–329

Bitns, M. 1960 The localization of acid phosphatase activity in the ameba, *Chaos chaos*. Exp. Cell Res., 20 203–205.

Brandes D H. Zetterqvist and H. Sheldon 1956 Histochemical techniques for electron microscopy alkaline phosphatase. Nature, *177* 382–383.

Brokaw C. J 1961 Movement and nucleoside polyphosphatase activity of isolated flagella from *Polytoma uvella*, Exp. Cell Res., *22*: 151–162.

Chèvremont, M., and H. Firket 1953 Alkaline phosphatase of the nucleus. Internat. Rev Cytol., *2* 261–288.

Clark, S. L., J 1959 The ingestion of proteins and colloidal materials by columnar absorptive cells of the small intestine in suckling rats and mice. J Biophys. Biochem. Cytol., *5* 41–50.

Danielli, J F 1946 A critical study of techniques for determining the cytological position of alkaline phosphatase. J Exp. Biol., *22*: 110–117

Dempsey E. W and H. W Deane 1946 The cytological localization, substrate specificity and pH optima of phosphatases in the duodenum of the mouse. J Cell. and Comp Physiol., *27* 159–179.

Essner E., A. B. Novikoff and B Masek 1958 Adenosinetriphosphatase and 5-nucleotidase activities in the plasma membrane of liver cells as revealed by electron microscopy J Biophys. Biochem. Cytol., *4* 711–716.

Gersh I. 1959 Some cytochemical studies with the electron microscope. In A Symposium on Molecular Biology R. E. Zirkle, ed. The University of Chicago Press, Chicago pp 230–247

Gomori, G. 1939 Microtechnical demonstration of phosphatase in tissue sections. Proc. Soc. Exp. Biol. Med., *42*: 23–26.

——— 1950 Sources of error in enzymatic histochemistry J Lab. Clin. Med., *35* 802–809

Kaplan, S. E., and A. B Novikoff 1959 The localization of adenosinetriphosphatase activity in rat kidney electron microscopic examination of reaction product in formol-calcium fixed frozen section. J Histochem. Cytochem., *7* 295–296.

Lansing, A. L, and F Lamy 1961 Fine structure of rotifer cilia. Anat. Rec., *139* 248.

Leduc, E. H., and E. W Dempsey 1951 Activation and diffusion as factors influencing the reliability of the histochemical method for alkaline phosphatase. J Anat., *85* 305–315.

Mölbert, E., F Duspiva and O von Deimling 1960a Die histochemische Lokalisation der Phosphatase in der Tubulusepithelzelle der Mäuseniere im elektronenmikroskopischen Bild. Z. Histochem., *2*: 5–22.

——— 1960b The demonstration of alkaline phosphatase in the electron microscope. J Biophys. Biochem. Cytol., *7* 387–390.

Mommaerts, W F H M. 1951 Phosphate metabolism in the activity of skeletal and cardiac muscle. In Phosphorus Metabolism, A Symposium on the Role of Phosphorus in the Metabolism of Plants and Animals. W D. McElroy and B. Glass, eds. The Johns Hopkins Press, Baltimore, vol. 1 pp. 551–568.

Moog, F 1958 The development of function in the adrenal cortex. In Comparative Endocrinology A. Gorbman, ed. John Wiley and Sons, Inc., New York, pp. 624–638

Neumann H. 1949 Dependence of the pH optimum of the phosphomonoesterase I on the substrate concentration and on inhibitors and activators. Biochem. Biophys. Acta, *3* 117–124.

Palade G. E. 1952 A study of fixation for electron microscopy J Exp. Med., *95* 285–298.

——— 1956 The endoplasmic reticulum. J Biophys. Biochem. Cytol., *2*: suppl. 85–98.

Porter K. R., and G. E. Palade 1957 Studies on the endoplasmic reticulum. III. Its form and distribution in striated muscle cells. J. Biophys. Biochem. Cytol., *3* 269–300.

Post, R. L., C. R. Merritt, C. R. Kinsolving and C. D Albright 1960 Membrane adenosine triphosphatase as participant in the active transport of sodium and potassium in the human erythrocyte. J Biol. Chem., *235* 1796–1802.

Roche, J 1950 Phosphatases. In The enzymes, chemistry and mechanism of action. J B. Sumner and K. Myrbäck, eds. Academic Press, Inc., New York, vol. 1, pp 473–510.

Sheldon, H H. Zetterqvist and D. Brandes 1955 Histochemical reactions for electron microscopy acid phosphatase. Exp. Cell Res., *9* 592–596.

Spater H. W A. B. Novikoff and B. Masek 1958 Adenosinetriphosphatase activity in the cell membranes of kidney tubule cells. J Biophys. Biochem. Cytol., *4* 765–770.

Takamatsu, H. 1939 Histologische und biochemische Studien über die Phosphatase (I. Mitteil ng) Histochemische Untersuchungsmethodik der Phosphatase und deren Verteilung in verschiedenen Organen und Geweben. Tr Soc. Path. Jap., *29* 492–498.

Tosteson, D. C., R. H. Moulton and M. Blaustein 1960 An enzymatic basis for the difference in active cation transport in two genetic types of sheep red cells. Fed. Proc., *19* 128.

von Deimling O., E. Mölbert and F Duspiva 1960 Elektronenmikroskopischer Nachweis eines Glucose-1-phosphat spaltenden Enzymes im Herzmuskel der Albinoratte, Beiträge Path. Anat., *123* 127–143

White, P R. 1954 The Cultivation of Animal and Plant Cells. The Ronald Press Co., New York, 1954 p. 90.

PLATES

PLATE 1

EXPLANATION OF FIGURES

All figures are electron micrographs of thin sections of tissues fixed three to 5 minutes and prepared according to the standard procedure described in Materials and Methods. Except where noted, they were obtained from mice between two and 6 months of age.

1 A control preparation of duodenum incubated 30 minutes at pH 8.6 in the absence of substrate. This section, taken near the end of a villus, includes several absorptive cells and a lymphoid cell (L) within the epithelium. The preservation of cytological structure is comparable to that obtained with the usual method of fixation in osmium tetroxide for electron microscopy indicating that incubation under the conditions of these experiments has not been seriously detrimental. The brush border (B) of the bsorptive cells consists of an orderly arrangement of microvilli. The apical cytoplasm is divided into three regions, subcuticular region (S) containing few organelles large intermediate region containing numerous mitochondria, and supranuclear region with prominent Golgi complex (G) Beneath the nucleus (N) is another prominent collection of mitochondria. (I, I intercellular spaces) × 4000.

2 The apical portion of duodenal absorptive cell from the same control preparation as figure 1 The microvilli of the brush border (B) are covered by the cell membrane, which extends as tubular invaginations, such as the one near B into the subcuticular cytoplasm (S) This region also contains smooth-walled vesicles or tubules (V) Deeper in the cell there are an abundance of mitochondria (M) and elements of the endoplasmic reticulum, both smooth-surfaced and covered with granules. The small dense particles contained in vesicles presumably are lipid (F) The lateral cell membranes (P P) of adjacent cells follow a tortuous but mostly parallel course, the lumenal end of which is marked by terminal bar (T) × 30,000.


B
L
2
C
B
F

PLATE 2

EXPLANATION OF FIGURES

3 An intestinal villus from 9-day-old mouse incubated 20 minutes at pH 8.8 in sodium β-glycerophosphate. The brush border (B) contains dense deposit, and the lateral cell membranes (P) appear somewhat darker than in control preparations. The dense body in the lower right corner is not granular and presumably is lipid such as is found in control preparations from such young animals. GC, goblet cell. × 4500.

4 Apical portions of several absorptive cells from the duodenum of an adult mouse incubated 10 minutes at pH 8.3 in disodium phenyl phosphate. There is dense deposit in the lumen of the intestine, in the region of the brush border (B), along lateral cell membranes (P) and scattered diffusely through the cytoplasm. The diffuse cytoplasmic reaction is more concentrated in the subcuticular region (S) than deeper in the cell, and it is found only in cells nearest the surface of the block. F F F; lipid droplets. × 19,000


3
4

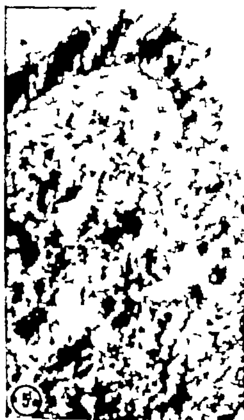
PLATE 3

EXPLANATION OF FIGURES

5 The apical portion of an absorptive cell from the duodenum, incubated 20 minutes at pH 8.6 in disodium para-nitrophenyl phosphate but placed in boiling water for one minute prior to incubation. There is no reaction, and no release of nitrophenol into the medium occurred during incubation, although cytological structure can still be recognized. B, brush border; S, subterminal region; P, lateral cell membrane. × 1 5 [illegible]

6 An intestinal absorptive cell from [illegible] 9-day-old mouse incubated 20 minutes at pH 8.6 in sodium β-glycerophosphate. In addition to [illegible] reaction in the brush border (B) and diffuse deposits in the cytoplasm, there is a deposit in the membranes surrounding vesicular structures (V) in the subterminal region. F, [illegible]; M, mitochondrion. ×4,000.

A duodenal absorptive cell incubated 10 minutes at pH 8.3 in disodium phenyl phosphate. The reaction in the brush border (B) can be resolved at this magnification into [illegible] coarse deposit in the lumen of the microvillus and [illegible] finely granular reaction in the region of the cell membrane surrounding each microvillus. There is a light, diffuse deposit in the subterminal cytoplasm. × 50,000.


5a


6

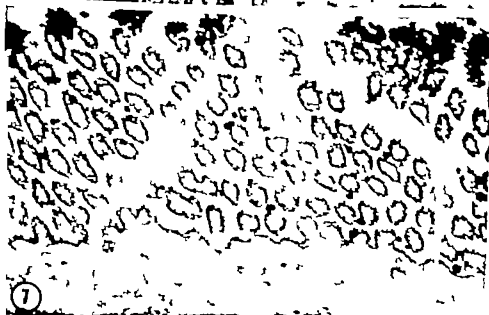

7

PLATE 4

EXPLANATION O FIGURES

8 The supranuclear cytoplasm of a duodenal absorptiv cell incubated 20 minutes t pH 8 6 in disodium para-nitrophenyl phosphate. The reaction is confined to the lateral cell membranes (P P) and none can be seen in any of the elements of the Golgi complex (G G, G) M, mitochondrion. × 25,000.

9 Intestinal absorptive cells from 9-day-old mouse sectioned t the level of the nuclei (N) The tissue was incubated 20 minutes at pH 8.6 in sodium β-glycerophosphate. At this level the reaction is again confined to the cell membrane (P) and nuclei (N) fail to react. I, intercellular space. × 10,000.



PLATE 5

EXPLAN TION O FIGURES

10 A goblet cell from the small intestine of a 9-day-old mouse incubated 20 minutes at pH 8 6 in sodium β-glycerophosph te. There is granular deposit in the cell membranes (P) of the goblet cell and the adjacent absorptive cells. N nucleus; MD mucus droplets. × 20,000

11 A lymphoid cell lying among the bsorptive cells of duodenal epithelium incubated 20 minutes at pH 8 3 in disodium phenyl phosph te The reaction is confined to the cell membranes (P) of the lymphoid and absorptive cells. N nucleus of lymphoid cell. × 19,000


10

PLATE 6

EXPLANATION OF FIGURE

12 Muscularis of the duodenum incubated two minutes at pH 7.3 in disodium phenyl phosphate. There are granules scattered diffusely both intra- and extracellularly but in addition, the reaction is localized discretely in the cell membranes of each of the several types of cells present, including an erythrocyte (R) capillary endothelium (E) smooth muscle (SM) and both the Schwann cell (SC) and axons (A) of a small branch of the myenteric plexus. Small vesicles (V) near the surface of smooth muscle cells also react. × 8500.


18
SM
SC
A
A
E
E

PLATE 7

EXPLAN TION FIGURES

13 A capillary in the duodenum, fixed 10 minutes and incubated 20 minutes t pH 7.3 in sodium β-glycerophosphate. In addition to deposits in the cell membranes of the endothelial cells and diffusely scattered through the cytoplasm, there is reaction in the walls of numerous small cytoplasmic vesicles (V) × 27,000.

14 Parts of 4 smooth muscle cells of the duodenum, incubated two minutes t pH 7.3 in disodium phenyl phosphate. There is reaction in the cell membranes (P) in the walls of small vesicles (V) near the cell membranes, and scattered diffusely through the cytoplasm Note the small reactive tubule or vesicle amid the group of mitochondria (M) N nucleus. × 19,000.

15 The serosa of the duodenum, incubated two minutes at pH 7.3 in disodium phenyl phosphate. There is diffuse deposit in the nucleus (N) of the serosal cell, as well as discrete reactions in the cell membrane (P) and the membranes of numerous cytoplasmic vesicles (V) At the top f the picture is bit of smooth muscle (SM) also containing reactive vesicles. P cell membrane on peritoneal surface of serosal cell. × 25,000.

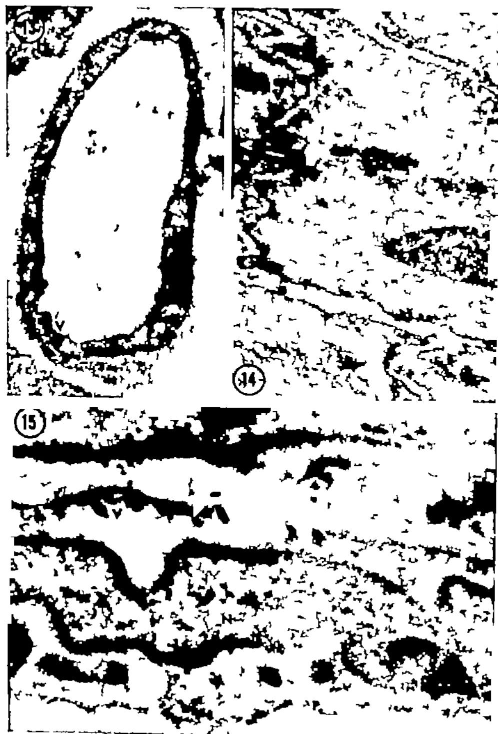

13
14
15

PLATE 8

EXPLANATION OF FIGURE

16 Striated muscle from the diaphragm, fixed 10 minutes and incubated 20 minutes at pH 7.3 in disodium phenyl phosphate. There is reaction in the cell membrane (P) and diffuse deposits in the nucleus (N) and the cytoplasm near the surface of the cell. Between the myofibrils (labeled Z, I, A for the various bands of which they consist) there are linear deposits in the area occupied by the sarcoplasmic reticulum, including very dense reactions at the level of the I bands, where the triads of the sarcoplasmic reticulum lie. M, mitochondria. × 34,000.



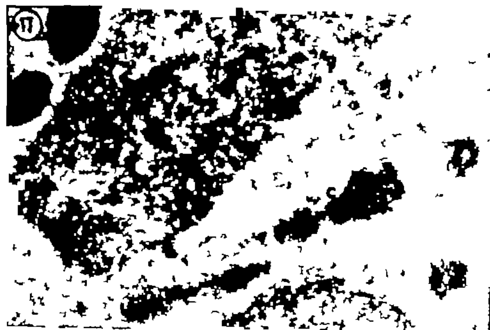
PLATE 9

EXPLANATION OF FIGURES

17 An eosinophil from the small intestine of 9-day-old mouse, incubated 20 minutes at pH 8.6 in sodium β-glycerophosphate. A pair of centrioles (C) sectioned obliquely is marked by reaction, and there is diffuse deposit in the nucleus (N) M, mitochondrion. × 44,000.

18 An eosinophil from the duodenum, incubated 20 minutes t pH7.3 in disodium phenyl phosph te. There is reaction in the paired centrioles (C) as well as a diffuse deposit in the nucleus (N) and cytoplasm, including the eosinophilic granules (EG) × 40,000.

19 Another eosinophil from the same preparation as figure 17 Again there is a reaction in the two centrioles (C, C) as well as diffuse deposits elsewhere. N nucleus; EG eosinophilic granule. × 26,000


17
C


18
C
EG
N


N
C
EG

PLATE 10

EXPLANATION OF FIGURES

20 The apical portion of tracheal epithelial cell incubated 20 minutes t pH 7.3 in disodium phenyl phosphate There is reaction in cilia (C) in basal bodies (BB) and in the cell membrane, including that covering the long microvilli (MV) which protrude between the cilia. The reaction lies within the substance of the basal bodies and cilia, except for the apparently hollow core of the basal bodies. × 45,000.

21 Tracheal epithelium incubated for 20 minutes t pH 8 3 without substrate. There is no reaction either in basal bodies (BB) or cilia (C) but the internal filaments of the cilia can be seen × 73,000

22 Tracheal epithelium from the same animal as figure 21 incubated 20 minutes at pH 8 3 in disodium phenyl phosphate A reaction is present within basal bodies (BB) and cilia (C) in the region of the internal filaments. The membrane covering the apical surface of the cell and the microvilli (MV) also reacted. × 66,000.


C
BB
21


C
MV
22

An Electron Microscopic Study of the Lymphatic Vessels in the Penile Skin of the Rat[1]

ELWIN E. FRALEY AND LEON WEISS
Harvard Medical School Boston Massachusetts and Department of Anatomy Johns Hopkins University School of Medicine Baltimore M ryland

Many reports have appeared in the recent literature concerning the fine structure of blood vessels (Palade '53 Moore and Ruska '57; Weiss '57; Bennett, '59 Fawcett, '59) These studies have in many instances caused either modification or complete revision of pre-existing concepts of capillary physiology For example, the mechanism whereby materials are exchanged with surrounding tissues has been long debated. Pappenheimer and his coworkers ('51) calculated that the measured rate of exchange between capillaries and interstitial tissue could be explained on the basis of endothelial pores with an effective radius of 30–45 A and a population density of $1-2 \times 10^{9}/cm$ of the capillary wall. The length of the pores was presumed to correspond to the thickness of the endothelial cell or 0 3 μ. However extensive electron microscopic studies of capillaries have with the exception of certain specialized vessels failed to demonstrate the existence of pores (Bennett, '58) Bennett ('59) in a recent publication, states that there is now sufficient morph ogical evi dence to doubt the pore r f c ry structure. Also it was e y h t the exchange of ma er als gh c p lary walls involves no xpen re of e ergy on the part c the endo al cells themselves (Lar s '34 Da li 1 Stock, 44 Char ers and Zweif h 4 The work of P de ('60) howe er suggests that en elium may be a ble of actively tran p ting certain s bst es by pinocytosis cytopempsis T su ct of pinocytosis v as reviewed by L tt ('58)

In cont to the situation h respect to blood illaries, little h s been added to our u er anding of the microscopic anatomy f mphatic vessels since th observations of on Recklinghausen (1870) Ranvier (1897) and Clark and Clark ('33 '38) Except for observations on the lacteal (Weiss, '55 Palay and Karlin, '59) and lymphatic sinuses in lymph nodes (Moe '60) studies on the structure of smaller lymphatic vessels with the electron microscope have not appeared

A fundamental question concerns the behavior of lymphatic endothelium in the presence of particulate matter Wislocki (16) reported that the lymphatic endothelium in the tails of certain amphibian larvae phagocytosed trypan blue Yoffey and Courtice ('56) state that under normal circumstances the lymphatic endothelium in adult animals is not phagocytic. In order to investigate the reactivity of lymphatic capillaries with the electron microscope morphological criteria for the identification of lymphatic vessels had to be established It is the purpose of this study to begin to set forth such criteria.

The penile skin was the site selected for this study This area was shown to be suitable because preliminary injection and light microscopic studies revealed a rich perficial plexus amenable to experimentation. This region is relatively easy to repare for electron icroscopy being free of such cutaneous dnexae as hair and sebaceous gl s.

MAT D THODS

Adult h f he Wistar strain wer k

Injected d preparations were st b li ht and electron microsc Injec s of the superficial lymph exus w made using a 1 cc yringe an an inje on mixture of equal

[1] This work was a d by grants C-3106 and C-5375 from the U S Public Health Service.

parts of Carbachrome Ink and Thorotrast[a] (a colloidal suspension of thorium dioxide) while the animals were under Nembutal anesthesia. Injections were made while the specimen was being viewed through a dissecting microscope

Material for both the light and electron microscopes was fixed in cold (3–5 C) buffered sucrose-1% osmium tetroxide according to Caulfield ('57) for 1½ hours at pH 7.2. After fixation the tissue was washed 5 minutes in distilled water dehydrated at room temperature in a graded series of ethyl alcohols (70 80 95 and 100%) for a total of 1½ hours and placed in a mixture of equal parts absolute alcohol and n-butyl methacrylate monomer (two changes in one hour) Finally the tissue was infiltrated with n-butyl methacrylate monomer (two changes in one hour) and embedded in a prepolymerized mixture of 9 parts n-butyl methacrylate and one part methyl methacrylate at 60 C for 24 hours. Sections were cut with a Porter Blum microtome at a thickness of 50 to 100 mμ for the electron microscope and at 2 μ for the light microscope using glass knives. Sections for the electron microscope were picked up on celloidion and carbon coated copper grids. The grids were examined without removing the plastic under the RCA model 3e and Siemens Elmiskop I electron microscopes Electron micrographs were taken on Kodak medium contrast lantern slide plates at varying magnifications and enlarged, photographically

Sections for the light microscope were stained with hematoxylin and periodic acid-Schiff as outlined by Weiss ('57)

OBSERVATIONS

Light microscopy

The penile skin possesses a rich lymphatic plexus demonstrable by injection. The smaller lymphatic vessels are typically found superficial to the blood capillaries (fig. 1) The lymphatic walls consist only of endothelial cells (fig. 2)

Electron microscopy

General orientation The lymphatic vessels studied have an average diameter of 14 μ and their walls are composed of thin endothelium (figs 3 4 10 11) The smaller lymphatic vessels tend to exist in a semicollapsed state (figs. 3 and 4) The vessels are intimately related to the surrounding connective tissue and no pericytes appear to be present (fig 3) The nuclei of lymphatic endothelial cells are large and often protrude into the vessel lumen (fig. 4)

The appearance of a lymphatic vessel differs from that of a blood capillary which is characterized by a thicker wall, smaller lumen and the presence of pericytes (fig. 3) Blood capillaries also possess a basement membrane (fig. 5) The presence of red blood cells in the vessel lumen is a useful but not definitive criteria for identifying blood vessels. Our observations on the fine structure of blood capillaries agree with previously cited studies on the subject.

Cytology of the lymphatic endothelium. The luminal surface of the endothelium displays numerous small cytoplasmic projections (fig 11) These endothelial projections appear to be similar to those reported in blood capillaries (Kisch '57) Larger abluminal endothelial projections extend into the surrounding connective tissue (figs. 6 and 7) The cytology of these projections is similar to the rest of the endothelial cell as described below

The cytoplasm of the endothelial cells contains mitochondria which appear to be similar in structure number and distribution to those found in the endothelium of blood capillaries (figs. 8 and 10) Extensive observations were not made on the Golgi apparatus but Golgi complexes tended to occupy a perinuclear location (fig. 6) The membranous component of the endoplasmic reticulum is scanty but numerous RNP particles are distributed throughout the cytoplasm (fig 10) No fibrillar structures similar to those described in well fixed blood capillary endothelium (Palade '53) were observed.

Vesicular structures are present at both the luminal and abluminal endothelial surfaces and in the intervening cytoplasm

---

Edward Gurr Ltd., 42 Upper Richmond Rd West, London S. W 14 England.

Testagar Inc. & Co., Detroit, Michigan.

(figs. 8 10 and 11) These range in diameter from 80 to 400 A. The vesicles appear to fuse with the plasma membrane at the luminal and abluminal surfaces (fig. 8) The vesicles appear to be more numerous at the cell surfaces than in the intervening cytoplasm. They appear similar in structure to the vesicles described in blood capillary endothelium (Palade '53) and may be concerned with pinocytotic activity

The endothelial endothelial junctions vary from simple edge-to-edge (fig. 10) or overlapping approximations (fig 8) to complexly plicated interdigitating structures (figs. 7 and 9) The intercellular space contains no discernible cement substance (figs 7 and 9) Desmosomes were not observed

The walls of these vessels are everywhere complete (figs. 3 4 10 and 11) No discontinuities were observed such as those reported to exist in the lacteal (Palay and Karlin, '53) The walls vary in thickness but for the most part are thin, having a minimal width of 0.2 μ (figs. 3 4 and 11)

Surrounding connective tissue Lymphatic capillaries lack a basement membrane (figs. 9 10 and 11) In rare places usually in larger capillaries a condensed ground material subjacent to a limited area of endothelium suggested the presence of a slender basement membrane (fig. 6) In no instance did the development of a basement membrane approach that of blood vessels (fig. 6) Therefore the abluminal endothelial surface is in direct contact with the surrounding ground substance and collagen of the connective tissue Although an intimate association exists between the endothelium and the collagen of the connective tissue no evidence of direct attachment of collagen t[illegible] he lymph[illegible] wall was observed (figs. 10 [illegible]nd 11)

The smaller [illegible]mphatic vessels do not possess any cel[illegible] similar to Rouget cells of blood capillar[illegible]

DISCUSSION

The obs[illegible]ations presented in this study have show[illegible] that the lymph[illegible]tic and blood capillaries in the penile skin of the rat have a fine s[illegible]ucture which is distinctive for each The salient morphological features characteristic of lymphatic and not of blood capillaries are the absence of a basement membrane the thinness of the wall abluminal endothelial projections extending into the surrounding connective tissue and the absence of either Rouget or adventitial cells. Thus, morphological criteria have been established to differentiate lymphatic from blood capillaries on the basis of fine structure

The structure of the lymphatics studied differs in some respect from that of the lacteal in that the lacteal apparently has a thicker wall than the blood capillaries in the intestinal villus its walls have occasional discontinuities and the lacteal does not have abluminal endothelial extensions (Weiss '55 Palay and Karlin '53) However both the lacteal (Weiss '55; Palay and Karlin '53) and the smaller peripheral lymphatic capillaries appear to lack a basement membrane

Wood ('60) has shown that a slender basement membrane was observed subjacent to the Kupffer cells in the rat after embedding in epoxy resin which was not seen in methacrylate-embedded material. In our material basement membranes were regularly observed in blood capillaries. In rare cases a slender discontinuous basement membrane may have been present in the larger lymphatic capillaries. In most lymphatic capillaries a basement membrane was not observed. Moreover collagen filaments and other structures were directly applied to the subjacent surface of the lymphatic endothelium.

No evidence was found to support the theory that connective tissue fibers are [illegible]ed to the lymphatic wall. The ob[illegible]ions of Pullinger and Florey ('35) [illegible]nd McMaster ('47) suggested that, in conditions leading [illegible] edema and connec[illegible] tissue sw[illegible] [illegible] tension of the con[illegible]ive tissu[illegible] [illegible]lling on the lymphatic wall [illegible]se in the calib[illegible]er of th[illegible] [illegible]ry would explain why [illegible] [illegible]res are not collapsed in [illegible] [illegible] as inflammation where the conn[illegible] tissue pressure is gr[illegible] than the [illegible]alymphatic pressure. How[illegible]er the [illegible]minal endothelial ext[illegible] [illegible]escribed in this study may subs[illegible] the function previously ascribed to the connect[illegible]e tissue fibers If these protoplasmic extensions serv[illegible] to anchor th

vessel wall to the surrounding connective tissue then expansions or contractions of the connective tissue would cause concomitant widening or narrowing of the vessel lumen.

In some cases these projections may represent branches of the lymphatic vessel in which the section passes through the wall but not through the lumen. However in most cases they appear to be abluminal endothelial projections.

In addition these spurs provide increased surface for transport from the connective tissue and by their extension into the surrounding tissue increase the volume of interstitial tissue drained by a given lymphatic vessel. The abluminal extensions the absence of a basement membrane which as an ultra-filter may discriminate against the passage of materials across the vessel wall, and the evidence presented here for active transport by the endothelium constitute a morphological basis for the rapid passage of a variety of materials across the lymphatic wall.

SUMMARY

The lymphatic vessels of the skin of the penis have been studied under the electron microscope. These vessels had an average diameter of 14 μ and consisted of an endothelium without a basement membrane. The endothelial wall was extremely thin, having a minimal width of 0.2 μ and was everywhere complete. The walls had both fine luminal and somewhat larger abluminal endothelial projections extending into the surrounding connective tissue. The endothelium contained numerous small mitochondria and a definitive Golgi apparatus. The membranous component of the endoplasmic reticulum was poorly developed. The cytoplasm contained many free RNP particles. Vesicular structures which varied in diameter from 80 to 400 A, were seen at the luminal and abluminal surfaces as well as in the intervening cytoplasm. These vesicles appeared to be concerned with pinocytosis. The endothelial-endothelial junction varied from complexly plicated to simple edge-to-edge approximations. The space between endothelial cells was approximately 90 A in width and appeared to contain no intercellular cement substance. The vessels were surrounded by connective tissue ground substance and collagen fibers. Pericytes were absent.

LITERATURE CITED

Bennett, H. S. 1956a In Electron Microscopy Proceedings of the First Regional Conference on Electron Microscopy in Asia and Oceania Electrotechnical Laboratory Nagata-cho, Chiyoda-ku Tokyo, p. 88.

——— 1956b The concepts of membrane flow and membrane vesiculation as mechanisms for active transport and ion pumping. J. Biophys. Biochem. Cytol., 2, 99–103.

Bennett, H. S. J. H. Luft and J. C. Hampton 1959 Morphological classification of vertebrate blood capillaries. Am. J Physiol., 196 381–390.

Caulfield, J. B. 1957 Effects of varying the vehicle for OsO in tissue fixation. J Biophys Biochem. Cytol., 3 827–829

Chambers, R., and B. W. Zweifach 1947 Intercellular cement and capillary permeability Physiol. Rev 27 431–463.

Clark, E. R., and F. L. Clark 1933 Further observations on living lymphatic vessels in the transparent chamber in the rabbits ear—their relationship to the tissue spaces. Am. J Anat., 52 273–305

——— 1938 Observations on isolated lymphatic capillaries in the living mammal. Ibid 62, 59–92.

Danielli J F and A. Stock 1944 The structure and permeability of blood capillaries. Biol. Rev 19 81–94.

Fawcett, D W 1959 The fine structure of capillaries, arterioles and small arteries. In The Microcirculation. Symposium on Factors Influencing Exchange of Substances Across Capillary Wall. The University of Illinois Press, Urbana, Ill.

Kisch B 1957 Electronmikroskopische Untersuchung des Herzens und der Kapillaren. Dtsch. Med. Wschr., 17 605–606.

——— 1957 Der ultramicroscopische bouder Capillarwand. Acta Physiol. Pharm. Néerl., 6 334–339

Landis, E. M. 1934 Capillary pressure and capillary permeability Physiol. Rev 14 404–481

McMaster P D 1947 The relative pressure within cutaneous lymphatic capillaries and the tissues. J Exp. Med 86 293–308.

Moe, R. 1960 Electron microscopic morphology of lymphatic sinuses. Anat. Rec 136 245 (abstract)

Moore D H., and H Ruska 1957 The fine structure of capillaries and small arteries. J Biophys. Biochem. Cytol., 3 457–462.

Palade G E. 1953 Fine structure of blood capillaries. J Appl. Phys., 24 1424

——— 1960 Transport in quanta across the endothelium of blood capillaries. Anat. Rec 136 254 (abstract)

Palay S L., and L. J Karlin 1959 An electron microscopic study of the intestinal villus. I

The fasting animal. J Biophys. Biochem. Cytol., 3 363–372.

Pappenheimer J R., E. M Renkin and L. M. Borrero 1951 Filtration, diffusion and molecular sieving through peripheral capillary membranes. Am. J Physiol., 167 13–46.

——— 1953 Passage of molecules through capillary walls. Physiol. Rev 33 387–423.

Pullinger B D., and H. W Florey 1935 Some observations on the structure and function of lymphatics their behavior in local oedema. Brit. J Exp. Path., 16 49–61

Ranvier L. 1897 Morphologie et développement des vaisseaux lymphatiques hez les mammifères. Arch d'Anat. Micr Paris, pp 69–81 nd 137 152.

von Recklinghausen, F 1862 Die Lymphgefässe und ihre Beziehung zum Bindgewebe Hirschwald, Berlin.

Weiss, J 1955 The rol of the Golgi complex in f t bsorption studied with the lectron microscope with observations on the cytology of duodenal bsorptive cells. J Exp. Med., 102 775–782.

Weiss, L. 1957 A study of the structure of splenic sinuses in man and in the albino rat with the light microscope and the electron microscope J Biophys. Biochem. Cytol., 3 599–610.

Wislocki, G. B 191 The staining of amphibian larvae with benzidine dyes with special reference to the behavior of lymphatic endothelium. Am. J Physiol., 42 1 4–132.

Wood, R. L. 1960 Observations on the fine structure of alf liver Anat. Rec., 136 304 (bstract)

Yoffey J M and F C. Courtice 1956 Lymphatics, Lymph and Lymphoid Tissue Edward Arnold Ltd London, England.

PLATE 1

EXPLANATION OF FIGURES

1 A whole-mount preparation of injected penile skin. The plane of focus is t the level of a very superficial lymphatic vessel (LV) The injection mass (IM) and the path of the injection mixture are indicated. Several other partially injected lymphatic vessels t somewhat different plane of focus are indicated by broken lines. Many blood vessels (BV) are visible at different level. × 250.

2 A section through an injected preparation. Note the thin wall of the lymphatic without pparent basement membrane and the closeness of the surrounding connective tissue fibers (CT) The injection mass (IM) fills most of the lumen (L) It surrounds some erythrocytes possibly arried in with the injection needle. Initial magnification. × 1300

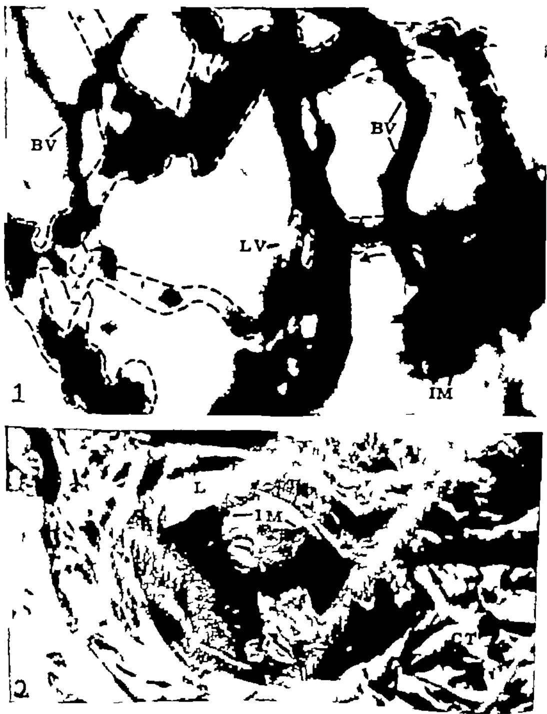

BV
BV
LV
IM
1
L
IM
CT
2

PLATE 2

EXPLANATION OF FIGURES

3 Electron micrograph of lymphatic (L CAP) and blood capillary (B CAP) and the surrounding connective tissue. The lymphatic capillary is extremely thin-walled. The close relationship between the lymphatic and the surrounding collagen (C) is apparent. The lymphatic vessel apparently lacks pericytes but pericyte (P) is seen in relationship to the blood capillary. The blood capillary has thicker wall than the lymphatic and red blood cells can be seen in the vessel lumen (L). × 4000.

4 A lymphatic vessel and surrounding connective tissue. The coagulated lymph in the vessel lumen (L) has finely reticulated ppearance. Luminal endothelial projections (LEP) are seen. Note the thinness of the endothelium (E) and its intimate relationship t the surrounding collagen (C). Prominent endothelial nuclei (N) protrude into the vessel lumen (L). See figure 11 for higher power of this wall. × 10,000

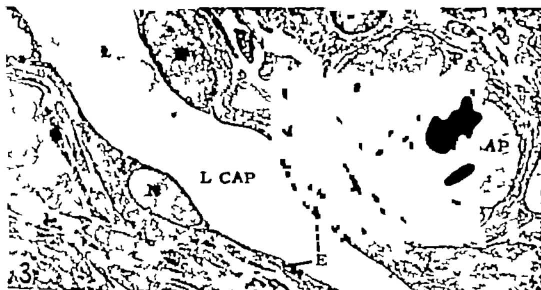

L
P
AP
L CAP
N
E
3

PLATE 3

EXPLANATION OF FIGURE

5 A blood capillary A red blood cell (RBC) is present in the vessel lumen (L) A slight basement membrane (BM) is seen subjacent to the endothelium (E) × 58,000.


RBC
L
EN
CT

PLATE 4

EXPLAN TION OF FIGURE

6 A wall of somewhat larger lymphatic vessel than shown heretofore. Prominent in this micrograph are two bluminal endothelial projections (AEP)—one of which is partially out of section. There appears to be some basement membrane (BM) material subjacent to certain sections of the wall. A definitive Golgi apparatus (G) perinuclear in location, is also seen. × 42,000

LYMPHATIC VESSELS IN PENILE RAT SKIN
Elwin E. Fraley and Leon Weiss



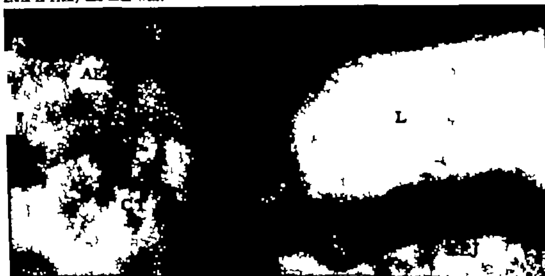
PLATE 5

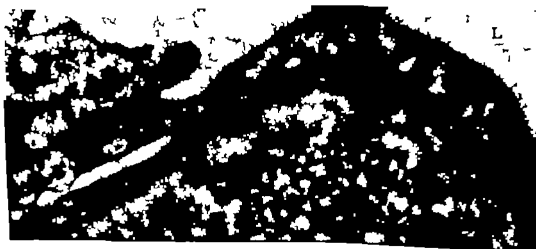
EXPLANATION OF FIGURES

7 A lymphatic wall at the level of several interdigitating endothelial-endothelial junctions (EEJ) The intercellular space measures approximately 90 A and contains no intercellular cement substance An abluminal endothelial projection (AEP) is also seen. × 50,000

8 An overlapping type of cell junction. Vesicles (V) which appear to fuse with the plasma membrane can be seen in the endothelium (E) The vesicles occur most frequently at the cell surfaces but are occasionally present in the intervening cytoplasm. × 40,000

9 Tongue and groove type of endothelial-endothelial junction (EEJ) The cell junction is close to nucleus (N) × 37,000


AE
C
L


L


L

PLATE 6

EXPLAN TION OF FIGURES

10 A section of lymphatic wall. Pinocytotic vesicles (V) are seen. Note the close rela tionship between the endothelium (E) and the surrounding collagen (C) nd ground ubstance (GS) The endothelial-endothelial junction (EEJ) ppears to be simple edge-to-edge approximation. A well-developed particulate (RNP) component is seen in the cytoplasm of the endothelium. The wall pparently lacks basement membrane. × 50,000.

11 A lymphatic wall which represe ts higher power of portion of the wall seen in fig ure 5. Note the luminal endothelial projections (LEP) × 42,000.

Sequence of Appearance of Primary Centers of Ossification in the Human Foot[1]

BERTRAM S. KRAUS
School of Dentistry University of Washington, Seattle Washington

INTRODUCTION

Since the appearance in 1737 of Albinus's *Icones ossium foetus humani* there has been a considerable literature devoted to the process and chronology of ossification of the human skeleton. Some investigators like Augier ('31) and Tiessandier ('44) have concentrated upon particular regions of the skeleton. Others (Noback and Robertson, '51; Mall, '06) have described the entire skeleton. The earlier methods were restricted to naked-eye observations of fetal bone development. Later techniques included roentgenography KOH clearing and alizarin staining and histological sectioning

In addition to the demonstration of ossification in the human skeleton there have been investigations of similar nature carried on in rats (Strong, '25; Walker and Wirtschafter '57; Wright, Asling Dougherty Nelson and Evans '58)

Although there are minor areas of disagreement, in general the sequence of initial ossification of the 19 post-tarsal bones of the human foot is described as beginning with the 5 metatarsals, followed by the 5 distal phalanges then the 5 proximal phalanges, and finally the 4 intermediate phalanges. Wright et al. ('58) cite Wood Jones as considering this sequence to be a generalized mammalian trait. These investigators find it applicable to their Long-Evans rats although within each phalangeal row the second and third digits were the first to ossify followed by the 4th 5th and 1st respectively

Beyond determination of the sequence of appearance of centers of ossification in the human foot by phalangeal and metatarsal groups, little attention has been paid to the precise digital sequence. Mall noted that in one fetus presumably 58 days old, the 2nd metatarsal and 1st distal phalanx were the only centers present. Of the 19 fetuses he examined this was the only specimen with as few as two centers present. The others showed 5 or more stained ossification centers. On the basis of 19 cleared and stained specimens Mall presented the following sequence of appearance

1. Metatarsal #2 and distal phalanx #1
2. Metatarsals #3 and #4 and distal phalanges #2, #3, and #4.
3. Metatarsals #1 and #5.
4. Distal phalanx #5 and proximal phalanx #1
5. Proximal phalange #2.
6. Proximal phalanges #3 #4 and #5.

Obviously with such a small sample size it was impossible to delineate the sequence of all 19 centers one at a time. Sampling size has thus far been a deterrent in attempts to establish the detailed sequence of appearance of ossification centers. Noback ('54) has pointed out that of the 590 embryos and fetuses examined by various investigators up to 1954 only 286 can be used, as published in a critical statistical analysis. He indicates that this number is a small quantity to do a statistical study of the time of appearance of 250 centers."

Noback and Robertson ('51) examined 136 cleared and stained human fetuses Their results as presented in table 9 are difficult to interpret in terms of sequence of appearance of ossification centers since their chief interest apparently lay in the chronology Although 9 f their specimens were in some stage of foot ossification they merely conclude that "the distal phalangeal centers of the foot appear after the metatarsal centers and are followed by the proximal phalanges and then the middle phalanges.

[1] This investigation was supported by Research Grant D-910 from the National Institute of Dental Research, United States Public Health Service.

Other than the work by Mall and by Noback and Robertson, there has been no published original material relating to the sequence of appearance of centers of ossification of the foot that is more specific. Statements that appear in general anatomy and embryology texts reflect the lack of precise information on this subject. For example Frazer (46) indicates that initial ossification occurs in regular sequence in the metatarsals from the first to the 5th digit. This regular sequence of appearance is followed in the distal next in the proximal, and finally in the intermediate phalanges. According to Wood Jones ('49) the process of calcification spreads from preaxial to postaxial digits in each row of phalanges but ossification commences in the proximal phalanges soon after it has appeared in the terminal phalanges of the preaxial side. He also indicated that the metatarsals are already elongated columns of bone before the centers for the distal phalanges are visible as more than "tiny points Hamilton, Boyd and Mossman ('57) present a line drawing of a 50 mm embryo (fig 386) showing the ossified centers of the first distal phalanx and the second third and 4th metatarsals.

The present study was undertaken in an attempt to determine if there is a distinguishable sequential pattern in the appearance of each of the 19 centers of ossification in the human foot. The need for such delineation has been aptly stated by Noback and Robertson (51)

> "The order of appearance and the intraregional patterns of ossification centers differentiating during the first 5 months of fetal lif are pparently under genetic control. This is expressed (1) by the rel tively regular sequence of the appearance of the primary ossification centers and (2) by the precise and orderly appearance of the ossification centers in the regions nd sub-regions of the body

We concern ourselves here with the relatively regular sequence of appearance Regularity in a biological developmental sequence bespeaks a genetic control. Departures from an est blished sequential pattern of events sugg st either interference with the environmental milieu in which the genes medi te their effects or defects in the genes themselves Since genes are known to have multiple effects, the observance of notable departures from the known order might signal the presence of one or more mutants and hence the probability of additional irregularities anomalies or abnormalities throughout the fetal body There is as yet no way of observing the fetal calcification process serially hence the establishment of a specific sequence must rest upon observations of aborted embryos and fetuses This obviates the potentiality of clinical significance is cases of marked deviations from the established sequence

There is, however a field in which the ability to detect the presence of mutant genes in aborted human fetuses has great potentialities. We refer to the study of the genetic effects of radiation in human populations. To date there is no direct evidence that radiation causes mutations in the sex cells of man. Studies by Neel and Schull ('56) to determine genetic damage in the offspring of irradiated Japanese parents by demonstrating higher frequencies of abnormalities in these offspring than in control groups have failed to disclose significant differences. If irradiated parents do, indeed, transmit increased numbers of mutated genes to their offspring, the effects presumably would be lethal in the great majority of cases within the first two weeks of gestation Sublethal effects might not be expressed as gross clinical defects or anomalies but rather as deviations from the normal sequence of biological events such as initial calcification of primary teeth (Kraus '59) appearance of centers of ossification and periods of acceleration and deceleration in growth of the shafts of long bones. (Kraus '58)

It is of interest, then to determine the specifically human sequential pattern of initial ossification of the bones of the foot. Deviations from this pattern might suggest the presence of mutant genes and spur the search for associated defects throughout the body Significant differences in the frequencies of such deviations between a series of aborted fetuses of irradiated parents and a control group might well be a measure of the genetic damage due to irradiation.

MATERIAL

A series of 138 human fetuses ranging in crown-rump length from 33–165 mm (or approximately from 8–18 weeks of age *in utero*) were cleared in KOH and stained with alizarin red S. Some of these were in addition, stained with methylene blue which has an affinity for cartilaginous tissue (Williams '41). The specimens were not differentiated as to race or sex and included some American Indian, Mexican and Negro representatives in addition to Whites, since they were obtained from hospitals in Tucson and Phoenix, Arizona and in Los Angeles. The fetuses were examined with a stereoscopic microscope under a magnification of 25×. A lower magnification sometimes failed to disclose minute centers of ossification. The age distribution of the specimens is presented in table 1.

TABLE 1

Crown-rump and age distribution of the sample (bilaterally symmetrical specimens only)

Crown rump	Estimated age	Number of specimens
mm	*week*	
18–35	8	3
36–46	9	16
47–58	10	27
59–71	11	16
72–85	12	11
86–99	13	18
100–113	14	10
114–127	15	12
128–141	16	8
142–154	17	12
155–167	18	3
		138

RESULTS

When the number of ossified centers is plotted against the crown-rump length of each specimen a parabolic distribution results (fig. 1). A number of interesting observations may be made. It would appear that the first 7 centers are present by the time the human fetus has attained a crown-rump length of 57 mm. The smallest specimen in which an ossified center was observed was 33 mm. Between 33 mm and 57 mm from zero to 7 centers may be expected to be present. There are however specimens as small as 45 mm with as many as 10 centers ossified, and two specimens of 55 mm with 12 and 15 centers. The range in crown-rump length from 1 to 12 centers is relatively small (20 mm on the average) but there is considerable overlapping. The range from

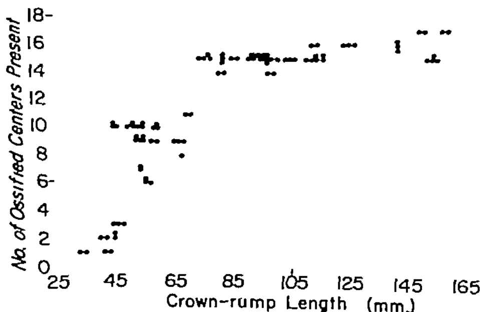


Fig. 1 Regression of number of ossified centers present on crown-rump length (= 138)

13 to 18 centers is on the other hand ex tremely broad but also with considerable overlap Fetuses with 15 centers for ex ample range from 55 mm to 165 mm. We may conclude, therefore that there is a differential time gradient in the ossification of the bones of the foot. Between 33 mm and about 70 mm the first 12 centers generally become ossified. Between 70 mm and 160 mm the remaining 7 centers will ossify Thus between 8½ and 11 weeks ossification proceeds rapidly but from 12 to 18 weeks there is a decelerating rate Approximately 10 weeks are required for the onset of ossification in the 19 bones of the foot. The relatively more rapid suc cession of ossified centers in the earlier stages may account for the fact that 22 4% of the sample in the first 12 stages are deviates whereas only 9 6% of the sample in the last 6 stages are deviates

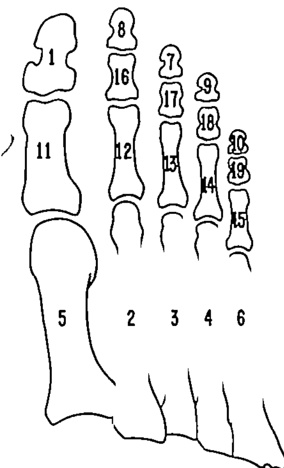


Fig. 2 Sequence of ppe nce of primary centers of ossification in the human foot (Kraus theory)

The sequence of appearance of centers of ossification in the foot that is derived from 138 observations is illustrated in figure 2. Of the 138 specimens 118 support this theory 20 do not. The distribution of the sample by number of centers present in accordance with support and non-support of the theory is presented in table 2. The 20 non-supporting specimens do not, however support any one other theory In fact, in some cases they offer more support to my theory (called Kraus theory for brevity) than to any one other theory The statistical analysis and computations are presented below in a separate section of the paper

It is interesting to note that the data of both Mall, and Noback and Robertson also support the Kraus theory Mall observed only 19 specimens 13 of which support the theory (table 3) Noback and Robertson found only 95 of their 136 cleared and stained specimens to be in some stage of ossification Of these 82 support the theory 13 do not (table 3) In both samples the non-supporting specimens are not consistently in support of any other theory When the two samples are combined with the present sample (table 4) we find 213

TABLE 2

Distribution of sample by support and non-support of Kraus theory

Centers present	Number pro	Number con	Total specimens
1	4	2	6
2	3	2	5
3	2	1	3
4	1	1	2
5	0	1	1
6	3	0	3
7	3	2	5
8	2	1	3
9	12	0	12
10	12	1	13
11	1	2	3
12	2	0	2
13	2	1	3
14	3	6	9
15	42	0	42
16	14	0	14
17	5	0	5
18	4	0	4
	118	20	138

TABLE 3

Calculated distribution of samples of Mall ('06) and Noback and Robertson ('51) according to support and non-support of Kraus theory

Centers present	Mall		Noback and Robertson	
	Pro	Con	Pro	Con
1	0	0	0	0
2	1	0	1	0
3	0	0	3	1
4	0	0	3	2
5	0	0	0	0
6	0	0	0	2
7	0	1	0	1
8	0	0	4	1
9	4	0	10	3
10	0	0	3	0
11	1	0	1	2
12	1	1	8	0
13	0	0	0	1
14	0	1	15	0
15	6	0	12	0
16	0	0	13	0
17	0	0	8	0
18	0	0	0	0
Totals	13	3	82	13

TABLE 4

Distribution of 3 samples (= 249) according to support and non-support of Kraus theory

Centers present	Pro	Con	
1	4	2	
2	5	2	
3	5	2	
4	4	3	
5	0	1	
6	3	2	
7	3	4	
8	6	2	
9	28	3	
10	15	1	
11	3	4	
12	11	1	
13	2	2	
14	18	7	
15	60	0	
16	27	0	
17	17	0	
18	4	0	
Totals	213	36	249

observations in support of the Kraus theory and 36 apparently against it. The percentage of each sample not supporting the theory are Kraus—14.5% Mall—18.7% and Noback and Robertson—13.7%.

The sample used in this report included only specimens in which the centers present appeared bilaterally. Those fetuses in which no ossified centers were present were obviously discarded. Thus a total of 200 fetuses made up the gross sample. With respect to bilateral asymmetry Noback and Roberson ('51) point out

> "The unilateral presence of one of a pair of bilateral centers is observed during the time when these centers normally appear and not observed after the time of their normal appearance. This suggests that the absent center of each of these bilateral pairs noted would normally appear shortly afterwards. (p. 18)

This observation is confirmed by the present study with only a few exceptions. Six specimens showed unilateral occurrence of a center which was early in the sequence of those present. For example in one specimen of 15 centers *the 5th distal* phalanx is unilaterally present. Normally this is the 10th center to appear (see fig. 2) The other 5 specimens where bilateral asymmetry was noted were also deviant with respect to the normal sequence postulated by both the literature and the Kraus theory

Figures 3–20 illustrate the 18 consecutive stages in the sequence of appearance *of ossified centers as postulated* in this paper. The centers are more easily observed under a microscope with the foot immersed in 100% glycerine.

STATISTICAL ANALYSIS

From the foregoing review of the literature we may assume that the current theory (Theory 1) holds that initial ossification occurs in the first metatarsal and that subsequent centers appear in the second third, 4th and 5th metatarsals, respectively. The next centers appear in regular sequence beginning with the first distal phalanx and followed by the second, third 4th and 5th distal phalanges. The proximal phalanges begin ossification next, in regular order from one through 5. These are followed by the second, third 4th and 5th intermediate phalanges respectively.

The theory advanced in this paper (Theory 2) differs *from Theory 1 in the* following respects the first distal phalanx is the first center to appear the first metatarsal is the 5th center to appear; the 5th metatarsal is the 6th center to appear the 3rd distal phalanx is the 7th center to ap-









F gs 3-6 (tages 1 2, 3 and 4)
(Arrow indic es last center theoretically to ppear)









Figs. 7-10 (stages 5 6, 7 and 8)
(Arrow indicates last center theoretically to ppear)









Figs 11 14 (stages 9, 10 11 and 12)
(Arrow indic tes last center theoretically to appear)









Figs. 15–18 (stages 13, 14 15 and 16)

(Arrow indicates last center, theoretically to appear)





Figs. 19–20 (stages 17 and 18)

(Arrow indicates last center theoretically to appear)

pear and the 2nd distal phalanx is the 8th center to appear The sequence of Theory 2 is illustrated in figure 2. The differences between the two theories can be designated for purposes of computation, as follows

Theory	PIII	Metatarsals					PIII			
	1	2	3	4	1	5	8	7	9	10
1	6	2	3	4	1	5	8	7	9	10
2	1	2	3	4	5	6	7	8	9	10

	PI					PI			
	11	12	13	14	16	16	17	18	19
1	11	12	13	14	15	16	17	18	19
2	11	12	13	14	15	16	17	16	19

We wish to determine whether or not the current theory and the new theory for the order of ossification of the bones in the foot are both significantly supported by the data, and in addition to determine if the support offered the new theory by the data is significantly greater than that offered the current theory The data available consist of 138 (bilaterally symmetrical) observations of fetuses, each observation showing the ossification centers present at the time of death To answer the above question we use a method elaborated by Tate ('60)

In determining the support offered a given theory we will consider the bony centers to be numbered in the order in which they are supposed to make their appearance according to that theory (Theory 2, see above)

Consider the following notation:

- n stage of the specimen (number of centers present)
- N_n number of specimens of stage n
- $(x_1, x_2, \ldots x_n)$ description of the specimen according to Theory 1
- $(y_1, y_2, \ldots y_n)$ description of the specimen according to Theory 2
- $S_1 = 20n - \Sigma x_i$ the support offered by specimen for Theory 1
- $S_2 = 20n - \Sigma y_i$ the support offered by specimen for Theory 2
- ΣS_1 the total support offered for Theory 1
- ΣS_2 the total support offered for Theory 2

It can be shown for each theory that the maximum and minimum support possible

for a single specimen is $\pm n(19-n)$. Thus ΣS_1 and ΣS_2 are both bounded by

$$\pm \sum^{18} n(19-n)N_n.$$

Columns 1, 2 and 8 of the Summary of Calculations (table 5) give n, N_n, and $n(19-n)$ respectively. $\Sigma n(19-n)N$ has been calculated to be 8612.

It is more or less obvious by inspection that both theories are given significant support by the data. A formal verification by a statistical test follows. Since we number according to the theory in question (Theory 2), the null hypothesis of no support for the theory specifies that we have a random set of n numbers for each specimen of stage n. Under the null hypothesis that, say, Theory 1 does not receive significant support it may be shown that

$$\mu_{\Sigma S_1} = 0 \quad \sigma_{\Sigma S_1} = \sqrt{\frac{20}{3}\Sigma n(19-n)N_n} = 239.6$$

In our example $\Sigma S_1 = 8106$ and $\Sigma S_2 = 8216$ (see columns 9 and 10 of the Summary). In view of the approximate normality for the chance quantities ΣS_1 and ΣS_2 we see that both null hypotheses are rejected.

To compare the support for Theory 1 with that for Theory 2 we use the Sign Test (Dixon and Massey '57, 280–286). The breakdown for all 138 specimens which is required for the test is shown in columns 5, 6, and 7 of the Summary. In condensed form it is

	$S_1 = S_2$	$S_1 > S_2$	$S_1 < S_2$	Total
Number of specimens	119	3	16	138

Of those cases in which ties do not occur 16 favor Theory 2 and 3 favor Theory 1. *This is sufficient to show that the difference* in support is highly significant in favor of Theory 2 (16 out of 19 would show significance at the 1% level).

We can also consider a third theory, say Theory 3, which is more or less between the other two. It is essentially the same

TABLE 5

Summary of calculations

Stage	N_n	Theory 1	Theory 2	Ties $S_1 = S_2$	Support theory 1 $S_1 > S_2$	Support theory 2 $S_1 < S_2$	Max. support possible—1 specimen	Magnitude of support theory 1	Magnitude of support theory 2
1	6	(4) 6	1	0	0	4	18	+32	+72
		(2) 2	2	2	0	0		+32	+32
2	5	(3) 28	12	0	0	3	34	+72	+102
		(2) 23	23	2	0	0		+60	+60
3	3	(2) 236	123	0	0	2	48	+76	+96
		(1) 123	235	0	1	0		+48	+40
4	2	(1) 2346	1234	0	0	1	60	+50	+60
		(1) 1234	2345	0	1	0		+60	+52
5	1	(1) 12345	23456	0	1	0	70	+70	+60
6	3	(3) 123456	123456	3	0	0	78	+234	+234
7	5	(3) 1234568	1234567	0	0	3	84	+246	+252
		(2) 2346789	1234789	0	0			+1[illegible]4	−144
8	1	(2) 12345678	12345678	2	0	0	89	+1[illegible]6	+178
		(1) 234678910	123478910	0	0	1		−[illegible]2	+72
9	16[1]			110	0	0	[illegible]	−6764	+6764
Totals	138			119	3	16		+8106	+8216
				(Maximum possible support for 138 specimens 8612)					

From stages 9 through 18 all specimens support equally Theories 1 and 2, hence are designated as ties. The total magnitude of support given by these 110 specimens is entered for purposes of comparison of grand totals. It will be seen that Theory 1 receives 94.1% of the maximum possible support, Theory 2, 95.4%.

as Theory 2 except for the fact that bones 7 and 8 in Theory 2 are reversed, that is are placed in the normal order of Theory 1 For Theory 3 the breakdown will be the same except for row 7 Instead of 0,0,5 we have 3,0,2. In condensed form it is:

	$S_1 = S_5$	$S_1 > S_5$	$S_1 < S_5$	Total
Number of specimens	122	3	13	138

Thus Theory 3 also receives significantly more support than does Theory 1

A comparison between Theory 2 and Theory 3 is inconclusive

	$S_1 = S_5$	$S_1 > S_5$	$S_1 < S_5$	Total
Number of specimens	135	3	0	138

The result, 3 out of 3 is short of significance at the 10% level.

The following two examples will show how support is computed

Example 1

N	[illegible]		[illegible]	[illegible]	[illegible]
4	6	+ 8	1	+18
2	2	+16	2	+16

$S_1 = S_5$ 2 $S_1 > S_5$ 0 $S_1 < S_5$ 4

Example 2

N	[illegible]	[illegible]	[illegible]	[illegible]
3	1234568	+82	1234567	+84
2	2346789	+62	1234789	+72

$S_1 = S_5$ 0 $S_1 > S_5$ 0 $S_1 < S_5$ 5

SUMMARY AND CONCLUSIONS

Utilizing 138 cleared and stained human fetuses ranging from 33 mm to 165 mm in crown-rump length a specific sequence of appearance of centers of ossification in the post-tarsal bones of th[illegible] foot has been proposed Support for this theory is determined by statistic[illegible]l an[illegible]lysi[illegible] based upon a method elabor[illegible]ted b[illegible] T[illegible]t[illegible] Comparison of different theor[illegible] [illegible] [illegible]rri[illegible]d out by the Sign Test.

The first 12 [illegible] p[illegible] [illegible]latively rapid successi[illegible] [illegible]when the [illegible] t[illegible] [illegible]s in the 8th to 11th w[illegible] [illegible]d[illegible]el [illegible]m[illegible] t[illegible] From the 11th to the [illegible] week th[illegible] remai[illegible] [illegible]g centers appear The seqence of appearance of centers of ossification appears to be as follows

Order	Center
1	1st distal phalanx
2	2nd metatarsal
3	3rd metatarsal
4	4th metatarsal
5	1st metatarsal
6	5th metatarsal
7	3rd distal phalanx
8	2nd distal phalanx
9	4th distal phalanx
10	5th distal phalanx
11	1st proximal phalanx
12	2nd proximal phalanx
13	3rd proximal phalanx
14	4th proximal phalanx
15	5th proximal phalanx
16	2nd intermediate phalanx
17	3rd intermediate phalanx
18	4th intermediate phalanx

Tested against the current theory the observations offer greater support for the theory proposed herein. Analysis of the reported observations of other investigators support the theory

Since a regular sequential pattern would seem to indicate rather rigid genetic control, it is suggested that significant deviations from this or any other biological sequential pattern might serve to indicate the presence of mutant genes. The use of such sequences is proposed to measure the genetic effects of irradiation.

ACKNOWLEDGMENT

I would like to express my gratitude to Dr Robert Tate for his construction of the statistical model, and to Mr Clifford Freebe for the photography

LITERATURE CITED

Augier M. 1931 Squelette cephalique. In Poirier P and Charpy editors, Traite d'Anatomie Humaine 1 89-630. Masson et Cie Paris.

Dixon, W and F Massey 1957 Introduction to statistical analysis. 2nd ed. McGraw-Hill, New York.

Frazer J 1946 The anatomy of the human skeleton. Fourth ed. J and A. Churchill Ltd London.

Hamilton W J Boyd, and H. Mossman 1952 Human embryology Second ed. Williams and Wilkins Co., Baltimore

Jones, F Wood 1949 Structure and function as seen in the foot. Second ed. Baillière Tindall and Cox London.

Kraus B and S Choi 1958 A factorial analysis of the prenatal growth of the human skeleton Growth 22 231 242.

Kraus, B. 1959 Calcification of the human deciduous teeth. J Am. Dent. Assoc., 59 1128–1136.

Neal, J., and W Schull 1956 The effect of exposure to the atomic bombs on pregnancy termination in Hiroshima and Nagasaki. Publication no. 461 Washington N tional Acad. Sci.—N tional Res. Council.

Noback, C., and G Robertson 1951 Sequences of appearance of ossification centers in the human skeleton during the first five prenatal months. Am. J Anat., 89 1–28.

Strong, R. M. 1925 The order time and rate of ossification of the albino rat (*Mus norvegicus albinus*) skeleton. Am. J Anat., 36 313–355.

Tate R. 1961 On the use of partially ordered observations in measuring the support for a complete order J Am. Stat. Assoc., 56 299–313.

Teissandier J 1944 L ossification des côtes et de la colonne vertébrale chez le foetus humain. Thèse Faculté de Médecine de Paris. (Cited in Noback and Robertson, '51.)

Walker D G., and Z. T Wirtschafter 195‑ The genesis of the rat skeleton. A laboratory atlas. Charles C Thomas, Springfield.

Williams, T W 1941 The differential staining of bone Stain Techn., 16. 23

Wright, H C. Asling, H. Dougherty M. Nelson, and H E ans 1958 Prenatal development of the skeleton in Long E ans rats. An t. Rec., 130 659–672.

Preadaptive Potentialities of the Mammalian Skull An Experiment in Growth and Form

E. LLOYD DuBRUL AND DANIEL M. LASKIN
U iversity of Illinois, Colleges of Medicine and Dentistry Chicago Ill nois

Theoretical propositions about the form of the vertebrate skull have come mainly from the study of the behavior of two basic tissues, cartilage and bone. The cranium of mammals first takes form from the development of a cartilaginous base—which in man is notably small—but it is quite certain that the base does not continue into a cartilaginous cranial roof in the embryos of higher mammals. The roof is made of membrane bone. This complex finally fuses into a rigid working unit when the cartilage is invaded and replaced by bone. But the cartilaginous base is not merely a memento of phylogenesis. We believe that it has always had potent preadaptive value. It is a firm, temporary but necessary scaffold for the organs of the head which will permit growth in differ ent rates and directions in differently adapted species. It acts as a template for the final definitive bony form of the skull.

Information about the growth behavior peculiar to each of these tissues can be ex tracted from the profusion of papers on the morphology of the skull base and roof. The studies encompass phylogeny ontog eny comparative anatomy and growth. Some stress the cartilaginous side of the story The skull base of a vigorously grow ing animal retains regularly spaced, resistant islands of active cartilage for vary ing lengths of time. Finally however these also are invaded and the adjacent bones fuse in animals that have finished growing. Thus many works that deal with the skull as a whole yield pertinent notes on the base (Huxley 1863; Topinard, 1891; Keith, '12 Dabelow '31 Kummer '52b Baer '54 Biegert, '57) Other works confine themselves solely to the base of the skull and this is evident in their titles (Virchow 1857; Bolk, 15 Pankow 49 '51 Schuchardt '50 Kummer '52a; Starck, '52; Bjork, '55 Schultz, '55 Zuck erman '55; Moss and Greenberg, '55 Moss '56 Ford '58 Scott, '58)

Now it is known that the sutures that separate the membrane bones of the roof of the skull are areas of bony accretion during cranial growth, but how this activity is initiated and controlled is not completely clear For this reason it is not sur prising to find reports of experiments on the vault and facial bones common enough in the literature (Giblin and Alley 44 Gans and Sarnat, '51; Moss, '54 '60 Watanabe Laskin and Brodie '57) It is said that sutures acting much like cartilaginous epiphyses are responsible for the active enlargement of the brain box. At tempts to obliterate these sutures have not been successful in substantiating this belief because even the resulting local mutilation does not measurably change cranial form.

Although the above is obviously no ex haustive representation of a century of literature (having omitted most embryology) it can still be said that little in the literature leads to a simple, coherent pic ture of the basic mammalian scheme from which the special adaptations could have radiated. Lately as noted above, experimental measures have been tried on the skull roof and face These areas are easily accessible. But little of such experimental attack on the skull base is to be found in the literature. Here of course access is less obvious. The only experimental work we could find was either accidental—due to the implantation of foreign material in the fetal braincase (Nicholas '30) or indirect—via the disturbance of the ac tivity of the endocrines (Baume '60)

If experimental tampering with the der mal bony parts of the skull shows no ef fects other than minor local mutilations

something deeper suggests itself as crucial in control of skull form. Consequently the present study was planned as a simple direct, experimental attack on certain specific cartilaginous sites in the cranial base. This is an attempt to define in clearer detail some fundamental mechanism concordant with both an innate common scheme and a wide adaptive diversity of the mammalian skull.

OBJECTIVES AND PROCEDURES

The immediate objective was to cut out completely the spheno-occipital synchondrosis in the skull bases of suitable animals. The underlying objective was to determine what effect this structure has upon the growth of the skull and hence its final form.

Rats were used for three reasons: (1) They are admirably hardy beasts and were soon found to survive the most severe surgical manipulation. (2) The mature rat cranium is certainly the most symmetrically rectilinear structure to be found in skulls of laboratory animals and this is especially so in the midsagittal plane (fig. 1) Any deviation from this outline is at once demonstrable and precisely measurable. (3) The cranial base has, visible in norma basalis two sharply defined cartilaginous plates traversing the midline. The anterior plate is seen just posterior to the rim of the bony palate. This is the spheno-presphenoid synchondrosis and it is the smaller of the two. The broader spheno-occipital synchondrosis lies several millimeters back of this It extends across the cranial base between the apices of the auditory bullae (fig 2)

The surgery was a minor modification of Ingle and Griffith's (49) approach to the hypophysis. In our procedure the animal is anesthetized with minimal doses of sodium pentobarbital. It is extended supine on an operating board with the head nestled in a specially designed cradle molded to the head form, because it is imperative to maintain maximum stability of the very young rat cranium. The bones are quite fragile and movable. The head and shoulders are extended by rubber bands on the upper incisor teeth and forelimbs to expose widely the front of the neck. The neck is then shaved and scrubbed to accommodate an incision in the midline from the dental papilla, just back of the mandibular symphysis to the sternum. The skin is freely undermined and the submaxillary gland bluntly dissected away from the front of the neck. Fibers of the omohyoid are retracted or separated just below their attachment to the hyoid bone and the exposed trachea and esophagus are then retracted to the left. The uncovered carotid and jugular vessels are retracted to the right. Now the longus capitus muscle is visible and both it and the underlying rectus capitus anterior are scraped away from the skull base to expose the spheno-occipital synchondrosis (fig. 3)

A small dental bur cut to a length equal to the supero-inferior thickness of the synchondrosis (1 0 to 2.0 mm) is used to cut the cartilage plate and a thin layer of bone anterior and posterior to it. The synchondrosis can be neatly excised in this way up to the meninges and transversely to the apex of each auditory bulla. Usually there is little bleeding. The area is cleaned the overlying structures repositioned and the skin closed with silk sutures.

About 100 albino rats of the Holtzman strain were used of which 23 were suitable for final critical measurement and 10 for histologic study Some animals were successfully operated upon as young as 15 days of age. All animals including litter mate controls were x rayed weekly and sacrificed at 6 weeks two months, three months 4–5 months, 6 months, and one year after operation Those prepared for histologic study were decalcified, sectioned at 8 µ, embedded and stained in the routine manner with hematoxylin and eosin.

Linear measurements were made under a hand lens with a Boley gauge whose ends were filed to a fine point. Accuracy is within 0.2 millimeters Angular measurements were made with a protractor Curvature of the cranial roof is expressed as the highest point above the line from nasal tip to inion. Cranial base curve is the farthest point of the base from a line drawn from basion to the spheno-ethmoidal junction (see table 1)

TABLE 1

Skull measurements in millimeters

Animal no.	Length of skull: (1) Nasal tip to occipital condyles	Length of skull: (2) Nasal tip to inion	Length of skull: Difference 1 > 2, 1 < 2	Length of skull base: Basion to spheno-occipital synchondrosis	Length of skull base: Spheno-occipital synchondrosis to presphenoid	Length of skull base: Total	Curvature of cranial roof	Curvature of cranial base[b]	Angle of medial plane with long axis of skull	Angle of bulla with long axis of skull: Left	Angle of bulla with long axis of skull: Right
									degrees	degrees	degrees
Experimentals, 6 weeks old											
44E	35.3	36.4	−1.1	5.9	4.5	10.4	3.4	−1.2	85	47.5	44.5
55E	36.6	37.8	−1.2	5.9	6.8	12.7	3.5	−1.2	83	49.0	56.5
06E	36.4	37.4	−1.1	5.1	5.2	10.3	3.0	−1.4	86	51.0	60.5
79E	38.7	40.7	−2.0	5.2	5.8	11.0	3.9	−2.5	81		
Controls, 6 weeks old											
38C	45.0	43.7	+1.3	6.8	7.4	14.2	0.7	+1.0	98	40.0	43.0
79C	41.5	41.0	+0.5	6.2	6.9	13.1	1.8	+0.8	90	42.0	44.5
Experimentals, 2 months old											
34E	41.2	40.7	+0.5	6.1	6.8	12.9	1.7	−0.3	85.5	54.0	59.0
69E	40.0	41.0	−1.0	5.4	6.0	11.4	2.6	−1.4	79	50.5	59.0
Controls, 2 months old											
65d3	42.3	41.2	+1.1	6.4	7.1	13.5	2.3	+1.0	94	45.0	45.0
65d4	42.8	42.0	+0.8	6.4	7.1	13.5	2.1	+0.8	95.0	43.0	45.0
Experimentals, 3–4 months old											
48E	45.9	45.3	+0.6	7.3	7.8	15.1	1.7	−0.4	80	51.5	54.0
10E	45.0	45.0	0.0	5.6	7.4	13.0	2.0	−1.4	88	59.5	60.0
17E	44.8	46.7	−1.9	6.7	6.5	13.2	2.5	−3.1	78	58.5	50.5
Controls, 3 months old											
89d1	47.1	45.9	+1.2	7.0	8.0	15.0	1.8	+0.8	96	41.0	43.0
89d3	47.2	45.7	+1.5	7.0	7.8	14.8	1.8	+0.9	102.5	45.0	45.0
Experimentals, 4–6 months old											
22E	43.2	44.1	−0.9	6.0	[illegible]	13.3	3.3	−1.0	87	60.0	58.0
35E	[illegible]	48.4	+1.3	[illegible]	8.4	15.7	0.0	0.0	96.5	53.0	48.0
62E	43.1	43.1	−3.0	6.4	5.7	12.1	[illegible]	−1.2	85.5	55.0	57.0
Controls, 6 months old											
6m8	46.2	45.3	+0.9	6.9	7.8	14.7	1.7	+0.4	98.0	37.5	42.0
6m9	46.2	45.2	+1	7.0	8.0	15.0	1.5	+0.7	98.0	38.0	45.0
Experimentals, 1 year old											
8E	46.0	46.2	−1.2	6.4	7.6	14.0	1.3	−0.8	89	56.5	54.0
Controls, 1 year old											
1y1	49.0	47.3	+1.7	7.4	8.6	16.0	1.0	+0.[illegible]	103	45.0	
1y9	49.3	47.6	+1.7	7.3	8.7	16.0	1.4	+0.8	103	43.0	43.0

[a] Bulla detached in maceration; position cannot be accurately measured.

[b] Concave, +; convex, −

RESULTS

Sagittal histologic sections of normal rat heads show actively growing cartilage at spheno-occipital and spheno-presphenoid synchondroses. The spheno-occipital cartilage plate is longer (almost 2.0 mm long) but narrower in this view than that of the spheno-presphenoid (about 1 5 mm long). Columns of cartilage cells are ranged fore-and-aft, in line with the long axis of the skull and in the direction of longitudinal growth as it is in the long bones (fig. 4)

The spheno-occipital cartilage is covered by the posterior tip of the hypophysis immediately above the dura. Both inner and outer cortical bony layers of occipital and sphenoid bones as well as numerous internal bony trabeculae, are interrupted by this cartilaginous slab On the underside of the skull the area of attachment of the longus capitus muscle includes: basioccipital bone perichondrium over the synchondrosis and part of the basisphenoid bone (fig 4) From the specimens studied proliferation of cartilage cells and growth activity seem to be greater in the *lower* half of the spheno-occipital synchondrosis, that is the side toward the external cortical bony plate. This activity seems to be reversed in the spheno-presphenoid synchondrosis, being greater in the *upper* half This may shift during different stages of growth.

Notable differences are seen in the experimental animals (fig. 5) (1) The spheno-occipital cartilage plate is completely absent. (2) Both inner and outer cortical bony layers of basioccipital and basisphenoid bones are continuous. (3) Medullary bone now has strong trabeculae running across the site previously occupied by the cartilage There is no sclerotic plate at the site to indicate the line of fus(as is found in the fused epiphyseal drosis of a long bone (4) T surface of the skull or outer shows much activity (bony apposition) concomitant with the ment of the muscles on its The inner plate shows none of ity the *dura is undisturbed*, the holding down the hypophysis is no inflammatory or reparative change found in the cranium In this p... case it is certainly shown that the surgical interference extended up to but did not penetrate the dura mater to touch the hypophysis (fig 5) (6) Peculiarly in the remaining synchondrosis (spheno-presphenoid) increase in growth activity now seems to have shifted toward the *lower* part of the cartilage. This may indicate a tendency to oppose the ventral bending of the neurocranium in compensation for the loss of the spheno-occipital cartilaginous growth site (see below)

Grossly animals whose synchondroses had been removed are now obviously different from the normal in skull outline. In lateral view the changes are: (1) a general shortness and roundness of the total skull, (2) a curvature of the cranial roof (3) a ventral migration of the nuchal crest, (4) a ventral and rostral swing of the nuchal plane around a *center of rotation* at inion and (5) a marked forward displacement of the occipital condyles (figs. 6 7 8 9 10) In basal view the changes are: (1) a ventral and forward rotation of the plane of the foramen magnum so that one can see directly into the cranial cavity (2) a ventral and forward rotation of the occipital condyles in addition to the forward displacement noted above (3) a marked shortening of the cranial base (4) a crowding forward of the auditory bullae onto the posterior margins of the temporomandibular joint (5) a shortening of the medial pterygoid plate and (6) a notable *increase* in the angle by the long axes of the 11 12) These conditi extent in all the but in varying d in each. lucidate the crania of changes unexpecte rat

spheno-occipital fusion. The back of this hollow houses the hypophysis (reminiscent of the hypophyseal hollow in primates). The plane of the basiocciput then bends sharply down to simulate a clivus as in man (fig. 8).

The linear and angular measurements in table 1 are illustrated in figures 1 and 2. From these measurements several cogent facts can be stressed. All animals with the synchondroses removed are shorter from nasal tip to occipital condyles than their controls except one number 35E. All experimental animals are also shorter than the controls from nasal tip to inion except three 35E, 17E and 22E. This might suggest that merely the skull length is lessened by the loss of the cartilage. But in normal animals the length from nasal tip to condyles is always longer than from nasal tip to inion. The reverse is *always* true in successful experiments. This is due of course to the forward swing of the nuchal plane around inion as center which carries the condyles forward to shorten the base (fig. 10). All these data seem to point to the cranial base as dominant in the control of skull growth because the growth of the base is distinctly reduced by loss of the cartilage. However as the brain still grows a bit, it must bulge out at the cranial roof.

The skulls of all experimental animals are shorter from basion to spheno-occipital synchondroses (basisphenoid bone) than the controls except 35E and 49E. They are shorter between spheno-occipital and spheno-presphenoid synchondroses — i.e., presphenoid bone—except 35E. The angle formed by the *nuchal plane with the long* axis of the skull is less than 90° in all experimentals except 35E. It is greater than 90° sometimes considerably greater in all controls. It is obvious that 35E is an aberrant animal. It shows up in all the exceptions. Close examination of the operation site reveals that its synchondrosis is only partly fused. This seemed to be a useful additional check on the efficacy of the procedure.

In general then the curvature of the cranial roof is greater in the experimentals than in the controls and in *all* experimental animals the cranial base is internally convex (kyphotic) while in all control it remains internally concave (lordotic). Again, the angle formed between the long axis of the skull and the nuchal plane is less in all experimental animals than in their controls. Table 1 shows that differences in length between experimentals and controls diminish with age. The remaining cartilage sites probably grow *more rapidly in compensation for loss of* the spheno-occipital contributions. However as stated above differences in form remain constant.

Complete removal of the synchondrosis in the base of the skull between occipital and sphenoid bones then, does drastically change the pattern of growth of the skull and hence its final form while tampering with the sutures of the vault does not. Although the changes in form are mostly restrained to the posterior half of the neurocranium both base and vault are affected!

DISCUSSION

The differences in mammalian skulls are at present best explained in terms of differences in the relative growth rates of various cranial parts (Huxley '32). This can lead to remarkable inferences of mechanism.

Weidenreich came to see the whole story as a feature of growth of the brain—especially in the case of man ('41)—although previously he had concluded convincingly that much of the morphology of the human skull was a result of mechanical readjustment to the upright posture ('24). The cerebral portion usually dominates skull contour in dwarf animals so, *it was said,* that man's present form reflects that of a dwarf in its swollen brain box and shrunken jaws. From this Weidenreich devised the thesis that man descended from gigantic ancestors ('46). Thus relative growth is ruled by brain size—small brain yields large jaws large brain yields small jaws. All this moves in the current of Bolk's fetalisationstheorie ('15) which still strongly molds interpretations of human evolution (Tobias, '57).

DeBeer on the other hand derives from comparative embryology the current concept that growth of the cranial vault is paced by growth of the brain but that skull base and jaws are independent of it.

He has written that the form of the chondrocranium may be devoid of phylogenetic significance it barely covers the floor of the brain ('37 p 450) But from the same source "It is true that the human chondrocranium presents a somewhat pathetic spectacle but that is only because of the relatively *huge* size of the brain ('37 p. 449) The last certainly is phylogenetically significant because one of the great features adapting man to his environment is his big brain!

Ford ('58) finds that growth in different parts of the skull base follows either neural or jaw growth rates. We prefer to say that segments of the skull base have growth rates similar to neural or jaw growth. Then, as we will show all the later works make sense if one thinks of the skull as a coordinated working unit.

It is clear that some emphasis on the evolution of the brain was inherent in the rise of mammals. This required a protective brain box that could expand quickly in early individual development. One can see in the skull vault that membrane bone has the capacity to appear simultaneously in widespread spots then quickly to connect in trabeculae radiating along lines of tension. This behavior gives such bone a greater potential for rapid expansion than cartilage But the bone that ultimately develops in the cartilage—although the cartilage itself expands at a fair rate by interstitial growth—must run through two processes First, the cartilage must be calcified, destroyed then removed, and second, the bone must replace the cartilage. The latter mechanism seems to fulfill the function of a strong, stable gradually stiffening but growing scaffold that can change the material of which it is made without relinquishing supporting power

The rat skull seems especially apropos for a beginning study of basic mammalian form because the metamerism of the primordial head is at least, recalled by the symmetrical repetition of cartilage plates along the base. At any rate this strategic array suggests a simple device for making the skull grow long The fetal head of the rat is rounded as in most mammals evidently it fits the largest mass—the brain—into the smallest space—a sphere—within the restricting confines of the uterus. The face is diminutive tucked in below and in front of the brain case. The skull need but unbend during growth to make the long rectangular shape of the adult. The final result is a shift in proportion whereby the length of the cranial vault decreases relative to the length of the face (Baer '54)

The mechanism for unbending is inherent in the growth of the cranial base at the cartilage plates. We have shown here that this unbending can be halted in part by obliterating the spheno-occipital cartilage. This is well illustrated in figure 10 What is most extraordinary is that the cranial floor actually kinks up at the site of the obliterated spheno-occipital synchondrosis. This is the negative of unbending that is the base gets very bent and the vault must adjust to it in some way Apparently the brain continues to grow as it now must, by bending around the sharp artificially created kyphosis at the base. But this rounds the cranial roof. Then, the roof of the skull follows the form of the brain which, cradled in the cranial base bends with the base. A reverse mechanical way of describing this effect is to picture what happens if a rectangular taffy bar is bent with the fingers. The bottom surface kinks up the top surface flows freely down at each end in a smooth round curve.

But the experimental changes we have here recorded are identical with some of the classical changes of the skull in its adaptation to the upright posture. They are (1) an increased vaulting of the dorsum, (2) a ventral shift of the foramen magnum and occipital condyles (3) a ventral migration of the nuchal crest, and (4) a change to a kyphotic or internally convex cranial base (Du Brul, '50) The skull in general is shortened. Also as pointed out by Weidenreich ('24) the bulla or pyramidal part of the temporal complex has swung from a more sagittal to a more coronal orientation in the skull. The whole skull base is severely crowded because of the shortening and bending. Thus the form and behavior of the cartilaginous part of the human cranium has great phylogenetic significance. The timing of appearance and disappearance of the cartilage plates their relative growth

the pattern of appearance and of fusion of bones of the skull base, all seem clearly to cause the adaptive changes of the skull.

All the life we know is grown in a gravitational field, it must be obvious that this force is one of the great molders of living form. Its effects are reflected in both the most subtle and manifest tissues—brains and bones. Nervous systems have no indwelling source of neural energy They depend on unremitting inputs from the environment for their very existence and brains deteriorate when these stimuli are diminished. The most reliable ubiquitous source of such input is found in stimuli arising from the pull of gravity (Stanley Jones, '60) It is certainly this source that instigates those changes of the skull which in mammals always accompany the same phylogenetic reorientation of the body axis in the gravitational field. It has been exhaustively demonstrated that the major changes in the mechanical features of the human head are of necessity simply adaptations to this total reorientation, which the upright posture is. All this became quite clear when orders in which the brain had not noticeably changed were used as controls in "the natural experiment to show that the skull was remodeled in a special way only by the change in habitual posture (DuBrul, '50 '58; DuBrul and Sicher '54) These broader investigations raised the crucial question "How is the basic mammalian skull equipped to respond always in the same way—even in the most widely diverse orders—to the same shifts in postural orientation?

We propose the following. Disregarding the distraction of detail, the basic plan of the mammalian skull is laid out along quite simple lines (fig. 13) The cranial base, as a forward extension of the vertebral axis, seems to govern its gross form. Growing vital organs are supported above and below the base. The brain, sitting on its upper surface is covered by a carapace of dermal bone which normally enlarges according to the dictates of brain growth The several organs of the face and neck, hanging from the lower basal surface, are also encased in dermal bone The snout is filled by a cartilaginous nasal capsule (an extension of the cartilage of the base) and its derivatives which crowd the casing forward in macrosmatic animals. The mandible acts as an added curved shield molded to fit around the tongue hyoid pharynx, larynx and the temporary remnant of the primary jaws Meckel's cartilage This is clearly demonstrated in completely upright man where the organs of the neck, running vertically so closely behind the jaw have remodeled the mandible and everted its lower border (DuBrul and Sicher '54) These dermal bony shields all grow according to the dictates of the organs they house. In the jaws this also includes the teeth.

Then a vault of dermal bones, separated by sutures, can accommodate the early speedy ballooning of the brain, and a facial scaffold of dermal bones can accommodate a later longer spurt of the snout and jaws bulged by the burgeoning organs they contain. The mandible is involved in a local complication at its contact with the skull base for its condyle contributes to jaw growth by a cartilaginous growth site It may be significant that this site is on the same plane as the other cartilaginous growth sites of the base (fig. 13) The cranial base is the intermediary governor of the system. Here the bone acts as a rack to hold cartilage plates placed at crucial sites in a series continuous with the metameric cartilage discs of the vertebral axis. This can best balance the various allometries between the growth of jaws and brains at different sites in the differently adapted heads of mammals. Extensions from these cartilages form the sense organ capsules (figs. 2 and 13)

In a horizontally oriented animal, the skull base is laid out along the horizontal When the animal rears toward the vertical the base swings up following closely the vertebral axis. The mouth and sense organs—olfactory visual and balancing elements—would have to be pushed down to keep the original functional, horizontal orientation with the outer environment. This renovation has in fact, happened in animals that have phylogenetically reared toward the vertical and adapted to erect or semi-erect, habitual postures. But the problem is to explain how this was done biologically

Studies of the peculiar short headed dwarf domestic animals establish that the

shortening and dwarfing mechanism is one that influences growth of cartilage and the formation of bone within it. This genetically directed process has been described in goats, sheep and cattle (Chang '49, Chang and Landauer '50, Julian et al., '57). It has been shown that the same gene is responsible for the phenomenon in several breeds of cattle (Gregory and Carroll, '56). The skull of the animal with the mutant gene is strikingly different from that of the normal phenotype. The essence of the genetic activity in the skull is fusion at the spheno-occipital synchondrosis! From photographs published by Julian et al. ('57) cranial changes can be seen to be: (1) an increased vaulting of the dorsum, (2) a ventral and forward shift of the foramen magnum and occipital condyles, (3) a ventral migration of the nuchal crest, (4) a shortening of the skull base and, (5) a raised rim at the site of fusion making a kinking up of the skull base. This kinked appearance is reinforced by the disappearance of the large basal tubercles normally found on the ventral (outer) surface of the synchondrosis. In sum, the mutant's morphologic features are the same as those we have produced experimentally!

Therefore it is further proposed that genes or gene complexes have as their target sites the cartilaginous growth sites in the base of the mammalian skull. Any mutations tending to shift growth patterns toward those we have produced experimentally will better balance a skull on a vertical column. Such mutations are certainly subject to strong selection pressure in animals that are phylogenetically shifting their orientation in the gravitational field toward the vertical.

Several interesting implications seem inescapable. First, there must be some basic genotypic complex common to mammals that governs the common phenotypic arrangement of the skull base. Second, these genes must be easily susceptible to similar mutations because the morphologic changes seem to be readily consummated in widely diverse groups of mammals whenever they indulge in postural reorientation. Third, the basic arrangement of the skull base allows many possible changes, but only as the changes can be managed by relative growth shifts at segmental cartilage sites. Therefore, fourth, the kinds of resultant forms are *limited*, that is, this basic plan is preadaptive within a knowable range and all possibilities may become predictable by special development of the mathematics of topology.

When, during its phylogeny, an animal uses its forelimbs more and more for prehension and feeding, it, perforce, throws the burden of bodily orientation and locomotion on the hindlimbs (DuBrul, '58). The basic plan of the mammalian skull base permits certain changes. Any mutations tending to shift growth patterns toward those we have experimentally produced, will better balance the skull on the vertically orienting vertebral column. These mutations are then subjected to strong selection pressure. This course of events is especially clear in man, an animal whose phylogeny has bulged its brain, bent its base, shrunk its jaws and otherwise accomplished the complete acquisition of the upright posture.

The ground plan of the mammalian skull, then, seems to embody an admirably preadaptive system. It has responded, repeatedly, in strikingly similar ways in those widely diverse orders whose skulls have had to find a better balance on the more vertical vertebral columns. But it may reveal much more in the adaptive radiation of mammals. By shifting allometries of growth from one specific site along the skull base to another, as suggested herein, we might as readily explain the relative longness of the polar bear's skull as the relative shortness of the spectacled bear's skull—even the long, sleek, slimness of the anteater's skull as opposed to the short broad bulk of that of the elephant.

SUMMARY

1. Because it has been so clearly shown that specific changes of the mammalian skull always accompany phylogenetic reorientation of the body axis in the gravitational field, the crucial question arises:

"How is the basic mammalian skull equipped to respond always in the same way—even in the most widely diverse orders—to the same shifts in postural orientation?

2. An experiment was devised to study he factors in the growth of the rat skull. n its mature form it is so symmetrically ectilinear that any deviation from this ox-like form is seen immediately

3 When the spheno-occipital synchon-lrosis is removed in young animals the adult form simulates the classical changes always associated with the upright posture.

4 The underlying growth mechanisms hus emerge and a model of the basic mam-malian skull is suggested which can ac-count for the major mammalian adaptive radiations.

LITERATURE CITED

Baer M. J 1954 Patterns of growth of the skull as revealed by vital staining. Human Biol., 26 80–126.

Baume, L. J 1960 Das Wachstum des Gebisses und des Gesichtes. In Nederlandsche Vereeniging voor Orthodontische Studie. Den Haag. Studieweek, 20 pp

Biegert, J 1957 Der Formwandel des Primatenschädels. Morph. Jahrb., 98 77–190.

Bjork, A. 1955 *Cranial base development.* Am. J Orthodont., 41 198–225.

Bolk, L. 1915 Über Lagerung, Verschiebung und Neigung des foramen magnum am Schädel der Primaten. Ztschr. Morph. Anthrop 17 611–692

Chang, T K. 1949 Morphological study on the skeleton of Ancon sheep Growth, 13 269–297

Chang, T K., W Landauer 1950 Observations on the skeleton of African dwarf goats. J Morph 86 367–378

Dabelow A. 1931 Über Korrelationen in der phylogenetischen Entwicklung der Schädelform II. Morph. Jahrb., 67 84–133.

DeBeer, G R. 1937 The Development of the Vertebrate Skull. Clarendon Press, Oxford, 552 pp.

DuBrul, E. L. 1950 Posture locomotion and the skull in lagomorpha. Am. J Anat., 87 277–313.

——— 1958 Evolution of the Speech Apparatus. Charles C Thomas, Springfield, 103 pp.

DuBrul, E. L., and H Sicher 1954 The Adaptive Chin. Charles C Thomas Springfield, 97 pp.

Ford, E. H. R. 1958 Growth of the human cranial base. Am. J Orthodon 44 498–506.

Gans, B. J and B G Sarnat 1951 Sutural facial growth of the Macac Rhesus monkey A cross and serial roentgenographic study by means of metallic implant Ibid., 37 827–841

Giblin, N., and A. Alley 1914 Studies in skull growth. Coronal suture fixation. Anat. Rec 88 143–153.

Gregory P W and F D Carroll 1956 Evidence for the same dwarf gene in Hereford, Aberdeen Angus, and certain other breeds of cattle J Hered 47 107 111

Huxley T H. 1863 Evidence as to Man Place in Nature. Williams and Norgate, Ltd., London, 159 pp

Huxley J S. 1932 Problems of Relative Growth. The Dial Press, New York, 276 pp.

Ingle, D J and J Q Griffith 1949 Surgery of the rat. In The Rat in Laboratory Investigation, 2nd ed. *Lippincott Co., Philadelphia,* pp. 434–452.

Julian, L. M., W S. Tyler T J Hage and P W Gregory 1957 Premature closure of the spheno-occipital synchondrosis in the horned Hereford dwarf of the short-headed" variety *Am. J Anat., 100:* 269–287

Keith, A. 1913 Abnormal crania—achondroplastic and acrocephalic. J Anat. Physiol., 47 189–206.

Kummer B 1952a Untersuchungen über die ontogenetische Entwicklung des menschlichen Schädelbasiswinkels. Ztschr Morph. Anthrop., 43: 331–360

——— 1952b Untersuchungen über die Entstehung der Schädelbasisform bei Mensch und Primaten. Anat. Anz., 99 123–126.

Moss, M. L. 1954 Growth of the calvaria in the rat. Am. J Anat., 94 333–361.

——— 1958 Malformations of the skull base associated with cleft palate deformity Plast. Reconstruct. Surg., 17 226–234

——— 1960 Inhibition and stimulation of sutural fusion in the rat calvaria. Anat. Rec., *136* 457–467

Moss, M. L., and S. N Greenberg 1955 Post natal growth of the human skull base. Angle Orthodont., 25 No. 2, 77–84.

Nicholas, J S. 1930 The effects of the separa *tion of the medulla and spinal cord from* the cerebral mechanism by the extirpation of the embryonic mesencephalon. J Exp. Zool., 55 1–22.

Pankow G. 1949 Untersuchungen über die *Schädelbasisknickung beim Menschen.* Ztschr Menschl. Vererb. Konstit. Lehre, 29 69–139

——— 1951 Über Gesetzmässigkeiten im Wachstum der Schädelbasis wahrend der menschlichen Ontogenese. Anat. Nachr., *1* 243–248.

Schuchardt, *E. 1950 Der Index der Schädel*basismitte in der Phylogenese Anat Anz., *97* 118–130.

Schultz, A H 1955 The position of the occipital condyles and of the *face* relative to the *skull* base in primates. Am. *J Phys. Anthrop., N.S 1 9–120*

Scott, J H 1958 The cranial base. Ibid., *16* 319–348

Stanley Jones D and K. Stanley Jones 1960 *The K ernetics of Natural Systems.* Pergamon Press New York, 145 pp.

Starck, D 1952 Form und Formbildung der Schädelbasis bei Chiropteren Anat. Anz 99 114–131

Tobias, P V *1957 B shmer f the* Kalahari Man, 57 33–40

Topinard, P 1891 La transformation du crâne animal en crâne humain. L Anthropologie 2 649–675.

Virchow Rudolf von 1857 *Untersuchungen* Über die Entwickelung Des Schädelgrundes Im Gesunden und Krankhaften Zustande Druck und Verlag von Georg Reimer Berlin, 128 pp.

Watanabe M., D M. Laskin and A. G. Brodie 1957 The effect of utotransplantation on growth of the zygomatico-maxillary suture. Am. J Anat., *100* 319–335

Weidenreich, F 1924 Die Sonderform des Menschenschädel als Anpassung an den uf rechten Gang. Ztschr Morph. Anthrop., *24* 157–169

——— 1941 The brain and its rôle in the phylogenetic transformation of the human skull. T Am. Phil. Soc., N.S., *31* Part V 321 442.

——— 1946 Apes, Giants, and Men. Univer sity of Chicago Press, Chicago, 122 pp

Zuckerman, S. 1955 Age changes in the basi-cranial axis of the human skull. Am. J Phys. Anthrop., N.S., *13* 521–539

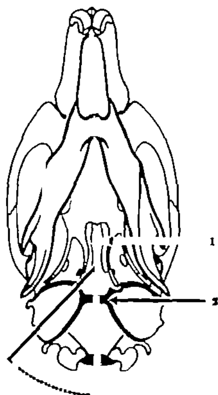
PLATE 1

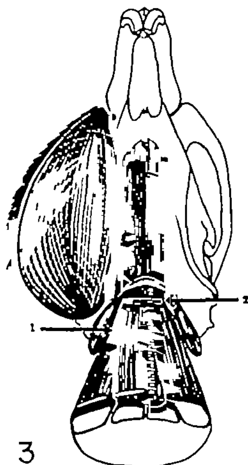
EXPLANATION OF FIGURES

1 Sagittal section of rat skull showing measurements recorded in text. Long axis indi cated by heavy line extending horizontally beyond the skull. Note rectangular regular ity 1 Length from nasal tip to occipital condyles. 2, Length from nasal tip to inion. 3 Length from spheno-presphenoid synchondrosis to spheno-occipital synchondrosis. 4 Length from spheno-occipital synchondrosis t basion. Arc indicated by dashed line with its center at inion, is th t around which the nuchal plane swings in the experi-mental animals.

2 Rat skull base with mandible in heavy outline 1, Spheno-presphenoid synchondrosis. 2, Spheno-occipital synchondrosis with lateral cartilage extensions for uditory bullae Arc indicated by dashed line is that around which bullae swings in the experimental animals.

3 Diagram ill strating experimental pproach. On the specimen right, the skin, masseter digastrics, sternohyoid and omohyoid muscles are indicated in their normal relations On the left the sternohyoid and omohyoid have been removed to show the positions of the trachea and esophagus and the skull outline shows the general relation to the whole skull. 1 Line of incision through the omohyoid muscle. 2, Position of the spheno-occipital synchondrosis behind the trachea, esophagus longus capitus and rectu capitus anterior muscles.


1
2
2


1
2
1
3

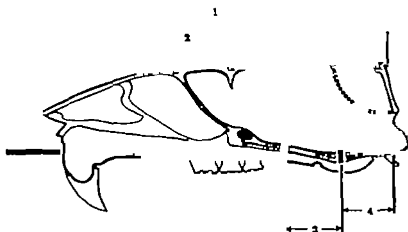

1
2
3
4

PLATE 2

EXPLANATION FIGURES

4 Sagittal section through normal rat skull base. The cartilage plate extend completely through the skull interrupting upper (inner) and lower (outer) cortical bony layers as well as medullary trabeculae. Horizontal rows of active cartilage cells can be seen with seemingly greater ctivity inferiorly Note the position of the posterior tip of the hypophysis just above the cartilage

5 Sagittal section through rat skull base after the spheno-occipital cartilage plate has been completely removed. Note the continuity of inner and outer cortical bony plates as well as medullary trabeculae. The sphenoid and occipital bones are continuous Note that the hypophysis shows no changes nd that the d ra mater has not been touched.


4.



PLATE 3

EXPLANATION OF FIGURES

6 Lateral view of the skull with synchondrosis removed.

7 Lateral view of the normal skull of the litter mate control.

8 Lateral radiograph of skull with synchondrosis removed. Note especially the kinked up contour of the inner outline of the skull base at the spheno-occipital fusion. (The outline has been lightened for clarity in printing.)

9 Lateral radiograph of normal skull of the same age. Note the smooth, flat, concave curve of the cranial base back to basion. (The outline has been lightened for clarity in printing.)

10 Outline of the experimental skull (solid line) superimposed on that of the normal skull (dashed line).

11 Skull base from which the spheno-occipital synchondrosis has been removed. The long axes of the auditory bullae indicated by the black line form a wide angle.

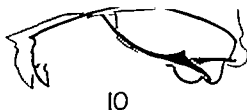
12 Skull base of normal litter mate control. The long axes and auditory bullae indicated by the black line form a narrow angle.


6.

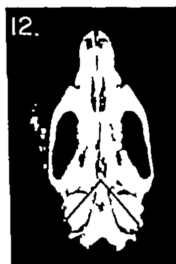

7.

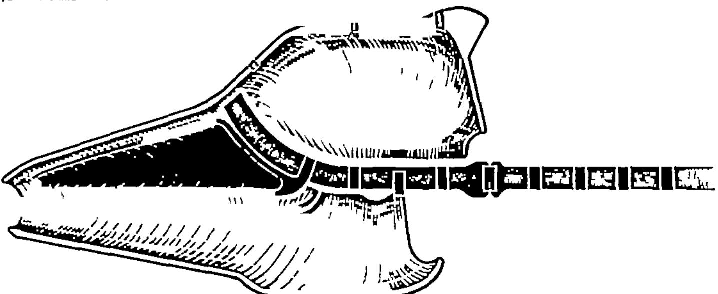

8.


9.


10


11.


12.



13 Model of the basic mammalian skull. Heavily stippled areas represent bone formed in cartilage. Black areas represent cartilage. The dermal bones form shell bove and below the plane of the skull base. Note th t the cartil ge of the condyle of the jaw is on the same plane as all other basal artilages and that the nasal capsule is n extension f the cartilage of the base (see text)

Regeneration of Gastric Mucosa in Rats[1,2]

SAMUEL FRANKLIN TOWNSEND[3,4]
Department of Anatomy The University of Michigan Medical School, Ann Arbor Michigan

Since Bensley's (1898) classical description of the specialized cell types in the gastric mucosal epithelium much uncertainty has existed concerning their life history Grant (45) Stevens and Leblond ('53) Hunt ('57) and Messier ('60) observed that both surface and mucous neck cells arise from the proliferation of cells in the neck region of the fundic gland and are sloughed off the mucous neck cells at their site of origin and the surface cells after moving to the surface of the mucosa. Hunt ('57) and Grant (45) concluded that other cell types in the glands are also lost. Harvey ('07) Ferguson ('28), and Hunt ('58) implied that parietal and chief cells are replaced by transformation from mucous neck cells but Stevens and Leblond ('53) and Messier ('60) denied the loss and replacement of these cell types.

In order to acquire more precise information concerning the origin of the various cell types in fundic glands, numerous investigators have studied their re-appearance in gastric mucosa following surgical or thermal injury to it (Harvey '07; Ferguson, '28; Gunter '50 Williams '53; Hunt, '58; Finckh and Milton, '60) These investigations revealed that (a) the first epithelial cells growing back into an injured area contain mucus and, at least in the newly-formed glands, come to resemble mucous neck cells except for their shape and nuclear structure and (b) the newly-formed chief and parietal cells seem to arise from these mucus-containing cells. However conclusive evidence for direct transformation of mucous cells to chief and parietal cells is lacking as is also information concerning the origin of argentophilic cells. Until such evidence is available the sources of these cells cannot be considered proven. Much of the difficulty in visualizing these transformations has arisen from the lack of techniques adequate for the demonstration of transitional forms.

The objective of this study was to secure cytological evidence concerning the cellular origin of the chief parietal and argentophilic cells as they arise in regenerating fundic stomach, utilizing newly modified staining techniques.

MATERIALS AND METHODS

Young adult female rats of the Sprague-Dawley strain were used. They were maintained in individual cages and were given water *ad libitum* throughout the experiment. All rats were fed a diet consisting of Purina Laboratory Chow supplemented weekly with fresh citrus fruit, vegetables and cod liver oil.

Seventy-two rats were utilized their mean body weight being 162 ± standard deviation of 22 gm before the lesion was placed in the stomach and 199 ± 40 gm at the time of sacrifice. In placement of the lesion, the stomach was exteriorized and a slit 6 mm in length was made in the forestomach while the animal was under sodium amytal anesthesia. The glandular mucosa was everted through this slit and stretched to smoothness over a blunt rod which was attached to the operating table. A circular piece of gastric mucosa 6 mm in diameter was removed from the glandular

---

[1] Supported in part by research grants to Dr Burton L. Baker from the National Institutes of Health, Public Health Service (A-131 C7 A 2841 C1) and the Upjohn Company

[2] Based on dissertation submitted in partial fulfillment of the requirements for the Doctor of Philosophy degree.

[3] This investigation was carried out during the tenure of Predoctoral Fellowship from the National Cancer Institute, United States Public Health Service. Deep appreciation is extended to Dr. Burton L. Baker for his direction of this investigation.

[4] Present address Department of Biology Kalamazoo College, Kalamazoo, Michigan.

stomach on the greater curvature and two to three millimeters inferior to the horizontal ridge. In doing this a skin punch 6 mm in diameter was applied to the stretched mucosa and an outline cut was made. With fine forceps one edge of the mucosa was lifted and the points of a pair of iridectomy scissors were slipped under the mucosa into the submucosa. This maneuver separated the mucosa from the submucosa and with the forceps the piece of mucosa was removed. The operated area was examined to make certain that all of the mucosa was excised. Following inversion of the glandular stomach the incision in the forestomach was sutured The time allowed for regeneration after excision of the mucosa and the number of rats used at each period were as follows: 4 hours 2 12 hours 1 1 day 2 36 hours, 2 2 days 2 4 days 2 5 days 1 6 days, 2; 7 days, 1 9 days 2; 10 days 8 11 days 3 12 days 1; 14 days 1; 15 days 6 20 days 9 21 days 1 25 days, 2; 28 days 2; 30 days, 9; 35 days, 4; 41 days 2 42 days, 2; 49 days 1; 56 days 2 63 days 1 70 days, 1

Histological and histochemical techniques Following killing of the rat by a blow on the head, the esophageal and duodenal ends of the stomach were ligated and 4 cc of either Zenker formol, Regaud's fluid or formalin-acetic acid-alcohol (FAA) fixative were injected into it subsequently the stomach was removed and placed in a bottle containing the fixative. This procedure stretched the stomach moderately and facilitated fixation. Six to 8 hours later the stomach was opened the lesion area was removed and fixation continued. The stomachs of 5 rats were stretched over corks after being opened along the lesser curvature. The lesion area was then removed, frozen and sectioned at 8 μ in a Cryostat. These sections were mounted on slides without albumen and incubated for 10 minutes at 37 C for the demonstration of succinic dehydrogenase (Nachlas et al. '57) Pieces of stomach that were fixed in Zenker formol for 24 hours and Regaud's fluid for 4 or 12 days were treated with 3% $K_2Cr_2O_7$ for three days dehydrated and embedded in celloidin and Tissuemat. They were sectioned at 2 to 4 μ. Pieces fixed in FAA for 48 hours were dehydrated cleared in carbon disulfide and embedded in Tissuemat. They were sectioned at 3 or 4 μ.

For the demonstration of mitochondria sections of the stomach fixed in Regaud's fluid were stained with the Severinghaus and Thompson ('39) Altmann Masson procedure. The colloidal iron and periodic acid-Schiff technique of Mowry ('58) was used on sections fixed in Regaud's fluid, Zenker formol or FAA for the demonstration of glycogen, acidic mucopolysaccharides and other carbohydrate-containing proteins and combined with 1% Bismarck brown in 1% acetic acid for nucleic acids. The Hotchkiss ('48) periodic acid-Schiff technique (PAS) for glycogen and carbohydrate-containing proteins was used in combination with Bodian protargol (Dawson and Barnett, 44) for argentophilic cells on sections fixed in FAA with Bowie's stain for pepsinogen granules (Bowie '36) on sections fixed in Regaud's fluid; and with methylene blue (0 05% solution containing 13.5% acetone and a citric acid-phosphate buffer at pH 5 6) and azure II-eosin (Lillie '54) for nucleic acids on sections fixed in Zenker formol FAA and Regaud's fluid. In order to determine whether or not the PAS-staining material was glycogen, some slides were incubated one hour at 37 C in a 1% solution of α-amylase in a 0 01 M Sorenson phosphate buffer (pH 7 0) before staining Control slides were incubated in the buffer solution without amylase

OBSERVATIONS

General histology

Four hours after the removal of a piece of mucosa bleeding had occurred into the lesion and the submucosa for some distance away from the lesion Microscopic examination verified the complete excision of mucosa and muscularis mucosae leaving the submucosa as the floor of the lesion. The size of the lesion varied considerably due to contraction of the surrounding muscularis mucosae

The established mucosa was normal except for a slight increase in blood cells

The term established mucosa will be used to indicate the mucosa adjacent to the lesion and "regenerating mucosa that which i newly formed in the lesion

in the lamina propria of some sections immediately adjacent to the lesion.

By the *12th hour* after the operation the lesion itself was unchanged while in the established mucosa the glands nearest the edge were tipped towards the lesion but still contained their normal types of cells (fig 3) The lamina propria was congested with blood for a considerable distance away from the lesion s edge, the degree of congestion being greatest adjacent to the edge (fig 1) Proximal to the lesion the congestion involved all of the mucosa but distally it was restricted to the superficial lamina propria.

Twenty-four hours after the operation bleeding had ceased and the lesion and neighboring submucosa contained clotted blood. Continuous with the surface cells of the established mucosa but lying out on the clot was a ledge of epithelial cells which was not composed of normal surface cells (fig. 2) They were oval to columnar in shape contained round to oval nuclei with prominent nucleoli and their cell membranes were not always distinguishable. The most superficial cells contained PAS-positive mucus apically; the deeper cells lacked mucus and close to the established mucosa a few flattened parietal cells were observed in the ledge

Congestion of the lamina propria of the established mucosa had increased and in some sections was so extensive that the glands were widely separated. Many of the epithelial cells of these glands were flattened but could still be distinguished as to type (fig. 12) The chief cells were smaller exhibited less cytoplasmic basophilia and contained fewer pepsinogen granules their nuclei and nucleoli were prominent. The parietal cells were small but more normal in appearance than the chief cells. Mitotic figures were prevalent in the established mucosa adjacent to the lesion which agrees with the observations of Hunt ('58) who showed that at this time the mitotic rate of foveolar and surface cells adjacent to the lesion was increased over that of the mucosa some distance away from the lesion.

Thirty-six hours after the operation the epithelial ledge had changed in form and extended further out onto the lesion. The ledge was composed of flattened cells with spindle-shaped nuclei which contained

EFFECTS OF THE OPERATION ON THE MUCOSA BORDERING THE LESION

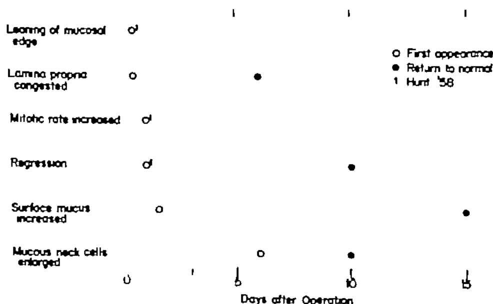


Figure 1

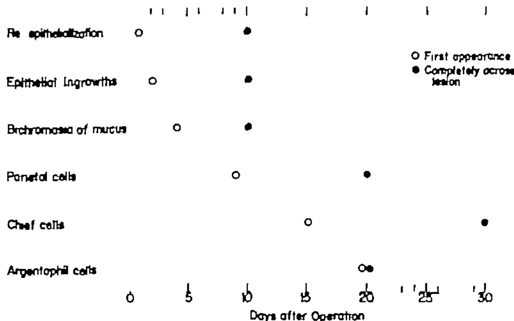


Figure 2

prominent nucleoli (fig 9) The ledge varied from one to about three cell layers in thickness. Sparsely distributed mucus continued to be present in the superficial cells.

The proximal one or two glands in the established mucosa showed evidence of regression (fig 13) They were lined by flat to oval, distinctly basophilic cells with prominent nuclei and nucleoli. No chief cells could be identified in these glands but a few flattened, elongated parietal cells were distinguished. Congestion of the lamina propria was often marked in these areas. Mitoses were observed at all levels in these regressed glands. The foveolar cells for some distance from the edge of the lesion were increased in number and in the density of their mucus content. The amount of mucus contained in surface cells was also increased.

At *two days* the submucosa under the lesion exhibited some evidence of granulation tissue formation. The epithelial ledge had advanced further out on the granulation tissue and had begun to send ingrowths into it. These ingrowths were composed of spindle-shaped cells some ingrowths exhibited narrow lumina while others were compact.

In the established mucosa the amount of mucus in surface and foveolar cells was increased over that in 36-hour specimens while the congestion of the lamina propria was decreased. The epithelial cells in the glands on the edge of the lesion had enlarged and become more intensely basophilic. Chief cells were indistinguishable in these glands and parietal cells were few in number

At *4 days* granulation tissue filled the lesion and epithelial ingrowths were numerous and more extensive (fig. 10) The cells in the ingrowths closest to the edge of the established mucosa were large and basophilic and contained large nuclei and distinct nucleoli. Some of these cells contained mucus which was stained bichromatically by colloidal iron and PAS some being purple and some red. The basal ends of the ingrowths were still composed of spindle-shaped cells. The epithelial ledge above the deepest ingrowths was composed of many layers of cells and the cells of the free surface were identical to surface and foveolar epithelial cells

In the regressed glands at the edge of the lesion, the mucous neck cells were increased in size and number The foveolar cells penetrated deeper into the lamina *propria* and the basophilic cells that lined the glands below the level of mucous neck cells also contained mucus scattered throughout their cytoplasm; it was most concentrated in the apical region (fig. 14) *Mitotic* figures were prevalent in these basophilic cells.

In the lesion area on the *6th day* the epithelial ingrowths from the ledge were deep and consisted of large basophilic cells which contained mucus (fig. 17) The cells lining the upper portion of the ingrowths were similar in staining characteristics to surface and foveolar cells while the mucus in those in the basal half was stained bichromatically by colloidal iron and PAS as were the mucous neck cells in the normal mucosa. The mucus in some cells was entirely purple and in others red, or both reactions were seen in the same cell. These ingrowths could be classified as glands or foveolae on the basis of this staining reaction. The leading portion of the ledge was composed of tall columnar cells which contained densely packed mucus in their apices and scattered granules throughout their cytoplasm (fig. 11)

The most striking feature of the established mucosa at the 6th day was the continued increase in surface and foveolar mucus (fig. 4) The enlarged foveolar cells extended one-half the distance to the muscularis mucosae at the edge of the lesion but more distally approximated normality in these characteristics. The enlarged mucous neck cells (figs. 15 and 16) lined the superficial three-quarters of the glands and chief and parietal cells the basal one-fourth except in the proximal few regressed glands where they were replaced by large basophilic mucus-containing cells. In the regressed glands transitional stages between mucous neck cells and chief and parietal cells were observed (fig. 19)

On the *9th day* the lesion was well filled with granulation tissue and the ledge of new growth had covered all but a small area (fig. 5) The epithelial ingrowths had for the most part reached a level that corresponded to that of the muscularis mucosae in the established mucosa. The ingrowths all exhibited lumina, many of which were large and irregular in shape. The lining was identical to that found at 6 days except for an occasional parietal cell located basally in the glands closest to the edge of the lesion.

The amount of surface mucus foveolar depth and size and number of mucous neck cells in the established mucosa were the *same as in the 6-day specimen. Regressive* changes in two or three glands proximal to the lesion in the established mucosa were no longer evident except for the presence of a few scattered large basophilic mucus-containing cells amongst the parietal and chief cells.

The lesion was re-covered by epithelium in all but one animal by the *10th day* and in all animals sacrificed subsequently (fig. 6) The epithelial ingrowths had increased in number and all of them could be subdivided into foveolae and glands. The depth and number of foveolar cells, the size and number of mucous neck cells and the amount of surface mucus in the established mucosa were nearly normal. The glands in the established mucosa immediately adjacent to the lesion were normal in cell content.

Fifteen days after the operation the mucosa bordering the lesion had resumed a normal appearance and the ledge itself had changed little from its condition at 10 days (fig. 1). The only [illegible] changes which occurred after 15 days were a further filling in of the lamina propria by branching of previous epithelial ingrowths and the formation of more of the special and epithelial cell types. At 70 days the newly formed mucosa differed from normal mucosa in the following ways: a muscularis mucosae was lacking, the number of specialized epithelial cell types was slightly lower and the mucous membrane was somewhat thinner than is true of normal mucosa.

Cytogenesis of special cell types

Chief cells A transformation from cells that contained mucus to chief cells was observed in three locations: between the 6th day and 9th day after the operation in the glands immediately adjacent to the lesion (fig. 19) on the 10th day and throughout the rest of the regeneration period [illegible]

epithelial ingrowths from the ledge (fig. 8) and in glands of the established mucosa regardless of the distance from the lesion (fig 20) In the regressed glands of the established mucosa the source cell was the usually cuboidal, basophilic cell that contained mucus scattered throughout its cytoplasm. In the established mucosa some distance away from the mucosa that was obviously affected by the operation the source cell was the mucous neck cell of the fundic gland. In the epithelial ingrowths the source cell was the basophilic cell that contained mucus with tinctorial and structural characteristics similar to those of the normal mucous neck cell.

In sections stained with PAS and Bowie's stain for pepsinogen granules the cells in transition exhibited the presence of blue pepsinogen granules encompassed by PAS-positive red mucus (figs. 18 and 20) As the Bowie-positive granules cytoplasmic basophilia cell size and nuclear size increased, the amount of mucus decreased until it was no longer present. In sections treated with α-amylase this transition was still observed since the enzyme did not remove the mucoprotein. In sections stained with PAS and azure II-eosin the cytoplasm above the nucleus contained mucus along with vacuoles in the transitional forms (fig. 19) These vacuoles were left by failure of the fixative to preserve granules

Parietal cells Sections treated for succinic dehydrogenase to reveal mitochondria and those stained with eosin demonstrated the presence of parietal cells in the basal portion of the epithelial ingrowths on the 9th day and the presence of parietal cells in all ingrowths across the lesion by the 20th day after the operation (fig. 7) Parietal cells arose in the same sites and from similar mucus-containing cells as was true for chief cells. This transformation was revealed most clearly in preparations stained with colloidal iron and PAS or with PAS and azure II. One of the most striking early changes was the development of dense cytoplasm around the nucleus (figs 21 and 22) The transition in all locations further involved a loss of cytoplasmic basophilia and mucus enlargement of the cell its nucleus and nucleolus and an increase in the number of mitochondria. The increase in size of the cell, nucleus and nucleolus occurred simultaneously with the decrease in basophilia. The resulting cell was parietal cell-like in all characteristics except the amount of mucus in its apical cytoplasm. This appeared to be pushed out of the cell into the lumen of the gland. With loss of the large mass of mucus from the cell delicately disposed material in the supranuclear region continued to stain with the colloidal iron-Prussian blue reaction and appeared to be associated with the intracellular canaliculi.

Argentophilic cells. Argentophilic cells appeared in the regenerating mucosa on the 20th day after the operation (fig. 23) The first ones appeared in the regenerating area in no spatial pattern and others followed in a random manner. In slides stained with PAS and Bodian protargol no transitional stages were observed between mucous cells and argentophilic cells in either the established mucosa or in the regenerating mucosa.

DISCUSSION

Factors influencing the timing of regenerative changes

The time required for general histological repair of the gastric mucosa resembled rather closely that observed by other authors. This is surprising because many variable factors make such a correlation difficult. First, varied methods have been used to injure the mucosa. These procedures include cautery (Williams, '53 Hunt '58; Skoryna et al. '58) scraping of the mucosa down to basal ends of the fundic glands (Finckh and Milton, '60) suction biopsy (Gunter '50) ulceration pursuant to pyloric ligation (Shay et al. 45) injury due to gastro-enterostomy (Harvey '07) and surgical excision of portions of the mucosa (Ferguson '28 Janowitz et al., '55 Myhre '56) Secondly previous studies have been carried out on several different species. Thirdly within a given experiment, partial closure of the lesion by contracture of surrounding tissue complicated the timing of cellular events.

Finally the regression of specialized epithelial cell types in glands bordering the lesion to a more nondifferentiated type made extremely difficult the precise identification of old regressed glands as opposed to newly regenerated ones particularly be-

tween the 4th and 9th days after placement of the lesion. The positional relationship of the glands to the cut end of the muscularis mucosae helped somewhat in making this determination. However since the glands of the established mucosa at the edge leaned over onto the lesion by the 12th hour some of the value of the muscularis mucosae as a landmark was lost. Somewhat similar regressive changes following injury to the gastric mucosa have been observed by Harvey ('07) Ferguson ('28) Hunt ('58) and Finckh and Milton ('60)

Similarity of regeneration to the processes of embryogenesis. During embryonic development of the fundic mucosa in cat and man all glands first became lined with mucoid cells and subsequently parietal and chief cells appeared in that order (Lim, '22) Kirk ('10) observed a similar order in the appearance of parietal and chief cells but did not find mucus in all of their progenitor cells. Thus, in the regenerating rat mucosa, the formation of ingrowths of mucoid cells from the early epithelial ledge, followed by the successive appearance of parietal and chief cells, duplicates in a general way the events of embryogenesis

Origin of specialized cell types. All previous workers are agreed that the first cell type to appear in regenerated glands is a mucus-containing cell. Ferguson ('28) and Hunt ('58) identified it as a mucous neck cell. As evidence in support of this identity can be cited the similar structure and staining capacity of the mucoprotein in the two types of cells as revealed by PAS and the bichromatic properties of the mucoprotein when stained with the colloidal iron-PAS procedure. Also, in sections of the lesion area, mucous neck cells formed a zone through the established mucosa which was continuous with the mucoid cells of the regenerated glands at the edge of the lesion. Finally by the 30th day and following neoformation of abundant chief and parietal cells in deeper portions of new glands mucoid cells remained in the superficial portions of the glands and were indistinguishable from mucous neck cells. Suggesting lack of identity of mucoid cells in regenerated glands with mucous neck cells were differences in size and shape of the cell as well as in size and structure of nuclei and nucleoli. Although the identity of the two cell forms is not established presently available evidence indicates that they are the same.

Harvey ('07) Ferguson ('28) and Hunt ('58) concluded previously that mucus-containing cells transform into parietal and chief cells. With respect to chief cells, Harvey reported the presence of mucus and zymogenic granules in the same cell. These demonstrations were not achieved contemporaneously but necessitated prior staining of zymogenic granules with neutral gentian followed by extraction of this dye and subsequent staining of mucus with mucihematin. Ferguson ('28) failed to demonstrate zymogenic granules in the dog. In parietal cells at the neck of fundic glands, Harvey ('07 fig 4) observed that neutral gentian stained large masses of material the nature of which was not established. This material was undoubtedly the mucus demonstrated in my study by staining with PAS and the colloidal iron-Prussian blue reaction. The present study reinforces the conclusion of these authors that mucous cells transform into chief and parietal cells by providing cytologic evidence of the existence of transitional forms. This was accomplished by combining the PAS procedure for mucoprotein with the Bowie technique for pepsinogen granules after fixation in Regaud's fluid followed by post-chromation. Similarly a combination of PAS colloidal iron (Mowry '58) and Bismarck brown provided an excellent demonstration of transitional parietal cells. The combination of PAS and azure II and eosin was helpful in the study of the origin of both chief and parietal cells. The conclusion that mucus-containing cells may transform into parietal and chief cells stands in contrast to that of Stevens and Leblond ('53) who were unable to find such evidence after staining with PAS and hematoxylin.

The presence of cells which are transitional between two other types does not by itself reveal the direction in which change is occurring. Indeed, Ferguson ('28) concluded that chief parietal and foveolar cells can change into mucous neck cells; in the present study evidence was obtained for the regression of chief and parietal cells

into a mucus-containing cell. However the order of appearance of cell types in the regenerating mucosa and the fact that immature surface mucous cells and mucous neck cells constitute the primary proliferating types in the normal gastric mucosa, make the transformation of mucous neck to chief and parietal cells more likely in the normal situation.

The failure to find transitional forms between mucoid cells and argentophilic cells indicates that the cellular source of argentophilic cells is different from that of the chief and parietal cells. The random pattern of appearance of these cells also sets them apart. In contrast, chief and parietal cells arose first basally in the new glands along the edge of the lesion and then appeared in the new glands farther out in the lesion area. Since mucoid cells were never observed in transition to argentophilic cells only the cells normally found in the connective tissue and in the blood stream are left as probable sources for this cell type.

Turnover of epithelial cells The present observations bear upon the currently debated problem of cell turnover in the rat stomach. Messier ('60), using H^3-thymidine labeling, observed that surface and mucous neck cells undergo turnover but concluded that chief and parietal cells do not. Myhre ('60) and Hunt and Hunt ('61) utilized the same approach and found that labeling did occur deep in the glands of the fundic stomach. The Hunts observed following the administration of 48/80 that the location of labeled cells moved progressively from the neck region to the basal portion of the gland and that the type of cell labeled changed from the mucous neck variety to chief and parietal cells. Therefore they concluded that mucous neck cells change into chief and parietal cells. My observations support their position.

SUMMARY

The origin of chief, parietal and argentophilic cells was studied in the regenerating and established gastric mucosa of rats after excision of a circular area of mucosa. In the *established* mucosa at the edge of the lesion between the first and 4th days the lamina propria was congested with blood, the amount of surface mucus was increased, mucous neck cells were enlarged, and the chief and parietal cells had become flattened and apparently transformed into basophilic mucus-producing cells. Between the 4th and 10th days, the amount of surface mucus remained high, the congestion of the lamina propria decreased, and the chief and parietal cells appeared to arise by direct transformation from mucus-containing cells.

In *healing of the lesion* an epithelial ledge composed of mucus-containing cells arose at the rim of the lesion from the surface epithelium on the first day It grew over the denuded submucosa and from it cellular projections extended into the underlying granulation tissue. These ingrowths developed lumina and mucus soon appeared in the constituent cells. The occurrence of transitional cell types was interpreted to indicate that these mucus-containing cells as well as mucous neck cells transform into chief and parietal cells. Argentophilic cells also arose in the regenerating mucosa but transitional stages from mucus-containing cells were not observed.

LITERATURE CITED

Bensley R. R. 1898 The structure of the mammalian gastric glands. Quart. J Micr. Sci., 41: 361–382.

Bowie, D. J 1935 A method for staining the pepsinogen granules in gastric glands. Anat. Rec., 64 357–368.

Dawson, A. B., and J Barnett 1944 Bodian protargol method applied to other than neurological preparations. Stain Technology 19. 115–118.

Ferguson, A. N 1928 A cytological study of the regeneration of gastric glands following the experimental removal of large areas of mucosa. Am. J Anat., 42: 403–441.

Finckh, E. S., and G. W Milton 1960 Regeneration of gastric mucosa from differentiated cells. J. Path. Bact., 80: 143–145.

Grant, R. 1945 Rate of replacement of the surface epithelial cells of the gastric mucosa. Anat. Rec., 91 175–185.

Gunter G. S. 1950 A histological investigation of the healing of acute gastric ulceration in the cat. Gastroenter., 15 709–717

Harvey B. C. H. 1907 A study of the structure of the gastric glands of the dog and of the changes they undergo after gastroenterostomy and occlusion of the pylorus. Am. J Anat., 6: 207–243.

Hotchkiss, R. D 1948 A microchemical reaction resulting in the staining of polysaccharide structures in fixed tissue preparations. Arch. Biochem., 16 131–141.

Hunt, T. E. 1957 Mitotic activity in the gastric mucosa of the rat after fasting and refeeding. Anat. Rec. 127 335-350.

——— 1958 Regeneration of the gastric mucosa in the rat. Ibid. 131 193-212.

Hunt, T. E. and E. A. Hunt 1961 The mitotic ... of the gastric mucosa of the ... after animal tion with ... compound 48/80. Ibid. 13 ... 45- ...

Janowitz, H. D. ... A. Weinstein ... F. H. Hollander 19... Effect of cortisone on the healing of experimental gastric ulcer. Fed. Proc. 14 79.

Kirk, E. G. 1910 On the histogenesis of gastric glands. Am. J. Anat. 10 473-19...

Lillie, R. D. 1954 Histopathologic Technic and Practical Histochemistry. The Blakiston Division, McGraw-Hill C... Inc., New York.

Lim, R. K. S. 1922 The gastric mucosa. Quart. J. Micr. Sci. 66 18-212.

Messier, B. 1960 Radioautographic evidence for the renewal of the mucous ... in the gastric mucosa of the ... A... Rec. 136 ... 42.

Mowry, R. W. 19...8 Improved procedure for the staining of acidic polysaccharides by Muller's colloidal (hydrous) ferric oxide and its combination with the Feulgen and periodic acid Schiff reactions. Lab. Invest. 7 ...-57...

Myhre, E. ... Regeneration of the fundic mucosa in ... effect of ... and of ... tion. A. M. A. Arch. Path. 62 30-3...

——— 19...2 Regeneration of the fundic mucosa ... radioautographic study on the effect of cortisone. Ibid. ... 476-483.

Nachlas, M. M., K. C. Tsou, E. de Souza, C. S. Cheng and A. M. Seligman 195... Cytochemical demonstration of succinic dehydrogenase by the use of a new p-nitrophenyl ... tetrazole (NBT). J. Histochem. Cytochem. 5 420-436.

Severinghaus, A. E. and K. W. Thompson 19... Cytologic ... produced ... the hypophysis ... prolonged administration of pituitary extract. Am. J. Path. 15 391-412.

Sh... H. S. A. Rowe ... S. ... D. M... M. Greenwood and H. S... 1945 A simple method for the uniform ... of ... ulceration in the ... Gastroenterology ... 43-61.

Skoryna, S. C., D. R. Webster ... D. S. Kahn 1958 A new method of production of experimental gastric ulcer. The effect of hormonal factors on healing. Ibid. 34 1-10.

Stevens, C. E. ... C. P. Leblond 1953 Renewal of the mucous cells in the gastric mucosa of the rat. Anat. Rec. 115 231-45.

Williams, A. W. 1953 Observations on the healing of experimental gastric ulcers in small laboratory animals. Brit. J. Surg. 41 315-3...

into a mucus-containing cell. However the order of appearance of cell types in the regenerating mucosa and the fact that immature surface mucous cells and mucous neck cells constitute the primary proliferating types in the normal gastric mucosa, make the transformation of mucous neck to chief and parietal cells more likely in the normal situation.

The failure to find transitional forms between *mucoid cells and argentophilic cells* indicates that the cellular source of argentophilic cells is different from that of the chief and parietal cells. The random pattern of appearance of these cells also sets them apart. In contrast, chief and parietal cells arose first basally in the new glands along the edge of the lesion and *then appeared in the new glands farther* out in the lesion area. Since mucoid cells were never observed in transition to argentophilic cells only the cells normally found in the connective tissue and in the blood stream are left as probable sources for this cell type.

Turnover of epithelial cells. The present observations bear upon the currently debated problem of cell turnover in the rat stomach. Messier ('60) using H^3-thymidine labeling, observed that surface and mucous neck cells undergo turnover but concluded that chief and parietal cells do not. Myhre ('60) and Hunt and Hunt ('61) utilized the same approach and found that labeling did occur deep in the glands of the fundic stomach. The Hunts observed following the administration of 48/80 that the location of labeled cells moved progressively from the neck region to the basal portion of the gland and that the type of cell labeled changed from the mucous neck variety to chief and parietal cells. Therefore, they concluded that mucous neck cells change into chief and parietal cells. My observations support their position.

SUMMARY

The origin of chief parietal and argentophilic cells was studied in the regenerating and established gastric mucosa of rats after excision of a circular area of mucosa. In the *established* mucosa at the edge of the lesion between the first and 4th days the lamina propria was congested with blood, the amount of surface mucus was increased, mucous neck cells were enlarged, and the chief and parietal cells had become flattened and apparently transformed into basophilic, mucus-producing cells. Between the 4th and 10th days the amount of surface mucus remained high the congestion of the lamina propria decreased, and the chief and parietal cells appeared to arise by direct transformation from mucus-containing cells.

In *healing of the lesion* an epithelial ledge composed of mucus-containing cells arose at the rim of the lesion from the surface epithelium on the first day It grew over the denuded submucosa and from it cellular projections extended into the underlying granulation tissue. These ingrowths developed lumina and mucus soon *appeared in the constituent cells.* The occurrence of transitional cell types was interpreted to indicate that these mucus-containing cells as well as mucous neck cells transform into chief and parietal cells. Argentophilic cells also arose in the regenerating mucosa but transitional stages from mucus-containing cells were not observed.

LITERATURE CITED

Bensley R. R. 1898 The structure of the mammalian gastric glands. Quart. J. Micr. Sci., 41 361–389

Bowie, D. J 1936 A method for staining the pepsinogen granules in gastric glands. Anat. Rec., 64 357–368

Dawson, A. B and J Barnett 1944 Bodian's protargol method applied to other than neurological preparations. Stain Technology 19 115–118.

Ferguson, A. N. 1928 A cytological study of the regeneration of gastric glands following the experimental removal of large areas of mucosa. Am. J Anat., 42: 403–441.

Florkh, E. S and G. W Millton 1960 Regeneration of gastric mucosa from differentiated cells. J Path. Bact., 80: 143–145.

Grant, R. 1945 Rate of replacement of the surface epithelial cells of the gastric mucosa. Anat. Rec., 91 175–185

Gunter G. S. 1950 A histological investigation of the healing of acute gastric ulceration in the cat. Gastroenter., 15 706–717

Harvey B. C. H. 1907 A study of the structure of the gastric glands of the dog and of the changes they undergo after gastroenterostomy and occlusion of the pylorus. Am. J. Anat., 6: 207–243.

Hotchkiss, R. D. 1948 A microchemical reaction resulting in the staining of polysaccharide structures in fixed tissue preparations. Arch. Biochem., 16 131–141.


E
4
5
7
8
P
M

PLATE 2

EXPLANATION OF FIGURES

The sections of gastric mucosa illustrated on this plate were fixed in Zenker-formol and stained with the PAS azure II-eosin technique.

9 Early epithelial ledge formation, 36 hours after injury A thin layer of epithelial cells continuous with the surface epithelium of the established mucosa has moved out onto the blood clot that fills the lesion. × 560.

10 Early epithelial ingrowths 4 days after surgery Epithelial ingrowths from the ledge are composed of basophilic cells with large nuclei and prominent nucleoli. Some ingrowths exhibit lumina, others are compact epithelial masses. × 360.

11 The epithelial ledge t 6 days. The leading edge of the ledge of epithelial cells and the formation of new glands are shown. Some of the cells in the new growth are dividing (arrows) × 736.

12 Regression 24 hours after surgery in the established mucosa adjacent to the lesion showing flattened parietal (RP) and chief (RC) cells. Compare RP and RC with more normal parietal (P) and chief (C) cells. × 560.

13 Regression 36 hours after surgery in the established mucosa adjacent t the lesion showing two normal glands (on the left) and several regressing glands (arrows) × 560.

14 Regression 4 days after surgery in the established mucosa adjacent to the lesion showing the extent of the process and the presence of mucus (arrow) in the regressed glands. × 96.


9
10
11
12
13
14
RC
RP

PLATE 3

EXPLANATION OF FIGURES

15 Enlarged mucous neck cells in the established mucosa adjacent to the lesion 6 days after injury Zenker formol fixation, PAS and azure II-eosin. × 1030.

16 Normal mucous neck cells in the established mucosa some distance way from the lesion 6 days after injury Zenker formol fixation, PAS and azure II-eosin. × 1030.

17 Epithelial ingrowth 6 d ys after surgery Large basophilic cells which contain mucus and ultimately give rise to other cell types are shown. Zenker formol fixation, PAS and azure II-eosin. × 1030.

18 Chief cell origin in epithelial ingrowth 15 days after injury At M is mucoid cell in which the mucus stained with PAS ppears gray At T are transitional cells in which the background mucus stained with PAS is gray but in which pepsinogen granules (black) are also revealed by the Bowie stain. Several other transitional cells are also present. Fixation in Regaud's fluid PAS and Bowie stain × 968

19 Chief cell restoration in regressed glands of the established mucosa adjacent t the lesion 6 days fter urgery showing chief cell with vacuolated cytoplasm nd small amount of perinuclear basophilia (C) mucoid cells with dark mucus (M) and transitional forms with enlarged nuclei, basophilic cytoplasm, mucus, and vacuoles left by nonpreserved pepsinogen granules. Zenker-formol fixation, PAS and azure II-eosin. × 1030.

20 Chief cell origin in established glands some distance way from the lesion. The evidence for cell metamorphosis is similar to that illustrated in the regenerating mucosa (fig. 18) At M are mucous neck cells, at T transitional cells containing both mucus and Bowie stained pepsinogen granules and t C and elsewhere, chief cells which no longer show mucus. Fixation in Regaud fluid, PAS and Bowi stain. × 1030.

21 Epithelial ingrowths in the regenerating mucosa 15 days after surgery showing transformation of mucoid cells to parietal cells. Several cells are illustrated (P_{1-3}) which basally contain the typical dense cytoplasm of parietal cells and in their pices, masses of mucus of variable size. These cells are regarded as transitional cells. Zenker-formol fix tion, colloidal iron and PAS. × 968

22 Parietal cell origin in the established mucosa some distance w y from the lesion 15 days after surgery Illustrated are an early stage (P) late stage (P) and mucous neck cell (M) Zenker formol fixation, colloidal iron nd PAS. × 968.

23 An argentophilic cell in an epithelial ingrowth 20 days after surgery Illustrated are an argentophilic cell (A) and mucoid cells (M) FAA fixation, PAS and protargol. × 1030.


15
16
M
17
18
M
T
T
C
19
C
M
M
20
M
T
T
C
21
P
M
22
P
M
P
23
M

The Transfer of Serum Proteins from Mother to Young in the Guinea Pig

I. PRENATAL RATES AND ROUTES[1]

JOHN C. LEISSRING[2] AND JOHN WALBERG ANDERSON
Department of Anatomy University of Wisconsin, Madison, Wisconsin

In recent years, the long recognized ability of mammals to provide a passive immunization of their young either before or shortly after birth or both (Ehrlich, 1892) has been the subject of an extended series of investigations, stemming primarily from Brambell's laboratory (see Brambell, '58 for review) In every mammal thus far studied, with the important exception of the rhesus monkey (Bangham, Hobbs and Terry '58) the chorioallantoic placenta has been ruled out as the route of prenatal immunization. This has been in contrast with the ideas of earlier workers (Mossman, '26 Mason Dalling and Gordon, '30) who attempted to correlate the prenatal transference of antibodies with the thickness of the chorioallantoic placental barrier as outlined in Grosser's scheme ('09 '26) The recent findings have focussed attention upon the vitelline circulation and/or the fetal gut as the routes of transfer of antibodies In the case of the rabbit, the yolk sac and the vitelline circulation have been shown to be the major route of absorption of antibodies (Brambell et al., 48 49 '50); while in the rat on the 19th day of gestation, both the vitelline circulation and the fetal gut are capable of this function (Brambell and Halliday '56)

Most of the mammals in which prenatal transference of immunity has been studied have a relatively short gestation period with the young born in an immature state. The guinea pig on the other hand, although its fetal membranes are like those of the rat and rabbit throughout most of gestation (see fig 1) has a relatively much longer gestation period (65–70 days) and the young are born in a very mature condition. A study of this animal was therefore undertaken with the idea of comparing the passive immunization of the young in this species with that in the rabbit. It will be seen that there are several features of the phenomenon which differ from those of the rabbit.

Although a considerable volume of work has appeared on the rates and routes of passive immunization of the young in some other mammals, reports on this phenomenon in the guinea pig are few Kitasato (1889) was the first to study the guinea pig, followed by Vaillard (1896) Remlinger (1899) and Staübli ('03) The prenatal nature of immunization of the young was stressed in the latter three reports, and Remlinger (1899) stated that agglutinins are not transmissible by the milk. In more recent years, Hartley's (48 '51) discovery of the selective preference for homologous antibodies in the transfer phenomenon was made using the guinea pig. Neither Hartley however nor Schneider and Szathmáry (40) nor Jo-Keiichiro ('53) presented information as to the varying rates or routes of prenatal transfer of antibodies in the guinea pig

The experiments of Barnes ('59) which appeared after the present study was begun, showed that beginning on about the 35th day of gestation antitoxins were secreted into the uterine lumen and were absorbed by the yolk sac and vitelline circulation. According to her the transfer reached a maximum between 60 and 66 days, and fell thereafter. No entry by way

---

[1] Supported by National Institutes of Health Grant H-3331 and by the Wisconsin Alumni Research Foundation.

[2] Part of the material reported in the three papers of this series was presented to the Faculty of the University of Wisconsin in partial fulfillment of the requirements for the degree of Master of Science, and was also presented at the VIIth International Congress of Anatomists, 1960.

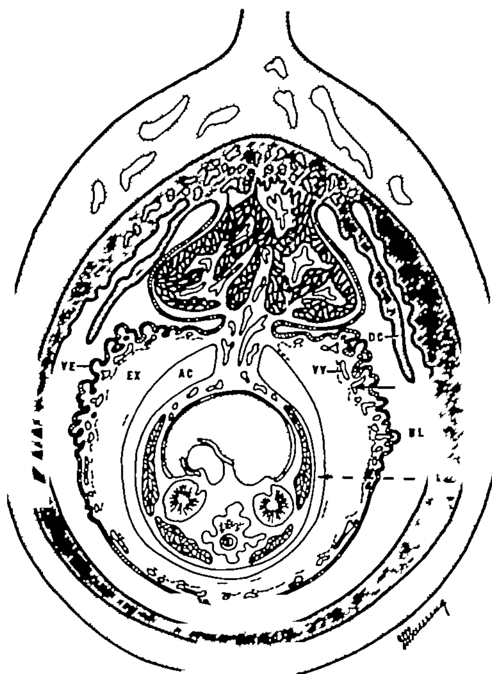


Diagram of the definitive guinea pig fetal membranes (after Moesman, '37) This condition persists from approximately 33 days until term. By this stage, the decidua capsularis has ruptured, but remains as a projection from the decidua basalis. At earlier stages, the decidua capsularis was in direct contact with the vascular splanchnopleure of the yolk sac; the parietal wall of the yolk sac never forms in this species.

Here, as in many rodents in the definitive condition the highly villous, vascular splanchnopleure is now in contact with the uterine luminal fluids. The predominant route of early antibody transfer is shown with the solid arrow the later route is bown with the dashed arrow

AC Amniotic cavity
DC Decidua capsularis
EX, Exocoelom
UL, Uterine lumen
VE, Visceral entoderm
VV Vitelline vessel

of the fetal gut was detected nor was any postnatal transfer noted. There are several points of the present report which differ from the results of Barnes.

MATERIALS AND METHODS

Nineteen timed-pregnant female guinea pigs (with a total of 50 fetuses) were actively immunized beginning on the first day of gestation using a saline suspension of phenol killed *Brucella abortus* These animals were killed at varying stages of gestation, and maternal sera, fetal sera and fetal fluids were collected for serological titration Sera from the mothers were used in passively immunizing 19 other pregnant females (with a total of 53 fetuses) at progressive stages of gestation 24 hours later these females were killed, and the same fluids were collected. The amount of serum used in the passive immunizations ranged from 5 to 14 ml.

The actively immunized mothers were studied at stages of gestation ranging from 16 to 68 days. The earliest stage at which pregnant females were passively immunized was 45 days and the young of the latest-stage experiments were born before the experiment had ended.

Since guinea pigs normally produce relatively low antibody titers as detected by standard agglutination technics, a modification of the "Coombs test was used in serological determinations (Coombs Mourant and Race, 45; Jones, '53 Wagner and Kuhns, '53; Brahic, Tamalet, Tamalet and Madet, '53) Guinea pig anti-*Brucella* serum with a titer of 1 320 in the agglutination test had a titer of 1 5120 with the "Coombs test. Repeated tests showed that washing the antiserum-absorbed *Brucella* organisms before addition of the Coombs serum had no effect on the titer and accordingly this step was eliminated. The definitive procedure was found to yield titers equal to those obtained by the Coombs test as presented by Jones ('53) It was concluded that the procedure was a reliable measure of the total amount of complete and "incomplete antibody in the sera tested.

Wherever possible, the titers of maternal and fetal sera were compared by means of concentration quotient (C.Q) a term introduced by Batty Brambell Hemmings and Oakley ('54) The C.Q is the ratio of fetal concentration/maternal concentration. By this means variations in maternal titers (and therefore in the amount of antibody available to the fetuses) are cancelled out in the calculations and the results of the different experiments can be directly compared.

Various surgical interventions were employed in an attempt to demonstrate the effective routes of transfer at different stages of gestation. The different procedures were as follows:

A. Uterine wall and fetal membranes incised parallel to major vessels fetus with attached membranes left free in uterine cavity

B As in A in addition vitelline vessels were ligated and yolk sac removed.

C. As in B; in addition, a ligature was placed around the mouth and nose of the fetus.

D Fetuses freed as in A mouth and nose ligated.

After the peritoneal cavity had been closed 5 ml of antiserum was injected into the maternal peritoneal cavity and two hours afterwards fluids were collected from the still viable fetuses.

OBSERVATIONS

The results of the prenatal transfer experiments both active and passive are expressed in tables 1 and 2. It can be seen that, in the actively immunized females transfer to the fetal circulation begins at a relatively low rate by 35 days (the earliest stage at which adequate blood samples could be obtained) increases until approximate equilibrium is reached by 50 days and continues at this high rate to term.

In the passively immunized females within 24 hours a titer about ¼th that of the mother was obtained at 45 days. Later stages showed an increasing C.Q within 24 hours and 60-day pregnant females came to equilibrium with their fetuses within this time period, as did females at later stages up to term. These data

Battey et al. ('54) have expressed the C.Q as the ratio fetal titer/maternal titer It seems to us that concentrations (reciprocals of titers) should be used.

TABLE 1

Antibody transfer in guinea pigs actively immunized since beginning of pregnancy

Gestation age	Maternal titer	Fetal titer	CQ
days			
16	1 2560	0(3)	—
25	1 2560	0(4)	—
27	1 2560	0(3)	—
30	1 2560	0(2)	—
35	1 2560	1 160(2)	1/16
35	1 1280	1 80(2)	1/16
40	1 2560	1 80	1/32
		1 160	1/16
45	1 640	1 80	1/8
		1 160	1/4
		1 320(2)	1/2
49	1 640	1 320	1/2
		1 640(2)	1
55	1 1280	1 1280(3)	1
60	1 320	1 160(2)	1/2
60	1 640	1 320(3)	1/2
60	1 1280	1 640(4)	1/2
60	1 1280	1 640(3)	1/2
60	1 2560	1 1280(3)	1/2
62	1 640	1 640(3)	1
65	1 1280	1 640	1/2
		1 1280(2)	1
68	1 640	1 640(3)	1
Newb.	1 640	1 320(3)	1/2

(Numbers in parentheses indicate the number of fetuses t that titer)

TABLE 2

Antibody transfer within 24 hours after passive immunization of mothers

Gestation age	Maternal titer	Fetal titer	CQ
days			
45	1 640	1 160(4)	1/4
49	1 1280	1 320(2)	1/4
53	1 1280	1 160(2)	1/8
55	1 640	1 320(2)	1/2
55	1 1280	1 640(5)	1/2
60	1 1280	1 1280(3)	1
60	1 1280	1 1280(2)	1
60	1 1280	1 1280(4)	1
60	1 640	1 640(3)	1
63	1 640	1 160(2)	1
63	1 2560	1 2560(2)	1
65	1 2560	1 2560(2)	1
65	1 640	1 640(4)	1
65	1 1280	1 1280(3)	1
65	1 640	1 640(2)	1
68	1 2560	1 2560(3)	1
Newb.	1 2560	1 2560(3)	1
Newb.	1 1280	1 1280(2)	1
Newb.	1 160	1 160(2)	1

(Numbers in parentheses indicate the number of fetuses at that titer)

probably do not reveal the rate at which equilibration occurs, since, in an isolated experiment with a 60-day pregnant animal, equilibration was attained within two hours. It would appear however that the C.Q attained in the active experiments before 60 days was somewhat higher than in the passively immunized females.

It became of some interest to determine which of the possible routes of transfer were operative in the guinea pig and ac cordingly a small series of surgical experiments was initiated. Insufficient numbers of animals were used to permit a final conclusion as to the routes involved but the data are highly suggestive The results of these experiments are summarized in table 3 Although the mothers undoubtedly absorbed antiserum from the peritoneal cavity the experimental situation differed so drastically from the normal that no attempt was made to obtain the C Q Thus the only possible comparison is between fetuses in any one experiment.

The experiments using 35-day pregnant females indicate that ligation of the vitelline vessels reduces significantly the amount of uptake, compared with the fetuses with vitelline circulation intact and additional ligation of the mouth did

TABLE 3

Effect of surgical interruption of the possible routes of antibody absorption

Gestation age	Fetus A	Fetus B	Fetus C	Fetus D
35	1 320	1 20	1 20	
	1 320	1 20		
43	1 2560	1 2560	1 160	
45	1 1280	1 40	1 20	
	1 1280	1 80	1 20	
50	1 2560	1 2560		
50	1 20			neg. 1 2.5(4)
55	1 640		1 40	
60	1 80			neg. 1 2.5(2)
65	1 20			neg. 1 2.5(2)

Fetus A—Uterine wall and fetal membranes incised parallel to major vessels; fetus with at tached membranes left free in terine cavity

Fetu B—As in A; in addition, vitelline vessels were ligated and yolk sac removed.

Fetus C—As in B; in addition, ligature was placed around the mouth and nose of the fetus.

Fetus D—Fetuses freed as in A; mouth and nose ligated.

(Numbers in parentheses indicate number of animals.)

not further reduce the uptake The reduction amounted to 4 tubes in the dilution series a factor of 16. The experiment with the 45-day-pregnant female resembles the 35-day experiment closely except that, in this case additional ligation of the mouth did further reduce the amount of uptake This would seem to indicate that there is some uptake by the fetal gut at this stage.

There is an apparent paradox in the experiment upon the 43-day pregnant female in that the results resemble those of the later stages much more than do those of the 45-day experiment. It will be seen that in the 43-day experiment ligation of the vitelline vessels had no effect on the uptake of antibodies whereas additional ligation of the mouth caused approximately the same reduction that ligation of the vitelline vessels did in the 35-day experiments (4 tubes). Histochemical analysis has shown that the gut and yolk sac of the fetuses at this stage were actually more mature than those of the 45-day experiment (Anderson and Leissring, '61)

The first experiment at 50 days showed no reduction in antibody uptake following ligation of the vitelline vessels. In subsequent experiments the titers were found to be much lower in the A fetuses, and consequently the titration series was modified to include 1 5 and 1:2.5 dilutions The second experiment at 50 days left the vitelline vessels intact; and the mouths of the fetuses were ligated following which the titers of all the operated fetuses were negative at 1 2.5 again a loss of at least 4 tubes in comparison with fetus A.

At 55 days ligation of both vitelline vessels and mouth resulted in a 4-tube loss; and at 60 and 65 days ligation of only the mouth resulted in a comparable or greater decrease in uptake

It seems reasonable to infer from this series of experiments which is not extensive enough to be definitive that the transfer of antibodies to the guinea pig fetus is primarily by way of the vitelline circulation until 40 days, and that there is a gradual shift in this function, until at 50 days and thereafter the fetal gut is the predominant active transfer organ.

It should be noted here that the amniotic fluid of embryos up to 30 days was negative at a dilution of 1 2.5 but from 35 days until term the titers of amniotic fluid exocoelomic fluid and fetal stomach contents were positive at 1:10

DISCUSSION

The present report constitutes the first recognition of a shift in the capacity for antibody absorption from one organ to another during the prenatal period The change from vitelline to intestinal absorption is not surprising The fetal membranes of the guinea pig closely resemble those of the rat which receives antibodies via the yolk sac and intestine before birth and by the intestine after birth. The guinea pig apparently accomplishes this evolution during its longer gestation period.

The morphological changes in the guinea pig yolk sac in the latter half of gestation have been noted by several authors including Wislocki, Deane and Dempsey ('46) Hard ('46) and Dempsey ('53) and are the subject of a study correlated with the present report (Anderson and Leissring '61) Histological and histochemical changes corroborate the idea that active absorption of proteins by the yolk sac decreases during the latter half of guinea pig development, and that its rôle in later stages is more probably passive

There are at present insufficient data at hand to explain the differences between our results and those of Barnes ('59) There are however several aspects of the methods employed which may account, at least in part, for these differences. Comparisons with Barnes study must be made cautiously since she studied antitoxins, while our titrations have detected "complete" plus "incomplete agglutinins. The differences between human agglutinins and antitoxins do not result in different rates of uptake of antibodies by the gut of the human neonate (Leissring Anderson and Smith, '61) but guinea pig neonates have been shown to take up "incomplete agglutinins from the gut at least several days beyond the time when uptake of complete agglutinins ceases (Leissring and Anderson, '61) The recent work

of Halliday and Kekwick ('60) is of interest here They have shown that 7S globulins are taken up by the gut of the young rat at a rate several times that of the 19S globulins; and that antibodies to the same antigen may lie in the one fraction following initial active immunization and in the other fraction in hyperimmunization. Obviously much more would have to be known about the ultracentrifugal mobilities of the antibodies used in our experiments and those used by Barnes ('59) for a valid comparison of the two experiments.

We have detected no decrease in the rate of transfer of antibodies just before term, as Barnes ('59) has reported. The nature of our test would not have permitted us to observe the very slight differences which she indicates however since the differences she reports lie within the normal range which she has observed at earlier stages we are forced to conclude that the curve which she has drawn cannot be regarded as meaningful.

SUMMARY

Pregnant guinea pigs actively immunized from the first day of gestation transferred anti-*Brucella abortus* antibodies to the young as early as 35 days as detected by the Coombs test. The C.Q. was about 1/16 at this time, and increased to 1/2 or 1/1 at around 50 days continuing until term.

Guinea pigs passively immunized with anti-*Brucella* serum transferred a detectable amount of antibody to the fetus within 24 hours as early as 45 days (C Q = 1/4) Equilibration within 24 hours was noted as early as 60 days and continued at this rate to term. The rate at which equilibration occurs is probably not reflected in our data, since, in a single experiment, a 60-day pregnant animal equilibrated with her young within two hours.

A small series of experiments employing surgical intervention with the different possible routes of transfer gave support to the idea that the vitelline vessels are the major site of entry of antibodies into the fetal circulation early in gestation whereas at later stages the fetal gut is of greater importance.

ACKNOWLEDGMENT

Thanks are due Mrs Judi L. Leissring for her careful rendition of the diagram of the guinea pig fetal membranes.

LITERATURE CITED

Anderson, J W and J C Leissring 1961 The transfer of serum proteins from mother to young in the guinea pig. II. Histochemical correlations with prenatal studies. Am. J Anat., *109:* 157–174.

Bangham, D R., K. R. Hobbs and R. J Terry 1958 Selective placental transfer of serum-proteins in the rhesus. Lancet, 2: 351–354.

Barnes, J M. 1959 Antitoxin transfer from mother to foetus in the guinea-pig. J Path. Bact., 77 371–380

Batty J F W R. Brambell, W A. Hemmings and C. L. Oakley 1954 Selection of antitoxins by the fetal membranes of rabbits. Proc. Roy Soc., B *142:* 452–471

Brahic, J J Tamalet, L.-J Tamalet and P Medat 1955 Sur l'utilisation du test de Coombs dans le diagnostic sérologique des brucelloses. Soc. Méd. Hop. Paris—Bull. et Mém., *71* 41–42.

Brambell, F W R. 1958 The passive immunity of the young mammal. Biol. Rev 33 488–531

Brambell, F W R., and R. Halliday 1956 The route by which passive immunity is transmitted from mother to foetus in the rat. Proc. Roy Soc., B *145* 170–185.

Brambell, F W R., W A. Hemmings and M Henderson 1951 Antibodies and embryos. The Athlone Press, London.

Brambell, F W R., W A. Hemmings, M Henderson, H. J Parry and W T Rowlands 1949 The route of antibodies passing from the maternal to the foetal circulation in rabbits. Proc. Roy Soc., B 136 131–144.

Brambell, F W R., W A. Hemmings, M. Henderson and W T Rowlands 1950 The selective admission of antibodies to the foetus by the yolk-sac splanchnopleur in rabbits. Ibid *137* 239–252.

Brambell, F W R., W A. Hemmings and W T Rowlands 1948 The passage of antibodies from the maternal circulation into the embryo in rabbits. Ibid., *135* 390–403.

Coombs, R. R., A. E. Mourant and R. Race 1945 A new test for the detection of weak and "incomplete Rh agglutinins. Brit. J Exp. P th., 26 255–266.

Dempsey E. W 1953 Electron microscopy of the visceral yolk-sac epithelium of the guinea pig. Am. J Anat., 93 331–363.

Ehrlich, P 1892 Ueber Immunität durch Vererbung und Säugung. Z. Hyg. Infektkr *12:* 183–203.

Grosser O 1909 Vergleichende Anatomie und Entwicklungsgeschichte der Eihäute und der Placenta. W Braumüller Wien.

——— 1936 Frühentwicklung Eihautbildung und Placentation des Menschen und der Säugetiere Deutsche Frauenheilkunde Bd. 5. J F Bergmann, München.

Halliday R., and R. A. Kekwick 1960 The selection of antibodies by the gut of the young rat. Proc. Roy Soc., B 153 279–286.
Hard, W H. 1946 A histochemical and quantitative study of phosphatase in the placenta and fetal membranes of the guinea pig. Am. J Anat., 78 47–78.
Hartley P 1948 The behavior of different types of homologous and heterologous diphtheria antitoxin when administered to pregnant guinea pigs. Month. Bull. Minist. Health (Lond.) 7 45–84
——— 1951 The effect of peptic digestion on the properties of diphtheria antitoxin. Proc. Roy Soc., B 138, 499–513.
Jo-Keichiro, K. 1951 On the transmission of antibodies from mothers to their offspring in experimental typhus fever; experiments in albino rats and guinea pigs. Jap. Journ. Med. Sci. Biol., 4 299–310.
Jones, L. M. 1953 Further studies of the pathogenicity and immunogenicity of mucoid variants of *Brucella abortus* for guinea pigs. J Inf. Dis., 92 26–32.
Kitasato, S. 1889 Ueber den Rauschbrandbacillus und sein Culturverfahren. Z. Hyg. Infektkr., 6 105–116.
Leissring, J C., J W Anderson and D. W Smith 1962 Uptake of antibodies by the gut of the newborn infant. A. M. A. J Dis. Child., in press.
Leissring, J C., and J W Anderson 1961 The transfer of serum proteins from mother to young in the guinea pig. III. Postnatal studies. Am. J Anat., 109 175–182.
Mason, J H., T Dalling and W S Gordon 1930 Transmission of maternal immunity J Path. Bact., 33 783–797
Mossman H. W 1926 The rabbit placenta and the problem of placental transmission. Am. J Anat., 37 433–497
——— 1937 Comparative morphogenesis of the fetal membranes and accessory uterine structures. Carnegie Contrib. Embryol., 26 129–246.
Remlinger P 1899 Contribution expérimentale à l'étude de la transmission héréditaire de l'immunité contre le bacille d'Eberth et du pouvoir agglutinant. Ann. Inst. Pasteur 13 129–135.
Schneider L., and J Szathmáry 1940 Ueber die Immunität der neugeborenen Meerschweinchen. Z. Immunforsch., 98 24–30.
Stäubli, C. 1903 Zur Frage des Ueberganges der Typhusagglutinine von der Mutter auf den Fötus. Centralbl. Bakt., 33 458–461
Vaillard, L. 1896 Sur l'hérédité de l'immunité acquise. Ann. Inst. Pasteur 10; 65–85.
Wagner B M., and D M. Kuhns 1953 Coombs type of antibodies in Brucellosis. Am. J Clin. Path., 23 185–189
Wislocki, G. B., H. W Deane and E. W Dempsey 1946 The histochemistry of the rodent' placenta. Am. J Anat., 78 281–345.

The Transfer of Serum Proteins from Mother to Young in the Guinea Pig

II. HISTOCHEMISTRY OF TISSUES INVOLVED IN PRENATAL TRANSFER[1]

JOHN WALBERG ANDERSON AND JOHN C. LEISSRING
Department of Anatomy, University of Wisconsin, Madison, Wisconsin

In the first paper of this series, it was shown that, in the guinea pig, little or no antibody is transferred from mother to fetus by way of the chorioallantoic placenta, and that the yolk sac and gut of the fetus are active in this process (Leissring and Anderson '61). It is of interest to correlate structural and histochemical changes of the various tissues involved with the protein transport phenomena recorded in the first paper.

Among the previous reports of the cytology and histochemistry of the guinea pig fetal membranes, have been those of Hard ('46), Wislocki, Deane and Dempsey ('46) and Dempsey ('53). All of these authors have demonstrated senescent changes in the yolk sac at later stages of gestation. Hard has shown a loss in alkaline phosphatase activity as gestation progresses and Dempsey ('53) has studied the yolk sac of the guinea pig with the electron microscope at a few gestation stages, finding additional evidence of degenerative changes.

Although previous reports of histological and histochemical studies of guinea pig fetal membranes have illustrated a variety of changes, it was considered that additional information could be obtained by a histochemical study of tissues whose abilities to transfer antibodies were known from concurrent immunological studies.

MATERIALS AND METHODS

Tissues were collected from all animals used in the previously reported paper. We shall report data obtained from fetuses and membranes of 35, 45, 55 and 65 days gestation age because these stages represent significant phases of guinea pig development with regard to protein transport.

Tissues fixed in Zenker's, Rossman's and Carnoy's fluids were graded up through alcohols and chloroform, infiltrated in a vacuum oven and embedded in paraffin. Other tissues fixed in 100% acetone were passed through chloroform and treated the same way. The tissues were processed uniformly, so that valid comparisons of concentrations of the various constituents could be made. The blocks of tissue were stored at 4 C, the sections were all made during a few days at the conclusion of the experiments, and the staining was performed immediately.

The passage of serum proteins through the various cell layers was visualized by the use of fluorescent-labeled serum. The method of Mayersbach ('58) was followed, using the fluorescent dye 1,1-dimethylamino-5-naphthalene sulfonyl chloride (DANS), whose fluorescence under ultraviolet illumination is bright yellow. Twenty milliliters of serum were mixed with 40 ml of buffered (pH 7.4) saline and to this was added slowly, with stirring in the cold, 12 ml of dioxane. Eighty milligrams of the dye was dissolved in 16 ml of acetone, and this mixture was added dropwise, in 4 aliquots at three hour intervals, to the combination of the other constituents at 5°C. The entire mixture was then dialyzed, with stirring, against several changes of physiological saline, and the mixture was concentrated by allowing the dialysis bag to hang in front of an electric fan. The labeled serum was utilized in

[1] Supported by National Institutes of Health Grant H-3331, and by the Wisconsin Alumni Research Foundation.

several different experiments The use of this substance in the experiments was considered valid for the mode of labeling made it unlikely that any dye released by uncoupling would re-couple to protein in a biological environment and Redetzki ('58) has shown that this label has no effect on the antigen-antibody reaction.

The labeled serum was injected into the peritoneal cavity of females at various stages of gestation. After 3–4 hours, the animals were killed and samples of the yolk sac amnion, fetal gut, and fetal liver were fixed in Carnoy's fluid for fluorescent studies. Tissues were also fixed in other reagents.

Labeled serum was employed in experiments performed upon several other animals which were bilaterally pregnant. Silk thread was used in ligating both ends of one uterine horn, into which 5 ml of the labeled serum was injected. The other horn was incised and the fetus or fetuses were carefully lifted out. The membranes were removed and 2 ml of the labeled serum was introduced into the stomach of each fetus, using a blunt needle. The fetuses were returned to the abdominal cavity which was then closed. After 90 minutes appropriate tissues were fixed in Carnoy's fluid

Labeled serum was used in the series of surgical experiments performed on pregnant animals at different stages of gestation as described in the previous paper Five milliliters of the labeled serum was introduced with the immune serum and tissue samples were fixed in various fluids two hours after administration of the serum.

Using the material fixed and embedded as above various histochemical technics were employed Alkaline phosphatase was determined in tissues fixed in cold acetone employing Na β-glycerophosphate as substrate at pH 9.2 (Leduc and Dempsey '51) The tissues were incubated in the substrate for 5 min 30 min. and 4 hr Polysaccharides were determined in tissues fixed in cold Rossman's fluid using the period acid Schiff (PAS) technic Control sections incubated in diastase verified the presence of glycogen Zenker-fixed material was stained with Weigert's iron hematoxylin and with methylene blue for 30 minutes at pH 5 1 Control sections, treated with perchloric acid at 4 C for 18 hours verified the presence of RNA. Sections of the Carnoy-fixed tissues were affixed to slides without albumin deparaffinized rehydrated, mounted with glycerin and studied with the ultraviolet microscope.

OBSERVATIONS

Yolk sac

The yolk sac at 35 days (fig 1) is quite vascular with a very cellular mesodermal layer Very few connective tissue fibers are present. Many of the distended blood vessels appear to be blood islands showing various stages of hemopoiesis. Underlying the endodermal cells is a thin PAS-positive basement membrane. Fusiform mesodermal cells form an almost continuous layer subtending this membrane; another continuous layer of low cuboidal mesodermal cells borders upon the exocoelom.

The endodermal cells form a tall columnar epithelial layer the majority of whose nuclei lie approximately halfway between apical and basal surfaces. Many mitotic figures are noted The cytoplasm of the endodermal cells shows numerous vacuoles most of which are sub-nuclear Some of the vacuoles, however are also seen in the peri and supra nuclear regions. The granular apical cytoplasm of each cell extends beyond the location of the terminal bar often giving a scalloped appearance to this region The apical cytoplasm is less heavily stained than the more basal regions although granules are present in larger numbers in the apical portion.

The PAS technic demonstrates that the apices of the cells are occupied by glycogen which would account for their lack of affinity for general histological stains. The glycogen is generally confined to the apical region but sometimes extends along the lateral plasmalemma. The cytoplasm exhibits intense basophilia which is strongest in the perinuclear zone. The subnuclear vacuoles remain unstained with either PAS or methylene blue.

Observations with the fluorescence microscope of yolk sacs exposed to the labeled serum proteins as described show an intense yellow fluorescence concen-

trated in the apical regions of the endodermal cells.

The mesodermal component of the yolk sac at 45 days (fig. 2) is more intensely vascular and has more collagenous fibers but the tissue is still predominantly cellular. The exocoelomic border appears to be a continuous layer of rounded cells. Many adult fibroblast nuclei can be identified. Blood islands are absent. The endodermal cells are still fairly tall columnar with the nuclei located near the bases of the cells. One or two prominent nucleoli can be found in most nuclei, and the chromatin is fairly sparse. Fewer mitotic figures are observed than at 35 days. In some cells, there is a single prominent subnuclear vacuole. An indistinct supranuclear vacuole such as has been described by Everett ('35) can be found in the Golgi region. The cytoplasm retains its granular appearance through this stage. There is a gradual change of the mesodermal component of the yolk sac throughout the rest of gestation (fig. 3 and 4). The exocoelomic lining cells become lower and the cellular layer subtending the basement membrane of the endoderm cannot be distinguished in later stages. The stroma changes from a mesenchymal condition to an adult type of areolar connective tissue.

The endodermal cells decrease in height and the nuclei become more rounded and more widely separated. The cytoplasm shows reduced tinctorial affinity resulting from less basophilia, particularly after 50 days. The glycogen content of the endodermal cells reaches a maximum at 45 days (fig. 17) and is progressively reduced until the endodermal cells at 65 days exhibit only trace quantities of glycogen. At all times, the glycogen is primarily confined to the apical regions, but may extend down along the lateral plasmalemma. Throughout gestation, there is a decrease in the subnuclear vacuoles; but some persist to term. In the Golgi region the coarse precipitate which forms following Helly fixation, shows an affinity for both methylene blue and iron hematoxylin. The granular nature of the cytoplasm remains characteristic throughout gestation. The nuclei do not show striking changes except that some of them are pyknotic at the latest stages. Visceral endoderm exposed to fluorescent-labeled serum shows a decrease in brightness beginning at 50 days and continuing until term during which period blue-white autofluorescence predominates.

Gut

At 35 days the endodermal cells of the gut are highly vacuolated (fig. 5). The nuclei are located in the apical halves of the cells but in many cells there is a variable amount of supranuclear cytoplasm. The vacuoles are occupied by glycogen, which constitutes the majority of the volume of the cell. Numerous mitotic figures can be discerned. Already at this stage, the surrounding connective tissue is intensely vascular.

At 45 days (fig. 6) the cells lining the gut have become differentiated into two distinct regions. The cells which are forming the tubular glands show an intense cytoplasmic basophilia and no vacuolization. The cells forming the villi, on the other hand, exhibit no cytoplasmic basophilia practically the entire cytoplasm is filled with glycogen (fig. 18). The nuclei of these large cells are irregular in shape and position, containing no prominent nucleoli. This is in contrast to the cells of the crypts in which prominent nucleoli can be seen.

At 55 days (fig. 7) the endodermal cells of the small intestine appear to have had a slight diminution in the amount of glycogen which they contain. The cytoplasm contains a significant number of granules which take up both methylene blue and the Biebrich's scarlet of Groat's stain.

At 65 days (fig. 8) there has been a further maturation of the cells of the intestine. In many of the cells, the glycogen vacuoles are reduced significantly and the cytoplasm shows an increased affinity for other stains. The brush border is more prominent. The cells of the crypts continue to show intense cytoplasmic basophilia, but the contrast between these cells and those of the villi is not so great because of the increased basophilia of the cells surrounding the villi. The granulation, first observed in significant amounts at 55 days, has become more intense. The

nuclei of the cells on the villi are quite evenly distributed towards the basal half of the cell, although some irregularity persists.

Alkaline phosphatase

As can be seen in figure 9 the yolk sac exhibits a very large amount of alkaline phosphatase early in gestation. The concentration of this enzyme decreases throughout the rest of gestation (figs. 10 11 and 12) until at 65 days the enzyme is lacking

On the other hand, reference to plate 4 shows that an exactly reverse situation exists in the gut. Alkaline phosphatase is first seen in the apices of the gut epithelium cells at 45 days at 55 and 65 days it is somewhat more intense fairly closely resembling the postnatal condition. Because of the variations in the tissues with respect to alkaline phosphatase, the relative amounts of alkaline phosphatase in both yolk sac and gut throughout gestation have been tabulated. They are reported as the subjective appearance on a scale from 0 to +++ in table 1

Surgical series

At all stages after 35 days maternal intraperitoneal injection of DMNS-labeled sera resulted in the finding of fluorescent areas in the fetal liver and kidneys In order to establish more clearly the differential roles of the yolk sac and/or fetal gut at different stages, a higher concentration of labeled protein was made available to the conceptuses. This was accomplished by intra-uterine injection of the labeled serum. The endodermal cells of the yolk sac at early stages exhibited intense yellowish fluorescence in the supranuclear portions being most marked beneath the apical plasmalemma. In addition, the fetal blood and liver exhibited strong yellow fluorescence which could be distinguished from the autofluorescence of control sections. The fetal gut exhibited no exogenous fluorescence at early stages, except in the blood.

At late stages injection of the labeled serum into the uterine lumen resulted in a much decreased yellow fluorescence of the yolk sac endodermal cells, and the appearance of labeled protein in the lumen and epithelium of the gut.

Feeding the labeled serum directly to the fetus by stomach tube early in gestation did not result in visible uptake of the protein by the intestinal epithelium. In later stages, however feeding of the labeled serum resulted in a fluorescence of the intestinal epithelium, even more intense than that following the injection into the uterine lumen.

Removal of the yolk sac and ligation of the vitelline vessels early in gestation, followed by injection of labeled serum into the maternal peritoneal cavity resulted in no visible fluorescence in the fetal liver or kidneys. But, surgical interruption of this vitelline route late in gestation did not interfere with the appearance of fluorescence in the fetal liver and kidneys. Ligation of the nose and mouth at these times however prevented the appearance of labeled proteins in these organs.

In the first paper of this series, the surgical procedures produced two cases which seemed to be contrary to the general trend. In one 43-day pregnancy the transfer of antibodies to the fetus appeared to be by way of the fetal gut whereas in a 45-day pregnant guinea pig the transfer was primarily by the vitelline circulation. It is interesting to note that

TABLE 1

The occurrence of alkaline phosphatase in fetal tissues

Age	Yolk sac	Fetal gut
16	0	0
22	+++	0
25	+++	0
27	+++	0
29	+++	0
30(2)	+++	0
35(3)	+++	0
40	+++	0
43	+++	+
45	+++	(±)
43	++	++
49	++	++
49	+	++
53	0	++
55	0	+++
63	0	++

Each section was incubated with sodium beta-glycerophosphate for 30 minutes. The results were interpreted subjectively and recorded on the basis of a scale which ranged from 0 to +++ depending upon the density of the precipitate.

the alkaline phosphatase of the yolk sac endoderm of the 43-day fetuses was lower in concentration than that of the 45-day fetuses, and that alkaline phosphatase was already present in the gut of the 43-day fetuses.

Amnion

The amnion (fig. 9) throughout the period studied, is a thin connective tissue membrane upon which rests a single layer of flattened ectodermal cells. The cells have a granular cytoplasm which is not basophilic and contains neither alkaline phosphatase nor glycogen. As observed with the fluorescence microscope, the cells appear to contain fluorescent labeled serum following injection of the labeled serum into the uterine cavity in late stages.

Uterus

It was not our intention to describe the endometrium in detail and consequently we do not have a complete series of samples of uterine wall taken throughout gestation. Some of the features that we have observed in late pregnancy however should be recorded here (fig. 20) The uterine epithelium exhibits in restricted areas a striking polarity in reverse of what might be expected. Many of the nuclei tend to be located in the apical half of the cell, as is the greater concentration of RNA. Glycogen is absent from the main body of these cells however a significant amount of PAS-positive diastase indigestible material is to be found in the lumen between these cells and the visceral wall of the yolk sac. This material also takes up the fast green of Groat's stain. In every cell of the uterine epithelium, there is a single, spherical, apical vacuole. The endometrial stroma is intensely vascular and contains a sparse population of uterine glands. These glands have extremely basophilic nuclei which are so closely packed as to make determination of the cytoplasmic basophilia difficult. It is clear however from studying the controls that there is a significant amount of RNA in the cytoplasm of these glandular cells.

DISCUSSION

The data obtained with the DMNS-labeled proteins corroborate completely the results of our previous immunologic studies It should be emphasized that the dye couples to all serum proteins and therefore it is impossible to determine which of the proteins are visualized by this method. Although neither the immunologic nor the fluorescent protein data following surgical procedures are presented as conclusive, the identical results of two entirely different technics give added strength to the idea of a change from vitelline to intestinal antibody absorption.

The histochemical findings reported here permit several correlations with the results of the immunologic studies reported in the first paper of this series (Leissring and Anderson, '61) and with the above data from the labeled protein experiments. These indicated that during the middle third of gestation the yolk sac and vitelline circulation are active in antibody transfer to the virtual exclusion of other routes. During the latter third of gestation, the vitelline circulation decreases in this function, and the fetal gut appears to be the major organ in antibody transfer to the fetus. This is of course, not an abrupt transition, but rather a gradual shift in capacity for antibody uptake.

It should be emphasized again that the change from vitelline to intestinal absorption of antibodies is not surprising on a comparative basis. Mice and rats have been shown to transmit antibodies *via* the vitelline route before birth and *via* the intestine after birth. Furthermore Brambell and Halliday ('56) have reported that the rat fetus at 19 and 20 days of gestation is capable of absorbing antibodies introduced into the stomach. The guinea pig, with its long gestation period, merely accomplishes the same transition entirely within the uterine lumen.

Our histochemical and general cytological observations have shown that the yolk sac endoderm appears to be fully mature during the middle third of gestation and that, in the latter third of gestation, these cells undergo senescent changes. These changes are most strikingly epitomized by the gradual change in alkaline phosphatase activity from the very intense reaction observed at 30 to 35 days to the virtual absence of this enzyme at 65 days

The fetal gut, on the other hand is in a very immature condition before 50 days gradually exhibiting a maturation thereafter until at 65 days the epithelium has become similar to the postnatal condition. These morphological changes are paralleled by the progressive alkaline phosphatase.

On the basis of these histochemical findings and their correlation with the immunologic studies, it would appear that the morphologic changes described indeed corroborate the physiologic data and, that in the guinea pig fetal tissues which we have studied, the presence of alkaline phosphatase correlates with the tissue s ability to transport antibodies. Since we know of no data associating directly the alkaline phosphatase enzymes with active protein transport, the most reasonable conclusion is that the presence of alkaline phosphatase is merely an indication of cell maturity In these studies, then the gain in alkaline phosphatase by the fetal gut is an indication of its maturation whereas the loss of these enzymes from the yolk sac endoderm is an indication of the altered physiological state of these cells.

Halliday ('59) has shown a correlation between the appearance of alkaline phosphatase in the duodenal mucosa (biochemical method di-sodium phenylphosphate substrate) the injection of adreno-corticoids, and the loss of ability of suckling rats to absorb antibodies. Earlier workers (Moog, '53 Moog and Kirsch '55) had shown that adrenal steroids can bring about the precocious differentiation of the intestinal epithelium, including the presence of alkaline phosphatase in the young mouse and the chick embryo. Halliday ('59) basing his studies on the observation of the above authors, found that concomitant with the precocious development of alkaline phosphatase induced by the injection of large doses of DOCA, there was a precocious reduction in the ability of the young rat to absorb antibodies. Although this is an interesting temporal relationship it does not necessarily imply that the presence of duodenal alkaline phosphatase is an indication of an animal's ability to absorb antibodies from the gut. Clark ('59) has pointed out that protein administered to suckling rats and mice is absorbed by the ileum and jejunum, but not by the duodenum. Clark's findings have been extended to the neonatal guinea pig by us in the third paper of this series. The inverse correlation between alkaline phosphatase activity and the absorption of antibodies by the gut of the suckling rat lends weight to the idea that alkaline phosphatase is not directly involved in the active transport of proteins.

A recent study by Moog ('61) gives further impetus to the concept that the appearance of alkaline phosphatase is not causally related to the cessation of antibody uptake.

The foregoing histochemical and cytological data correlate with the findings of Dempsey ('53) Using the electron microscope, he has presented evidence of structural details of the endodermal cells which are unresolved with the light microscope. Most germane to our considerations are his findings of a complex microvillous apical border with small vacuoles in the apical cytoplasm whose invagination from the surface plasmalemma can be followed. The vacuoles which Dempsey ('53) has described are much less numerous and occupy a much less significant proportion of the cell than do the vesicles described by Clark ('59) in the jejunum and ileum of the suckling rat. The youngest stage described by Dempsey is 75 mm C-R length corresponding to approximately 45 days. By this stage we have shown that there is already a decrease in the alkaline phosphatase activity and some decrease in the number of vacuoles visible with the light microscope.

Dempsey ('53) has also noted the degenerative changes in the endoderm late in gestation although he has not followed a closely graded series of specimens. Notable among the senescent changes are the swelling and degeneration of mitochondria, the reduction in complexity of the microvillous border the decrease in number and size of the apical vacuoles and the increase in thickness of the basement membrane. Unfortunately it is not possible to ascertain from Dempsey's ('53) illustrations the fine structure of the fetal capillaries throughout gestation, which may well hold an important key to our

fuller understanding of protein transport by the yolk sac.

Dempsey's ('53) description of edge canals which are found wherever the plasmalemma of three adjacent endodermal cells are contiguous, is of particular interest. These canals can be seen to form a continuous space, extending from the uterine lumen to the basement membrane and they have been observed to contain material having an appearance similar to that of material found in the uterine lumen.

It is apparent that the major organ by which the fetus obtains its antibodies early in gestation is the yolk sac later the fetal gut is of greater significance. While loss of a particular function by the yolk sac is implied by this transition, it is essential to recognize that, in order to reach the gut, the antibodies must still cross the yolk sac. The decline in activity by the vitelline circulation may result in part from changes in the vitelline capillary walls.

Since the third paper of this series adduces information which bears directly upon any generalized schema which would account for the intracellular transfer of serum proteins across cellular barriers, the discussion of this area is postponed to that paper

ACKNOWLEDGMENT

It is a pleasure to acknowledge the technical assistance of Mrs. Frances Simandl and Mrs. Aud B Pedersen.

LITERATURE CITED

Brambell, F W R., and R. Halliday 1956 The route by which passive immunity is transmitted from mother to foetus in the rat. Proc. Roy Soc., B 145 170–178

Clark, S. L., J 1959 The ingestion of proteins and colloidal materials by columnar absorptive cells of the small intestine in suckling rats and mice. J Biophys. Biochem. Cytol., 5 41–50.

Dempsey E. W 1953 Electron microscopy of the visceral yolk-sac epithelium of the guinea pig. Am. J Anat., 93: 331–363.

Everett, J W 1935 Morphological and physiological studies of the placenta of the albino rat. J Exp. Zool., 70 243–285.

Halliday R. 1959 The effect of steroid hormones on the absorption of antibody by the young rat. J Endroc., 18: 56–66.

Hard, W H. 1946 A histochemical and quantitative study of phosphatase in the placenta and fetal membranes of the guinea pig. Am. J Anat., 78 47–78.

Leduc E., and E. Dempsey 1951 Activation and diffusion as factors influencing the reliability of the histochemical method for alkaline phosphatase. J Anat., 85 308–318.

Leissring, J C and J W Anderson 1961 The transfer of serum proteins from mother to young in the guinea pig. I. Prenatal rates and routes. Am. J Anat., 109 149–156.

Mayersbach, H. 1958 Zur Frage des Proteinüberganges von der Mutter zum Foeten, I. Befunde an Ratten am Ende der Schwangerschaft. Z. Zellforsch., 48 479–504.

Moog, F 1953 The functional differentiation of the small intestine. III. The influence of the pituitary-adrenal system on the differentiation of phosphatase of the suckling mouse. J. Exp. Zool., 124: 329–346.

——— 1961 The functional differentiation of the small intestine. VIII. Regional differences in the alkaline phosphatases of the small intestine of the mouse from birth to one year Devel. Biol., 3 153–174

Moog, F and M. Kirsch 1955 Quantitative determination of phosphatase activity in chick embryo duodenum cultured in fluid media with and without hydrocortisone. Nature, 175: 722–723.

Redetzki, H. M. 1958 Labelling of antibodies by 5-dimethylamino-1-sulfonyl chloride its effect on antigen-antibody reactions. Proc. Soc. Exp. Biol. Med., 98 34–30.

Wislocki, G. B H. W Deane and E. W Dempsey 1946 The histochemistry of the rodent' placenta. Am. J Anat., 78 281–346.

PLATE 1

EXPLANATION O FIGURES

Yolk sac at progressive stages of gestation. The endodermal cells show a gradual decrease in height, vacuolation and granulation. The nuclei at late stages show degenerative changes. The change from cellular mesoderm at 35 days to a more fibrous layer at 65 days is also shown. All × 830; 1 and 2, methylene blue; 3 and 4 Groat's tetrachrome.

1 35 days.

2 45 days.

3 55 days.

4 65 days.

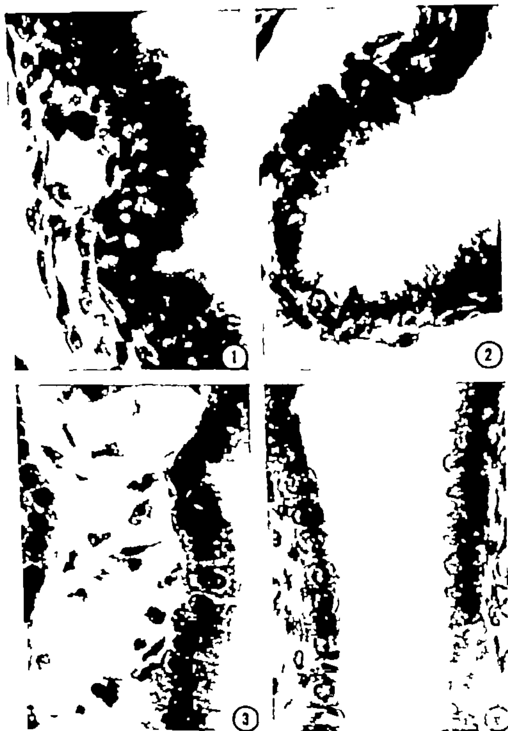

1
2
3

PLATE 2

EXPLANATION OF FIGURES

Alkaline phosphatase reaction of yolk sac at progressive stages of gestation, showing the gradual loss of this enzyme. Substrate, sodium beta glycerophosphate; incubation time 30 minutes. No counterstain was used; high contrast photographic methods have revealed greater cellular detail, but there is actually almost no staining other than in the apices of the cells. × 250.

5 35 days.

6 45 days.

7 55 days.

8 65 days.


5


6


7



PLATE 3

EXPLANATION OF FIGURES

Small intestine of fetuses at progressive stages of gestation. The supra- and subnuclear glycogen vacuoles are particularly prominent at 35, 45 and 55 days, and the basophilia of the tubular glands is strongest at 65 days. × 290

9 35 days.

10 45 days.

11 55 days.

12 65 days.


9


10


11



PLATE 4

EXPLANATION OF FIGURES

Alkaline phosphatase reaction of fetal gut at progressive stages of gestation.

The histochemical and photographic methods were the same as in plate 2. × 250

13 35 days.

14 45 days.

15 55 days.

16 65 days.


13


14


15



PLATE 5

EXPLANATION OF FIGURES

17 PAS-positive material in the yolk sac at 45 days of gestation. The heavy glycogen content of the apices of the endodermal cells, and the distinct basement membrane can be seen. × 290.

18 PAS-positive material in the small intestine of the fetus t 45 days of gestation. The extremely heavy deposits of dye in the cells of the villi obscure all other details. × 290.

19 Amnion at 65 days of gestation, showing the squamous ectoderm, and the condensation of mesoderm at the exocoelomic lining. A—amniotic cavity; E—exocoelom. × 490.

20 Endometrial wall and adjacent visceral yolk sac at 65 days of gestation. Some of the supranuclear vacuoles can be seen in the epithelium. The yolk-sac endodermal cells are much lower here than near the placental surface (cf. fig. 8) The intense basophilia of the nuclei of the uterine glands is also shown. U—uterine lumen; E—exocoelom. × 180.


17


18


A
E
19


E
U

The Transfer of Serum Proteins from Mother to Young in the Guinea Pig

III POSTNATAL STUDIES[1]

JOHN C. LEISSRING AND JOHN WALBERG ANDERSON
Department of Anatomy University of Wiscon i Madison Wisconsi

Following Kitasato s (1889) original re port on passive immunization of the young guinea pig reports by several authors in dicated that there was no postnatal transmission of antibodies from mother to young in this animal. Vaillard (1896) and Remlinger (1899) concluded that this was the case as did Schneider and Szathmáry ('40) Jo-keiichiro ('53) was unable to detect a titer of complement-fixing antibodies in newborn guinea pigs nursing upon immune foster mothers.

On the other hand, Brogi and Biagini ('30) were able to produce a marked hemolytic anemia in guinea pigs within a few days of birth by feeding hemolytic serum. The effect was exacerbated by simultaneous administration of bile salts. The hemolysis could not be produced in 20-day-old guinea pigs even with addition of bile salts.

Barnes ('59) reported that, in her ex periments, the gut of the guinea pig fetus was not involved in passive immunization. The results of our immunologic and histochemical experiments have shown that the passive immunization of the fetal guinea pig during the last half of gestation most likely occurs through the absorptive functions of the yolk sac and fetal intestine (Leissring and Anderson '61; Anderson and Leissring, '61) In view of the foregoing conflicting reports a correlated immunologic and histochemical study was undertaken.

MATERIALS AND METHODS

Guinea pig anti-*Brucella abortus* serum was produced as described in an earlier report (Leissring and Anderson, '61) and was fed in amounts of either 1 or 2 ml to 64 non-immune guinea pigs ranging in age from immediately postnatal to 7 days. Twenty four hours after introduction of the antiserum into the stomach the animals were bled from the heart and samples of intestine were fixed for histological and histochemical study as reported previously (Anderson and Leissring '61) Two milliliters of guinea pig serum labeled with a fluorescent dye 1-dimethylaminonaphthalene-5-sulfonyl chloride (Mayersbach '58) were similarly fed to 15 guinea pigs 0 to 7 days of age After three hours samples of intestine liver and kidney were fixed in Carnoy s fluid and prepared for observation with the ultraviolet microscope.

Antibody titration included the tube agglutination test (Brambell et al. 48) and the Coombs modification of this test (Jones '53)

OBSERVATIONS

The results of the immunologic titrations are summarized in tables 1 and 2 and in figure 1 The agglutination test reflects complete antibodies which are capable of forming polymeric aggregates and thus are capable of agglutination while the Coombs test detects in addition to the complete antibodies incomplete or univalent molecules which are not themselves able to cause clumping. "Complete antibodies are absorbed in progressively diminishing amounts until the third day of life after which absorption of this antibody type is not detected by our methods. A different pattern is se fo the absorption of "incomplete n l de There is a high initial absorptio nd a continuing high level of app ce of "incomplete antibodies in the s r m of the

[1] Supported by N tional Insti — of Heal h Grant H-3331 and by the Wisconsin Alumni Research Foundation.

animals 24 hours after feeding throughout the 7 postnatal days of our experiments

The histochemical properties of the intestinal epithelium during the first week of life do not differ materially from the prenatal condition described earlier (Anderson and Leissring, '61) Heavy deposits of glycogen, dense cytoplasmic basophilia of the cells of the crypts and acidophilic granules (figs. 2 and 3) were observed. The granules were present also in the lu-

TABLE 1

Agglutination titers 24 hours after feeding 1 ml of serum

Age (when fed)	Agglutination titer of fed serum	Agglutination titer of recipients serum after 24 hours	C.Q.
Newborn	1 320	1 160(3)	1/2
One day	1 1280	1 160(4)	1/2
		1 80(2)	1/16
Two day	1 1280	1 80(2)	1/16
		1 40(1)	1/32
		1 20(1)	1/64
		1 10(1)	1/128
Three day	1 1280	1 160(2)	1/8
		0(6)	—
Four day	1 1280	0(4)	—
Five day	1 1280	0(2)	—
Seven day	1 1280	0(4)	—

Numbers in parentheses indicate number of animals used.

TABLE 2

"Coombs" titers 24 hours after feeding 2 ml of serum

Age (when fed)	"Coombs" titer of fed serum	"Coombs" titer of recipients' serum	C Q
Newborn	1 5120	1 5120(2)	1
One day	1 5120	1 5120(4)	1
Two day	1 5120	1 2560(4)	1/2
		1 1280(1)	1/4
Three day	1 5120	1 640(4)	1/8
Four day	1 1280	1 640(1)	1/2
Five day	1 1280	1 640(1)	1/2
		1 320(1)	1/4
		1 160(1)	1/8
Seven day	1 2560	1 1280(3)	1/2

Numbers in parentheses indicate number of animals used.

men of the gut and could be followed into the lacteals of the intestinal villi. Alkaline phosphatase was present in significant amounts in the apical borders of the intestinal cells (figs. 4 and 5) The acidophilic granules were present to a much greater extent in the cells and lacteals of the ileum than in the duodenum.

Exogenous fluorescence in tissues from newborn animals fed labeled serum was seen in the apical portions of the epithelial cell, in the lacteals, and in the connective tissue of the submucosa. The fluorescence was much brighter in the ileal tissues than in the duodenum and was also found in sections of the kidney and liver

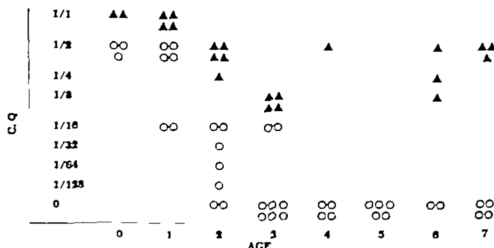


Fig. 1 Concentratior (C Q = recipient' serum concentration/donor serum concentration) 21 hr aft The ge is given t the time of feeding. ○ = Agglutination titer ▲ = "Coombs

DISCUSSION

The present experiments have shown that the newborn guinea pig can absorb complete agglutinins until the third day after birth and "incomplete" antibodies for at least 7 days postnatally. Histological and histochemical findings parallel the immunologic results. The apparent higher rate of absorption in the ileum compared with the duodenum as reflected by greater fluorescence after feeding of labeled serum is in agreement with studies in the rat by Clark ('59).

The failure of Jo-Keiichiro ('53) to demonstrate a titer of complement-fixing antibodies in his experiments gives no direct information about the ability of the intestine to absorb antibodies. If his negative results are confirmed, it would appear that the failure of passive immunization must be explained by factors other than the lack of absorption in the intestinal epithelium. Several possible explanations may be advanced: (1) failure of the antibodies to appear in adequate concentration in the milk, (2) insufficiently sensitive tests to detect a low absorption rate and (3) alteration of the antibody molecules during passage such that the test used fails to detect the resulting molecules.

Brambell ('58) has suggested a possible mechanism for the intracellular events attendant upon protein transfer across cells based upon a series of papers which he reviewed. He indicated that in the one instance where the uptake of protein by endodermal cells has been studied (Hemmings '57) the phenomenon was found to be nonselective. He suggested that the most likely mechanism for this uptake is by pinocytosis which suggestion has received strong support from the work of Clark ('59). Brambell ('58) has advanced the idea that a protein recognition mechanism exists and that there is competition for acceptance by this mechanism. Two phenomena which give strongest support to this idea are those of selection of homologous gamma-globulin over heterologous gamma-globulin, and of "interference" (the degree to which the uptake of homologous gamma-globulins is mitigated by heterologous antibodies simultaneously presented to the endodermal cells). Furthermore, Brambell suggested that the active sites of the antibody molecule must remain intact following passage to the circulation of the young animal and that the passage of the intact molecule through the cell would depend upon the degree to which its surface configuration would fit the protein recognition mechanism. The phenomena of selection and interference could thus both be explained on an intracellular basis. Selection of course would depend upon the destruction of the heterologous gamma globulins by intracellular proteolytic enzymes.

Subsequent studies using pepsin refined antibodies (Brambell, Hemmings and Oakley '59) and papain digested antibodies (Brambell et al. '60) have suggested that one part of the antibody molecule is the protein recognition unit and is itself transported more readily than are the other two fractions produced by papain digestion. It is of interest that the protein recognition unit corresponds to the antigenic site of the antibody molecule as found by Porter ('58).

Brambell ('58) has postulated that the mechanism of protein recognition may involve a template, possibly RNA. We should like to suggest that the template (the molecular configuration responsible for protein recognition) resides in the protein of the plasmalemma. The configuration of the protein of the plasmalemma would ultimately of course reflect the template configuration of the RNA of the cell.

The protection of the antibodies which remain intact during passage might result from the following events. Protein is taken up in the pinocytotic vesicles which are derived from the apical plasmalemma. Then depending upon the degree to which the protein resembles homologous gamma-globulins, it will be more or less tightly adsorbed to the walls of the vesicles, thus providing a degree of protection of the protein against the action of intravesicular proteolytic enzymes. Changes (pH, redox potential, Everett, '35) in the supranuclear regions of the entodermal cells might activate the proteolytic enzymes. After the action the only remaining protein would be that which was adsorbed to the surface of the

vesicles. The findings of Anderson ('59) in the rat yolk sac suggest that the supranuclear region is the site of destruction of the majority of adsorbed proteins. Clark's paper ('59) lends strong support to the theory that adsorption to the walls of the pinocytotic vesicles provides protection from the effects of proteolytic enzymes. Figure 11 of his paper indicates that all of the intracellular protein which remains is adsorbed to the surfaces of the pinocytotic vesicles.

The results of the present study show that neonatal guinea pigs obtain a significant titer of "incomplete" antibodies from fed antiserum for at least several days beyond the time at which the uptake of "complete" antibodies ceases. (The results of Brogi and Biagini ('50) suggest that antibody uptake continues for less than 20 days.) This difference may have resulted from either a selective transport of "incomplete" antibodies or a conversion of "complete" antibodies to "incomplete" ones during passage across the endodermal cell, by the proteolytic removal of one antigen-reactive site. The theory of differential adsorption to the walls of pinocytotic vesicles as the means of protein "recognition" would permit both of the above mechanisms to apply "Incomplete" or univalent homologous antibodies would be adsorbed to the walls of the vesicles, and the protection thus provided would permit their passage through the cell "Complete" or divalent antibodies would also become adsorbed but one of the antibody radicals would be removed thus rendering it univalent or "incomplete."

The phenomena of selection and interference could well be explained by this theory Heterologous proteins would be only loosely adsorbed to the walls of the vesicles and would block a globulin recognition site preventing the adsorption of an homologous globulin The bond however would be too loose to prevent its destruction by proteolytic enzymes. The fact that there is [illegible] limit to the rate at which homolog[illegible] [illegible]ntibodies can be taken into the circul[illegible] [illegible]s also compatible with this theory [illegible]med that the rate of formation [illegible] [illegible]ytotic vesicles is also limited [illegible] [illegible]molecular occurrences still req[illegible] [illegible] this hypothesis is supported by the available data.

One further remark is required concerning the experiments of Brogi and Biagini ('50) It is likely that their results stem from a fortunate choice of antibodies. The end-point used was hemolysis of guinea pig erythrocytes *in vitro*. Human anti-Rh hemolysins responsible for the clinical picture of erythroblastosis fetalis, remained undetectable by classical methods until the evolution of the Coombs test (Coombs et al '54) showed them to be "incomplete" antibodies. If the same is true in the guinea pig, the antibodies responsible for the hemolysis in the experiments of Brogi and Giagini ('50) were probably "incomplete" and their results are thereby corroborated by the present studies.

LITERATURE CITED

Anderson, J W 1959 The placental barrier to gamma-globulins in the rat. Am. J Anat., 104 403–429

Anderson, J W and J C. Leissring 1961 The transfer of serum proteins from mother to young in the guinea pig. II. Histochemistry of tissues involved in prenatal transfer. Am. J Anat., *109* 157–174.

Barnes, J M. 1959 Antitoxin transfer from mother to foetus in the guinea pig J Path. Bact., *77* 371–380.

Brambell, F W R., R. Halliday and I. G. Morris 1958 Interference by human and bovine serum and serum proteins fractions with the absorption of antibodies by suckling rats and mice. Proc. Roy Soc *B 149*: 1 11

Brambell F W R., W A. Hemmings and C. L. Oakley 1959 The relative transmission of natural and pepsin-refined homologous antitoxin from the uterine cavity to the foetal circulation in the rabbit. Ibid., *B 150*. 312–317

Brambell F W R., W A. Hemmings, C. L. Oakley and R. R. Porter 1960 The relative transmission of the fractions of papain hydrolysed homologous gamma-globulin from the uterine cavity to the foetal circulation in the rabbit. Ibid., *B 151* 478–482.

Brambell, F W R., W A. Hemmings, and W T Rowlands 1948 The passage of antibodies from the maternal circulation into the embryo in rabbits. Ibid., *B 135*: 390–403.

Brogi, G and R. Biagini 1950 L assorbimento intestinale delle emolisine in cavie lattanti. Clin. Ped., 32 685–695.

Coombs, R. R., A. E. Mourant and R. R. Race 1954 A new test for the detection of weak and "incomplete" Rh agglutinins. Brit. J. Exp Path., 26 255–260

Clark, S. L., J 1959 The ingestion of proteins and colloidal materials by columnar absorp-

tive cells of the small intestine in suckling rats and mice. J Biophys. Biochem. Cytol., 5 41–50.

Everett, J W 1935 Morphological and physiological studies of the placenta of the albino rat. J Exp. Zool., 70: 243–285.

Hemmings, W A. 1957 Protein selection in the yolk-sac splanchnopleure of the rabbit the total uptake estimated as loss from the uterus. Proc. Roy Soc., B *148* 76–83.

Jo-Kehchiro, K. 1953 On the transmission of antibodies from mothers to their offspring in experimental typhus fever experiments in albino rats and guinea pigs. J p. J Med. Sci. Biol., 6 299–310.

Jones, L. M. 1953 Further studies of the pathogenicity and immunogenicity of mucoid variants of *Brucella* bortus for guinea pigs. J Infect. Dis., 92. 26–32.

Kitasato, S. 1889 Ueber den Rauschbrandbacillus und sein Culturverfahren. Z. Hyg. Infektkr 6 105–116.

Leissring, J. C., and J W Anderson 1961 The transfer of serum proteins from mother to young in the guinea pig. I. Prenatal rates and routes. Am. J Anat., *109:* 149–156.

Mayersbach, H. 1958 Zur Frage des Protein-überganges von der M tter zum Foeten, I. Befunde an Ratten am Ende der Schwanger schaft. Z. Zellforsch., *48* 479–504.

Porter R. R. 1958 Separation and isolation of fractions of rabbit gamma-globulin containing the antibody and antigenic combining sites. Nature *182:* 670–671.

Remlinger P 1899 Contribution expérimentale l'étude de la transmission héréditaire de l'immunite contre le bacille d'Eberth et du pouvoir agglutinant. Ann. Inst. Pasteur *13:* 129–135.

Schneider L., and J. Szathmary 1940 Ueber die Immunität der neugeborenen Säugetiere. Z. Immun-Forsch., 95 465–474

Vaillard, L. 1896 Sur L'hérédité de L'immunité acquise. Ann. Inst. Pasteur *10:* 65–85.

PLATE 1

EXPLANATION OF FIGURES

2 Jejunal villus of guinea pig on day of birth, showing the granular cytoplasm. Some of the granules (arrows) can be traced from the lumen, through the cells, and into the lacteal. Methylene blue, × 500.

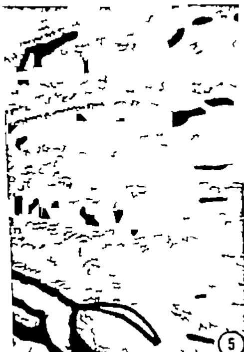
3 Jejunal villus of guinea pig 3 days old. The cytoplasm is still granular although it has not been possible to trace granules in transit as in figure 1. Groat's stain, × 500.

4 and 5 Alkaline phosphatase reaction of jejunum of new-born and 3-day-old guinea pigs, respectively. Substrate, sodium β-glycerophosphate; incubation time 30 minutes. × 125.


2


3


4


5

The Ultrastructure of the Mesenteric Lymph Node of the Rat[1,2]

SEONG SOO HAN
Department of Anatomy The University of Michigan Medical School, Ann Arbor Michigan

Although the ultrastructure of lymphocytes and monocytes from peripheral blood has been described (Kautz and De Marsh '54 Bernhard, Haguenau and Leplus, '55 Low and Freeman, '58) the lymph nodes themselves have received little attention. Recently Moe ('60) described by abstract the ultrastructure of lymph nodes in mice and Sorenson ('60) reported a similar study on rabbits. Bernhard and Granboulan ('60) and Granboulan ('60) described some features of the lymph node, emphasizing in particular the development of lymphocytes and plasma cells. The ultrastructure of mature plasma cells has been described by Braunsteiner Fellinger and Pakesch ('53a '53b and '57) Stoeckenius and Naumann ('57) and Thiéry ('58)

Many problems remain which merit continued study With respect to reticular cells these include determination of the different types of cells their developmental interrelationships, their relationship to fibers and their structural participation in phagocytic activity In regard to lymphocytes the ultrastructural modifications occurring during development of mature forms are not fully known. The origin of plasma cells remains under debate and their fate has not been fully revealed. It is to these problems that this study has been addressed.

MATERIALS AND METHODS

The lymph nodes of 37 young female Sprague-Dawley rats of 200 gm body weight were used. Under ether anesthesia pieces approximately 1 mm³ in size were cut from mesenteric lymph nodes and fixed immediately in either 1% osmium tetroxide solution (Palade '52) or in 2 4% potassium permanganate (Luft '56). Both solutions were buffered with 0 14 M veronal acetate to pH 7 4 Sucrose was added to the OsO at a concentration of 45 mg/ml of the fixative (Caulfield, '57) Fixation in OsO was carried out at 0 C and in KMnO at room temperature.

Dehydration of tissues fixed in 1% OsO was performed at the temperature of fixation until the last change of 95% ethanol when the tissues were brought back to room temperature. Dehydration of the $KMnO_4$-fixed tissues was done at room temperature. In both cases dehydration was completed within two hours.

Purified methacrylate was used as the embedding medium, 2% Luperco CDB (50% 2,4-dichlorobenzoyl peroxide with dibutyl phthalate) being added as catalyst to 20% methyl methacrylate in n-butyl methacrylate. The methacrylate infiltrated tissue was de-aerated by subjecting the gelatin capsules containing tissue and embedding medium to negative pressure prior to polymerization. The methacrylate was polymerized for 12 to 24 hours at 60 C After mounting on grids some of the sections were stained with lead hydroxide lead acetate, uranium acetate or phosphotungstic acid (Watson, '58)

OBSERVATIONS

In the subsequent description subdivision of cells into types will be avoided as much as possible in order to minimize the possibility of erroneous classification. The

---

Supported in part by research grants to Dr Burton L. Baker from the National Institutes of Health, Public Health Service, University of Michigan-Memorial Phoenix Project no. 145, and The Upjohn Company

Based on dissertation submitted in partial fulfillment of the requirements for the Doctor of Philosophy degree.

features observed with the light microscope have been used as the starting point for the identification of cells. Thus under reticular connective cells will be described all of those cells which would be so classified if the light microscope were used.

The usual double membrane structure of the nuclear envelope was clearly visible in most cell types. Pores were also observed in the nuclear membrane. In the lymphocytic and plasma cell series obscurely demarcated channels separated the peripheral condensations of electron-dense material and led out to the nuclear pores creating through them continuity with the surrounding cytoplasm.

Reticular cells

Nondifferentiated reticular cells. The nondifferentiated reticular cell was found in cortical nodules and medullary cords. It was irregular in shape (fig. 2) usually being elongate with cytoplasmic processes which insinuated themselves between adjacent cells. The cell membrane was indistinct and when in contact with other cells its visualization was frequently difficult. The cytoplasm of the nondifferentiated reticular cell was characterized by irregular density, small areas near the periphery being almost clear and giving the cytoplasm a somewhat mottled appearance.

The cytoplasmic organelles were poorly developed as compared with other cell types to be described. The endoplasmic reticulum was composed of rare vesicles or small flattened sacs scattered randomly in the cytoplasm (figs. 3 and 4). These sacs were occasionally dilated so that the caliber of the cisternae was somewhat variable. Some dense granules which appeared to be ribosomes were present but they were not numerous. They usually formed small aggregates but occasionally were associated with the endoplasmic reticulum.

Mitochondria were few in number (fig. 3). They were oval to ellipsoid in shape although often the contour was quite irregular. Their size was variable but many of them were quite small in comparison with the size of the nucl[illegible]. The internal structure of mitochondr[illegible] [illegible]xceedingly irregular, cristae being poorly developed and randomly arranged. In some cases the matrix was quite electron-lucent. That this feature was not due to poor fixation was indicated by the well-preserved cristae and limiting membranes in these mitochondria as well as in the mitochondria of adjacent cells. Dense bodies of lesser diameter than that of mitochondria were distributed sparsely in the cytoplasm. They were quite homogeneous and resembled the microbodies of other authors (Rouiller and Bernhard '56).

The Golgi apparatus could not be identified conclusively in photographs of many cells. A paranuclear accumulation of small vesicles located in a matrix denser than the remainder of the cytoplasm (fig. 2) appeared to be the basic component of the Golgi body. The Golgi apparatus in the primitive cell of the rabbit lymph node has a similar structure (Sorenson '60).

The shape of the nucleus in the nondifferentiated reticular cell varied from spherical to ellipsoid. The nucleoplasm consisted of fine electron-dense structures in a less dense matrix. These dense structures aggregated peripherally and formed a very thin rim along the inner membrane of the nuclear envelope. Otherwise they were distributed randomly throughout the nucleus. Irregularly-shaped electron-lucent areas also characterized the nucleoplasm. A poorly formed nucleolus was seen in some cells.

Reticular cells associated with fibers. The structure of cells located adjacent to fibers varied considerably and it is probable that many inadequately discerned transitional forms existed between the nondifferentiated reticular cell and the reticular cell associated with fibers. The fiber associated reticular cell was found in sinuses as well as in cortical nodules and medullary cords. It was distinguished from the nondifferentiated cell by the greater density of both cytoplasm and nucleoplasm, as well as by finer details to be described (figs. 5 and 7). The main body of the cell had an irregular contour with a thin rim of cytoplasm surrounding the nucleus. However from this part of the cell extended long attenuated cytoplasmic processes which encompassed the collage-

nous fibers. The plasma membrane extended inwards to surround the fibers the contour of the membrane suggesting that the cytoplasm had rotated around the long axis of the fiber (figs. 5 and 7) The cell membrane was usually clearly defined even alongside fibers (figs 5 and 8) although in some locations it was indistinct. Occasionally fibers were so deeply enfolded by the cell that they were brought close to and indented the nucleus (fig 7) Nevertheless, the fibers were always separated from the nuclear membrane by cytoplasm.

The endoplasmic reticulum present in the perinuclear cytoplasm consisted of randomly distributed small flattened sacs or tubes which partly because of the extreme density of the cytoplasm, were not easily discerned. In the cytoplasmic processes adjacent to fibers the endoplasmic reticulum was drawn out into extensive flattened sacs which were oriented parallel to the fibers (figs. 6 and 8) Ribosomes were present in small numbers throughout the perinuclear cytoplasm. However in the peripheral cell processes which covered the fibers they were more numerous and almost all were associated closely with the endoplasmic reticulum (fig. 8)

Mitochondria were frequent and often clustered around the cell center They were less frequently present in cell processes. Mitochondria tended to be quite elongate and contained numerous prominent and regularly arranged cristae The matrix was uniformly dense. Facing the cell center the nuclear membrane was often indented. Mitochondria were found in these indentations and bore a close positional relation to the nuclear membrane Mitochondria-containing areas of the cytoplasm also revealed microbodies whose size equaled or was less than that of the mitochondria (figs. 5 and 7) Inclusions similar to fat droplets were also found occasionally The structure of the Golgi apparatus was not clearly revealed. In some cells it consisted of a cluster of small thick-walled vesicles in the perinuclear cytoplasm (fig. 5) while in others it included also groups of parallel membranes.

The nuclear membrane was somewhat wrinkled (fig. 7) The nucleoplasm consisted of electron-dense structures superimposed on a mottled matrix which was denser than that in the nondifferentiated reticular cell the greatest density occurring near the nuclear membrane The nucleolus was large (fig 7)

Flattened *endothelioid* cells were found at the outer edge of some sinuses lying against collagenous fibers. Their relationship to the fiber associated reticular cell was not fully clarified. Thinned out cytoplasm extended out away from the nucleus of this cell and made close overlapping contact with adjacent cells. KMnO fixation revealed with unusual clarity many infoldings of the cell membrane on both the luminal and fiber facing surfaces. Associated with these infoldings were a number of vesicles especially in the thinned out portions of the cell. As compared with the reticular cells associated with fibers endoplasmic reticulum was poorly developed and there were few ribosomes. The sparse mitochondria tended to aggregate at the ends of the flattened nucleus. Cristae were less numerous and regularly arranged than in the mitochondria of reticular cells associated with fibers. A small number of microbodies with a dense matrix were present. The elongate nucleus resembled that of the fiber associated reticular cell in the structure of its nucleoplasm. With KMnO fixation the peripheral nucleoplasm appeared denser than that more centrally located.

Phagocytic reticular cells Reticular cells containing phagocytized bodies were found in the cortex and medulla. Their cytoplasm was voluminous with processes that extended between other cells. Phagocytic reticular cells often bridged across a sinus making contact with cells associated with fibers.

The external cellular membrane folded inwards, particularly along the borders facing the spaces of sinuses. Th the outer membrane seemed to becom [illegible]

Since electron microscopic studies in [illegible] ate an identity between the essential fibrils of collagenous and reticular (argyrophilic [illegible] in this paper reticular fibers are designated as being collagenous.

The term cell center is used to designate only the general area of cytoplasm near the nucleus in which were located the centrioles centrosome and Golgi pparatus.

tinuous with endoplasmic reticulum (fig. 10) The endoplasmic reticulum was extensive and diffusely distributed in an irregular pattern throughout the cytoplasm Portions of the endoplasmic reticulum possessed attached ribosomes others did not (fig 11) In regions containing inclusion bodies the cisternae were associated with a greater number of ribosomes (fig. 10) and some were quite expansive The endoplasmic reticulum was folded around some mitochondria in close apposition to them Mitochondria were spherical to ellipsoid and of variable size Their cristae exhibited an irregular arrangement but nevertheless were organized more regularly than those of the nondifferentiated reticular cell (fig. 11) The Golgi apparatus consisted of clusters of double membranes and small vesicles. The clusters were found in multiple foci in and around the cell center (figs. 9 and 10)

The ground cytoplasm varied in density In those regions of the cell containing many inclusion bodies it was much less dense than that in the perinuclear area (fig. 9) Free ribosomes were distributed in small groups throughout the cytoplasm (fig. 11)

A variety of inclusion bodies which presumably represented phagocytized material were present. Although their morphology was highly diverse they could be grouped roughly into three categories The first type (A) attained a diameter over half that of the nucleus and possessed a moderately electron-opaque interior (figs. 9 and 10) It was irregular in shape and surrounded by an outer limiting membrane Its matrix sometimes encompassed smaller dense round bodies which occasionally contained ferritin-like granules (fig 15) The neighboring cytoplasm was not dense

The second type of inclusion body (B) was distinguished by its frequent myelin like formation (figs 12 13 and 14) The size of this body ranged upwards from that of mitochondria. Th[illegible] finely granular matrix in general was m[illegible]derat[illegible]ly dense but less so than that of type A H[illegible]ever some sharply circumscrib[illegible] a[illegible] ex tremely dense. This [illegible]ed to arise in previously la[illegible]lat[illegible] [illegible]This

kind of inclusion body often possessed two limiting membranes the external one being continuous with other membranes in the cytoplasm (fig. 12) while the inner membrane extended into the interior to form myelin figures The frequent incomplete union of two bodies suggested either fusion of two or splitting of one (fig. 13) Ferritin-like granules and crystalloids were present.

The third form of inclusion body (C) was small and ovoid or of more irregular shape Its size approximated that of mitochondria An electron-dense outer rim surrounded a clear center and from the outer rim projections extended inward No external limiting membrane was seen (figs. 12 and 13) In addition to the three types of inclusion bodies described the cytoplasm included other cellular fragments.

The nucleus of the phagocytic reticular cell possessed an irregular contour often being elongated. The nucleoplasm was similar to that of the nondifferentiated reticular cell A small nucleolus was seen in some nuclei.

The free rounded macrophage was structurally closely related to the fixed phagocytic reticular cell The endoplasmic reticulum ribosomes mitochondria Golgi apparatus and inclusion bodies were quite similar in structure and distribution (figs. 16 and 17) The free macrophage was found most frequently in sinuses and was generally in contact with reticular cells which surrounded fibers. The cell reached a diameter of over 15 μ The plasma membrane was frequently infolded and the cytoplasm was often raised up in pseudopod-like projections beside these invaginations (fig. 16) Some cytoplasmic processes were finger like and touched those of other cells (fig 17) The infoldings of the outer membrane extended deeply into the interior and appeared to give off small vesicles at the deep end Although of variable structure the inclusion bodies were usually of type B The nucleus was eccentrically placed, and contained nucleoplasm of variable density The density of the cytoplasm varied in different cells and in different parts of the same cell. The peripheral cytoplasm and that in the processes frequently had a hydropic appear

ance. The cytoplasm contained many vacuoles of varied sizes most of which were empty The vacuoles reached their greatest size at the periphery (fig 17)

Lymphocytic cells

On the basis of differences in size ultra structure and nucleocytoplasmic ration, lymphocytic cells were divided into lymphoblasts medium-sized lymphocytes and small lymphocytes to facilitate description (fig 1) As is true with features seen with the light microscope the ultrastructural characteristics did not permit sharp subdivision of these cells into developmental stages.

Lymphoblasts Figure 19 illustrates a lymphoblast while the cell shown in figure 18 appears to be intermediate in development between the nondifferentiated cell and lymphoblast. In contrast to the primitive reticular cell the lymphoblast (fig. 19)

Fig. 1 Cellular interrelationships in the lymph node Although the cellular transformations shown in this figure are indicated by the arrows to be unidirectional, the author recognizes that purely morphological study does not reveal direction of change with certainty and that some of the transformations shown may move in the opposite direction also.

was more rounded in shape and usually possessed a greater volume of cytoplasm in relation to that of the nucleus. In areas where cells were crowded the cell membrane was contorted and vaguely defined

The endoplasmic reticulum consisting of flattened sacs or tubules was irregularly and sparsely distributed. However it was much more extensive than that of the nondifferentiated reticular cell Similarly ribosomes were somewhat more frequent, most of them being distributed freely and only a few being attached to the endoplasmic reticulum. Mitochondria were ovoid and tended to accumulate near the cell center (fig 19) Their cristae were fairly numerous but irregularly arranged The matrix was generally dense With increasing maturity of the cell (figs. 18 and 19) cristae were more compactly arranged within a more uniformly dense matrix. Occasional small dense microbodies were present.

The Golgi apparatus located in the cell center consisted of clusters of short parallel double membranes stacked together Near the parallel membranes and elsewhere in the cell center were small vesicles. Other larger vacuoles were associated with the Golgi complex A paired centriole was located near the center of the area. The ground cytoplasm supporting the centrioles was somewhat denser than elsewhere in the cell and was devoid of ribosomes.

The nucleus was rounded and flattened on one side The nucleoplasm was considerably denser than that in the nondifferentiated reticular cell Large nucleoli were clearly revealed

Medium sized lymphocytes Since the *transformation of lymphoblasts to mature* lymphocytes was characterized by gradual structural change the ultrastructure of the medium-sized form will be described chiefly in terms of its contrast with the lymphoblast The volume of cytoplasm in relation to that of th nucleus was reduced The medi m [illegible] mphocyte was rounded but when [illegible] ntact with other cells its periph[illegible] n d irregular projections (fig 20 [illegible] triking ultrastructural charact[illegible] ppar ent in and about the ce[illegible] h nucleus

The endoplasmic reticulum was poorly developed and when visible consisted of small flattened sacs or tubules Ribosomes were reduced in number and distributed singly and in clusters throughout the cell *less commonly they were attached to the* endoplasmic reticulum or outer nuclear membrane (figs. 20 and 21)

The changing structure of mitochondria constituted one of the most distinctive features of lymphocytopoiesis Of oval form they were distinguished by the regularity and sharpness of their membranous constitution (fig 21) Some of them were elongated. The cristae were uniformly oriented on the same plane and evenly spaced one from the other Direct continuity of the lamellae of the cristae with the internal lamella of the outer limiting membrane was established at some points The thickness of the outer limiting membrane was less than that of the cristae Some *cristae extended almost completely across* the interior of the organelle The matrix was uniformly dense Not all mitochondria possessed such regular internal organization. Occasional ones were almost devoid of cristae; others presented bizarre arrangements of the cristae. Some microbodies were present

Mitochondria were clustered in and around the cell center (figs. 20 and 21) Many established direct contact with the nucleus Facing the cell center the nucleus exhibited one or more infoldings of its outer membrane some of them being quite deep These infoldings often encompassed mitochondria At such points of intimate contact the outer membranes of both mitochondria and nucleus were *blurred and poorly defined When more* than one mitochondrion appeared within the indentation of the nucleus the deeper one was smaller and exhibited less regular internal structure (fig. 23 insert) Similarly cristae were less well-defined in those portions of mitochondria proximal to points of contact with the nucleus than in the more distal portions

Components of the Golgi apparatus, similar in organization to those of the lymphoblast were present in the cell center At least in more mature lymphocytes (fig 20 insert) these components ex

tended into the nuclear indentations and came into close contact with the nucleus.

In addition to the membranes of the endoplasmic reticulum and Golgi apparatus, the cell center also included other prominent vesicular structures (fig. 22). These vesicles were bordered by a membrane consisting of two electron-dense lamellae separated by a more electron-lucent layer. The interior possessed the same electron density as the external ground cytoplasm. Most of the vesicles were about 0.1 μ or less in diameter. However some were considerably larger. Some of the larger ones contained secondary internal vesicles of similar structure (fig. 22). Larger vacuoles with a rather clear center were also present.

Particularly striking in the cell center was an extensive region of uniformly dense cytoplasm which encompassed the centriole and was designated the centrosome (fig. 21). This cytoplasm was composed of densely packed granules of low electron density. Except for a few ribosomes, the centrosome was devoid of the other structures which characterized the cell center.

The nucleus possessed densely packed electron-dense material interrupted peripherally by electron-lucent channels which led out to the pores of the nuclear membrane (fig. 20).

Small lymphocytes. In addition to its narrow rim of cytoplasm, the mature lymphocyte differed from the medium-sized lymphocyte in several respects (fig. 1). Endoplasmic reticulum was rarely observed. It consisted of vesicles of varied shapes and seldom were ribosomes associated with it or with the outer nuclear membrane (fig. 23). Aggregations of free ribosomes were distributed sparsely throughout the cell. Their concentration was somewhat less than in the larger lymphocytes (fig. 25).

The small lymphocyte contained fewer mitochondria; most of those present were located around the cell center. They were somewhat smaller and often possessed fewer cristae than those of larger lymphocytes. "Microbodies" were occasionally present. The Golgi apparatus was more restricted in extent and consisted chiefly of thick-walled vesicles (figs. 23 and 24). The centrosome which appeared less extensive than in the medium-sized lymphocytes encompassed the centrioles (fig. 24). Except for smaller size and fewer and more shallow infoldings of the membrane nuclear structure was not greatly altered from that of the larger lymphocytes. The nuclear infoldings continued to contain mitochondria (fig. 24).

Plasma cells

The medullary cords contained clusters of plasma cells in various stages of development interspersed with nondifferentiated reticular and phagocytic cells, all of these types being grouped around blood capillaries (fig. 26).

Immature plasma cells. The most immature plasma cells possessed several characteristics which indicated their close structural similarity to and probable derivation from the nondifferentiated reticular cell. The most immature plasma cells were polygonal in shape and possessed indistinct cell membranes (figs. 1 and 27). The nucleus was roughly central in location and, except for patchy areas of electron-dense material, contained nucleoplasm of low density.

On the other hand, the direction of differentiation of the nondifferentiated reticular cell to a plasma cell was shown by several other ultrastructural features. The earliest indication was the appearance of elongated profiles of endoplasmic reticulum with flattened cisternae oriented parallel to the nuclear surface and in the immediate vicinity of the nucleus (fig. 27). Attached ribosomes also appeared early. With increasing maturity the branching membranes of the endoplasmic reticulum came to extend throughout the cytoplasm except for the Golgi area, and enclosed extensively anastomosed cisternae (fig. 28). Concurrently the number of ribosomes increased. The cisternae were narrow and contained a material of somewhat less density than that of the ground cytoplasm (fig. 28). Some ribosomes were scattered free in the cytoplasm. Another characteristic which indicated that nondifferentiated reticular cells develop into plasma cells was the appearance in the youngest plasma cells of electron-dense

material at the periphery of the nucleus (fig 27) Subsequently this material was aggregated into peripheral clumps around a large central nucleolus, creating the typical spoke-like pattern which is characteristic of the cell as seen with light microscopy (figs. 1 and 28) Mitochondria were ovoid and of somewhat varied size. Some contained well-developed and densely arranged cristae. "Microbodies were frequently present. The Golgi apparatus was not a prominent feature of the younger forms (fig 27)

Mature plasma cells Mature plasma cells were more round in shape and the nuclear-cytoplasmic ratio was less than in younger forms The nucleus had assumed an eccentric position and appeared to be actually smaller than in the young plasma cell (fig 29)

The endoplasmic reticulum extended throughout the voluminous cytoplasm with the exception of the Golgi area. The anastomosing cisternae were generally flattened while some were dilated and filled with a cloudy material. The numerous ribosomes were generally associated with the outer surface of the endoplasmic reticulum. Mitochondria were large and ovoid and located in the rather dense ground cytoplasm between cisternae. Most mitochondria were situated near the cell center Their cristae consisted of thin lamellae which were more numerous and more closely arranged than those of any other cell type

The Golgi apparatus was large in relation to size of the cell It consisted of several layers of double membranes which in somes cases appeared to encircle the cell center (fig. 30) In other cells the double membranes were arranged in stacks. Adjacent to these membranes were large vacuoles. In the cytoplasm of the cell center and in that just outside the parallel Golgi membranes were many vesicles which contained material of variable density The outer wall of these vesicles appeared to be thick which in at lea[illegible]ome instances may have resulted from [illegible] lane at which the vesicles were sect[illegible]d Within the cell center were freq[illegible] bodies (fig. 30 D) which rar[illegible]e from that of the small vesicl[illegible] the size of the clear vacuoles. [illegible] bodies possessed irregular contours and were surrounded by dense limiting membranes. The cell center contained a few dense granules which appeared to be ribosomes (fig. 30)

The nucleus exhibited the same pattern as that of the more advanced immature plasma cell except that it was smaller and of a more regularly round contour Also the nucleoplasm was denser but with the spoke-like pattern remaining clearly evident.

Modifications in the structure of plasma cells Several modifications in the structure of plasma cells were observed (fig. 1) *In the first type of modification (type A)* the cytoplasm became voluminous with the cisternae being greatly expanded and of irregular contour (fig. 31) The cisternae contained a flocculent material of low electron density Mitochondria retained the structure seen in those of mature plasma cells. Being located in the narrow strands of ground cytoplasm they appeared to cause the endoplasmic reticulum to bulge into the cisternae The dense cell center Golgi components and a centriole typical of the mature plasma cell, were retained.

The second form (type B) was characterized by great enlargement of the cisternae of the endoplasmic reticulum due to the accumulation within them of an amorphous material which except for its somewhat greater electron density was similar to that in the cisternae of mature plasma cells (fig 32) Further condensation of this material appeared to result in formation of Russell bodies which were almost homogeneous (fig. 33) although direct transformation was not demonstrated. In such cells the intervening endoplasmic reticulum and ribosomes remained fairly distinct. The ground cytoplasm appeared only as narrow strands bordered by the endoplasmic reticulum Mitochondria were located within these narrow strands of ground cytoplasm. The nucleus was deformed, and exhibited a rather marked increase in the density of its nucleoplasm (fig. 32)

A third type (C) of modified plasma cell differed from the preceding two in that it was much smaller and appeared to be in an exhausted state (fig. 26 PG) The cis-

ternae were narrow and contained only a small amount of flocculent material. The cell center with its associated Golgi appa ratus was exceedingly dense. Ribosomes were numerous and associated with an endoplasmic reticulum which was well-developed. The nucleus was small, contained denser nucleoplasm and exhibited invaginations of the nuclear membrane. A few mitochondria remained.

DISCUSSION

The reticular cells

Maximow distinguished two types of cells associated with reticular fibers ('27) namely a phagocytic and a non-phagocytic or nondifferentiated cell which with others was said to form a syncytium. However morphological distinctions between these two types of cells have never been clearly established. In the spleen of the rabbit, Stoeckenius and Naumann ('57) recognized large light and small dark reticular cells with the electron microscope. The light reticular cells were interpreted to be closely similar to the primitive reticular cell of Maximow The details of the ultrastructure of reticular cells in my study permitted their subdivision into a nondifferentiated form, one associated with fibers and a phagocytic type.

Nondifferentiated reticular cells Little attention has been given to the electron microscopy of nondifferentiated cells in general. Porter ('54) Munger ('58) and Bernhard and Granboulan ('60) have noted that various types of nondifferentiated cells are characterized by a lack of devel opment in the endoplasmic reticulum Golgi apparatus, and mitochondria and by an absence of other specialized struc tures. In agreement with their observa tions are the simplicity of the cytoplasmic membranous structures, the presence of fairly numerous ribosomes, and the poorly developed Golgi apparatus and mitochondria in the nondifferentiated reticular cell of the lymph node from the rat. In general, these observations agree with those made on this cell type by Bernhard and Granboulan ('60) in man.

The constant presence of electron-lucent foci in the nucleoplasm mitochondria and ground cytoplasm of the nondifferentiated reticular cell may have resulted in part from damage occurring during the technical procedures. However if this is true the differences cited must have stemmed from the unique intrinsic constitution of the cell because adjacent cells of other types did not reveal similar alterations.

Although using a different fixative Sorenson ('60) described a large nucleolus in the nondifferentiated reticular cell of the rabbit. It was much smaller in the rat. Since Brachet ('57) and Prescott ('59) have concluded that ribonucleic acid is synthesized in the nucleolus the small size of this structure may indicate that ribonucleic acid is synthesized at a low rate Although a fair number of ribosomes were present, the poor development of the endoplasmic reticulum would suggest that protein synthesis was proceeding slowly Similarly the lack of intramitochondrial development might be indicative of a low concentration of oxidative enzyme activity within this organelle (Green and Hatefi, '61)

Reticular cells associated with fibers Moe ('60) described the reticulum of lymphatic sinuses in the mouse as consisting of a tube of reticuloendothelial cells en compassing an extracellular connective tissue component. Sorenson ('60) noted that the internal framework of the lymph node in the rabbit is made up of large groups of collagenous fibers which are covered by elongated flattened endothelial or reticular cells In my study of lymph nodes in the rat, collagenous fibers likewise were shown to be encompassed by cytoplasm throughout their extent In fact, no fiber was observed which presented a bare surface to the lumen of a sinus or other tissue space. Thus, it has now been shown in three species that collagenous fibers composing the reticular framework of the lymph node are totally encased in cytoplasm. This arrangement leads one to expect a more continuing participation of cellular activity in the metabolism of collagen and its associated ground substance in the lymph node than may be true of fibro-elastic connective tissue. Since these fibers are the argyrophilic ones of light microscopy the interesting possibility is raised that this cellular associa-

tion may account for their silver-staining property

The infolding of the plasma membrane of reticular cells to surround enclosed fibers is a striking feature of these cells. Although not reported by Sorenson ('60) it is seen clearly in several of his photographs (figs. 2 and 4) This relationship raises the following intriguing possibility regarding the functional relationship of cells to the fibers. If fibrils are formed at the surface of the cell it may be inferred that the cytoplasm subsequently flows around them in a rotational pattern with respect to the long axis of the fibrils. Then enlargement and development of fibers might continue while encased by the cytoplasm Immaturity of many of the fibers is probably indicated by the sparsity of the fibrils.

The frequent occurrence in the processes of reticular cells of a well-developed endoplasmic reticulum with many associated ribosomes has particular significance with respect to the formation of protein a relationship which has been stressed by many workers including Porter ('53 '54) Braunsteiner and Pakesch ('55) and Palade ('56) Porter and Pappas ('59) presented convincing evidence that collagenous fibers are formed at the surface of chick fibroblasts which contain extensive endoplasmic reticulum with associated ribosomes in their elongated pseudopodia. It appears quite probable that the similar processes of reticular cells in the rat lymph node are concerned with synthesis and deposition of tropocollagen The frequent perinuclear ribosomes also may be related to active protein synthesis. Indeed additional study is required to determine whether any significant structural difference exists between the fiber-associated reticular cell and the fibroblast.

The reticular cells of lymph nodes are generally regarded by histologists as existing in a syncytial arrangement It is pertinent that in all reticular cells observed in the lymph node of the rat the cytoplasm intervening between nuclei was always compartmentalized by a cell membrane Thus the existence of a true reticular syncytium is highly improbable

Phagocytic reticular cells Phagocytosis is regarded currently as being a process essentially similar to pinocytosis (Palade '55 '56 Bennett '58 Karrer '58 '60) The plasma membrane participates by folding inwards in areas where foreign particles have become attached to the cell (Karrer '60) Enclosure of these particles is completed by the formation of cytoplasmic pseudopods (Essner '60) or ruffles (Karrer '60) adjacent to the infoldings which permit external closure of the plasma membrane. Thus the included bodies are surrounded by a membrane which is derived from the plasma membrane and possesses the same intrinsic structure. However there is not yet complete agreement on the general interrelations of the outer cell membrane with the internal membranes of the cell. In the splenic macrophage of the chick and rat Palade ('55 '56) concluded that the plasma membrane is continuous with the endoplasmic reticulum and Robertson ('59) observed that both membranes are of identical structure These observations have not been confirmed and Karrer ('60) disagrees with the conclusions drawn from them. Thus the possible relationship of the membrane surrounding inclusion bodies to endoplasmic reticulum is unresolved In this study the limiting membrane of the type B inclusion body was continuous with other intracellular membranes which may have been a component of the endoplasmic reticulum

Assuming the validity of the concept that phagocytosis is essentially similar to pinocytosis several ultrastructural characteristics of the phagocytic reticular cell may be explained The rarefaction of cytoplasm in the neighborhood of inclusion bodies a condition not observed previously by others in other types of phagocytic cells may have resulted from engulfment of external fluid during phagocytosis. Further the limiting membranes surrounding inclusion bodies of types A and B a feature observed by Karrer ('58) in alveolar macrophages of the lung, may have been derived from the cell membrane when the material was taken up Although continuity of the limiting membrane around inclusion bodies with the cell membrane was not established in this study frequent infoldings of the latter membrane were

seen which at their internal ends appeared to continue into vesicles.

Schulz ('58) and Karrer ('60) have arranged the different types of inclusion bodies in the probable order of their ingestion and subsequent development. Type B without myelin figures was described in the macrophages of the lung (Karrer '60) as being representative of material just after its ingestion. The appearance of myelin figures was thought to represent a subsequent step in modification of this material. Indeed, formations of this type have been described in a wide variety of cells some of which are not generally regarded as being phagocytes (reviewed by Miller '60) Evidence indicates that the newly formed membranes are composed of lipoprotein (Miller '60) of unknown origin. The presence of ferritin-like granules in this type of body indicates that at least some of the inclusions represent fragments of erythrocytes. No inclusion bodies comparable to the third type have been described previously The small size and extreme density of this body indicate that it may have arisen from further condensation of one of the other types.

The accumulation of endoplasmic reticulum and ribosomes in the region of phagocytized bodies suggests participation of these organelles in the destruction of ingested materials by the synthesis of essential enzymes. Essner ('60) observed high acid phosphatase activity in phagocytic vacuoles following ingestion of erythrocytes. The presence of high concentrations of acid phosphatase and other hydrolytic enzymes in lysosomes may be pertinent (de Duve '59 Straus '59) because of the possible identity of lysosomes and inclusion bodies The presence of rough-surfaced endoplasmic reticulum in the neighborhood of phagocytized material has not been a general observation (Miller '60)

The formation of lymphocytic cells

Only Bernhard, Haguenau and Leplus ('55) and Bernhard and Granboulan ('60) have described the ultrastructural changes which characterize lymphocyte formation The fine structure of the cells representing various stages in lymphocyte formation in the rat resembles in many respects that described for the human lymph node by Bernhard and Granboulan. Several additional important features were observed. The transformation of the nondifferentiated reticular cell to the lymphoblast (fig. 1) in the rat was characterized by rounding up the cell with increase in volume of cytoplasm by cytoplasmic differentiation which included the appearance of a more extensive endoplasmic reticulum consisting of flattened vesicles increase in the number of free and attached ribosomes an increase in the number of mitochondria as well as in the number and regularity of cristae which were supported by a denser matrix, enhanced prominence of the Golgi apparatus and increased density of the nucleoplasm

In the continued development of lymphoblasts into small lymphocytes a different trend of changes took place which in many respects reversed the structural modifications which occurred in the development of the lymphoblast from the nondifferentiated reticular cell. With declining size of the cell and cytoplasmic volume the endoplasmic reticulum ribosomes and Golgi apparatus became less prominent and the mitochondria smaller and fewer in number Similarly the nucleolus became smaller while the density of nucleoplasm increased These changes can be taken to indicate a reduced rate of protein synthesis. Indeed the mature lymphocyte gives the ultrastructural appearance of a rather inactive cell. Other ultrastructural characteristics of the lymphocyte not previously observed require further consideration

The centrosome The frequent occurrence of centrioles in the cell center confirms the classical observations of light microscopy Furthermore the exceedingly dense homogeneous cytoplasm in which the centrioles were located demonstrates the presence of cytoplasmic specialization in this area. Although the term centrosome has been used with varied connotations by different workers (Wilson '53) it is probably the most desirable term for designation of this area, particularly since the region is devoid of other organelles

Spatial relation of mitochondria to nucleus The apposition of mitochondria to the nuclear membrane suggests (a) that

transport occurs between the two structures or (b) that mitochondria arise from the nucleus. The time-lapse cinematography of Frederic (54) and the electron micrographs of Ornstein ('56) have revealed the more general occurrence of this relationship in other types of cells. Previous studies suggest the involvement of the nucleus in the synthesis of mitochondrial diphosphopyridine nucleotide (Brachet, '57) The possibility that transport occurs between nucleus and mitochondria appears feasible. Furthermore, the blurring of nuclear and mitochondrial membranes at these points of contact occurs so regularly that functional significance is implied. With respect to the possible origin of mitochondria from the nucleus Brandt and Pappas ('59) showed that this occurs in some lower forms. In the lymphocyte, mitochondria encompassed by the indentation of the nuclear membrane were smaller and contained less well-developed cristae than those outside of the indentation and situated farther away from the nucleus. These variations may well suggest the maturation of mitochondria as they move away from the nucleus although origin directly from the nucleus is not necessarily indicated.

Vesicles with double electron dense membranes The vesicles observed in this study which possessed double electron-dense membranes may be identical with the compound vacuoles described in lymphocytes by Low and Freeman ('58) as judged on the basis of similarity in distribution and size However these workers did not observe the triple-layered structure of the wall as was observed in this study No indication of the functional significance of these vesicles was obtained.

Nuclear structure Bernhard and Granboulan ('60) described the nucleus of lymphocytes as being uniformly dense This was not the case in this study where material of high electron density became increasingly clumped toward the periphery of the nucleus as development progressed from the lymphoblast to the mature lymphocyte These aggregations were separated by less dense areas or ill-defined channels leading to and through nuclear pores. The nuclear channels may serve as passageways through which metabolites move into and out of the compact nucleus of lymphocytes.

The plasma cells

It is now clear that the cytoplasm of the mature plasma cell is distinguished by an extensive endoplasmic reticulum associated with a multitude of ribosomes (Braunsteiner and Pakesch '55 Thiéry '55 '58 Kautz, De Marsh and Thornburg '57; and Bernhard and Granboulan '60) The origin of the cell is less certain. According to most investigators utilizing the light microscope the plasma cell arises by direct transformation from the lymphocyte (Trowell, '58 Roberts, Dixon and Weigle '57) Thus far convincing electron microscopic evidence for this transformation has not been presented, and was not secured in this study The electron microscope offers a distinct advantage in resolving this dilemma because endoplasmic reticulum with its associated ribosomes constitutes a much more precise microscopic criterion for identification than does cytoplasmic basophilia as viewed with the light microscope This criterion makes possible the differentiation of the lymphoblast from the most immature plasma cell (plasmablast) The incipient development in nondifferentiated reticular cells of endoplasmic reticulum with the distinctive form and orientation which characterize it in mature plasma cells in addition to the early changes in nuclear structure, provide strong support for the concept that in the normal lymph node plasma cells are derived from the nondifferentiated reticular cell. This viewpoint was advanced previously by Braunsteiner and Pakesch ('55) Thiéry ('60) and Bernhard and Granboulan ('60) Thus it appears that the lymphocytes and plasma cells represent different cell lines arising from the nondifferentiated reticular cell and that if lymphocytes do transform into plasma cells the transformation might involve prior dedifferentiation toward the nondifferentiated reticular cell

The significant development of mitochondria and the Golgi apparatus in plasma cells may be interpreted as being indicative of a metabolically active cell A large nucleolus in other cell types has

been associated with rapid synthesis of ribonucleic acid (Brachet, '57; Prescott, '59) which can be correlated with the presence of many cytoplasmic ribosomes. These features combined with the extensive endoplasmic reticulum are the structural counterparts of active protein synthesis.

The material located within the cisternae of the endoplasmic reticulum may represent the protein synthesized by the plasma cell. Numerous studies with the light (Fagraeus, '48) and electron microscopes (Braunsteiner and Pakesch '55 Thiéry '55 '58) point to participation of the plasma cell in antibody formation. This concept raises the possibility that the intracisternal material may be composed of or contain antibody protein. Furthermore Russell bodies appear to arise from a further increase in the concentration of intracisternal substance (Thiéry '58). When the fluorescent antibody technique was applied to Russell bodies their periphery fluoresced brilliantly (White '54).

The frequent clusters of plasma cells around phagocytic reticular and nondifferentiated reticular cells is suggestive of a similar arrangement observed by Bessis ('58) in the bone marrow. Sorenson ('60) noted this relationship in the lymph node of the rabbit and described a unique extension of the plasma cell cytoplasm into the cytoplasm of neighboring cells which he suggested may be concerned with the interchange of substances between these cells.

SUMMARY

The ultrastructure of the mesenteric lymph node of the rat was described with emphasis being placed on cellular interrelationships. Reticular cells were divided into three types nondifferentiated reticular cells reticular cells associated with fibers and phagocytic reticular cells. Collagenous fibers were surrounded invariably by the cytoplasm of reticular cells. A syncytial arrangement of reticular cells could not be demonstrated. Inclusion bodies in the phagocytic reticular cells were grouped into three types. Type A was large and dense and surrounded by a limiting membrane. Type B was less dense and often contained myelin figures. Type C was small with an extremely dense periphery and a clear interior.

The development of lymphoblasts from nondifferentiated reticular cells was characterized by augmentation of cytoplasmic volume expansion of endoplasmic reticulum, increase in the number of ribosomes development in the structure of mitochondria and of the Golgi apparatus and by an increase in the density of nucleoplasm. In development of lymphoblasts to mature lymphocytes all of these trends were reversed except for changes in the nucleus. In addition, a prominent centrosome encompassed the centrioles. Some mitochondria were in contact with the nuclear membrane. Evidence was presented which indicates that the plasma cell differentiates directly from the nondifferentiated reticular cell. In its later stages the plasma cell underwent various forms of structural modification. Intracisternal material appeared to condense to form Russell bodies.

ACKNOWLEDGMENTS

To Professor Burton L. Baker I owe my deepest appreciation for his encouragement and advice during this work.

LITERATURE CITED

Bennett, H. S. 1956 The concepts of membrane flow and membrane vesiculation as mechanisms for active transport and ion pumping. J. Biophys. Biochem. Cytol., 2 (No. 4 suppl.) 99–103.

Bernhard, W. and N. Granboulan 1960 Ultrastructure of immunologically competent cells. Ciba Foundation Symposium. Cellular Aspects of Immunity. Little Brown and Co. Boston, pp. 9[illegible]–11

Bernhard, W., F. Haguenau and R. Leplus 1955 Coupes [illegible] d'éléments sanguins et de ganglions lymphatiques étudiées [illegible] microscope électronique. Rev. Hémat. 10 [illegible].

Bessis [illegible] 56 L'îlot erythroblastique [illegible] fonc[illegible] de la moelle osseuse [illegible] 8–11

——— 1959 Différents aspects du [illegible] dans l'organisme. II. Différentes formes de l'hémosidérine. J. Biophys. Biochem. Cytol. 6 237–240.

Brachet, J. 1957 Biochemical Cytology. Acad. Press, Inc., New York.

Brandt, P. W. and G. D. Pappas 1959 Mitochondria. II. The nuclear-mitochondrial relationship in *Pelomyxa carolinensis* Wilson (Chaos chaos L.) J. Biophys. Biochem. Cytol., 6. 91–96.

Braunsteiner H., K. Pellinger and F Pakesch 1953a Demonstration of cytoplasmic structure in plasma cells. Blood, 8 916–922.
——— 1953b Elektronmikroskopische Untersuchung der Plasmazellen im lymphareticulären Gewebe. Deut. Arch. klin. Med., 200 657–663.
——— 1957 Electron microscopic investigations on sections from lymph nodes and bone marrow in malignant diseases. Blood, 12 278–294
Braunsteiner H and F Pakesch 1955 Electron microscopy and the functional significance of a new cellular tructure in plasmacytes A review Ibid., 10 650–654
C ulfeld, J B. 1957 Effects of varying hicle for OsO in tissue fixation J Biophys. Biochem. Cytol 3 827–830
de Duve C. 1959 Lysosomes, new group of cytoplasmic particles. In S bcellular Particles. T H yashi, ed. Ronald Press Co., New York, pp. 128–159
Essner E. 1960 An electron microscopic study of erythrophagocytosis. J Biophys. Biochem. Cytol., 7 329–334
Fagraeus A. 1948 Antibody production in relation to the development of plasm cells. Acta Med. Scand., 130 (suppl. 204) 5–122.
Frederic J 1954 Action of various substances on the mitochondria of living cells cultivated i vitro Ann. N Y Acad. Sci., 58 1246–63
Granboulan N 1960 Étude u microscope électronique des cell les de la lignée lymphocytaire normale Rev Hémat., 15 52 71
Green, D E., nd Y Hatefi 1961 The mitohondrion and biochemical machines. Science 133 13–19
Karrer H E 1958 The ltrastructure of the mouse lung the alveolar macrophage. J Biophys. Biochem. Cytol 4 693–700.
——— 1960 Electron microscopic study of the phagocytosis process in the lung Ibid., 7 357–366.
Kautz, J and Q B De Marsh 1954 An electron microscope study of sectioned cell of peripheral blood and bone marrow Blood 9 24–38.
Kautz, J Q B De Marsh and W Thornburg 1957 A polarizing and electron microscope study of plasma cell Exp. Cell Res 13 596–599
Low F N and J A Freeman 1958 Electron Microscopic Atlas of Normal and Leukemic Human Blood. McGraw Hill Book Co., Inc New York
Luft, J H 1956 Permangan te A new fixat for electron microscopy J Biophys Biochem. Cytol 2 799–802
M ximow A. 1927 Bindegewebe und blutbildende Gewebe H ndbuch der mikroskopischen Anatomie des Menschen (Möllendorff) II/1 232–583 Berlin
Miller F 1960 Hemoglobin bsorption by the cell of the proximal onvol ted tubule in mouse kidney J Biophys Biochem. Cytol 8 689–718.
Moe R. 1960 Electron microscopic morphology of lymphatic sinuses An Rec 136 215 (abstract)
Munger B L. 1958 A phase and electron microscopic study of cellular differentiation in pancreatic acinar cells of the mouse Am. J An t., 103 1–35.
Ornstein L. 1956 Mitochondrial and nuclear interaction. J Biophys. Biochem. Cytol 2 (No. 4 suppl.) 351–352.
Palade G E. 1952 A study of fixation for lectron microscopy J Exp. Med., 95 285–298
——— 1955 Rel tions between the endoplasmic reticulum and the plasma membrane in macrophages. Anat. Rec., 121 445 (abstract)
——— 1956 The endoplasmic reticulum. J Biophys. Biochem. Cytol., 2 (No. 4 suppl.) 85–98.
Porter K. R. 1953 Observations on submicroscopic basophilic component of cytoplasm. J Exp. Med., 97 727–750.
——— 1954 Electron microscopy of basophilic components of cytoplasm. J Histochem. Cytochem., 2 346–373.
Porter K. R., and G D P ppas 1959 Collagen formation by fibroblasts of the chick embryo dermis. J Biophys. Biochem. Cytol. 5 153–166.
Prescott, D M. 1959 Nuclear synthesi of cytoplasmic ribonucleic acid in Amoeba proteus. Ibid 6 203–206.
Roberts, J C., J F J Dixon and W O. Weigle 1957 Antibody-producing lymph node cells and peritoneal exudate cells. A M A Arch Path. 64 324–332
Robertson, J D 1959 The ultrastructure of cell membranes nd thei derivati es Biochem Soc Symp., 16 3–43
Rouiller C and W Bernhard 1956 "Microbodies" and the problem of mitochondrial regeneration in liver cell J Biophys Biochem Cytol., 2 (N 4 suppl) 355–360
Schulz, H 1958 Die submikroskopische Pathologie der Cytosomen in den Alveolarmakrophagen der Lu ge Beitr path Anat allg. P th. 119 71–91
Sorenson C D 1960 An electron microscopic study of popliteal lymph nodes from rabbits Am J A t 107 73–90.
Stoeckenius, W and P N ma 195 Elektronenmikroskopische U tersuchungen zur Antikörperbildung in der Milz. Proc VI Congr Europ Soc Haemat. 2 81–89
Straus W 1959 Rapid cytochemical identification of phagosomes in various tissues of the rat nd thei differenti tion from mitochondria by the pero idase method J Biophys. Biochem Cytol 5 193–204
Thiéry J P 1955 L erg stoplasme des plasmocytes l'état vi ant Rev Hémat 10 715–732
——— 1958 Étude ur le plasmocyte con traste de phase et en microscopie électronique III. Plasmocytes à corps de Russell et à cri taux Ibid. 13 61 78.
——— 1960 Microcinem togr phic contributions to the study of pl sma cells. Ciba Foundation Symposium. Cellular Aspect of Imm nity Little Brown and Co Boston, pp. 59– 1
Trowell, O A 1958 The lymphocyt I t Rev Cytol 7 235–293

Watson, M. L. 1958 Staining of tissue section for electron microscopy with heavy metals. II. Application of solutions containing lead and barium. J Biophys. Biochem. Cytol., 4 727 729.

White R. G. 1954 Observations on the formation and nature of Russell bodies. Brit. J Exp Path., 35 365–376.

Wilson E. B 1953 The Cell in Development and Heredity Macmillan Co., New York.

Abbreviation to plates

C, cell center	IB type B inclusion body
CM, cell membrane	IC, type C inclusion body
Co, centriole	L, lymphocyte
Cr crystalloid	Li, lipid droplet
Cs, centrosome	M, mitochondria
ER, endoplasmic reticulum	No, nucleolus
F collagenous fiber	P plasma cell
G Golgi pparatu	PR, ph gocytic reticular cell
IA, type A inclusion body	V vacuole

PLATE 1

EXPLAN TION OF FIGURES

Unless stated to the contrary all illustrations are of tissues fixed in OsO_4.

2 A nondifferentiated reticular cell showing irregular cytoplasmic processes and an indistinct cell membrane The Golgi apparatus appears to consist primarily of thick walled vesicles. The electron-dense material of the nucleoplasm is sparsely distributed. × approximately 10,000.

3 A portion of nondifferentiated reticular cell. Mitochondria are of irregular shape and have few cristae and matrix of low density The nucleus contains small nucleolus × 13,200

4 Another region of the nondifferentiated reticular cell illustrated in figure 2. Here the cell membrane is more clearly defined. Present in the cytoplasm are ggregates of free ribosomes and sparse endoplasmic reticulum. × 13,200.


OM
G
M
2


No
GM
ER
3


GM
ER
4

PLATE 2

EXPLANATION O FIGURES

5 A reticular cell associated with fibers illustrates the greater cytopl smic density as compared with that of the nondifferentiated reticular cell (fig. 2) and of the phagocytic reticular cell. A portion of phagocytic reticular cell is shown at the right. The cell membrane ppears to be infolded (arrows) to surround bundles of fibrils. × 14,200

6 A portion f the cytoplasmic process of fiber-associated reticular cell showing extensive rough-surfaced endoplasmic reticulum and longated mitochondria with umerous, well-organized cristae in dense matrix. × 15,600.


PRC
6
M
PR
CM
L
5

PLATE 3

EXPLAN TION OF FIGURES

7 This reticula cell is associated with fibers and ill str tes the lose proximity of fibers to the nucleus in addition to the numerous infoldings of the cell membrane (arrows) to encompass bundles of fibrils. These fibril are not densely packed. Irregularity of the nuclear contour large ucleolus and lipid incl sions are evident. × 12,800

8 The extensive endoplasmic reticulum with ssociated ribosomes extends throughout the cytoplasmic process of fiber-associ ted reticular cell The fiber is completely surrounded by cytoplasm the two being separated by the cell membrane × 15,000.


F
F
F
F
F
F
7
8

PLATE 4

EXPLAN TION O FIGURE

9 A phagocytic reticular cell is surrounded by several plasmacytes (P) Much of the voluminous cytoplasm of the phagocytic cell is occupied by type A inclusion body Above it is rarefied region f cytoplasm which is rich in endoplasmic reticulum. T the right of the ucleus is prominent aggregation of Golgi components. Mitochondria are well-developed, although their size is vari ble × 11,000.

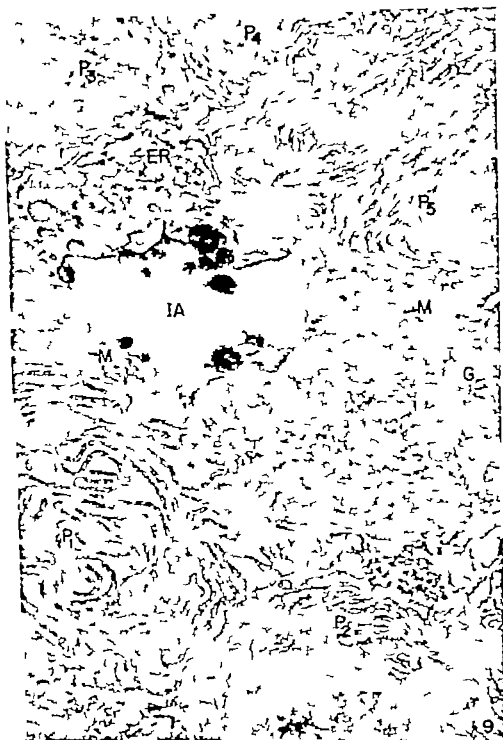

P4
P3
ER
P5
IA
M
M
G
P1
F
P2
9

PLATE 5

EXPLAN TION OF FIGURES

10 A portion of the cytoplasm of phagocytic reticular cell showing large type A inclusion body enclosed by a limiting membrane; within the inclusion body are additional smaller dense globular bodies. Other similar bodies are contained in the rarefied portion of the cytoplasm which is rich in rough-surfaced endoplasmic reticulum. The Golgi apparatus is at the right. × 11,200

11 A portion of the cytoplasm of phagocytic reticular cell illustrating the irregularity in form of the cisternae. Long profiles of the endoplasmic reticulum have both smooth- and rough-surfaced portions. Free ribosomes are scattered in the form of small gregates (arrows) Mitochondria are also irregular in structure × 28,000.


M
ER
M

PLATE 6

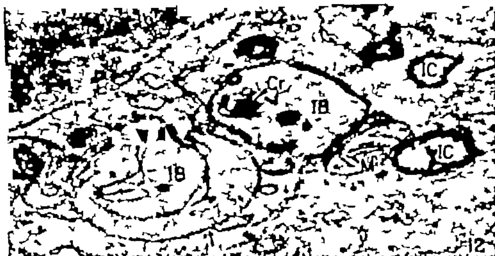
EXPLANATION OF FIGURES

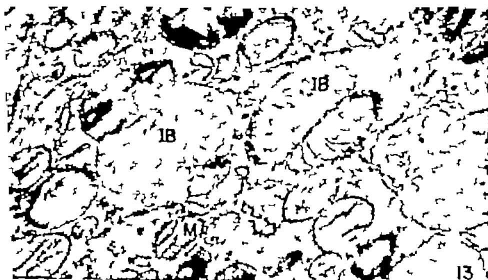
12 A portion of the cytoplasm of phagocytic reticular cell after KMnO fixation. Two large type B inclusion bodies of low electron density are shown. The limiting membrane of the one on the left is continuous with other intracytoplasmic membranes (arrow) Small crystalloid (Cr) are seen within a type B inclusion. Type C inclusion bodies ppear on the right with their clear interior nd extremely dense periphery The presence of a limiting membrane around them is uncertain. × 27,500.

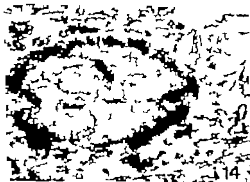
13 A portion of ph gocytic reticul cell imil to th t in figure 12, showing type B inclusion bodies of varying sizes. The large one at the right illustrates the formation of myelin structure while the large one t the left appears to represent either fusion of two bodies or fission of one. A type C inclusion body is at the lower right. × 27,000.

14 A type B inclusion body with "myelin figure. Fine dense particles within the body may be ferritin granules. A highly irregular pattern of cristae i seen i the mitochondrion t the right. × 30,000.

15 A portion f type A inclusion body possesses dense matrix in which are numerous gran les (arrow) which ppear to be ferritin. × 56,000.


IC
Cr
IB
IB
IC
M
12


IB
IB
M
13


14


15

PLATE 7

EXPLANATION O FIGURES

16 A portion of rounded macrophage shows irregularity in contour of the plasma membrane which is folded inwards (arrows) suggesting the presence of pinocytotic activity There are numerous small intracytoplasmic vesicles along with many mitochondria, an endoplasmic reticulum and some vacuoles. The nucleus is fairly electron-lucent. × 12,000.

17 A portion of rounded macroph ge which bows many peripheral finger-like projection (arrows) which make contact with others. Inclusion bodies are of type B The largest vacuoles are peripheral. × 10 400.

PLATE 8

EXPLAN TION OF FIGURES

18 This cell is probably transitional form between the nondifferentiated reticular cell and lymphoblast. The cell is irregular in shape. Mitochondria are large and have poorly developed cristae within matrix of variable density The cytoplasm contains little endoplasmic reticulum but many ribosomes. The Golgi pparatus consist of ( ) stacks of double membranes many of which end in vesicles, and (b) numerou vesicles. The nucleoplasm has increased electron density × 10,800.

19 This lymphoblast and its nucleu are rounded. Numerous mitochondria are cl stered near the cell center and have dense matrix. The endoplasmic reticulum is both rough- and smooth-surfaced and is fairly abundant. Although the plane of section did not pass through the cell center some of the Golgi components are discernible t the right side of the flattened nuclear face The nucleolus is conspicuous. × 8960.

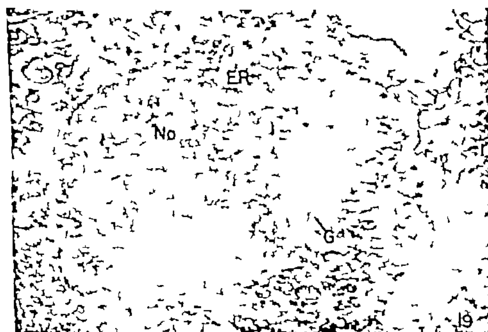

ER
No
G
19

PLATE 9

EXPLAN TION O FIGURES

20 A medium-sized lymphocyte. The cell membrane i jagged. The endoplasmic reticulum is sparse. The nuclear membrane is indented deeply In the cytoplasm opposing the indentation are mitochondria and the Golgi pparatus. × 11,200. The insert illu trates the close proximity of Golgi profiles to the nuclear indentation. At the upper left is an obliquely sectioned centriole. × 16,200

21 The cell center of medium-sized lymphocyte. Ovoid mitochondria with extremely well-developed cristae are clustered in this region. Some of the cristae extend across the entire width of the dense mitochondrial matrix. In addition to the stacks of paired membranes in the Golgi pparatus, many thick-walled vesicles are also present and are probably component of this organelle. Fine granules compose the centrosome in which no other structures are found except for a few ribosomes. The surrounding cytoplasm contains free ribosomes and few small ttened cisternae. × 22,000

22 A region of the cytoplasm from medium-size ows several vesicles of -r.ed sizes with double electron-dense me ndary vesicles 66,000


Gs
ER
G



PLATE 9

EXPLANATION OF FIGURES

20 A medium-sized lymphocyte. The cell membrane is jagged The endoplasmic reticulum is sparse The nuclear membrane is indented deeply In the cytoplasm opposing the indentation are mitochondria and the Golgi pparatus. × 11,200 The insert illustrates the lose proximity of Golgi profiles to the nuclear indentation. At the upper left is an obliquely sectioned centriole × 16,200.

21 The cell center of medium-sized lymphocyte Ovoid mitochondria with extremely well developed cristae are clustered in this region. Some of the cristae extend across the entire width of the dense mitochondrial matrix. In addition to the stacks of paired membranes in the Golgi pparatus many thick-walled vesicles re also present and are probably component of this organelle Fine granules compose the centrosome in which no other structures are found except for few ribosomes. The surrounding cytoplasm contains free ribosomes and few small flattened ci ternae × 22,000

22 A region of the cytoplasm from medium-sized lymphocyte shows several vesicles of ..r.e.l ..tes with double lectron-dense membrane and secondary vesicles I side × 66,000


Cs
ER
23
Co
M
G
25

PLATE 10

EXPLANATION OF FIGURES

23 A small lymphocyte. The cell center has a large centrosome of dense cytoplasm, but fewer mitochondria than the larger lymphocytes. The cristae mitochondriales are less concentrated and the Golgi apparatus appears to be composed primarily of vesicular components. A few large vacuoles often appear in the cell center. Endoplasmic reticulum and free ribosomes are sparse, the latter generally being freely disposed. Nucleoplasm is exceedingly dense. × 17,600. The insert shows the position of mitochondria in the nuclear indentation. The structure of the deeper mitochondrion and of the lower end of the outer one is obscure. × 15,800.

24 The cell center of a mature lymphocyte shows the centrosome and its contained centriole. In addition to some vesicular Golgi components a few triple-layered vesicles are seen (arrows). Mitochondrial contact with the nucleus is well shown. Membranes are blurred at points of contact. × 24,000

25 A small lymphocyte illustrates the paucity of ribosomes and endoplasmic reticulum, and the presence of clear nuclear channels (arrows). The outer nuclear membrane is almost completely devoid of ribosomes. × 10,200.


Cs
V
ER
G
23
Co
G
24
25

PLATE 11

EXPLANATION OF FIGURE

"6 A portion of medullary cord which is rich in plasma cells, shows various stages in their lif history Near the capillary t the lower left is phagocytic reticular cell with many inclusion bodies. × 6800.

8


P5
PH
26

PLATE 12

EXPLANATION OF FIGURES

27 A very immature plasma cell which still show many of the haracteristics of nondifferentiated reticular cells. Flat profiles of endoplasmic reticulum are arranged parallel to the nuclear membrane Many ribosomes are located freely in the cytopla m. Although cytoplasmic condensation above the central nucleus indicates early maturation of the cell center the Golgi apparatus is only vaguely defined and mitochondria re small. × 10,800.

28 An imm ture plasma cell is further advanced than the one shown in figure 27 The extensive cisternae of the endoplasmic reticulum are often confluent and most f the ribosomes are associated with the endoplasmic reticulum. The nucleus is still centrally loc ted but the peripheral ggregation of electron-dense m terial is apparent. The nucleolus is very large × 11,200.



PLATE 13

EXPLANATION OF FIGURES

29 A mature plasma cell shows an extensive endoplasmic reticulum with somewhat dilated cisternae which contain a cloudy material. Mitochondria are large and well-organized. The Golgi apparatus is large. The nucleus contains dense nucleoplasm and is eccentrically located. × 11,200.

30 This is typical Golgi apparatus of the mature plasma cell. Extensive bilaminated membranes encompass the cell center which contains dense ground cytoplasm. The membranes are associated with vacuoles. Numerous thick-walled vesicles (arrows) with an interior of variable density are found both inside and outside the paired membranes. Irregularly shaped dense bodies (D) with thick walls appear to have arisen by transformation from the smaller vesicles. A portion of the nucleus is visible below. × 46,000.



G
D

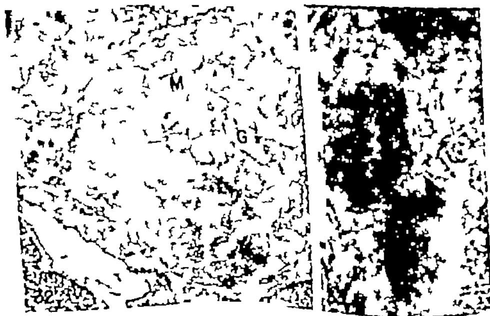
PLATE 14

EXPLANATION OF FIGURES

31 A plasma cell illustrates the type A modification. Greatly enlarged cisternae contain less dense flocculent material than that in the mature plasma cell. Mitochondria in the narrow strands of ground cytoplasm bulge toward the cisternae. The centrally located Golgi body is large and dense and contains a centriole which is cut transversely. The nucleus is sectioned far from its equatorial plane. × 8000.

32 This plasma cell shows the type B modification. The cisternae are more rounded and contain denser material than is true of the mature plasma cell. Several mitochondria are packed in between the cisternae. × 7600.

33 Dense globular bodies in the cytoplasm of cell somewhat similar to the one shown in figure 31. They are within the cisternae of rough-surfaced endoplasmic reticulum and are believed t be Russell bodies. × 48,000


M
G
32

A Study of Lumbrical Muscles in the Human Hand

H. J MEHTA AND W U GARDNER
Department of Anatomy Yale University School of Medicine New Haven, Connecticut

Much of the versatility and deftness of the human hand depends upon its intrinsic musculature. Improvements in technic have enabled surgeons to consider these muscles more frequently Certain finer aspects, that seemed unimportant a few decades ago are now of surgical significance (Bunnel, '60)

Because the lumbrical muscles usually arise from the tendons of flexor digitorum profundus and insert into the expansion of the extensor tendons, they act on all the digital joints of the respective fingers. Their importance in delicate balance of digital movements is disproportionate to their size.

Lizars (1824) noted that the lumbrical muscles had been described prior to his work under such names as (1) musculi quatuor digitos pollici adducentes (2) quatuor qui parve admodum in vola paer ent chordis secundi; (3) quatuor extreme manus musculi post primum; (4) flectentes primus internodium; (5) les musculis lombricaux les palmiphalangiens; (6) annuli tendino phalangiens. His plates and descriptions are accurate.

The variations of body musculature in general have been treated extensively by Wood (1866 1868) and by Macalister (1875) who reviewed many pertinent previous reports. Russel and Sunderland ('38) and Basu and Hazary ('60) discuss variations of the lumbrical muscles of the human hand.

The normal anatomy of lumbricals has been described in detail by Bunnel ('56) Fairly detailed accounts are included in textbooks of human anatomy (Morris '53 Spalteholz, 48; Piersol, '30 and Gray '60). Isolated and peculiar anomalies have been reported (du Bois Reymonds, 1894 Lane 1887; Wood, 1868 and Macalister 1875) The innervation of lumbricals and their variations have been described by Brooks (1887) and Cliffton (48) The functional aspects of the intrinsic muscles of the hand are well discussed by Sunderland (45)

The morphology and comparative anatomy of these muscles have been studied and summarized (Bunnel, '56 McMurrich '03 and Straus, 42) The anatomy of these muscles especially in anthropoid apes, was discussed by Hepburn (1892) Murphy ('56) Cunningham (1892) Keith (1894) and Jones (42)

MATERIALS AND METHODS

The hands of 33 male and 5 female cadavers were dissected. Both hands of all except one cadaver were dissected; in all 75 hands were observed.

The dissections were started by the students but in most cases instructors had assisted them. All hands were dissected further before the muscles were measured and then innervations, origins and insertions ascertained. The data were recorded and a sketch made.

Calipers, with a vernier scale were used for measuring the following lengths (fig. 1)

(a) of origin, the length between the farthest points of the attachment

(b) of the muscle belly from the most proximal point of origin to the most distal point where muscular fibers ended

(c) of the tendon, from the most proximal point of its appearance to its distal end in insertion;

(d) total muscle (TL) from the most proximal point of the origin to the point of merger of the tendon at the curved proximal point in the extensor expansion (EE) or the far

International Cooperation Administration Fellow, 1960. Permanent address B. J Medical College, Ahmedabad, India. Present address New York Medical College.

thest point of bony attachment if the muscle did not insert in EE,

(e) distance from the distal border of flexor retinaculum (FrL) the distance between the most proximal point of the origin to the nearest point on the distal border of flexer retinaculum (FR) results recorded as (+) if distal to (−) if proximal to and (O) if at the distal border

When a muscle was inserted into two fingers the length of the common part and the separate parts of the belly both the tendons and two total lengths were measured. The proportion of the muscle fibers going to each finger was estimated.

The measurements were recorded by the nearest whole millimeter Averages and percentages are reported to the first decimal point.

A steel tape was used to measure the length of the finger (FnL) The distance between the tip of the finger and the nearest point on a line extending from the scaphoid tubercule and distal border of the pisiform bone was used as the length of the finger The middle digit was invariably the longest and represented the maximum hand length.

OBSERVATIONS

The patterns of origin and insertion of the several lumbrical muscles are summarized in tables 1 and 2 and the several measurements that were made recorded in table 3 The first lumbrical muscle resembled the usual text-book description in 62 hands (82.7 per cent, fig. 1) Of the variations 7 were in right hands and 6 in left hands. Although muscle usually arose from the radial side of the first tendon of flexor digitorum profundus (FDP) in 11 hands (14 7%) it also came from the anterior surface of the tendon. Additional origins in the palm were the first tendon of flexor digitorum superficialis (FDS,) the first metacarpal and the third metacarpal (table 1) Origins in the forearm were from muscles FDS and flexor pollicis longus (FPL)

The origin from the third metacarpal was located on the palmar aspect immediately distal to the origin of the transverse head of adductor pollicis (fig. 3) The normal origin from FDP was absent. The belly curved towards the lateral side of head of the second metacarpal and inserted in EE,

TABLE 1

Patterns of origins of the lumbrical muscles
(Study of 75 hands)

Lumbrical muscle	Textbook type		Incomplete normal origin	Additional palmar origins			Additional forearm origins		
				Adjacent FDP	Same FDS	Metacarpal	FDP	FDS	FPL
no.	%	no.	no.	no.	no.	no.	no.	no.	no.
1	98 7	74	1	0	9 rl = 1 l = 4 r = 3	2 = l = meta I l = l = meta III	0	2 rl = 1	1 l = 1
2	100	75	0	21 rl = 6 = 4 l = 5	1 r = 1	0	2 rl = 1	1 = 1	0
3	93.3	70	3 = 1 l = 2	0	0	0	0	2 rl = 1	0
4	86.7	65	6[1] l = 1 = 3 l = 1	0	0	0	0	0	0

[1] Does not include 4 instances of the absence of the m scle

Abbreviations r right; l, left; meta, metacarpal; FDP flexor digitorum profund FDS, flexor digitorum superficiali ; FPL, flexor pollicis longus EE, extensor expansion

TABLE 2

Patterns of insertion of lumbrical muscles
(Study of 75 hands)

Lumbrical muscle	Textbook type		"Split" insertion	Misplaced insertion	E.E. and base of I phalanx	I Phalanx base (exclusive)	Fibrous flexor sheath	Transverse metacarpal ligament	FDS
no.	%	no.	no.	no.	no.	no.	no.	no.	no.
1	100	75	0	0	3 = 2 l = 1	0	1 l = 1	0	0
2	89.3	67	1 = 1	0	6 r = 5 l = 1	0	1 l = 1	1 l = 1	0
3	48	36	29 rl = 9 r = 2 l = 9	7 rl = 1 r = 3 l = 2	13 rl = 3 = 3 l = 4	2 = 1 l = 1	0	1 l = 1	1 l = 1
4	60*	45	6 rl = 1 = 2 l = 2	6 rl = 3	46 rl = 21 = 2 l = 2	8 rl = 2 l = 4	0	0	0

Insertions in EE_4 alone occurred only in 17.3% (13) hands.
For abbreviation see footnote table 1

TABLE 3

Measurements of the lumbrical muscles
(Study of 75 hands)

Lumbrical muscle	Length of origin: Lateral	Length of origin: Medical	Length of muscle belly	Length of tendon: Lateral	Length of tendon: Medical	Total length	Finger length	Distance from flexor retinaculum
	Range and mean ± SD	Range and mean ± SD	Range and mean ± SD	Range and mean ± SD	Range and mean ± SD	Range and mean ± SD	Range and mean ± SD	Range and average
	mm	mm	mm	mm	mm	mm	mm	mm
1	16–48 26.7 ±6.76		41–75 57.3 ±6.91	9–33 18.6 ±5.80		47–86 68.5 ±8.50	130–181 159.5 ±11.09	(+20)–(−13) +2.1
2	7–53 27.2 ±8.93	6–33 15.1 ±8.57	39–81 61.3 ±9.46	5–31 13.5 ±5.83		49–95 72.8 ±9.21	140–194 170.4 ±11.26	(+12)–(−23) −3.25
3	7–35 14.5 ±5.22	7–30 18.3 ±5.10	31–69 52.0 ±8.32	0–16 8.2 ±4.33	5–19 11.2 ±2.57	41–77 59.3 ±7.41	137–181 158.9 ±11.40	(+19)–(−9) +7.6
4	5–23 14.1 ±4.71	5–25 10.5 ±4.81	27–67 47.5 ±7.34	0–17 9.3 ±3.83	0–17 7.9 ±3.56	36–63 49.5 ±7.50	112–156 137.5 ±11.30	(+33)–(−27) +13.9

In 21 instances of bipennate origins.
All measurement figures in millimeters.

The forearm origins were tendinous and came either from the belly of FDS for the index finger or from medial border of FPL. Each tendon formed a muscle belly dorsal to the flexor retinaculum and joined distally with the palmar part of the first lumbrical muscle.

The muscle was always unipenniform and the belly was usually large. The tendon was long, appeared first on the ante-

Fig. 1 Diagrammatic presentation of the usual description of the palmar lumbrical muscles and schematic presentation of the points used for the measurements made.

Fig. 2 Diagrammatic presentation of some of the more frequent variations in insertion and of the points of innervation of the lumbrical muscles. Insertion on the proximal phalanx of the 4th and 5th digit and insertion on the ulnar side of the extensor expansion of the third digit were noted frequently

rior or anteromedial aspect and its junction with the muscle belly was dovetailed. Muscle fibers continued for a longer distance posteroradially (fig. 2)

The muscle was always inserted on the radial side of EE_1 and in addition on the radial side and base of the proximal phalanx and the fibrous flexor sheath in 4 instances (table 2)

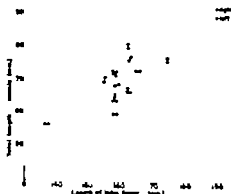
The muscle received its nerve supply from the median nerve via its radial digital branch to the index finger The nerve always entered the muscle at the anterior border opposite the distal point of origin. A definite neurovascular hilus was present in all but 10 hands (86.7%) Additional innervation came from (a) additional branch from the same source in 7 hands (9 3%) and (b) a deep branch of ulnar nerve in one

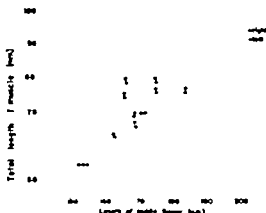
The muscle s total length was roughly related to the length of the index finger (correlation coefficient 0.2944 fig. 4)

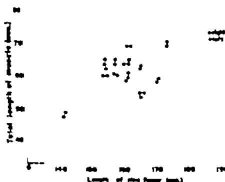
The *second lumbrical muscle* adhered to the textbook pattern less closely than the first lumbrical (68% or 51 of 75 hands) Thirty-two per cent of the deviations from the normal pattern, were bilateral in 5 cadavers in right hands in 10 and in left hands in 4

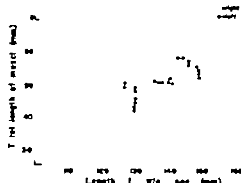
The muscle usually arose from the radial side of FDP_2. The origin extended to the anterior aspect of FDP in 29.3% (22) hands and/or the posterior aspect in 6 7% (5) hands.

Fig. 3 Diagram of additional anomalous origins and insertions of lumbrical muscles.


Figure 4


Figure 5


Figure 6


Figure 7

Figs. 4, 5, 6, 7 Relationship between total length of lumbrical muscles and length of the respective digits. (See figure 1 for points of measurement.)

Additional origins were (a) in the palm (1) ulnar side of FDP (2) FDS₄, and (3) in an isolate example there was a common mass of origin for second and third lumbricals occupying the anterior aspect of FDP (b) in the forearm a tendinous origin from (1) the portion of the FDP muscle to the middle finger and (2) corresponding part of the FDS muscle. The muscles were bipenniform in 28% of hands. The long muscle belly usually the longest in any given hand was narrower than that to the index finger. The usual form of musculotendinous junction was an oblique line, muscle fibers extending more distally on the radial side. Sometimes the junction was of "spike-dovetailed" type like the one of the first lumbrical.

The muscle was inserted in all instances, on the radial side of EE₄. Additional insertion variants were (a) the split-insertion, (b) insertion in the base of the proximal phalanx, (c) insertion in the fibrous flexor sheath and (d) insertion in the transverse metacarpal ligment (table 2)

The muscles were innervated by the median nerve via its digital branch for the adjacent sides of index and middle fingers. The nerve usually entered the anterior aspect of the muscle, a little more distally than in the first lumbrical. A definite neurovascular hilus was present in 12% of hands (R = 3, L = 6). A deep branch of the ulnar nerve supplied one muscle in a left hand.

The measurements of the components of the muscle are listed in table 3

The coefficient of correlation between the muscle's total length and the length of

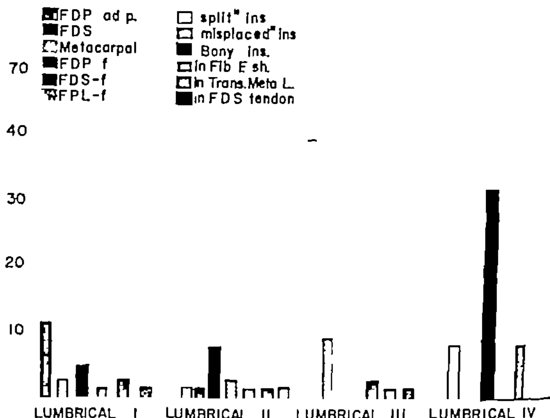


Fig 8 Incidence (per cent) of variations in origin and insertion of the lumbrical muscles.
FDP adp — adjacent palmar flexor digitorum profundus.
FDS — palmar part of flexor digitorum superficialis.
f — forearm.
FPL — flexor digitorum longus.
ins. — insertion.
Fib. F sh. — insertion fibrous flexor he th.

the digit was 0.3393 This was the highest correlation of all 4 lumbricals. Even so the total muscle length only moderately correlated with finger length (fig 5)

The *third lumbrical muscle* has been labeled the most variable lumbrical. The textbook type was observed in 45.3% (34 of 75) of the hands dissected The vari ants were distributed thus 14 cadavers had bilateral variations 5 had variations in the right hand and 8 in the left hand. The more frequent variations involved insertions rather than the origins of this lumbrical.

The muscle usually arose from adjacent sides of the tendons FDP and FDP. Ori gins from FDP alone occurred in 4% of hands (R = 1 L = 2) Additional origin from the forearm from the corresponding part of FDS occurred in the same subject which had a similar origin for the second lumbrical.

Usually bipenniform the muscle was unipenniform in three hands. The belly was usually slender and joined the tendon in a more or less transverse line In hands in which the insertion was split the length of the common part of the belly ranged from 10–50 mm.

The insertion in EE, as described in textbooks occurred in only 48% of the hands (table 2) Variant insertions were (a) split or "bifid" insertion to EE and EE (b) misplaced insertion to EE, (c) additional insertion in the base of the first phalanx, (d) exclusive insertion in the first phalanx (e) insertions in the transverse metacarpal ligament and (f) in the

tendon of FDS_4 in order of decreasing frequency In the last type of insertion the muscle split, about 80% of fibers inserted in EE_4 and 20% *constituting the medial* portion joined the tendon FDS_4 at the level of metacarpophalangeal joint, just before the flexor tendons entered the fibrous flexor sheaths. Incidentally this was the same cadaver in which the left first lumbrical arose from the third metacarpal and the 4th lumbrical was absent bilaterally

The innervation came from the deep division of the ulnar nerve in all but three hands. Usually the nerve entered the posterior aspect of the muscle. Additional branches entered the superficial surface of the muscle from (a) the loop between superficial division of the ulnar and the median nerve in 14 hands (19 7%) (b) the most lateral palmar digital branch of ulnar nerve in 4 hands (5 3%) and (c) from the most medial digital branch of the median nerve in 28 hands (37.3%) In 7 hands of last group (9.3%) no loop existed between the median and the ulnar nerves.

The measurements of the component of the muscle are listed in table 3

The total lengths of the muscles were not closely correlated with length of the ring finger (correlation coefficient 0.2595 fig 6)

The *4th lumbrical muscle* was the smallest and adhered to the textbook pattern in 45 hands (60%) if the additional insertion in the base of the first phalanx is considered normal. This "bony insertion, sometimes exclusive, is the characteristic quality of the muscle. Forty per cent of the muscles did not conform to the normal pattern as follows (a) absent in both hands of two male cadavers (5 3%) and (b) deviating in insertion in 26 hands, bilaterally in 7 cadavers, 5 in the right hand of 5 cadavers and 7 in the left hand of 7 cadavers.

The muscle usually arose from the adjacent sides of tendons FDP and FDP_4. The variations of origin were the lack of origin either from FDP or from FDP (table 1)

The muscle was bipenniform in all but 6 hands and the belly was small and delicate. In cases of split-insertion the common part of the belly ranged in length from 27–34 mm. The tendon was shorter delicate joined the muscle in a horizontal line and was absent in cases of "exclusive *bony insertions.*

The insertion in EE_4 alone occurred in 13 hands (bilateral in 5, right in 2 and left in 1) Variation in insertion pattern include bony insertions "additional or exclusive split-insertions and "misplaced insertions to EE_4 (table 2)

The usual nerve supply was from the deep division of the ulnar nerve a branch of which entered the deep aspect of the muscle In two hands a branch from the most medial digital branch of the ulnar nerve supplied the muscle. Additional sources of innervation were an extra branch from deep division of the ulnar nerve in two hands and superficial division of ulnar nerve in three hands.

The total muscle length was not appreciably correlated with the length of the little finger (correlation coefficient 0 1872 fig. 7)

DISCUSSION

A normal hand would be an uncommon entity if exact concurrence with the textbook descriptions of lumbricals was used to define the normal (Buchanan, '50; Anson and Maddock, '58; Cunningham '51 Gardner '60 Grant '58 Gray '60 Last '54; Mainland, 45 Morris, '53; Piersol, '30; Spalteholz, 48; and Woodburne, '57) In only one of 38 cadavers would both hands have been considered normal. Twelve hands (16% three bilaterally 4 right, two left) correspond to the textbook pattern if the differences of innervations and additional insertions into the proximal phalanx are not taken into account. Thirty-nine per cent of the hands corresponded to this classical description in the series of Kopsch (1898) and Reinhardt ('01)

The incidence of variation has been reported previously on the per cent of individuals or per cent of hands. The available data are compared with the present series (table 4) The incidence of variations reported by these two different patterns is not strictly comparable. Sunderland ('45) states that regardless of the manner in which results have been treated both the incidence and range of variation in lumbricals must be high.

TABLE 4
Incidence of variations of the lumbrical muscles

Per cent of variations	No. of subjects	No. of hands	Investigator
13	300	—	Le Double (1897)
12.5	400	—	Macalister (1875)
18.6	102	—	Wood (1868)
45	?	?	Froment (1853)
58.3	—	72	Basu and Hazary ('60)
61	—	100	Kopsch (1898)
61	—	100	Reinhardt ('01)
84	—	75	Present series

The lumbrical muscles may be reduced in number by the absence of one or more of them in a given hand. Textbooks report that they may be reduced to two (Gray '60 Cunningham, '51). Wood (1868) states that the absence of lumbricals was observed by earlier anatomists. Macalister (1875) reported that both the hands of one cadaver lacked lumbrical muscles. The first and second lumbrical muscles were lacking and the third and 4th lumbricals were vestigial in both the hands of a cadaver (Russel and Sunderland, '38). That third and 4th lumbricals may be absent has been reported (Morris '53 Eyler and Markee '54).

The 4th lumbrical is most frequently absent. Wood (1868) reported three instances in 110 subjects dissected and Macalister (1875) 4 in 400. Basu and Hazary ('60) reported one such absence in 72 hands. In the present series 4th lumbrical was absent in both the hands of two cadavers (5.3% i.e. in 4 of 75 hands).

Five lumbricals may be present (Cunningham, '51) or 6 (Gray '60). Braithewaite et al. ('48) state that the increase in the number of the lumbricals is more common than the reduction. The third or 4th lumbricals may be doubled (Morris '53). Macalister (1875) reports that each of Walther Petsche Böhmer and Carver had observed 5 lumbricals in one hand. He has reported an instance of double first lumbrical and mentions Wood to have observed one such example. It is assumed here that all his predecessors used the same criteria as Macalister's in reckoning a doubling of a lumbrical. Applying his criteria to the present series all the 8 forearm origins would have to be listed as examples of double or supernumerary lumbricals. The fibers from the forearm origins merge at a varying point with the belly coming from the palmar origin and in no case reach the insertion in EE independently. Hence they are reported as "additional forearm origins" and not as "double lumbricals."

The origin of a muscle is the most variable in different species whereas the innervation as well as the insertion are more fixed and afford a better clue to morphological lineage, Cunningham, 188.. Keith (1894) considered that linear segmentation of a muscle had little morphological value for example the different species of primates show considerable individual variation in segmentation of the flexor digitorum profundus. In the gibbon this muscle's belly may split in 7 parts or may be fused into a very slightly segmented mass.

The lumbricals may arise from the front as well as the sides of FDP tendons (Woodburne '37 Cruveilhier 1871). That they may also arise from the dorsum of FDP tendons has not been reported apparently. In addition to arising from the lateral or medial margins of FDP tendons the lumbricals arose also (a) anteriorly in 40 instances (lumbricals I = 11 II = 18 III = 5 IV = 6) (b) anteriorly and posteriorly in 5 instances (II = 4 and III = 1) and (c) only posteriorly in one instance (II) out of a total of 296 muscles examined. Lum-

TABLE 5
Altered form of the lumbrical muscles

Lumb. 2 (Bipennate)		Lumb. 3 (Unipennate)		Lumb. 4 (Unipennate)		No. of hand examined	Investigator
Per cent	No.	Per cent	No.	Per cent	No.		
	6		4		0	102	Wood (1868)
22.2	16	0	0	2.8	2	72	Basu and Hazary ('60)
28	21	4	3	8	6	75	Present series

bricals arise from the side front, and back of the corresponding flexor tendon in the tapir (Campbell, '36)

The origin often overlaps the overlying FDS tendon (Bunnel, '56; and Lizars 1824)

Lack of an origin from a FDP tendon or an additional one from the adjacent deep flexor tendon alters the form of the muscle, thus, a usually bipennate muscle becomes unipennate and vice versa The incidence of altered form has been compared with the reported data from other sources (table 5) The 4th lumbrical may arise from FDP alone (Lizars, 1824) All the lumbricals in a monotreme are bipennate, there are three of them and arise between the 4 superficial podial flexors (the deep flexors of this species correspond to dorsal interossei) (Howell, '36)

Lumbricals have been reported to derive origins from other sources either in the palm or in the forearm. Such origins as an occasional possibility have been reported (Kopsch, 1898 Morris, '53 and Grüber [quoted by Macalister 1875]) In the present series no example was observed with an origin from either an interosseous muscle (Wood 1868, one first lumbrical) or a metacarpophalangeal ligament (Lane, 1887 first lumbrical in both the hands of one cadaver)

The intrinsic muscles of the palm constitute several layers of flexores breves muscles in amphibia and reptiles. The flexor muscles of the forearm end at the wrist. The first forearm flexor muscle to reach the digits is FDP in the alligator (Bunnel, '56) by incorporating part of the fascia which intervenes between the flexores breves superficiales and medius (McMurrich, '03)

Flexor digitorum superficialis and pal maris longus, however are peculiar to therian mammals and have no homologues in other tetrapods (Straus 42) FDS gets linked with its palmar part which seems to be derived from flexores breves super ficiales.

The lumbricals differentiate from the superficial stratum of the flexor brevis medius the deep stratum contributing to the adductor pollicis and the interossei. Apes have 4 lumbricals which diminish in size from the first to the 4th and which differ greatly in site of origin. In the orang the 4th lumbrical arises from only FDP (Hepburn, 1892) Muscles contrahentes digitorum of the gibbons hand are supposed to be equivalents of human lumbri cals (Murphy '36)

The usual origins from FDP tendons and occasional ones from FDS as well as from the metacarpals in man have counter parts in other species.

The usual and less frequent insertions of the lumbrical muscles have been studied more frequently than other aspects of their gross structure. That, variations occur has been mentioned in textbooks (Cunningham, '51; Gardiner '60 Grant, '58 and Last, '54) and reported in some detail or by illustration in other textbooks (Morris '53 Spalteholz, 48 Grant, 47) The third lumbrical has been considered the most variable primarily because of the variations of its insertion, and especially its split-insertion.

The double or split-insertions of the lumbricals observed in the present series are compared with other reported data (table 6) The misplaced insertions to the adjacent digit have been recorded and

TABLE 6

"Split insertion of the lumbrical muscles"[1]

Lumb. 2		Lumb. 3		Lumb. 4		No. of hands	No. of subjects	Investigator
Per cent	No.	Per cent	No.	Per cent	No.			
2.8	2	20.8	15	11.1	8	72	36	Basu and Hazary ('60)
0	0	15.6	5	6.3	2	32		Eyler and Markee ('54)
—	—	43	47	9	10	110		Kopsch (1898) Q. by McMurrich
—	—	43	43	10	10	100		Reimhardt ('02) Q. by McMurrich
	50	—	—	—	—	—		Spalteholz (48)
	1	—	6	—	1	72		Wood (1868)
1.3	1	38.7	29	8	6	75	38	Present series

[1] Also called "Double or "Bifid" insertion.

TABLE 4
Incidence of variations of the lumbrical muscles

Per cent of variations	No. of subjects	No. of hands	Investigator
12	200	—	Le Double (1897)
12.5	400	—	Macalister (1875)
18.6	102	—	Wood (1868)
45	?	?	Froment (1853)
58.2	—	72	Basu and Hazary ('60)
61	—	100	Kopsch (1898)
61	—	100	Reinhardt ('01)
84	—	75	Present series

The lumbrical muscles may be reduced in number by the absence of one or more of them in a given hand. Textbooks report that they may be reduced to two (Gray '60 Cunningham, '51) Wood (1868) states that the absence of lumbricals was observed by earlier anatomists. Macalister (1875) reported that both the hands of one cadaver lacked lumbrical muscles. The first and second lumbrical muscles were lacking and the third and 4th lumbricals were vestigial in both the hands of a cadaver (Russel and Sunderland '38) That third and 4th lumbricals may be absent has been reported (Morris, '53; Eyler and Markee '54)

The 4th lumbrical is most frequently absent. Wood (1868) *reported* three instances in 110 subjects dissected and Macalister (1875) 4 in 400 Basu and Hazary ('60) reported *one* such absence *in* 72 *hands.* In the present series, 4th lumbrical was absent in both the hands of two cadavers (5.3% i.e in 4 of 75 hands)

Five lumbricals *may be* present (Cunningham, '51) *or 6* (*Gray* '60) *Braithewaite et al.* (48) *state that the increase in the number of the lumbricals is more common than the reduction. The third or 4th lumbricals may be doubled* (Morris '53) Macalister (1875) reports that each of Walther Petsche Böhmer and Carver had observed 5 lumbricals in one hand. He has reported an instance of double first lumbrical and mentions Wood to have observed one such example. It is assumed here that all his predecessors used the same criteria as Macalister's in reckoning a doubling of *a lumbrical. Applying his criteria to the* present series all the 8 forearm origins would have to be listed as examples of double or supernumerary lumbricals. The fibers from the forearm origins merge at a varying point with the belly coming from the palmar origin and in no case reach the insertion in EE independently Hence they are reported as "additional forearm origins" and not as double lumbricals.

The origin of a muscle is the most variable in different species whereas the innervation as well as the insertion are *more fixed and afford a better clue to morphological* lineage Cunningham, 1882 Keith (1894) considered that linear segmentation of a muscle had little morphological value *for* example the different species of primates show considerable individual variation in segmentation of the flexor digitorum profundus *In the gibbon this* muscle's belly may split in 7 parts or may *be fused into a very slightly segmented* mass.

The lumbricals may arise from the front as well as the sides of FDP tendons (Woodburne, '57; Cruveilhier 1871) That they may also arise from the dorsum of FDP tendons has not been reported, apparently In addition to arising from the lateral or medial margins of FDP tendons the lumbricals arose also (a) anteriorly *in 40 instances* (lumbricals I = 11 II = 18 III = 5 IV = 6) (b) anteriorly and posteriorly in 5 instances (II = 4 and III = 1) and (c) only posteriorly in one instance (II) out of a total of 296 muscles examined Lum-

TABLE 5
Altered form of the lumbrical muscles

Lumb. 2 (Bipennate)		Lumb. 3 (Unipennate)		Lumb. 4 (Unipennate)		No. of hands examined	Investigator
Per cent	No.	Per cent	No.	Per cent	No.		
	8		4		0	102	Wood (1868)
22.2	16	0	0	2.8	2	72	Basu and Hazary ('60)
28	21	4	3	8	6	75	Present series

two and three instances respectively replacing branches were derived from the most medial digital branch of the median nerve and the digital branch of the superficial division of the ulnar nerve, respectively. When replaced by median innervation there was no loop between the median and the ulnar nerves. Brook's series (1887) had three (of 21) corresponding examples.

Additional branches to the third lumbrical were derived from (a) medial most branch of median nerve, (b) the loop (c) deep division of ulnar nerve and the superficial division of the ulnar nerve. Similar branches to the 4th lumbrical were less frequent and came from deep ulnar and digital branch of superficial ulnar. In Brook's series (1887) the superficial division of the ulnar nerve was the source of additional nerve supply for the third and 4th lumbricals.

A definite neurovascular hilus was present in 87% of the first and in 32% of the second lumbricals. There was no neurovascular hilus in the third and 4th lumbricals. Observations in man, orang, gibbon, and macaque have led Brooks (1887) to believe that the lumbricals were originally supplied on their superficial aspect and that the deep ulnar is gradually displacing the superficial. The variations in innervation have a tremendous importance in diagnosis, planning of treatment and judging the recovery in nerve repair operations (Cliffton, 48). In the present series the loop was absent in 20% (15) of the hands.

SUMMARY

1. The lumbrical muscles were studied in dissections of 75 hands and forearms. Their attachments, form, innervation, and component parts were ascertained and measured when practical.

2. The first lumbrical was the most constant and differed from the textbook descriptions in 17.3% (13) of the hands. The origin was located on an average 2.1 mm distal to the distal border of the flexor retinaculum. The muscle was always inserted in the extensor expansion and innervated by a branch from the median nerve which entered the muscle in a neurovascular hilus on the anterior surface.

The principal variations were in origin, (a) in the palm from FDS, first and third metacarpals and, (b) in the forearm from bellies of flexor digitorum superficialis and flexor pollicis longus.

3. The second lumbrical was the longest and differed from the textbook descriptions in 24 of the hands. The origin was located, on an average 3.25 mm proximal to the distal border of flexor retinaculum. Innervation was from median nerve. A neurovascular hilus was found in 12% of the muscles.

The principal variants of the muscles were (a) additional origins from the adjacent flexor digitorum profundus, (bipennate muscle) and in the forearm from bellies of flexor digitorum superficialis and profundus; (b) unusual insertion as "split-insertion" to extensor expansions of the index and middle finger and in the base of the proximal phalanx, in the fibrous flexor sheath and in the transverse metacarpal ligament.

4. The third lumbrical was most variable and did not conform to the textbook description in 54.7% (41) of the hands. The origin was located on an average 7.6 mm distal to the distal border of the flexor retinaculum. The usual innervation was from the deep division of the ulnar nerve. Additional innervation came from (1) the loop between the ulnar and the median nerve (19.7%) (2) digital branch of the ulnar nerve (5.3%) and (3) the digital branch of the median nerve (37.3%).

The variations of the muscle were a unipennate origin, origin from belly of flexor digitorum superficialis and misplaced insertions to the extensor expansion of the middle finger to the base of the proximal phalanx, to the transverse metacarpal ligament, to the third digital flexor digitorum superficialis tendon and split-insertions into extensor expansions of the ring and middle fingers (38.7%). The insertion in the flexor digitorum superficialis is probably reported for the first time.

5. The 4th lumbrical, the muscle of "bony insertion," did not conform to the textbook descriptions in 25 hands. The origin was located, on an average, 13.9 mm distal to the distal border of flexor retinaculum. The innervation was usually from the deep division of the ulnar nerve.

The variations of the muscle were (a) the absence of muscle, (b) a unipennate

origin, (c) a split insertion in the extensor expansion of the ring and little finger and insertion (normal) in the base of the proximal phalanx in 72% of hands.

6 The lumbricals arose usually from radial margins of the tendons of flexor digitorum profundus, but may arise from the ventral aspect and/or dorsal aspect.

7 The total lengths of the muscles were not closely correlated to the length of respective fingers.

8. These observations have been compared with the reported data.

LITERATURE CITED

Anson, B J and W C. Maddock 1958 Callander's Surgical Anatomy 4th ed., W B Saunders, Philadelphia.

Basu, S., and S. S. Hazary 1960 Variations of the lumbrical muscle of the hand. Anat. Rec., 136 501–504.

Braithwaite, F., G. D Channel, F T Moore and J Whillis 1948 The applied anatomy of the lumbrical and interosseous muscles of the hand. Guy s Hosp Reports, 97 185–195.

Brooks, H. St. John 1887 Variations in the nerve supply of the lumbrical muscles in the hand and foot, with some observations on the innervation of the perforating flexors. J Anat. Physiol., 21 575–585.

Buchanan s Manual of Anatomy 8th ed. 1950 ed. F Wood Jones, Williams and Wilkins, Baltimore.

Bunnel, S. 1956 Surgery of the Hand, J B. Lippincott Company Philadelphia.

Campbell, B. 1936 Comparative myology of the *forelimb of Hippopotamus T pir Pig* and Pecary Am. J Anat., 59 201

Clifton E. E. 1948 Unusual innervation of the intrinsic muscle of the hand by the median and ulnar nerves. Surgery 23 12–21.

Cruveilhier J 1853 The Anatomy of the Human Body 1 t American ed., Harper Brothers, New York.

Cunningham, D J 1892 Relation of nerve supply to muscle-homology J. Anat. Physiol. Lond., 16 1–9

——— 1951 Textbook of Anatomy 9th ed., ed., J C. Brash, Oxford University Press, London.

duBois, Reymond, R. 1894 Beschreibung einer Anzahl Muskel-variatäten an einem Individuum. Anat. Anz., 9 431

Eyler D. L., and J E. Markee 1954 The anatomy and function of the intrinsic musculature of the fingers. J Bone and Joint Surg., 36-A: 1–9

Gardner E., J Gray and O O'Rahilly 1960 A regional study of human tructure. W B. Saunders, Philadelphia.

Grant, J C. B. 1958 A Method of Anatomy — descriptive and deductive. Williams and Wilkins Co Baltimore

——— 1947 An Atlas of Anatomy Ibid.

Gray H. 1960 Anatomy of the Human Body 27th ed., ed C. M. Goss Le and F biger Philadelphia.

Hepburn, D. 1892 Comparative anatomy of muscles and nerves of superior and inferior extremities of anthropoid apes. J Anat. Physiol., 26. 149.

Howell, A. B. 1936 The musculature of antebrachium and manus in the platypus. Amer. J Anat., 59 425.

Jones, F W 1942 The principles of anatomy as seen in the hand. Williams and Wilkins Co., Baltimore.

Kajava, Y 1910 Die kurzen Muskeln und langen Beugemuskeln der saugetier hand. I Monotremata und Marsupalia. Anat. Heft, Bd., 42 S. 1–94.

Keith, Sir Arthur 1894 Notes on theory to account for the various arrangements of the flexor profundus digitorum in the hand and foot of primates. J Anat. Physiol., 28 335–339.

Kopsch, F 1898 Die Insertion der Musculi lumbricales an der Hand des Menschen. Inter. J Anat. Physiol., Bd., 15 S. 70.

Lane, W A. 1887 Abnormal muscle of the hand. J. Anat. Physiol., 21 674

Lane, W A., J Poland and L. A. Dunn 1887 Abnormalities observed in the dissection room of Guy' Hospital during the sessions, 1885–86 and 1886–87 Guy' Hosp. Report, 44 396–412.

Last, R. J. 1954 Anatomy regional and pplied. Little Brown and Co., Boston.

Lizars, John 1824 A system of Anatomical Plates accompanied with descriptions and physiological, pathological and surgical observations. Part V Plates X, XI, Lizars, Edinburgh.

Macalister A. 1875 Muscular Anomalies in Human Anatomy Trans. Roy Irish Acad., 25. 1–130

Mainland D. 1945 Anatomy as basis for medical and dental practice. Paul B Hoeber, Inc., New York.

McMurrich, J P 1903 Phylogeny of Palmar Musculature. Amer J Anat., 2: 463–500.

Morris, H. 1953 Human Anatomy 11th ed ed., J P Schaeffer Blakiston Co., Philadelphia.

Murphy R. C. 1956 Notes on musculature of the forearm and hand of the gibbon (hylobates Lar) Anat. Rec., 124 338.

Piersol, G. A. 1930 Human Anatomy ed. Huber A. C., J. B Lippincott Co., Philadelphia.

Reinhardt, E. 1901 Über der Ansatz der Musculi Lumbricals an der Hand des Menschen. Anat. Anz. Bd., 20 S. 129

Rowsel, K. F., and S. Sunderland 1938 Abnormalities of the lumbrical muscles of the hand J Anat., 72: 306–307

Spalteholz, W 1948 Hand-Atlas of Human Anatomy 7th ed., J B. Lippincott Co., Philadelphia.

Straus, W L., J 1942 The homologies of the forearm flexors urodeles lizards, mammals Amer J Anat., 70 281–316.

Sunderland, S. 1945 The actions of the extensor digitorum communis interosseous and lumbrical muscles. Ibid., 77 189

Wood, J 1866 I. Variations in human myology Proc. Roy Soc. Lond 15 518–546.

——— 1868 II. Variations in human myology Ibid., 16 483–525.

Woodburne R. J 1952 Essential of Human Anatomy Oxford University Press, New York

Body Proportions of Didelphid (and some other) Marsupials with Emphasis on Variability

MILTON HILDEBRAND
Department of Zoology University of California, Davis

The initial objective of this study was to present and interpret certain body proportions of didelphid marsupials with particular attention to allometric growth. The analysis was made difficult by an unexpected degree of individual variation among the animals of each sample. Accordingly an investigation of the relative variability of body proportions between marsupial and eutherian mammals became a further objective of the study. The problem has been in part biological (to describe and analyze animal proportions) and in part statistical (to cope with problems inherent in the analysis). It is desirable to explain these factors more fully.

Some years ago I made a study of skeletal proportions in the Canidae (dog family) (Hildebrand, '52) wherein it was shown that body proportions are sometimes difficult to correlate with general body size in work with mammalian materials. The problem may be summarized as follows. It is convenient to express body proportions as ratios or numerical indexes. If significant differences are found among mean values for corresponding ratios determined from samples of various populations, one may then wish to learn if the different proportions correlate with differences in general body size. To do this scatter diagrams are prepared by plotting, for each individual of each population, the log of one variable against the log of the other. Regression lines are then fitted independently to each array. If populations differing both in general body size and in the ratio under consideration share the same regression, then a correlation between size and proportion has been demonstrated. Conversely if the regressions are significantly different, then any variation in body proportion does not correlate directly with body size. This method of analyzing allometric growth is well known and widely applied.

In even the larger collections of the country however many genera of mammals are represented by fewer than 15 measurable skeletons. Most of these are of adult or subadult animals, and therefore of closely similar size. When a scatter diagram is prepared to relate the size of one bone to that of another the plotted points tend to cluster in a more or less oval area. A regression can be calculated that is mathematically exact, yet it is evident that it has limited significance—the addition of several specimens might materially alter the regression.

Because of these difficulties the results of my work on canid body proportions were unsatisfactory and I decided to make another study this time adapting the material to the method. I had observed that "adult" marsupials are more variable in body size than are typical eutherian mammals. It was supposed therefore that scatter diagrams prepared to analyze their skeletal proportions would spread out in a more linear pattern. The Didelphidae (opossums) were selected because this family is relatively well represented in American collections and includes genera of widely differing body sizes. Ratios were calculated to express selected body proportions and scatter diagrams were prepared when significant differences were found among the species. True, there was more variation of body size within species than had been noted for canid material so the plotted points did spread out lengthwise on the graphs. But the arrays also spread out in depth because of marked individual variation in body proportions. Instead of small clusters of points I had large clusters of points. It then seemed

worthwhile to test the relative variability of marsupial and eutherian body proportions in terms of other selected measurements and ratios of genera for which relatively large samples are available.

MATERIALS AND ACKNOWLEDGMENTS

Original data consist of one or more pairs of skeletal or external measurements of about 800 specimens representing the 26 mammalian genera listed in the appropriate figures. I am indebted to the curators of the following collections for making specimens available: American Museum of Natural History, British Museum of Natural History, Chicago Natural History Museum, Museum of Comparative Zoology, Museum of Vertebrate Zoology and United States National Museum. Other sources of raw data include charts of measurements in Tate ('33, 45a, 45b) and Grinnell et al. ('37). Parameters of variation shown in Gould and Kreeger ('48) and Clark ('41) were also used.

The long bones and spine were measured as described and figured in Hildebrand ('52). The combined lengths of cervical, thoracic, and lumbar vertebrae are totaled to derive what is called spine or back length. The lengths of the humerus, radius, and longest metacarpal are added to derive what is called forelimb length; similarly the lengths of the femur, tibia, and longest metatarsal are totaled to derive the hindlimb length.

Unless otherwise noted, only adult and subadult animals are included. Several of the species are represented by two or more subspecies; where sample size permitted analysis it was determined that only trivial differences existed among subspecies for the characters tested. Further comments on materials and methods are included in the following sections.

Relative variability of proportions and size of marsupial and Eutherian mammals

Limb proportions. The variation of each of 6 limb proportions was estimated for the 5 species of didelphid marsupials (opossums) for which 5 or more skeletons were available and was contrasted with the corresponding variation of similar samples of 5 species of canids (coyote and foxes). Figures 1 and 2 show the ratios tested, the species used, sizes of samples (averaging 13) and results. Each sample includes animals of each sex. Vertical lines indicate coefficients of variation, V. Rectangles, shaded for marsupials and open for canids, include the limits of V ± one standard error, S_V. Since the magnitude of S_V tends to increase with the mag

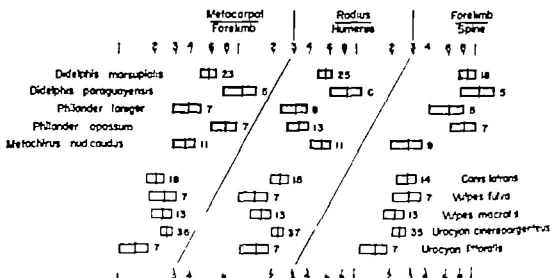


Fig. 1 Coefficient of variation plus and minus one standard error for 3 forelimb proportions of 5 species of didelphids and 5 of canids. Symbols explained in text.

nitude of V the values are plotted on logarithmic grid to facilitate visual comparison. It is emphasized that the data figured show the variation, not the magnitude, of the ratios.

It is evident that variation is greater among the marsupials. For only one of the 6 ratios, Forelimb/Spine does any V for a didelphid have a lower value than the highest V for a canid. In every instance the value of the pooled V less two S, of the didelphid samples exceeds the value of the pooled V plus two S, of the canids.

Likely to be more satisfying for the statistician is another measure of the significance of the differences between the various body proportions. A one-sided null hypothesis is set up (that the variation of one group does not exceed that of the other) and the probability of the hypothesis is tested by the observations. The ratio of the pooled variance of the didelphids to that of the canids is calculated for each body proportion, and then, using the appropriate number of degrees of freedom (here 4/4) the probabilities are found in tables (Pearson and Hartley '54 table 18) One of these 6 ratios has a probability of 15 and the others range from 06 to .01 The significance of the differences is therefore, striking. However there is one reservation. The statistician does not permit variances to be pooled unless they are homogeneous. Applying Bartlett's test for the homogeneity of variances to these 12 samples (2 groups for each of 6 proportions) we find that 7 lie comfortably below the .90 significance level, whereas the remaining 5 are clearly not homogeneous. Stepping back into the role of the zoologist, we do not find these results surprising. Indeed, it would surprise us to find that various kinds of opossums (or foxes, etc.) *did* have closely similar variability for any given body proportion. In biology homogeneity is relative. We postulated only that in regard to the proportions tested, these didelphids and these canids are less homogeneous when taken together than when taken as individual groups, and that the didelphids are almost always more variable than the canids. The data strongly support this hypothesis and encourage us to believe that any didelphid is likely to exceed any canid in the variability of any proportion of the post-cranial skeleton.

Cranial proportions It would be desirable to know if the conclusions of the preceding paragraph can be extended to marsupials as a group and eutherian mam-

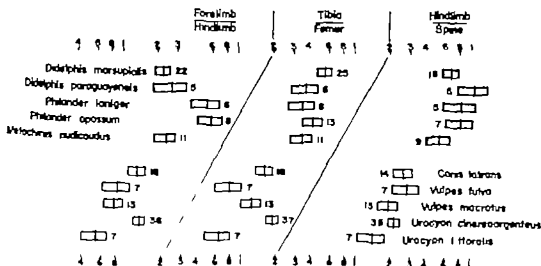


Fig. 2 Coefficients of variation, plus and minus one standard error for 2 hindlimb proportions and an intermembral proportion of 5 species of didelphids and 5 of canids. Symbols explained in text.

mals as a group A cranial proportion Basal Length/Zygomatic Breadth was selected for study because there are not enough marsupial skeletons in the entire country to permit a sufficiently broad analysis of post-cranial dimensions. Figure 3 shows the 13 species of marsupials and 14 species of eutherian mammals tested, their classification into 5 families and 5 orders respectively sample sizes (averaging 30) sources of raw data and results. Again, the figure shows the variation not the magnitude, of the ratio Symbols are the same as for the preceding figures. *Didelphis paraguayensis* is represented only by males and *Ictonyx striatus* only by females all other samples include both sexes. Separate analysis by sex for *Citellus Ondatra* and *Spilogale* revealed only trivial differences between the sexes and it is believed that none of the species is sexually dimorphic to an important degree for the ratio tested.

The value of the pooled V less one S. for the marsupials exceeds the value of the pooled V plus one S. for the eutherian mammals. The variances are not homogeneous for either group yet if following the reasoning of the previous section we use the ratio of the pooled variances of the two groups to determine the significance of the difference between their variabilities, we derive a confidence level of 14 which is only fair

Further tests of the hypothesis that skeletal proportions tend to be more variable *in marsupials than in eutherian mammals* would require study of other proportions using adequate samples of many representative species from each group. These requirements would be difficult to meet. Unfortunately the inadequacies of mar

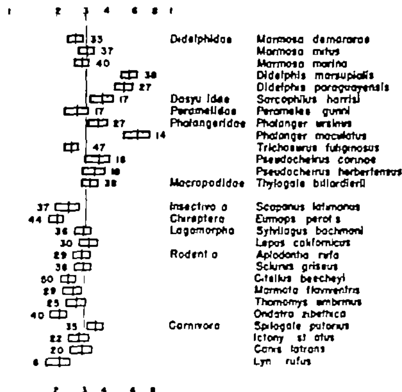


Fig. 3 Coefficients of variation, plus and minus one standard error for the ratio of basal length of skull to zygomatic breadth of 13 species of marsupial (arranged by families) and 14 species of eutherian mammals (arranged by orders) Sources *Marmosa* from T te '33 *Phalanger* from T te 45a; *Pseudocheirus* from T te, 45b; *Canis* and *Lynx* from Grinnell et al., '37; others original. Symbols explained in text.

supial collections outside of Australia would restrict such a study to cranial materials, and the selection of proportions suitable for analysis would also be limited by the desirability of finding ratios that vary independently of one another Further, I believe that cranial proportions may be expected to be less variable within or between species, than postcranial proportions. I cannot cite quantitative data (though such may be scattered in the literature) yet experience in handling skeletal materials leaves me with the impression that the skull is a relatively precision-made structure that natural selection holds within narrow tolerance limits. The functional demands on the carpus and tarsus may similarly restrict the variability of their elements. The form of the vertebrae, long bones, and (particularly) ribs and sternum in contrast, can vary more without adversely affecting function

I conclude that the data here presented support, though they do not prove the hypothesis that the skeletal proportions of marsupials are generally somewhat more variable than the corresponding proportions of eutherian mammals.

Linear measurements This study postulates that marsupials more often than other mammals, continue their growth long into adult life and are therefore more variable in linear measurement. We could hardly expect that this hypothesis would be easy to test. Size variation resulting from sexual dimorphism can be eliminated if enough specimens of one sex are available, but samples would not be random, or different samples homogeneous, in regard to age distribution museum collections commonly include many subadults of some kinds of mammals (*e g Marmota, Aplodontia*) but few of other kinds (many bats) Nevertheless, since most of the needed data were at hand (analyses of large samples by Clark, 41 and Gould and Kreeger 48 were also considered) analyzing them seemed worthwhile, and the results merit brief comment.

When variability of the basal length and zygomatic breadth of the skull of marsupials as a group (represented by 12 species from 5 families) was contrasted with that of eutherian mammals as a group (represented by 16 species from 5 orders) it was found that coefficients of variation averaged about 6 for the marsupials and 4 for the other mammals. There was such wide overlap of variability for particular samples of the two groups however that the results are of no importance for systematics.

Total body length and tail length were recorded from study skin labels for 30 to 40 specimens each of 10 species of marsupials and 10 species of eutherian mammals. No significant differences in variability were found between the two groups and variation of these external measurements markedly exceeded variation of the skeletal measurements analyzed. This difference (between external and skeletal variation) has been reported for other vertebrates and is doubtless real. Nevertheless the external dimensions of each animal are recorded by its collector and techniques for measuring vary in detail Injuries and rigor mortis introduce errors. Recorded tail lengths of short-tailed animals (rabbits mountain beaver) are particularly variable and, one suspects unreliable.

DISCUSSION

It is not clear why certain marsupials have a relatively high variability of postcranial, and probably of cranial, skeletal proportions. Bader ('65) summarizes evidence from the studies of other investigators as well as his own, that high variability tends to correlate with a low rate of evolution. In support of this view he cites high values of V for 16 metric cranial characters of three populations of *Didelphis*. My results for postcranial proportions of this, and other didelphid genera are consistent with that hypothesis. Within the order Marsupialia I did not find that variation of a cranial proportion was less among relatively specialized genera (*Sarcophilus Perameles Thylogale*) than among more generalized genera (*Marmosa, Phalanger Pseudocheirus*) but the inference may be invalid that the more specialized genera are now evolving more rapidly

Selected body proportions of Didelphid marsupials

Habits and body size Before presenting the body proportions of the didelphid

marsupials brief consideration of their habits and body sizes is desirable so as to relate them where possible, to generic differences in proportions. My data on habits are taken largely from Cabrera ('40) Osgood (43) and Tate ('31 '33 45a) The following grouping of my material is adequate for our purpose. *Lutreolina* is sometimes riparian in habits and is a good swimmer but is not aquatic.

Arboreal	Semiarboreal	Terrestrial	Aquatic
Dromiciops Marmosa (chapmani, cinerea, domina, germana, mexicana, murina, rustanica) Metachirus Philander (laniger philander)	Didelphis Marmosa (agilis, caucae micro-tarsus, noctivaga) Philander opossum	Lutreolin Monodelphis	Chironectes

Relative body size of the species studied can be determined from the scatter diagrams that follow Since such diagrams are not shown for each proportion and since not all genera are shown on each diagram, it is desirable also to indicate relative body size here. Using spine length exclusive of tail and sacrum as an index of size the genera can be grouped as shown below (The back lengths indicated are, in some instances based on few specimens.) There is considerable size variation among the numerous species of *Marmosa*. *Dromiciops* is a little smaller than *Monodelphis* and *Lutreolina* is probably a little larger than the other genera with which it is grouped.

LENGTH OF BACK

45–105 mm	115–180 mm	160–200 mm
Dromiciops Marmosa Monodelphis	*Chironectes* Lutreolina Metachirus Philander	*Didelphis*

Graphic representation of data The percentage ratios that follow list the animals by habits in the order shown above except that all species of *Marmosa* and of *Philander* are combined unless significant differences were found between their arboreal and semiarboreal species Size of sample observed range (horizontal line) value of the mean (vertical line) and extent of two standard errors to each side of the mean (rectangle) are shown for each species. The numerical values of the ranges means, and standard errors of the means are available on request.

Forelimb in relation to spine (fig 4). The forelimb of *Chironectes* was found (on the basis of two immature specimens) to be relatively long. Single specimens of *Dromiciops* and *Lutreolina* respectively seem to indicate long and short forelimbs for these animals. The remaining genera have similar and intermediate proportions the limb of *Metachirus* may be slightly shorter than those of *Philander Marmosa* and *Didelphis*

It is not clear why *Chironectes* has relatively long legs: most aquatic mammals have normal or short legs. *Lutreolina* is said to conceal itself on occasion in the grass and low relief of relatively open country; short legs may be advantageous for such behavior

No correlation between forelimb length and body size can be demonstrated because of the difficulties discussed in the first part of this paper Except with *Chironectes* and possibly *Dromiciops* and *Lutreolina* plots for all the didelphids studied could be related by a regression line (indicated on the figure) having a slope of 45

Radius in relation to humerus (fig 5). The didelphids are about equally divided between animals with radius longer than humerus and animals with radius shorter than humerus. The radius is apparently longest in *Dromiciops* (single specimen) and a little longer in *Marmosa* and *Chironectes* than in other genera Except for *Didelphis* and perhaps *Lutreolina* the same genera that tend to have long forelimbs also tend to have the radius long in relation to the humerus

Correlation of this ratio with habits is doubtful The more terrestrial animals

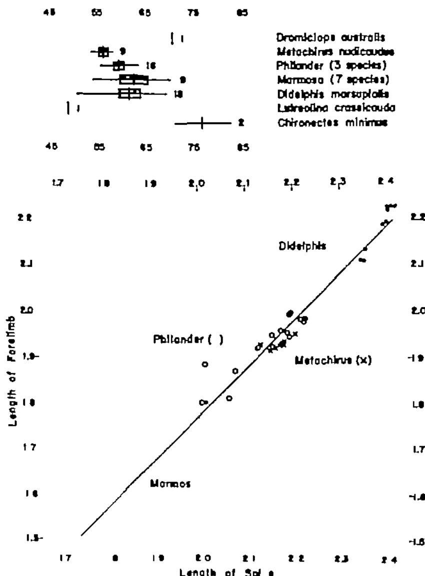


Fig. 4 Above: percentage ratio, length of forelimb to length of spine. Below: logs of same measurements plotted as scatter diagram. Symbols explained in text.

have a relatively short radius, but the arboreal animals do not necessarily have a long radius.

The scatter diagram shows less individual variation than for the previous ratio, but there is still no clear correlation between the magnitude of the ratio and the body size. The diagram is not figured.

Metacarpus in relation to forelimb (*fig 6*). Foot length as represented by the longest metacarpal, is relatively as long in *Chironectes* as in canids. It is considerably shorter in the other didelphids but is longer in *Metachirus Philander opossum Didelphis* and *Lutreolina* than in the remaining animals.

It was to be expected that aquatic *Chironectes* would have the largest foot, yet it should be mentioned that the two available skeletons were both of immature ani-

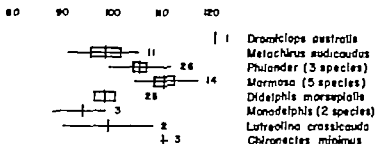


Fig. 5 Percentage ratio, length of radius to length of humerus. Symbols explained in text.

8 10 12 14 16

Dromiciops australis 1
Metachirus nudicaudus 12
Philander laniger & philander 12
Marmosa (8 species) 11
Philander opossum 8
Didelphis marsupialis 23
Lutreolina crassicauda 1
Chironectes minimus 2

8 10 12 14 16

Chironectes

Didelphis

Metachirus

Philander laniger & philander

Marmosa

Length of Metacarpus

Length of Forelimb

Fig 6 Above percentage ratio length of metacarpus to length of forelimb. Below, logs of same measurements plotted in scatter diagram. Symbols explained in text

mals, and immature mammals tend to have relatively larger feet than adults. Riparian *Lutreolina* may also have large feet (judging by a single specimen) The animal sometimes frequents swampy areas, where large feet would be advanta geous. No further correlation with habits can be noted.

Regression analysis is relatively satisfactory for this ratio. *Didelphis* and *Meta chirus* could be considered to lie on the same regression line having a slope of 45 (k = 1 in the familiar regression for mula, $y = bx^k$) or alternatively *Didelphis* and *Marmosa* could be considered to share a regression having a slope of about 48 (k > 1) which would exclude *Metachirus*. In either event *Philander laniger* and P *philander* fall on a different, and probably even steeper regression line. The plotted points for *Philander opossum* are too clumped for analysis.

Hindlimb in relation to spine (fig 7). As expected, this ratio varies among the genera in nearly the same way that the ratio of forelimb to spine was found to vary The position of *Metachirus* is how ever, somewhat different. *Chironectes* has a relatively long leg, and, judging from single specimens, *Dromiciops* may have a long leg and *Lutreolina* a short leg. All the remaining genera have nearly identical values for this ratio, regardless of habits or body size.

Tibia in relation to femur (fig 8). The tibia of didelphids is nearly always longer than the femur. The ratio of tibia to femur varies among the genera in a pat tern that recalls the ratio of radius to humerus the more distal segment is relatively long in *Dromiciops Marmosa*, and *Chironectes* and is relatively short in *Didelphis Monodelphis* and *Lutreolina*. *Philander opossum* has a longer tibia than the other species of *Philander* studied.

No association was found between this ratio and the habits of the animals. Al though the relatively terrestrial genera *Didelphis Monodelphis* and *Lutreolina* have a short tibia, the less arboreal species of *Marmosa* and *Philander* have a longer tibia than their more arboreal relatives. On the scatter diagram, plots for *Meta chirus* and *Philander opossum* fall along an extension of the regression line of *Di delphis* The slope of this line is 45 (k = 1) The regression for *Marmosa* is less steep (k > 1) It is not clear to which of these lines the remaining species of *Philander* can better be related.

Forelimb in relation to hindlimb (fig 9). *Metachirus* has relatively short forelimbs. All the other genera have about equal values for this ratio, although *Didelphis* tends to have slightly longer forelimbs than the others. No association is appar ent between the intermembral index and habits or body size.

DISCUSSION

Chironectes Lutreolina and *Dromiciops* have relatively distinctive body propor tions. *Chironectes* has long legs, long radius in relation to humerus, long tibia in relation to femur and long metacarpus in relation to length of forelimb. Each of these proportions except the first is to be expected of an aquatic animal, but the reason for the long legs is not clear.

It appears (from meager material) that *Lutreolina* has moderately large feet for a didelphid, probably in adaptation for

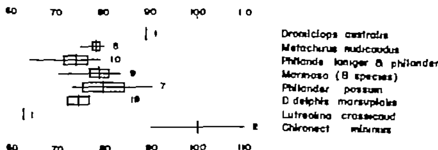


Fig. 7 Percentage ratio, length of hindlimb to length of spine. Symbols explained in text.

100 110 120 130

Dromiciops australis 1
Metachirus nudicaudus 12
Philander laniger & philander 13
Marmosa (6 arboreal species) 9
Philander opossum 13
Marmosa (3 semiarboreal species) 6
Didelphis marsupialis 25
Monodelphis (2 species) 3
Lutreolina crassicauda 2
Chironectes minimus 3

100 110 120 130

Didelphis
Metachirus (x)
Philander laniger & philander ( )
Marmosa
Length of Tibia
Length of Femur

Fig 8 *Above* percentage ratio, length of tibia to length of femur *Below* logs of same measurements plotted as scatter diagram. Symbols explained in text

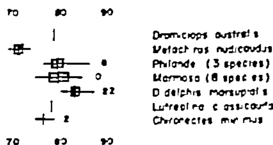


Fig. 9 Percentage ratio, length of forelimb to length of hindlimb. Symbols explained in text

walking on wet ground and swimming and short legs, which may be in adaptation for concealment on open ground.

Little *Dromiciops* has long legs, long radius in relation to humerus, and long tibia in relation to femur It is doubtful that these proportions can be related to its highly arboreal habits.

Metachirus is distinctive for its relatively short front legs in relation to hind legs. The remaining genera, *Monodelphis* *Didelphis* *Phalanger* and *Marmosa*, have similar body proportions. Such variations as are found among them do not correlate with habits so far as this study reveals, the more arboreal animals differ from the semiarboreal and terrestrial animals in behavior patterns but not in morphology Any of them could climb or walk well if it "wanted" to.

Philander opossum has a slightly longer metacarpus in relation to forelimb and longer tibia in relation to femur than *P philander* and *P laniger*

No important instance of allometric growth was demonstrated, because of individual variation and because the largest and smallest genera that are represented by adequate samples have closely similar body proportions.

SUMMARY

The variation of 6 postcranial body proportions of 5 species of didelphid marsupials was contrasted with the variation of the same proportions of 5 species of canids. Also, variation of a cranial proportion and some internal and external linear measurements of 12 to 13 species of marsupials was contrasted with the variation of the same proportion and measurements of 14 to 16 species of eutherian mammals. It was concluded that any didelphid is likely to exceed any canid in the variability of any proportion of the postcranial skeleton, and that the skeletal proportions of marsupials in general probably have somewhat more variability than the corresponding proportions of eutherian mammals.

Six body proportions of 8 genera of didelphid marsupials were analyzed. *Chironectes* *Lutreolina*, and *Dromiciops* have relatively distinctive proportions. Within the family some correlation between body proportions and habits is demonstrated for aquatic and riparian species but not for arboreal, semiarboreal or terrestrial species. Analysis for allometric growth was not rewarding, because of individual variation and because the species that differ most in body proportions tend to be of similar body size.

LITERATURE CITED

Bader R. S. 1955 Variability and evolutionary rate in the oreodonts. Evolution, 9 119–140.

Cabrera, A., and J Yepes 1940 Mamíferos Sud-americanos (Vida, Costumbres y Descripción) Historia Natural Ediar Buenos Aires, Compañía Argentina de Editores.

Clark, F H. 1941 Correlation and body proportions in mature mice of the genus *Peromyscus* Genetics, 26 283–300.

Gould, H. N and F B. Kreeger 1948 The skull of the Louisiana muskrat (*Ondatra zibethica* Bangs) I *The skull in advanced age* J Mammalogy 29 138–149

Grinnell, J J Dixon, and J M. Linsdale 1937 Fur-bearing Mammals of California Their Natural History Systematic Status, and Relations to Man. Univ Calif. Press, Berkeley vol. 2.

Hildebrand, M. 1952 An analysis of body proportions in the Canidae. Am. J Anat., 90: 217–256.

Osgood, W H. 1943 Mammals of Chile. Field Mus. Nat. Hist., Zool. Series, vol. 30.

Pearson, E. W and H. O. Hartley 1954 Biometrika tables for statisticians. Cambridge Univ Press, vol. 1

Tate, G. H. H. 1931 Random observations on habits of South American mammals. J Mammalogy 12: 248–256.

——— 1933 A systematic revision of the marsupial genus *Marmosa*. Bull. Amer Mus. N t. Hist., 66, article 1

——— 1945a Results of the Archbold Expeditions. No. 53 the marsupial genus *Phalanger* Amer. Mus. Novitates, no. 1283.

——— 1945b Results of the Archbold Expeditions. No. 54 the marsupial genus *Pseudocheirus* and its subgenera. Ibid., no. 1287

Ultrastructure of Articular Cartilage of Mice of Various Ages[1,2]

RUTH SILBERBERG, MARTIN SILBERBERG, ALFRED VOGEL AND WALLY WETTSTEIN

Department of Pathology, Washington University School of Medicine, St. Louis, Missouri, and Histopathological Institute of the University of Zürich, Switzerland

Aging of the articular cartilage manifests itself in growth as well as in regressive changes. These processes are at least partly under genetic control. Accordingly they vary in degree and rapidity of progress with species and strain. Non-genetic influences are exerted on the skeletal time curve by metabolic factors such as endocrine secretions and nutritional influences (Silberberg and Silberberg, '41, '59, '60, '61). Articular aging changes are considered by many investigators to be forerunners or pacemakers of osteoarthrosis and transitions exist between the simple changes of aging and degenerative joint disease of old age (Weichselbaum, 1877; Payr, '34; Bennett, Waine and Bauer, '41; Silberberg and Silberberg, '41, '61). An understanding of articular aging is therefore not only of basic but also of practical interest. The sequelae of these changes can be followed readily in mice which develop an analogue of the human disease (Silberberg and Silberberg, '41; Sokoloff, '56). One of the unresolved problems centers about the question whether the growth processes observed in aging joints are of primary nature or whether they are preceded by regressive changes in the matrix. This question could not be answered by light microscopy. In continuation of our earlier investigations dealing with development and aging of cartilage we therefore began systematic studies of the ultrastructure of articular cartilage of mice. The present report deals primarily with one aspect of the problem, namely the formation and fate of fibers in the articular cartilage during the lifespan of the mouse.

MATERIAL AND METHODS

Mice of strains C57BL, JAX 6, C3H and Swiss albino varying in age from one day to more than two years were used. The animals were killed with chloroform or by severing the cervical spine. The femur heads were exposed, removed quickly and transferred into one of the following fixing fluids: 10% neutral formalin, 1% potassium permanganate, 1% osmium tetroxide in Palade's Veronal-acetate buffer or first to 10% neutral formalin followed by 1% osmium tetroxide. Since the use of decalcifying agents resulted in too much distortion and destruction of cells, the tissues were dehydrated in alcohol or acetone without previous decalcification, and embedded in methacrylate — three parts of the butyl and one part of the methyl compound — or in Araldite obtained from the Ciba Company, Basle, Switzerland. Accurate orientation is essential for the study of articular surfaces; therefore an attempt was made to embed the blocks uniformly with the insertion of the ligament facing outward in the embedding capsule. This part of the femoral head was sectioned off and discarded, and sections for phase microscopy were taken from a level near the center of the specimen or slightly above (fig. 1).

Some care had to be taken in order not to cut too deeply into the specimen and to avoid the epiphyseal growth zone. In some instances the growth zone merges gradually with the cartilage of the head of the femur and ossification of the latter

[1] These investigations were carried out during the stay of the senior authors in Zürich; they were supported by Grant A-1679 (C2) of the National Institute of Arthritis and Metabolic Diseases, National Institute of Health, Public Health Service.

[2] We are greatly indebted to Professors Drs. A. von Albertini and K. Mühlethaler for their interest shown and generous advice given during the course of these studies.

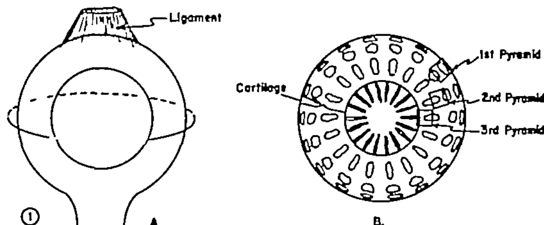


Fig. 1 Diagram demonstrating the preparation of the tissue for sectioning. A shows how part of the head of the femur was cut off and discarded; B indicates areas where "pyramids" may be trimmed for thin sectioning.

proceeds from there without formation of a secondary center of ossification. Remnants of the growth zone may persist into late adulthood but in senile animals they have usually disappeared. These conditions have been described in detail (Johnson '33; Sokoloff and Jay '56) If the precaution mentioned above was observed, the cut surface gave an accurate view of the articular cartilage in its entire thickness and, from a certain stage of development on of the underlying spongiosa and of the bone marrow cavity Difficulties were encountered in obtaining good complete sections for phase contrast microscopy of the heavily calcified bones of old animals. However as a rule such sections were at least adequate for orientation and selection of an area for thin sectioning (figs. 2, 3) After a field was chosen its precise location was determined according to a method described in detail elsewhere (Vogel '60 '61) and a diagram of the section was made with the aid of a drawing prism. The distance of the center of the area to be cut from two points on the margin of the section was measured with an object micrometer and the measurements were entered on the sketch. In this way it was easy to localize the desired field even after some time had elapsed after preparation of the phase section and even by a person other than the one who cut the phase section For the preparation of the pyramid the block was transferred to a special holder designed for use with the Zeiss dissecting microscope (Vogel '60) With the help of a micrometer ocular the area to be sectioned was identified a rectangular field measuring about 0.2 × 0.4 mm was marked off with a razor blade as the apex of a pyramid to be cut out of the block. The latter was then trimmed to leave a pyramid about 0.1 mm high to be sectioned with the ultramicrotome The smallness of such a pyramid makes it possible to cut further pyramids from a nearby or another area of the tissue block, if the first pyramid has been cut down.

The specimens were cut with the Porter Blum or the LKB ultramicrotome using hard glass knives (Scott and Gen. Mainz, Germany) or a diamond knife. Sections were mounted on 400 mesh copper grids coated with formvar reinforced by carbon shadowing; some were left unstained; others were stained for one to two hours with a 1% solution of phosphotungstic acid or uranyl acetate respectively Most of the material was studied with the Philips electron microscope model 11980/03 (1952) and micrographs were made on 35 mm film; a few micrographs were taken with the Siemens Elmiscope.

Diffraction studies were carried out on some mineralized areas. We are indebted

We are indebted to Dr A. R. Stefer for the preparation of the phase microphotographs.

to Dr Robert M. Frank, Institut Dentaire Faculté de Médicine Strasbourg, France and to Professor Dr W Epprecht and to Dr. A. Niggli, both of Zürich for their help in preparing the diffractograms and interpreting the findings.

OBSERVATIONS

Newborn animals

Phase microscopy The head of the femur was entirely cartilaginous with at best only a vessel in the center indicating the site of incipient ossification. The outer layers were composed of numerous ovoid cartilage cells separated by comparatively little intervening matrix. The intermedi ate layer contained similar cells which were slightly more spherical; they had vesicular cytoplasm and showed a little tendency to form territories or short columns, the center of the section was made up of vesiculated cartilage cells of hyper trophic type with large nuclei and vacuolated cytoplasm.

Electronmicroscopic findings The sur face failed to show a continuous layer of either cells or a limiting membrane. There were abundant amounts of homogeneous slightly opaque ground substance containing a few delicate fibrils. Some of these reached the surface, running in various directions and lacking preferential orienta tion. These linear filaments varied in length; they measured 100 to 130 A in width and showed a fairly distinct periodicity which varied from 150 to somewhat over 300 A with an average of about 250 A. They thus correspond to protofibrils (Poli card and Baud, '58) and will subsequently be referred to as class 1 — or primitive fibrils (fig. 4) In more central locations they were more numerous longer and thicker and the periods were wider than in the surface layers. Cells were in close contact with the surrounding matrix they were round or polygonal with a large nucleus and a comparatively narrow cytoplasm which extended into the matrix as narrow footlets. Mitochondria were infrequent, but the ergastoplasm was distinct and extended into the cytoplasmic footlets. It formed sac-like structures containing homogeneous material which was darker than the surrounding cytoplasm.

Animals one and two weeks old

Phase microscopy The cells began to form groups of two or more enclosed by a refractile capsule. These territories were the more distinct towards the center of the section. On the whole there was more matrix present than in the newborn and it was more abundant in the deep layers than near the articular surface. In the center of specimens of two week-old animals beginning ossification and formation of spicules were noted.

Electronmicroscopic findings Cells were ovoid or polygonal the nucleo-cytoplasmic ratio varied, the cytoplasm being more abundant and more vacuolated than in the newborn. Mitochondria were still scarce but the endoplasmic reticulum was well defined and contained cisterns (fig. 6) Here and there, an extremely fine very electron-dense material was seen on the surface of a cell or in the matrix between cytoplasmic footlets or occasionally inside the cell. This material appeared as tiny rods in linear array with fairly regular spacing and alternating with more electron-lucent material. These rods had a diameter of about 70 A and were thus only immaterially larger than the RNA granules of the ergastoplasmic membranes they were identifiable only in material that had been fixed in osmic acid or in the combination of osmic acid and formalin (fig. 7) In the vicinity of the superficial cells only primitive fibrils were identified. However at some distance from the cells a new type of fibers had appeared. They were less delicate than class 1 fibrils, their width varied from 200 to 400 A, they were long and showed the 600 to 700 A periodicity of collagen but only indistinct subbanding if any These fibers will be subsequently referred to as class 2 fibers. They were swinging about or lying radially to the cell periphery but did not disclose any specific orientation in relation to the joint surface. In the deep articular layer fibers of the same type were found but they were more closely packed and formed a denser network than the fibers in more superficial locations.

Animals three weeks or one month old

Phase microscopy The cartilage was now distinctly stratified. The uppermost layer consisted of flat or ovoid cells and the intermediate layer contained cell territories composed of ovoid or polygonal cells which towards the center reached considerable size. The interterritorial matrix was abundant near the center of the specimen calcification and ossification were in progress.

Electronmicroscopic findings The surface cells were essentially similar to those seen at the previous stage with well defined nuclei, cytoplasmic reticulum and rather few mitochondria. The dense finely granular material was still present at the cell surfaces, but it was also seen inside the cytoplasm of several large cells. Occasionally it was located in close proximity to the nucleus Near to the cells class 1 fibrils were identified. However they were fewer than at the earlier ages while class 2 fibers had become prominent. They coursed in slight curves around the periphery of the cells and were also seen somewhat farther out in the matrix. At some distance from the cells a third type of fibers was noted They showed the characteristic banding and subbanding of native collagen and had diameters up to more than 800 A with an average of 600 A. These fibers will hereafter be referred to as class 3 fibers (fig. 5) Their number was limited as compared to that of class 2 fibers which by far outnumbered all other types

In the deep layers of the articular cartilage cells with a comparatively dense nucleus and increasingly vacuolated cytoplasm were found In such cells ergastoplasmic lamellae were less conspicuous than in cells located more superficially However not all cells had this appearance others were less vacuolated, and the ergastoplasm was well defined Mitochondria were on the whole not numerous. About the vacuolated cells only fibers of class 2 and 3 were seen. Where the calcification front was approached small very electron dense rods measuring about 100 × 400 A appeared which in many places tended to accentuate the periodicity of the fibers In the deepest layers examined calcification had encroached upon the cartilage cells which disintegrated in their capsules and left many of these as empty spaces. In some instances a narrow rim of undecalcified matrix persisted lining the capsules. In areas of advanced calcification, no other structural details could be made out. Wherever the deposits permitted visualization of the underlying structures, banded fibers of class 3 type were present.

Animals six months old

Phase microscopy The articular surface showed shallow indentations and curving as is normal for this age. However there was no roughening or fraying of the surface layer The cartilaginous layer was thinner and less cellular than early in life Territories were larger and there was more interterritorial matrix found than during the preceding stages of observation. Stratification of the cartilage was distinct and a layer of cancellous bone was present underneath the former

Electronmicroscopic findings The surface layer was still fairly cellular However the matrix had increased in amount as compared to conditions observed before. The cells had large compact nuclei and dense ergastoplasmic lamellae Mitochondria were present in varying numbers. Occasionally delicate fibrils of class 1 seemed to radiate from the cytoplasmic borders into the surrounding intercellular substance Class 2 fibers were seen chiefly in the vicinity of cells some curving around the periphery and others arranged in a haphazard manner In areas farther away from the cells type 1 fibrils were no longer identified however many fibers of class 3 measuring 800 A and more in width were in evidence In the deepest layer of the cartilage next to the zone of calcification class 3 fibers predominated over those of class 2 they were running parallel to each other and were closely packed In the zone of calcification they were associated with deposits of crystallites which tended to bring out the 640 A periodicity As the mineral deposits increased in density towards the zones of ossification the fibers became obliterated Mineral deposits also encroached upon the periphery of the hypertrophic cartilage

cells which in increasing numbers were in a state of dissolution.

Animals one year old

Phase microscopy The cartilage was thinned out. The surface showed occasional slight irregularities and some cells were seen to protrude over the surface. There were comparatively fewer cells and more intervening matrix than at earlier ages. However there were scattered multicellular territories in the intermediate layer of the cartilage. The cancellous bone underlying the cartilage was less delicate than in young animals.

Electronmicroscopic findings The layer of non-calcified cartilage was in some areas as thin as 35 μ, and only two cell layers were present with the calcification front encroaching upon cells of the second layer. While many cells resembled those seen at 6 months of age, some were in less intimate contact with the matrix inasmuch as their cytoplasm appeared to be more sharply set off from the latter. This might represent an age change of the cells owing to a shortening of the cytoplasmic processes which seemed to anchor the young cells in the matrix. The isolation of the cell body might appear accentuated due to condensation of the matrix. The latter contained numerous fibers with little intervening ground substance. While particularly near the cells fibers of class 2 could still be seen they were far outnumbered by fibers of class 3 (fig. 8). In most places no preferential orientation was noted. However between closely approximated cells, the fibers often paralleled the opposing surfaces of the latter.

A few areas within the uncalcified cartilage were strikingly different from the rest of the tissue. Some cells were almost completely isolated from the surrounding matrix, the fibers, most of which were now of class 3 with a diameter over 800 A, were straighter than elsewhere they were packed in strands or bundles which intersected in an irregular manner without specific orientation. Little if any ground substance was identifiable between these fibers so that they appeared almost naked (fig. 9). This pattern suggested that of asbestos transformation of cartilage seen in the light microscope. In the deep layers the findings in calcified and ossifying cartilage resembled those seen at the age of 6 months.

Animals two years old and older

Phase microscopy A narrow layer of cartilage often not more than two cells deep covered the cancellous bone both together forming a thin shell about the narrow cavity. The cartilage of one of the 10 mice examined showed disarrangement typical of osteoarthrosis. The pathological findings observed in diseased joints will be reported elsewhere. The cartilage of the remaining 9 mice did not seem to be fundamentally changed from that seen at one year of age.

Electronmicroscopic findings. The layer of non-calcified cartilage was in some areas narrowed down to 25 μ, and a single section included both the free surface and the zone of beginning calcification. In some animals, the surface was frayed with ragged bundles of fibers protruding from the cartilaginous layer. Many of these bundles were oriented perpendicularly but some were running obliquely or horizontally (fig. 10). Parts of disintegrated cells such as fragments of endoplasmic reticulum, came to lie free in the intercellular matrix. Other cells were well preserved. The nuclei were distinct, the ergastoplasmic lamellae were narrow but well defined, and there were few but also distinct mitochondria. The cytoplasm was vacuolated to a varying degree and contained osmiophilic inclusions of varying size (fig. 11). Some cells were binucleated, an indication of resumption of growth. About these cells the matrix was often more electron-dense than at some distance from them this density was partly caused by closely packed fibers many of which were of class 2. In areas in which there was no resumption of growth, the contact between some cells and matrix seemed less close than in young animals. Cells near the surface were then separated from each other by abundant matrix containing numerous thick fibers. While occasionally class 2 fibers were seen, the vast majority were of class 3 with diameters of up to 800 A. These fibers formed a dense interlacing

The ultrastructural changes observed in the articular cartilage of our mice during growth and development correlate well with those reported in the epiphyseal growth zone of rats (Policard and Baud, '58 Godman and Porter '60 Knese and Knoop '61) and kittens (Scott and Pease '56) and in the joints of chickens (Martin, '54) and one-year-old mice (Zelander '59) In view of the fact that epiphyseal and articular cartilage are histogenetically alike it is not surprising that growth of cells as well as the production of matrix are similar in both locations. In both the chondrocytes contain ergastoplasmic cisterns which presumably are sites of production of ground substance Early fibril formation was seen near the cell surfaces and possibly within the cells. Finely granular material possibly constituting prefibrillar elements and found in bead-like arrangement along the cytoplasmic processes appeared denser in our micrographs than in previously published material (Zelander '59) This may be due to a rather intense staining of these elements with uranylacetate or phosphotungstic acid in our preparations. Interpretation of the nature of the dense juxtanuclear granules is difficult. They might be identical with the material accompanying the cytoplasmatic footlets and the peculiar localization may result from cutting the cell border tangentially The closeness of the material to the nucleus would not necessarily rule out this interpretation since the perinuclear cytoplasmic rim is extremely narrow in some places. There is, however also the possibility that the surface structures and the intracytoplasmic aggregates are not identical chemically in spite of their similarity in electron density Since glycogen has been shown to appear as electron-dense granules following staining with phosphotungstic acid (Revel Napolitano and Fawcett '60) this material may represent glycogen. However it would be surprising if glycogen were present in young cells but not demonstrable in the older ones which by light microscopy contain considerable amounts of glycogen (Silberberg and Silberberg, '61) This finding requires further study especially since the more superficial cells may contain glycogen in a special form or a similar substance taking part in the production of the matrix. Cells with double nuclei and territory formation present in some fairly superficial cells indicate a resumption of proliferative activity even at a late age. The counterpart of this condition was observed by light microscopy and is considered an essential feature of aging cartilage (Silberberg and Silberberg, 41)

Variations in the time of appearance of the different types of fibers observed by different investigators are easily explained by differences in species, strain and location of the tissues studied. The age at which the various types of fibers develop apparently varies not only with species and strain but may also differ in different joints and conform in some way to the age order of development of the individual joints (Silberberg and Silberberg, '61) The lack of uniformity in the development of the femur head of the mouse has been pointed out previously (Johnson '33; Sokoloff and Jay '56) The absence of transitional forms between primitive fibrils and fibers with the typical collagen periodicity and the steady decrease of the former with advancing age raises the questions as to whether primitive fibrils cease to be produced and what their fate is, once they have come to lie in the intercellular matrix. Views differ as to whether or not they become incorporated into large fibers (Martin '54) Even after the primitive fibrils have become scanty and mature collagen fibers of varying diameter have appeared the thinner fibers are frequent in the vicinity of cells while thick fibers are usually found at some distance from the cell periphery This suggests that fibers grow by accretion from material derived from the ground substance In aged mice thick collagen fibers were also seen in the immediate vicinity of the cells, a finding that might indicate the cessation of new formation of class 2 fibers. Actually the loss of close contact between the cells and matrix in some areas of aging cartilage may suggest a change with age in the functional relationships of cells and matrix. The reappearance in senile cartilage of young fibers at the periphery of cells which have begun to proliferate might indicate an attempt to

restore function in addition to growth. This point needs further clarification.

As to the distribution of the various types of fibers and their orientation, findings in young mice are at variance with those in infants (Cameron and Robinson, '58): in the former thick fibers were present in the deep layers of the cartilage and not close to the surface as in infants. Bundles of closely packed fibers were found in the upper layers of the articular cartilage only in mice one year of age and older. A focal change of unmasking of fibers was interpreted as a sign of regression occurring with advancing age and related to the simultaneous loss of chondroitin sulfate from the matrix. Such loss of matrix with advancing age has been demonstrated in the costal cartilage of humans (Hass '56) and of dogs (Eichelberger and Roma '54) and it may be presumed to occur in aging cartilage in locations other than the ribs. Histologically the unmasking of collagen fibers due to loss of ground substance has long been known as asbestos transformation.

At all ages observed, fibers were seen to course in all directions although in an individual section preferential orientation in one or another direction might predominate. The change in orientation of fibers with advancing age from a horizontal to a vertical arrangement in regard to the articular surface was thus less conspicuous in the mouse than in human joints (Trueta and Little '60). The question may be raised whether there is actually a reorientation of fibers with age or whether as a consequence of sloughing of those fibers that run parallel to the surface, the perpendicular ones become prominent. If the matrix becomes defective horizontally placed elements may lose their connections more readily than the vertical ones which are anchored more deeply in the cartilage and resist sloughing for a longer period of time than the former.

Calcification so far as could be ascertained occurred only in association with mature collagen fibers irrespective of whether the deposition of mineral constituted a step in the development of the articular cartilage or whether it was an old-age change. The failure of the true surface layer to calcify irrespective of age even in the presence of mature collagen fibers guarantees normal joint function. It has been suggested that mineralization of tissue is contingent upon the presence of a highly specific molecular configuration of both collagen and ground substance (Glimcher '60). This configuration is apparently absent in the surface layer of the joint of young as well as of aged individuals. Neither is calcifiability necessarily imparted to the cartilage by certain age changes in the ground substance although it apparently is by other changes. It is tempting to speculate whether or not calcifiability of the aging matrix may be related to the occurrence or non-occurrence of osteoarthrosis of the aging joint.

SUMMARY

Developmental and old age changes occurring in the articular cartilage of the head of the femur were studied on the ultrastructural level in mice varying in age from birth to two and a half years. During the lifespan of the mouse the cartilage of the femur was transformed from a solid structure to a thin shell covering the underlying spongiosa. In the newborn animal the cartilaginous matrix consisted of abundant ground substance containing a loose network of primitive fibrils which was most dense near the cells. During the first weeks of life young thin collagen fibers with typical periodicity but indistinct subbanding, and soon thereafter thick mature collagen fibers with characteristic subbanding, appeared. These fibers also formed an irregular network with little if any preferential orientation in any direction. With advancing age the fibers became arranged in irregularly interlacing bundles while the intervening ground substance decreased so much that in some foci the fibers seemed to lie free within the tissue. Fibers were coursing haphazardly through the cartilage at all ages although especially in areas of fraying of the surface vertical arrangement predominated. Mineralization of cartilage regardless of whether it occurred as a phase of ossification during growth and development or as an old-age change in senile cartilage was not observed in the absence of thick collagen fibers. With advancing age cartilage cells showed structural

changes indicating transition from an apparently highly functional to a more inactive state However in old animals proliferation of cartilage cells and possibly resumption of fibrogenesis were observed.

LITERATURE CITED

Bennett, G. A., H. Waine and W Bauer 1942 Changes in the knee joint t various ages, with particular reference to the nature of degenerative joint disease The Commonwealth Fund, New York.

Bondi M., and M. Montaleone 1957 L ultrastruttura della cartilagine articolare in condizioni normali in alcune condizioni patologico. Ricerche con il microscopio elettronico Ortop. Traum. App. Mot., 25 279–335.

Cameron, D A., and R. A. Robinson 1958 Electron microscopy of epiphyseal and articular cartilage matrix in the femur of the newborn infant. J Bone and Joint Surg., 40A: 163–170

Cecchi, E. 1958 Articular cartilage in osteoarthritis. Rheumatism, 4: 101–107

Eichelberger L., and M. Roma 1954 Effect of age on the histochemical haracterization of costal cartilage. Am. J Physiol., 178 296–304

Glimcher M. J 1960 Specificity of the molecular structure of organic matrices in mineralization. In Calcification in Biological Systems. A.A.A.S. Washington, D C., 421–487

Godman, G C., and K. R. Porter 1960 Chondrogenesis, studied with the electronmicroscope. J Biophys. nd Biochem. Cytol., 8 719–760

Hass, G. M. 1956 P thological calcification. In The Biochemistry and Physiology of Bone. Ed. G H. Bourne. Academic Press Inc., New York, 767–810.

Johnson, M. L. 1933 The time nd order of appearance of ossification centers in the albino mouse. Am. J Anat 52: 241–271

Knese, K-H and A. M. Knoop 1961 Über den Ort der Bildung des M kopolysaccharid-Proteinkomplexes im Knorpelgewebe Elektronenmikroskopische und Histochemische Untersuchungen. Z. f Zellforsch. und Mikroskop Anat., 53 201 258.

Little K., L. H Pimm and J Trueta 1958 Osteoarthritis the hip joint An electron microscope study J Bone and Joint Surg 40B 123–131

Martin, A. V W 1954 An electron microscope study of the car-lagineous matrix in the developing tibia of the fowl. J Embryol and Exper Morphol 38–48

Payr E. 1934 Gel nkstoffen und Ge k s tik. Part I. Julius pringer Berlin

Policard, A., et C. A. Baud 1958 Les structures inframicroscopiques normales et pathologiques des cellules et des tissues. Masson et Cie, Paris.

Revel, J P L. Napolitano and D W Fawcett 1960 Identification of glycogen in electron micrographs of thin tissue sections. J Biophys. and Biochem. Cytol., 8 575–589.

Robinson, R. A., and M. L. Watson 1952 Collagen-crystal relationships in bones as seen in the electron microscope Anat. Rec 114 383–409

Silberberg, M., and R. Silberberg 1941 Age changes of bones and joints in various strains f mice. Am. J Anat., 68 69–95.

——— 1961 Ageing hanges in cartilage and bone In Structural Aspects of Ageing. Ed. G. H. Bourne (in press) Pitman Med. Publishing Company London.

Silberberg, R., and M. Silberberg 1939 Einfluss einer fettreichen Kost auf die Entwicklung der Arthrosis deformans. Schweiz. Ztschr f. allg. P thol. und Bakt., 22. 447–458.

——— 1960 Articular geing and osteoarthrosis of female mice bearing anterior hypophyseal grafts. Pathol. et Microbiol., 23 103–112.

Sokoloff L. 1956 Nature of degenerative joint disease in small laboratory animals. 1. Pathological anatomy of degenerative joint disease in mice. Arch. P thol 62 118–128

Sokoloff L., and G. E. Jay Jr. 1956 Nature of degenerative joint disease in small laboratory animals. 3. Variations in epiphyseal maturation in the head of the femur among inbred strain of mice. Ibid., 62 136–139.

Trueta, J and K. Little 1960 The vascular contribution to osteogenesis. II. Studies with the electron microscope. J Bone and Joint Surg., 42B 367–376.

Vogel A. 1960 Die Herstellung von Schnitten für das Elektronenmikroskop durch lichtmikroskopisch ausgewählte Gewebsbezirke. Ztschr f wissenschaftl. Mikroskop und mikroskop Technik, 64 468–473

——— 1961 Centering device for tissue blocks on the Porter Blum microtome. Stain Technol

W tson, M L., and R. A Robinson 1953 Collagen-crystal rel tionship in bone. II. Electron microscope study of basic alcium phosphate crystals. Am. J Anat., 93 25–60.

Weichselbaum, A. 1877 Die senilen Veränderungen der Gelenke und deren Zusammenhang mit der Arthritis deformans. Sitzungsber. d. kaiserl Akad d. Wissensch. Wien, 75 193–240

Zbinden, G. 1953 Über Feinstruktur und Altersveränderungen des hyalinen Knorpels im elektronenmikroskopischen Schnittpräparat und Beitrag zur Kenntnis der Verfettung der Knorpelgrundsubstanz. Schweiz. Ztschr. f. allg. Pathol. und Bakt., 16 165–189

Zelander, T 1959 Ultrastructure of articular cartilage. Ztschr. f. Zellforsch., 49 720–738.

PLATES

PLATE 1

EXPLAN TION F FIGURES

2 Cross section of a fully developed femoral head of mouse. Phase microphotograph × 83.

3 Ossification progressing from an epiphyseal growth zone in the bsence of secondary center of ossification. Phase microphotograph × 83


2


3

PLATE 2

EXPLANATION OF FIGURES

4 Electronmicrograph of the upper layer of the articular cartilage. Newborn mouse. Primitive fibrils are seen showing indistinct periodicity and forming loose network in bundant ground substance. × 43,000 Insert shows detail of primitive fibrils with delicate banding. Periods are less conspicuous than those of the mature collagen fibers. Arrow points to bands. × 100,000.

5 Electronmicrograph of the surface layer One month-old mouse. Class 2 and class 3 collagen fibers are coursing in various directions. × 50,000


4
5

PLATE 4

EXPLANATION OF FIGURES

8 Electronmicrograph of the surface layer One month-old mouse. Class 2 and 3 collagen fibers are running in various directions. × 65,000.

9 Electronmicrograph of the surface layer One-year-old mouse. Bundles of densely packed thick collagen fibers in parallel alignment are seen with little intervening ground ubstance (Asbestos transformation.) × 40,000 Insert shows detail of class 3 fibers. × 130,000


8

PLATE 5

EXPLANATION OF FIGURE

10 Electronmicrograph of the surface layer. Two-and-a-half-year-old mouse. There is roughening and fraying of the surface. Binucleated cartilage cell and fibrils coursing in various directions are seen. × 5,000

PLATE 5



PLATE 6

EXPLANATION OF FIGURE

11 Electronmicrograph of the intermediate layer. Two-and-a-half-year-old mouse. There is artefactual retraction of the cartilage cell from the matrix; probable mitochondrion (arrow) juxtanuclear vacuoles (Golgi apparatus) and ergastoplasm are noticeable. There are areas of hyalinization outside the ergastoplasmic lamellae. × 15,000.

PLATE 6



PLATE 7

EXPLANATION OF FIGURE

12 Electronmicrograph of deep layer of the cartilage. Two-and-a-half year-old mouse. Densely packed collagen fibers with needle-shaped mineral deposits are seen. Undecalcified. Araldite embedding, staining with uranyl acetate. Taken with Siemens Elmiskop. Arrows point to banding of fibers. $\times$ 60,000.


12

The Relationship of the Sarcoplasmic Reticulum to Sarcolemma in Crayfish Stretch Receptor Muscle[1,2]

R. PRICE PETERSON AND FRANK A. PEPE
Institute of Neurological Science and Department of Anatomy University of Pennsylvania, Philadelphia, Pennsylvania

Since the first description of the crustacean stretch receptor by Alexandrowicz ('51 '52) this structure has become the object of intense physiological investigation by many workers. Due to its relative simplicity it has been used to study muscle activation (Eyzaguirre et al. '55 Kuffler '54) generator potentials (Eyzaguirre et al., 55 Eyzaguirre et al. '55) neurone activation (Eyzaguirre et al., '55 Eyzaguirre et al. '55 Kuffler '54) site of impulse initiation (Edwards et al. '58) neurone inhibition and aspects of the general inhibitory process (Edwards et al '59 Edwards et al. '59 Hagiwara et al. '60- Kuffler '58 Kuffler '58–'59; Kuffler et al., '58 Kuffler et al '55) Also it has provided a place to study "twitch" and "slow" muscle processes as well as fast and slow neurone adaptation (Eyzaguirre et al. '55 Kuffler '54)

Using the light microscope the structure of the crayfish stretch receptors (which were used exclusively in the present investigation) has been studied by Wiersma et al. ('53) and more extensively by Florey and Florey ('55). The receptors lie dorsally in the animal, just beneath the carapace in the thoracic and abdominal segments. In the abdomen there are 4 receptor organs per segment, two on each side. Those of the abdominal segments were used in this study. Each receptor organ consists of a sensory neurone adjacent to a small group of thin muscle fibers. The dendrites of the sensory neurone extend into the muscle bundle in several large trunks which divide and send slender branches parallel to the muscle fibers. The axon of the sensory neurone runs centrally in the company of several other axons. These other axons provide motor innervation to the muscle (Kuffler '54) inhibitory innervation to the muscle (Kuffler '60) and direct inhibitory innervation to the sensory neurone cell body and its dendrites (Eyzaguirre et al. '55 Eyzaguirre et al '55 Kuffler et al '55)

The two receptors on each side of the abdomen differ in the physiological characteristics of both the sensory neurone and the receptor muscles. The more medial receptor consists of a sensory neurone which is fast adapting in association with the larger group of receptor muscle fibers (RM 2). These fibers have been shown by Kuffler ('54) to be fast or "twitch" fibers which when stimulated via their motor nerves, usually show a spike depolarization of the membrane potential, and each stimulus elicits a twitch-like contraction. On the other hand the smaller muscle bundle (RM 1) shows only a partial depolarization of the membrane potential, when stimulated, and mechanically gives a very slow contraction the degree of which is dependent on the frequency of stimulation. Thus in this context, the terms "fast" (RM 2) and "slow" (RM 1) may be applied to these muscles. In part it was one of the aims of this work to determine whether these physiological characteristics could be correlated with any differences in arrangement of the sarco-tubular system.

Due to the simplicity of these sensory receptors they have proven to be an ideal system to study morphological bases for some of these physiological phenomena. In addition to the subject of this paper further work is being done on the inhibitory synaptic endings dendrite-muscle re

[1] This work was supported by USPHS 2G-281 (C1)

[2] This work was reported in part at the Biophysical Society meetings February 1961 held in St. Louis, Missouri.

lationships and the fine structure of the muscle components.

METHODS

The crayfish used in this study *Orconectes virilis* were obtained from Wisconsin in the summer and fall. After leaving the animals in the refrigerator overnight to cool, the dissection and fixation were carried out as follows. The abdomen was detached and the carapace removed by cutting it away at the dorsolateral corner on both sides. Usually the ventral musculature and gut were stripped off as the dorsal carapace was removed. This left the dorsal musculature (including the stretch receptors) exposed and *in situ* on the carapace. The carapace was then clamped into a special dissecting chamber (chamber instruments and fluids were all ice cold) and flooded with Van Harreveld's solution ('36). The stretch receptors were dissected free of connective tissue and the Van Harreveld's solution replaced with fixative. The chamber was placed on ice for the remainder of the fixation period (1–1½ hours) the fixing fluid being replaced with fresh fixative every 15–20 minutes. At the end of the fixing period the receptors were stiff enough to dissect out without loss of shape. They were then dehydrated through increasing concentrations of ethanol and embedded. The fixative used was 1.5% osmium tetroxide buffered to pH 7.4 with s-Collidine (Bennett et al. '59). This gave as good, if not better preservation when prepared in distilled water than when various concentrations of sucrose were added. The embedding material was Araldite epoxy resin, which was used according to the modified formula of Finck ('60). The embedding was usually done in polyethylene molds. This made it easier to orient the receptors for sectioning than when they were embedded in gelatin capsules.

Gold, silver and gray sections were cut on a Porter-Blum microtome using glass knives and were examined with a Hitachi HS-6 electron microscope. Routinely sections were stained in a 1 solution of phosphotungstic acid (PTA) in absolute ethanol. After immersing the grid for 1–2 minutes, it was washed for several minutes in two changes of absolute ethanol. In some cases a thin layer of carbon was then evaporated on top of the grid. No substrate formvar or collodion was used on the grids.

RESULTS

In one of the earlier electron microscope accounts of the sarcoplasmic reticulum (Porter et al., '57) this system was described (in rats and Amblystoma) as consisting of membrane-limited vesicles tubules, and cisternae associated in a continuous reticular structure which forms lace-like sleeves around the myofibrils. In this account particular emphasis was placed on the large cisternal structures in between the myofibrils as being the essence of the sarcoplasmic reticulum in these animals. Also it was felt that the term sarcoplasmic reticulum, like its parent term endoplasmic reticulum, referred to an internal system i.e. one which did not have any relation to the cell membrane.

In the muscles of the crayfish stretch receptor no cisternal structures were observed between the myofibrils. The tubular system which is described below consists of many tubules of relatively constant diameter which form a reticular complex within the sarcoplasm. Although this system in the crayfish is not identical morphologically with the sarcoplasmic reticulum of rats and Amblystoma, it is nonetheless believed to be sarcoplasmic reticulum. Since this is the only reticular system observed in these muscles it is concluded that identification as sarcoplasmic reticulum is preferable to concluding that this muscle is entirely devoid of an endoplasmic reticular structure.

Essentially there is no difference between the sarcoplasmic reticulum of the slow and fast receptor muscles (RM 1 and RM 2 in Florey's terminology ('55)). In cross and longitudinal sections through the muscle fibers the sarcoplasmic reticulum appears either as small elongated profiles (200–250 A. in diameter fig. 10) or as a row of circular profiles giving the impression of a string of beads (figs. 1 and 2). These appear among the myofibrils and do not penetrate in between the myofilaments.

In the central part of the fiber these formations are seen running between the

myofibrils where they form an incomplete network connecting various interfibrillar areas. In the central part of the fiber these tubules practically never dilate to form either cisternal sacs or sheet like expansions. Only the tubular or beaded form is seen with the very rarest exceptions.

At the periphery of the fiber the sarcoplasmic reticulum appears to come from the sarcolemma (in this paper referring to the electron-dense line which represents the muscle plasma membrane) and to run between the myofibrils (fig. 3) In both muscles at low magnification the sarcoplasmic reticulum seems to approach the sarcolemma and to form an intimate relationship At higher magnification in micrographs obtained from thin sections it appears that the sarcoplasmic reticulum is continuous with the sarcolemma and in fact, appears to be an invagination of this membrane (figs. 4–9) The layers outside the sarcolemma are layers of connective tissue cell cytoplasm and extracellular fibrous material. These are not part of the sarcolemma.

In longitudinal section the sarcoplasmic reticulum in the form of long strings of beads is nearly always seen between the first one or two myofibrils below the sarcolemma. These rows of circular profiles often run the length of the fibers (fig 1) On the other hand, after about the third fibril in from the membrane, the sarcoplasmic reticulum loses this organization decreases in amount and appears a discontinuous small circular and tubular profiles more randomly arranged (fig. 2). The same appearance of continuity between sarcoplasmic reticulum and sarcolemma is also often seen in longitudinal section but less clearly than in cross section

Many authors (Andersson Cedergren '59 Huxley '58 Porter '56 Porter et al '57 Robertson '56) have reported so-called "triad" structures occurring at definite places along the sarcomere in other types of muscles. These structures consist of elements of the discontinuous sarcoplasmic reticulum of adjacent sarcomeres, and a small, interposed transverse tubular element In some animals the triads appear at the Z line (Huxley '58 Porter '56) and in others at the junction of the A and I bands (Andersson-Cedergren, '59; Huxley '58 Porter et al '57 Robertson, 58) The crayfish receptor muscle was carefully examined to see whether the sarcoplasmic reticulum had any particular relationship with any part of the sarcomere but none was found.

As has been reported the membranes of the sarcoplasmic reticulum of adult muscle do not have small granules along their borders. This is also true of cray fish receptor muscles. Even after PTA or uranyl nitrate staining no accumulations of this material were seen.

Before describing the end-plate regions it should be understood that both motor and direct inhibitory endings occur When an end plate is seen it is impossible at present, to distinguish excitatory from inhibitory endings on morphological grounds The only variation in pattern of the sarcoplasmic reticulum seems to occur at the end-plate regions. This variation consists of a wide dilation (about 500 Å across) of the sarcoplasmic reticulum (or the infolded sarcolemma) in the sub-sarcolemmal area. Because of this dilation the continuity between the membranes is particularly clear (figs. 8 and 9) This is characteristic of the end plate areas. Usually the wider area extends approximately 0 5 to 2 μ in from the plasma membrane before branching into the smaller tubular type of sarcoplasmic reticulum. From the fact that this dilated area (1) may be followed in for some distance without interruption and (2) may be followed in serial sections for several microns, it is concluded that in this area the sarcoplasmic reticulum (or sarcolemma) is in the form of double-membraned sheets or cisternae These run longitudinally along the fiber i e as sheet-like invaginations of the sarcolemma in a longitudinal plane

Figure 10 was obtained from a longitudinal section through the slow receptor muscle. The section passes through in a nearly longitudinal plane a row of sarcoplasmic reticulum tubules near the sarcolemma Here the close packing and convolutions of the tubules may be seen

DISCUSSION

There are at least two possible interpretations of the relationship between the sarcolemma and the sarcoplasmic reticu

lum in this muscle based upon this evidence. The first interpretation would entail two membranous systems one a series of infoldings of the sarcolemma and the second a completely internal sarcoplasmic reticulum which is not continuous with the sarcolemmal infoldings The appearance of discontinuity which is encountered could give weight to this interpretation.

The second interpretation is that there is a single continuous system in which tubules of sarcoplasmic reticulum are continuous with the sarcolemma. This interpretation is shown diagrammatically in figure 11 Coming in from the sarcolemma is a system of 200–250 A tubules the membranes of which are interpreted as being continuous with the sarcolemma. These tubules are convoluted and radiate in from the sarcolemma at intervals of about 600 A along the fiber They maintain a roughly parallel arrangement at least to a point beyond the first row of myofibrils. At this point they appear to divide sending branches longitudinally up and down the fiber and laterally around the myofibrils. The only observed variation in this pattern occurs at the end-plate regions where the sarcoplasmic reticulum originates as long, narrow cisternae instead of parallel tubules It is this second interpretation which the authors prefer for the following reasons

In many places continuity between sarcolemma and sarcoplasmic reticulum is not apparent At first this observation led us to believe that continuity did not exist Later when structure suggesting continuity had been seen often enough it was realized that in many instances the appearance of discontinuity was due to vagaries caused by thickness and plane of section. This is shown diagrammatically in figure 12 which is an *en face* view of a portion of sarcolemma in the center of which is a hole representing the origin of a sarcoplasmic reticulum tubule A B and C represent three possible sections cut in a plane perpendicular to the sarcolemma. Obviously only a section exactly corresponding to A and of less than 200 A thickness, would give the appearance of continuity of sarcolemma and sarcoplasmic reticulum, without showing any membrane continuing across the lumen of the tubule. The second example of the obscuring of the true three-dimensional structure by section thickness is shown in figure 4 Here it appears that only a nipple-like protrusion extends from the sarcolemma. This appearance is due to the plane of section as illustrated in figure 12, D In this diagram the undulation of a tubule into and out of the plane of section gives the impression of a discontinuity Thus these two variations in plane and thickness of section may often give rise to a false impression of discontinuity between sarcolemma and sarcoplasmic reticulum.

Another observation supporting this interpretation may be seen in figures 3–8 Wherever there is an infolding of the sarcolemma, there is always a string of sarcoplasmic reticulum vesicles and tubules adjacent to it, i.e. the infoldings do not occur along the sarcolemma independent of a string of sarcoplasmic reticulum. Although this observation does not prove continuity between the infoldings and the sarcoplasmic reticulum it does indicate that they are morphologically related, and not independent, structures

It should be recalled that much of this conclusion, that there is continuity between sarcolemma and sarcoplasmic reticulum, is based upon interpretation As mentioned above due to the irregularity and convolutions of the tubules it is difficult to definitely prove either continuity or lack of continuity Thus the possibility does exist, as mentioned above that rather than having a single system of interconnected sarcoplasmic reticulum tubules and invaginated sarcolemma, this muscle may have two discontinuous systems However for the reason given, it is presently believed that the interpretation of a single continuous system is favored by the results.

The work of Huxley and co-workers ('57 '58) has suggested a possible role of the sarcoplasmic reticulum in excitation-contraction coupling Using single fiber preparations from various animals they produced a local decrease of the membrane potential at discrete loci along the sarcomere This was done by applying a current-passing micropipette to the muscle fiber under microscopic observation. In frog sartorius muscle, local excitation

occurred when the pipette was opposite the Z line (Huxley et al. '55 '58) but nowhere else along the sarcomere In the muscle of the lizard (Huxley et al '58) and crab (Huxley et al. '58) excitation occurred with the micropipette opposite the junction of the A and I bands but again nowhere else These results showed correlation with the electron microscopic observations demonstrating that in salamander larvae the triad is at the Z line (Porter '56 Porter et al '57) while in the lizard it is at the A I junction (Huxley 58 Robertson, '56) From these and other observations it was hypothesized that the sarcoplasmic reticulum might conduct the membrane excitation into the *myofilaments* where the contractile events are thought to occur

The crayfish receptor muscle shows neither (1) any sort of triad structure nor (2) any longitudinal discontinuity in origin of tubules, i.e. discontinuity between Z lines or A I junctions. If the sarcoplasmic reticulum does carry the excitation to the myofilaments, as indicated by the work of Huxley and collaborators mentioned above, then the receptor muscles observed in crayfish should not show any longitudinal variations in sensitivity to local stimulation by lowering of the membrane potential That is it should not show a specific sensitivity at the Z line or at the A-I junction. By this reasoning also it should show the circumferential discontinuities in sensitivity to an external negative field which have been described in frog muscle (Huxley et al 58) This would be due to the arrangement of the tubules in longitudinal rows with spaces in between these rows These physiological characteristics of crayfish receptor muscles have not been examined

It may well be appreciated by means of the membrane continuities suggested in this paper how the sarcolemmal membrane potential could be extended into the sarcoplasmic reticulum as a sarcoplasmic reticulum membrane potential. Whether this actually occurs or not is purely a matter of speculation at this time The evidence cited above only implies that this might be possible

SUMMARY

1 The sarcoplasmic retic l of th slow and fast muscles of th r sh stretch receptor have been des l as a system of 225 A. tubules w l ate in from the sarcolemma in p r ows This pattern is varied at th d plates where long dilated cisterns are stituted for the tubules.

2 The membranes of the sarc len m and the sarcoplasmic reticulum are t t tatively interpreted as being continu u This finding has been related to the v c k of Huxley and co-workers on excitation of muscle fibers at specific loci on the sarcomere In other muscles this work has suggested that excitation-contraction coupling may occur by means of the sarcoplasmic reticulum

ACKNOWLEDGMENTS

It is with great pleasure that the authors thank Dr Henry Finck of the University of Pittsburgh for his help and for introducing them to the fine art of electron microscopy

LITERATURE CITED

Alexandrowicz, J S. 1951 Muscle receptor organs in the abdomen of *Homarus* ... and *P l narus vulgaris*. Quart. J Micr Sci., 92 163–199

——— 1952 Receptor elements in the thoracic muscles of *Homarus vulgaris* and *P linurus vulgaris*. Ibid., 93 315–346.

Andersson-Cedergren E. 1959 Ultrastructure of motor end plates and sarcoplasmic components of mouse skeletal muscle fiber J Ultrastructure Res., Suppl 1

Bennett, H S ... nd J H Luf 1959 s-Collidine as ... basis for buffering fixatives. J Biophys and Biochem. Cytol 6 113–114

Edwards, C., and D Ottoson 1958 The site of impulse initiation in ... nerve cell of crustacean stretch ... eceptor J Physiol (London) 143 138–148.

Edwards, C and S Hagiwara 1959 Potassium ions and the inhibitory process in the crayfish stretch receptor J Gen Physiol 43 315–321

Edwards, C and S Kuffler 1959 The blocking effect of GABA and the action of related compounds on single nerve cells. J Neurochem., 4 19–30

Eyzaguirre C and S Kuffler 1955 Processes of excitation in the dendrites and in the soma of single isolated sensory nerve cells of the lobster and crayfish. J Gen Physiol 39 87–119

——— 1955 Further study of soma, dendrites and axon excitation in single axons Ibid 39 121 153

Finck, H. 1960 Epoxy resins in electron microscopy J Biophys. and Biochem. Cytol., 7 27–30.

Florey E., and E. Florey 1955 Microanatomy of the abdominal stretch receptors of the crayfish. J Gen. Physiol., 39 69–85.

Hagiwara, S., K. Kusano and S. Saito 1960 Membrane changes in crayfish stretch receptor neurons during synaptic inhibition and under action of GABA. J Neurophysiol., 23 505–515.

Harreveld, A. V 1936 A physiological solution for freshwater crustaceans. Proc. Soc. Exper Biol. and Med., 34 428–432.

Huxley A. F 1957 Local activation of striated muscle from the frog and the crab. J Physiol., 135 17P

——— 1959 Local activation of muscle. Ann. N Y Acad Sci., 81 446–452.

Huxley A. F and R. W Straub 1958 Local activation and interfibrillar structures in striated muscle J Physiol., 143 40P

Huxley A. F and R. E. Taylor 1955 Activation of single sarcomere. Ibid 130; 49P

——— 1958 Local activation of striated muscles. Ibid., 144 426–441

Kuffler S W 1954 Mechanisms of activation and motor control of stretch receptors of lobsters and crayfish. J Neurophysiol., 17 558–574

——— 1958 Synaptic inhibitory mechanisms. Properties of dendrites and problems of excitation in isolated sensory nerve cells. Exp. Cell Res., Suppl., 5 493–519.

——— 1958–59 Excitation and inhibition in single nerve cells. The Harvey Lectures p. 176–218.

——— 1960 Personal communication.

Kuffler S. W and C. Edwards 1958 Mechanisms of gamma aminobutyric acid (GABA) action and its relation to synaptic inhibition. J Neurophysiol., 21 589–610.

Kuffler S. W and C Eyzaguirre 1955 Synaptic inhibition in an isolated nerve cell. J Gen. Physiol., 39 155–184

Porter K. R. 1956 The sarcoplasmic reticulum in muscle cells of Amblystoma larvae. J Biophys. and Biochem. Cytol., 2 163–170 Suppl.

Porter K. R., and G. E. Palade 1957 Studies on the endoplasmic reticulum. III Its form and distribution in striated muscle cells. Ibid 3: 269–300

Robertson, J D. 1956 Some features of the ultrastructure of reptilian skeletal muscle. Ibid., 2: 369–380

Wiersma, C. A. G E. Furshpan and E. Florey 1953 Physiological and pharmacological observations on muscle receptor organs of the crayfish, Cambarus clarkii Girard. J Exp Biol 30: 136–150.

PLATE 1

EXPLANATION OF FIGURES

1a This shows a longitudinal section through slow receptor muscle near the upper or lower border of the fiber Profiles of sarcoplasmic reticulum (SR) are seen between the myofibrils. In the center the reticulum runs from deep indentations of the sarcolemma (S) into the fiber. The dark transverse lines are Z lines. 18,400 ×

1b This is higher magnification micrograph of the central area in figure 1a. It demonstrates the beaded appearance of the sarcoplasmic reticulum tubules in cross section The relatively regular spacing of the circular profiles indicates that these tubules are near their origin from the sarcolemma. 50,000 ×

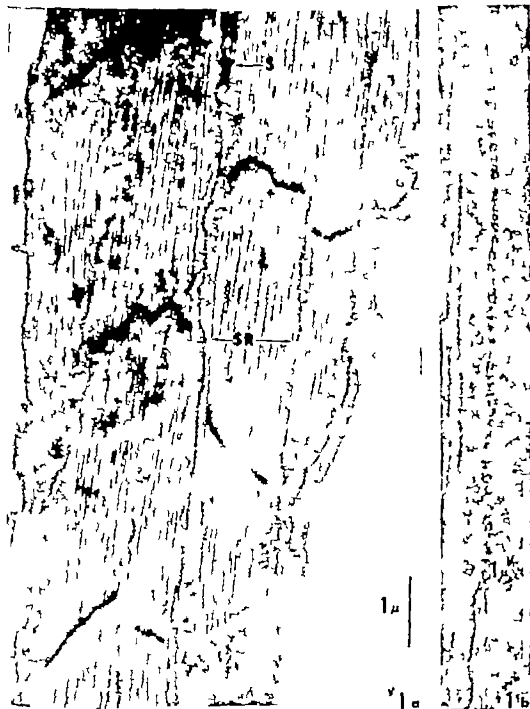

S
SR
1μ
1a
1b

PLATE 2

EXPLAN TION FIGURE

2 This is a micrograph of longitudinal section through the central part of fast muscle fiber Z lines are indicated. Other transverse dark bands are due to sectioning artifact. This shows the more irregular distribution of sarcoplasmic reticulum (SR) in the central part of the fiber as well as the lack of any triad structure. One of the rarely occurring dilated structures is indicated (D) 42,400 ×


SR
2

PLATE 3

EXPLANATION OF FIGURE

3 This shows a low power micrograph of cross section through parts of 4 slow muscle fibers. The relationship of sarcolemm (S) sarcoplasmic reticulum (SR) and myofibrils (MF) can be seen. 16,000 X

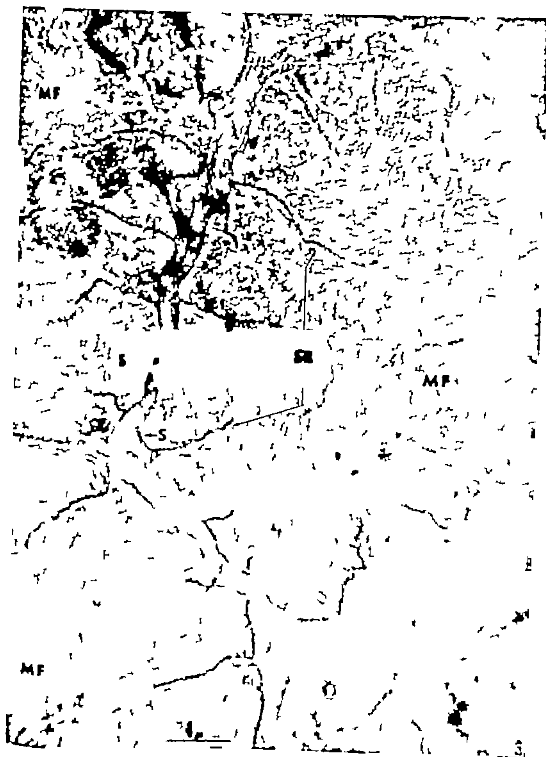

MF
S
SR
MF
S
MF
3

PLATE 4

EXPLANATION OF FIGURES

4 through 7 These micrographs all show examples of sarcoplasmic reticulum — sarcolemmal relationship. Note the dense connective tissue (CT) layers outside the sarcolemma. Figure 4 shows the nipple-like (N) appearance resulting from section as in figure 12d. Figure 6 suggests an appearance resulting from section as in figure 12b. Figure 4 36,000 × figure 5 61,600 ×; figure 6 56,000 × figure 7 56,000 ×





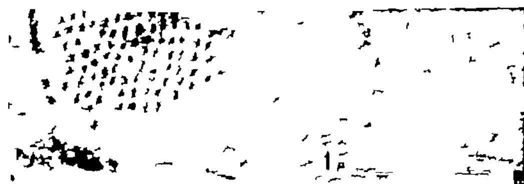




PLATE 6

EXPLAN TION OF FIGURE

8 This is low power micrograph of cros section through an end-plate region of fast fiber Synaptic vesicles (SV) mitochondria (M) and increased osmophilia (O) of pre- and post-synaptic membranes are apparent. Dilated and regular appearances of sarcoplasmic reticulum (SR) are indicated. Also interesting is the cross-hatched appearance of the Z line in cross section, in the lower left portion of the micrograph. 28,400 ×


M
SR

PLATE 6

EXPLANATION OF FIGURE

9 This shows cross section through an end-plate region. Here the sarcoplasmic reticulum (SR) — sarcolemmal continuity is particularly clear. Synaptic membranes (SYN) are indicated. 32,000 ×

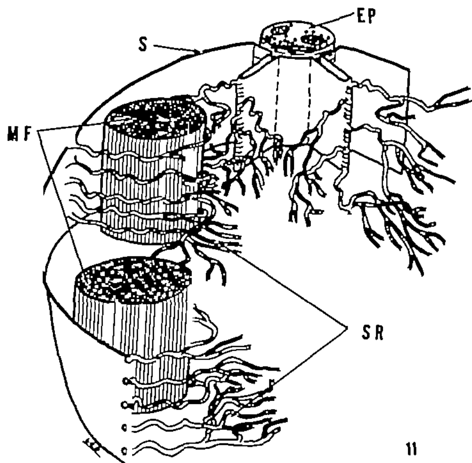

SR
1μ

PLATE 7

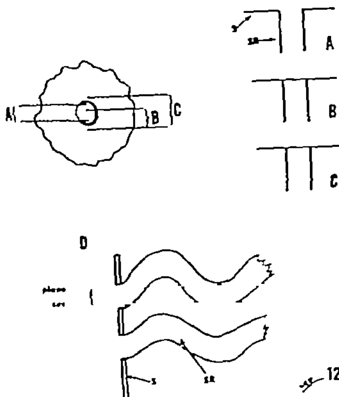
EXPLAN TION F FIGURE

10 This is micrograph of longitudinal section through slow muscle fiber In some areas the plane of section coincides with that of the longitudinal row of sarcoplasmic reticulum (SR) tubules. This points out not only the close packing and convolutions of the tubules, but also verifies the tubular as opposed to cisicular nature of these structures. Z lines and sarcolemma (S) are indicated. 25,600 ×


Z
SR



11 This is diagrammatic representation of section of crayfish receptor muscle fiber The rows of sarcoplasmic reticulum (SR) tubules are seen radiating in from the sarcolemma (S) and around the myofibrils (MF) The modifications t the end-plate (EP) are apparent.



12 This diagram shows an en face view of portion of sarcolemma. The hole in the center represents the origin of sarcoplasmic reticulum tubule. A, B, and C are three possible planes and thicknesses of sections normal to the sarcolemma. The smaller diagrams, A, B, and C show diagrammatically how these sections would portray the relationship of sarcoplasmic reticulum to sarcolemma. Diagram D shows the type of section giving rise to the nipple-like protrusions seen in figure 4

The Definitive Architecture of the Placentae of Nutria, *Myocastor coypus* (Molina)[1]

HOWARD H. HILLEMANN AND ALTA L. GAYNOR
Department of Zoology Oregon State University
Corvallis, Oregon

Information on the development and organization of the placentae of those rodents comprising the Suborder Hystricomorpha is limited to a few papers. For details of the placenta in the guinea pig, we are indebted to Duval (1892) Samson and Hill ('31) Amoroso ('52) Hard ('46), and Davies et al. ('59). Perrotta ('56 '59) studied the placenta of the porcupine, and the agouti placenta was investigated by Strahl ('05) and Becher ('20 '21). A paper on the placenta of the chinchilla appeared in '59 (Tibbitts and Hillemann). Nothing has been noted in the literature relating to the placentae of the hystricomorph *Myocastor coypus*

In the course of other work on the reproductive biology of nutria (Hillemann, Gaynor and Stanley '58 Stanley and Hillemann, '59) a number of pregnant nutrias were made available, and it was decided to learn as much as possible about the mature placentae of this animal. Since fetal membranes have a phylogenetic significance (Mossman, '37 '53) it is particularly pertinent to compare the observations made on the nutria placentae with those of other hystricomorphs so far studied, namely those of the guinea pig, the agouti, the Canadian porcupine, and the chinchilla.

MATERIALS AND METHODS

Most of the pregnant females donated by local ranchers had been accidentally killed or died from various causes but a limited number of live females were also obtained.

The deep freeze placental material, even though necrotic was useful for obtaining various measurements and for vascular injections with colored vinylites, gelatin and India ink. All vessels, uterine arteries and veins, allantoic arteries and vein, and vitelline artery and vein, were injected in various combinations with contrasting colors. Some of the resulting preparations were cleared, and others were corroded with potassium hydroxide to yield casts of the vascular channels.

The live pregnant females were anesthetized and some of the placentae were injected with India ink, colored vinylites, and colored gelatins. These and others were fixed with Bouin's solution and prepared as serial paraffin sections cut at 10–15 μ. A number of sections were treated with connective tissue stains Foot's method for reticulum, Masson's trichrome for collagen, and Macallum's modification of Verhoeff's stain for elastic fibers. These stains also helped to identify demarcate and establish the boundaries of fetal and maternal tissues.

OBSERVATIONS AND DISCUSSION

Form of allantoic and yolk sac placentae and their gross relations to the uterus

The allantoic placenta, mesometrially attached is discoid, tending to be elongated in the diameter parallel with the long axis of the uterus. The thickness of the disc is the smallest dimension (table 1). On the mesometrial aspect there is an

[1] Aided largely by grant-in-aid, RG-3778, from the Public Health Service, and by General Research Grant from the Graduate Council of Oregon State University Research Paper No. 415, Department of Zoology School of Science. Published under the auspices of the Oregon State University Monographs Committee.

Special appreciation is here expressed for the artistic assistance rendered to the authors by Hugh P Stanley (predoctoral fellow N.I.H.) in the representation of placental relationships featured in figures 1 2, 3 and 4.

The central zone of a lobe which may be oblong or spheroidal, depending on the shape of the lobe is composed of multiple small terminal branches of the maternal blood supply which here open to release maternal blood (fig. 13) Included here also are the many *small tributaries of the* umbilical vein, which collect blood from the tubes of the intermediate zone. The central zone is thus composed of a net work of larger and smaller branches and tributaries of maternal arteries" and fetal "veins along with connective tissue to be mentioned below

The intermediate zone (labyrinth) of a lobe is composed of numerous long and slender vascular channels which extend from the central zone to the trophospongium (figs. 3 21) There exist some anastomoses among the fetal endothelial *channels* as well as among the trophoblast tubes The labyrinthine zone is striated in appearance due to the alignment of the allantoic capillaries and the trophoblast tubes. Each fetal channel, about 7 μ in diameter consists of an endothelium and carries over its outer surface a *simple lining of chorionic ectoderm (fig.*

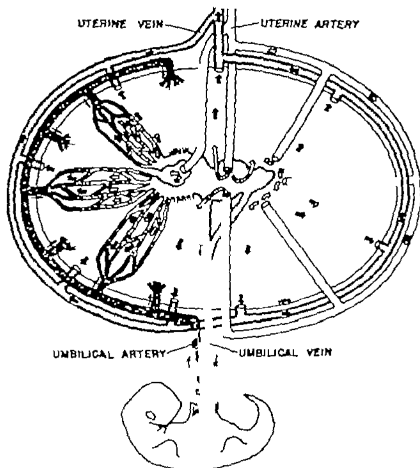


Fig. 3 The maternal and fetal blood supply of single lobe of the nutria placenta. Comparison of this with figure 4 clearly demonstrates that in vascular architecture, one-half lobe of nutria placenta is the morphological equivalent *of the entire* hamster placenta. The block arrows refer only to maternal blood circulating in the trophoblastic tubules. The progressive loss of oxygen *from the maternal blood is indicated by the block arrows graded* from clear to crossed to complete black. The fetal blood, similarly shaded in degrees of black, is represented by India ink dots within vessels.

F The nuclei of the endothelium are ... and stain a deeper hue than do the ... nuclei of the trophoblast syncytium ... simple chorionic ectoderm is viewed ... comprising a numerous series of tropho... ...ic tubes (two to 5 times the diameter of the fetal capillaries) through which ... the maternal blood Since the endo... ...lial tubes carry fetal blood, two epithe... separate the two blood streams here ... of the exchange area of the placenta is ... ...ed as hemochorial in its finer mor... ...logy (fig 16) as in *chinchilla* (Tibbitts and Hillemann, '59) The cytoplasm of ...blast syncytium is attenuated be... ...een adjacent nuclei, forming a thin ...brane in contact with the fetal capil... ...ry tubes The nuclei of the trophoblast ...ytium are large and spheroidal

A section through endothelial and troph... ...blast tubes at right angles to their long ... presents an arrangement reminiscent of the rete mirabile or star pattern (Schol... ...tz, '57) A variable number of capil... ...ry tubes are arranged on the peripheral ...rgin of the trophoblast tubes but these ... capillaries contact adjoining tropho... ...blast tubes as well (fig. 16)

The outer zone or trophospongium is a ...ncytium and composed for the most part of residual chorionic ectoderm through which pass branches of the umbilical ar... ...terial vessels (figs. 17 21) which in turn ...ibute into capillaries in the labyrinth ... Maternal blood is collected in the inter... ...tices of the trophospongium and passes ... maternal veins.

A few giant cells are found in the junc... ...tional zone next to the decidua basalis. There is also a broad cortex-like zone or band of giant cells many vacuolated and ...otic, around the free surface of the placental disc. Immediately peripl erally this "cortex" is invested by Rei hert's membrane and the non-vascular yolk sac epithelium. This combination of "cortex" ...toderm and the non-vascular yolk sac ...toderm represents a persistence to term of bilaminar omphalopleure in this area The cortex-like giant cell zone is markedly channeled and serves as a drainage path-way for maternal blood from the more peripherally located trophospongium (fig 17).

One may regard the early trophoblast as having differentiated into 4 c... ...gions (1) giant cells (compact primary tropho-blast remnant) (2) the trophospongium (with a transition to the giant cell layer) (3) the syncytial trophoblast tubes or canals which harbor maternal blood (4) and the primary trophoblast (mostly syn cytial) of the subplacenta As in the por cupine (Perrotta '59) the subplacental tissue on its fetal aspect grades into the trophospongium of the lobes but it does so with very little intergrading tissue the zone of demarcation is very narrow in sec tion (figs 18 19)

Perrotta ('59) states that there is no allantoic vesicle (entoderm) in the por cupine On the basis of one early speci men of nutria (from female 43) the al lantoic projection consisted likewise of only splanchnic mesoderm and its vessels, with no entodermal epithelium present There was another somewhat older pla centa (not definitive) and in the chorio-allantoic disc there were several circles of epithelium (cross sections) suggestive of remnants of fingers or diverticula from some earlier vesicle (fig 9) The possi bility that these circles indicate rest of the visceral entoderm isolated in the inter stices of the early chorioallantois has not been ruled out even though *they neither* contain nor are surrounded by mesoderm *(no cavity present).*

A large subplacenta (no cavity present) found consistently at term *in all* discs sectioned occupies a central area and ex tends to the mesometrial aspect of the disc. Thus lobes cover the fetal aspect as well as the remaining mesometrial surface of the placenta (*figs* 2 7 18 19) The subplacenta like the chorioallantoic pla centa proper *is also lobed* Along its fetal border the *subplacenta* is scalloped and this margin interdigitates with the lobes of the placenta proper Nutria shares the *subplacenta as a major* aspect of mem brane specialization along with the guinea pig agouti *porcupine* and chinchilla.

The cells of the subplacenta are *small* and of *uniform size,* and occur in nests and strands *bound* in a matrix *of loose* connective tissue and permeated *by allan*-toic vessels (*derived* from allantoic meso-derm) Centrally and mesometrially some of the subplacenta has degenerated and

is represented here by necrotic nuclear material and a hyaline matrix containing fibrin

Perrotta ('59) regards the subplacenta *of the porcupine as a potentially germinal* region of trophoblast and allantoic mesoderm from which new lobes of the labyrinth may be differentiated and added to the chorioallantoic placental disc during its later growth a process which Perrotta regards as ceasing in late gestation when the subplacenta degenerates. From a study of the chinchilla placenta (Tibbitts and Hillemann '59) and the nutria placenta the authors regard the subplacenta as being residual trophoblast along with some allantoic mesoderm which has not fully organized into lobes Perrotta refers to a transition from compact to spongy trophoblast at the junction of the subplacenta with the lobes, where new lobes would be proliferated and differentiated. This view is also consistent with the persistence in nutria of a large subplacenta to term and with a degenerated central mesometrial area within it. Whether or not the subplacenta performs an endocrine function during gestation, as suggested by Davies, Amoroso and Dempsey ('59) it [illegible]ains at all events more or less full [illegible]n to term in both chinchilla and [illegible]

The bulk of the decidua basalis at term consists of a narrow pedicle (figs 2 5 20) as also in the porcupine (Perrotta '59) The zone of junction is markedly necrotic

Uterine arterial supply and venous drainage of the chorioallantois

A few uterine arteries extend from the mesometrial region of the uterus directly to the central depression on the mesometrial aspect of the placenta passing there via a slender basal pedicle of decidual tissue (figs. 2 5 20)

Upon reaching the placental disc these arterial channels subdivide repeatedly as they pass through the trophospongium investing the lobes of the placenta Smaller branches penetrate to the central zone of each lobe (figs 3 13) where they further subdivide and release maternal blood among the anastomosing elements of the umbilical vein tributaries.

Maternal blood flows from the central zone peripherally through the many parallel radiating and anastomosing trophoblast tubes (figs. 3 16 21) en route to the *trophospongium. After* percolating through the interstices of the trophospongial zone the maternal blood is directed into a net work of venous channels on the surface of the trophospongium (figs. 3 17). These vessels pass through the zone of junction to the decidua basalis veins. Maternal blood also drains from the peripheral inter lobar partitions and thence into the channeled peripheral giant cell zone en route to the venous channels of the junctional zone, whence in turn this blood reaches the decidua basalis veins. The vessels convey the blood toward the mesometrial aspect of the placenta where it is taken up, almost invariably by two large sinusoidal veins one on either side of the margin of the central depression on the maternal aspect of the placenta (fig. 20) The two veins follow the basal pedicle and reach the mesometrial decidua.

Perrotta ('59) refers to sinuses of the *subplacenta of the porcupine* as being filled with maternal blood. Sectioned material in nutria which had previously been injected with colored masses provided evidence for the existence of fetal vessels alone in the subplacenta (fig. 15) The maternal arteries largely bypass the subplacenta. A few pass between subplacental lobes, but most of them pass outside the subplacental area and thence between adjacent chorioallantoic lobes en route to the central zones of the lobes.

No endovascular plasmodial cells were identified in any uterine vessels or elsewhere

Umbilical arterial supply and venous drainage of the chorioallantois

From the allantoic stalk a single umbilical vein in company with two umbilical arteries penetrates centrally into the fetal aspect of the placenta (fig. 14) By means of serial cross-sections prepared *from one* embryo it was determined that it was the *right* umbilical vein which was involved As the umbilical arteries enter the disc they establish between them a short and intimate anastomosis (fig. 10) Beyond

this level and within the substance of the trophospongium which envelopes the lobes, these arteries subdivide and send numerous branches to the placental lobes. A complex network ramifies about each lobe and the component small vessels penetrate the trophospongium centrally in each lobe (fig. 3) Upon reaching the fringe of the middle or labyrinthine zone these vessels branch into numerous capillaries which pass as slender roughly parallel and converging tubes among the trophoblast tubes (figs. 17 21) Several allantoic capillaries are associated with each trophoblast tube and in turn with other adjacent tubes an arrangement mentioned above (fig 16)

When the allantoic capillaries reach the central zone, there develops a complex anastomosis which forms progressively larger veins (figs. 3 13) and these in turn emerge from the lobe and form tributaries of the allantoic vein.

It was mentioned above that maternal blood flows from the central zone peripherally through the trophoblast tubes of the lobe and thence to the trophospongium [illegible] But the fetal blood passes from [illegible] spongium centrally through the [illegible] and thence to the central [illegible] placenta as in chinchilla [illegible] Hillemann '39) the matern[illegible] blood streams course in [illegible] adjacent but opposite dir[illegible] lishing an exchange gradi[illegible] these two fluids. This hystricom[illegible] illustrates the counter flow ex[illegible] dient first announced by Moss[illegible] in the rabbit.

The vascular pattern and the d[illegible] tion of vessels to and from the lob[illegible] be understood by visualizing a single [illegible] of the nutria placenta as the equivalent of two whole hamster placentae (chorioallantoic) as described by Adams and Hillemann ('50 '53) Figures 3 and 4 were made to illustrate this point.

In the hamster (fig 4) maternal arteries penetrate the exchange area to the chorionic plate, where they open antimesometrially Maternal blood then flows meso-

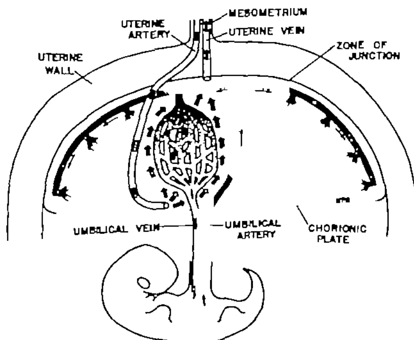


Fig. 4 The orientation of the vascular supply pattern in the hamster placenta for comparison with the vascular architecture in the nutria placenta As in figure 3, the black arrows refer only to maternal blood and its degree of oxygen loss to the fetal blood stream the fetal blood is similarly shaded with dots within vessels.

metrially among the endothelial tubes and *collects into open veins which* pass to the mesometrium. The allantoic arteries on the other hand penetrate the chorionic plate pass through the exchange area and near the zone of junction and break up into a network of smaller vessels from which groups of capillaries are suspended" and which transmit the fetal blood antimesometrially In the area of the chorionic plate these vessels coalesce to form the umbilical vein. The two blood streams course in opposite directions mesometrially-antimesometrially in this hemoendothelial placenta.

Another way of comparing the nutria and hamster placentae is to state that the entire hamster allantoic disc is the equivalent of one-half of one lobe only of the nutria placenta These then would be morphological equivalents. The nutria placenta is compound and therefore fetal arterial blood can enter while at the same time maternal venous blood can leave, from multiple sites distributed over the entire surface of each lobe. But in the hamster placenta, arterial blood enters and maternal blood leaves, from the mesometrial surface of the single lobe (a "hemisphere) The chorionic plate area of the hamster placenta which accommodates the opening maternal arterial channels as well as umbilical veins in process of coalescence is the morphological and *functional equivalent of* the central zone in each lobe of the nutria chorioallantois. This structural and physiological comparison may be clarified with reference to figures 3 and 4

The interpretation given above for the pattern of circulation in the nutria placenta, which is also the same as given previously for the chinchilla (Tibbitts and Hillemann '59) was based on corrosion casts following injections of contrasting color media, on cleared whole placentae following similar injections and on histological sections made of placentae which had been injected with contrasting colored gelatins, vinylites and India ink. In view of all this it is difficult to reconcile the following statement of Perrotta ('59) about the placental circulation of the Canadian porcupine even though this is a different animal it is nevertheless also a hystricomorph: "Fetal arterioles arising from arteries in the central area of the lobule traverse the lobule to the periphery where they empty into fetal capillaries of the labyrinth. From these capillaries the fetal blood drains into the veins in the centers of the lobule. We could not find in nutria and chinchilla such arterioles arising from the central area and passing to the periphery The arterial supply in nutria and chinchilla comes from branches of the umbilical arteries among the lobes. These arteries break up in the trophospongium and then feed the allantoic capillaries which in turn are drained by umbilical vein tributaries in the central zone in both chinchilla and nutria. Perrotta did not state any evidence for the alleged passage of such arterioles in the porcupine neither was any mention made of any identifying injections

Female 43 yielded an early embryo and adnexa. The embryo measured 5 mm crown rump in its highly flexed condition. Stretched out it was estimated to measure about 12 mm in length. Besides a yolk sac and stalk considered below it had an early allantois of splanchnic mesoderm only and associated with the yolk stalk This allantoic mass was about 2 mm wide and about 3 mm in length Its shape was somewhat irregular and the entire mass was closely attached to the embryo

Collagenic connective tissue fibers of the chorioallantoic disc have been demonstrated to be present in the somatic mesodermal stroma of the chorionic plate These fibers also surround the interlobar derivatives of the umbilical arteries and vein and are also scattered within the splanchnic mesodermal matrix of these vessels Collagenic fibers if present at all are very scant they are seen adjacent to the vessels of the trophospongium as well as along the endothelio-trophoblast tubes of the labyrinth they are both sparse and scattered within the connective tissue matrix of the central zone of the lobe and also poorly represented around the contained vessels of this zone Collagenic fibers are heavily represented within the large subplacenta and comprise much of its framework. On the mesometrial aspect of the disc collagenic fibers are distributed around the maternal arteries and veins.

Elastic fibers surround the vessels making transit through the trophospongium of the placental lobe. These fibers also occur as scattered wavy threads coursing along with the endothelio-trophoblast tubes of the labyrinth of the lobe and are especially heavy around the vessels of the central zone of each lobe. A good representation of elastic fibers surrounds the vessels of the subplacenta. Elastic fibers occur in the walls of the umbilical vessels in the chorionic plate stroma (somatic mesoderm) as well as in the walls of the maternal vessels on the mesometrial aspect of the disc.

Reticular fibers are very numerous within the subplacenta, where they are heavy and dense (fig 12). Reticular fibers are well represented in the trophospongial zone of the lobe where they form an interlacing network of heavy fibers (fig 21). These fibers also surround the contained vessels of this zone, and there are very numerous heavier and lighter wavy lines of anastomosing reticular fibers coursing along with the endothelio-trophoblast tubes of the labyrinthine zone (fig 21). Reticular fibers are also numerous around the vessels of the central zone and form much of the diffuse ground work of the stroma of this zone (fig. 21). These fibers are well represented within the walls of the umbilical vessels in the chorionic plate.

Histological organization of the yolk sac

The yolk sac is solely visceral there being no evidence for a parietal component existing in the mature placenta. The full-term yolk sac placenta is completely inverted but it is not known when the inversion occurs. This vascular splanchnopleure bears branched villi in a broad zone near the placental disc.

Within the circle circumscribed by the sinus terminalis the somatic mesoderm is a thick layer (fig. 2). Adherent to it in places (but distinct from it) is the amnion (fig. 1).

The non-vascular portion of the yolk sac adheres to the peripheral fetal aspect of the chorioallantoic disc but is structurally continuous with the rest of the sac which is highly vascularized (fig. 2). The limit between the vascular and non-vascular portions is marked by the sinus terminalis. The non-vascular yolk sac is markedly tufted in some areas.

Collagenic connective tissue fibers occur in the splanchnic mesodermal stroma of this free visceral yolk sac and also surround its contained vessels. Reichert's hyaline membrane is clearly and heavily outlined beneath the non-vascular portion of the yolk sac and separates the yolk sac from the trophoblast of the disc. Reichert's membrane adheres to the disc as it extends from the sinus terminalis area and around the margins of the disc over which it has proliferated as far as the site of attachment of the disc at the decidua basalis (pedicel).

Reticular fibers are present in the walls of the vessels of the free yolk sac.

The walls of the larger vessels of the free yolk sac contain the characteristic elastic fibers of vessels.

Female 43 provided an early yolk sac measuring about 22 mm in diameter. The yolk stalk measured 10 mm in length and about 0.75 mm in diameter. The yolk stalk was attached at the antimesometrial pole of the yolk sac and at this point the vitelline artery arose and coursed as a single straight vessel in the yolk sac wall directly to the place where the yolk sac attached to the placental disc. The vitelline vein also extended out from this point of attachment and branched several times over a limited area of the antimesometrial aspect of the yolk sac. The bulk of this visceral yolk sac was well vascularized with many fine capillaries packed with nucleated R.B.C.

The only way to date this yolk sac was to refer to the measurements of the embryo contained within the sac. The embryo was highly flexed so that the tip of its forehead extended back about 3.3 mm. The crown-rump measurement of the flexed embryo was 5 mm. When stretched out, the total length of this embryo from head to tail was about 12 mm. Closely associated with the yolk stalk where it joined the embryo was an allantoic mass of splanchnic mesoderm only.

Maternal arterial supply and venous drainage of the choriovitelline placenta

If there is in the fully differentiated nutria placenta any passage of materials through the uterine epithelium to the yolk sac epithelium then the finer branches of the maternal circumferential arteries and veins would constitute the maternal vascular supply and drainage Similarly any materials emitted by the yolk sac epithelium may traverse the uterine epithelium to enter the maternal vessels. The yolk sac epithelium does come into intimate contact with the uterine epithelium over much of its surface, insinuating itself among the leaf-like folds of the uterine endometrium

Vitelline arterial supply and venous drainage of the choriovitelline placenta

The single vitelline artery (fig. 22) leaves the umbilical cord near the middle of the cord's length and continues via the vitelline stalk to the yolk sac proper in company with the vitelline vein The yolk sac touches the placental disc on its fetal aspect near its periphery Upon reaching disc, the vitelline artery divides at an - angle into two branches which separate to form arcs within the substance of the yolk sac and encircle the placental surface as the sinus terminalis (fig 2) This sinus courses within a fibro-vascular ring as also in the guinea pig and chinchilla (Perrotta '59)

The terminations of these two arcs on the side of the placenta opposite their insertions come close together but presumably anastomosis does not occur unless among some of the many tufts of fine capillaries given off here (fig. 22)

Arterial branches extend peripherally from the sinus terminalis in the yolk sac as it passes over the margin of the placental disc (fig 1) These vessels form a complex network of arterioles and capillaries

The network of capillaries and venules which drain the yolk sac coalesce into progressively larger veins which in turn fuse to form the vitelline vein proper This vein has its roots of origin at the site where the vitelline artery bifurcates to form the sinus terminalis. The vitelline vein courses in the vitelline stalk and thence into the umbilical cord en route to the fetus.

The umbilical cord

The umbilical cord, ventrally inserted on the fetal aspect of the term placenta is about 65 mm long and about 4 5 mm in diameter (fig. 1) It harbors two umbilical arteries of equal diameter a larger umbilical vein (figs 10 14) one small vitelline artery and one small vitelline vein. There are also scattered within the substance of the cord small vascular channels but the sites of origin and drainage of their contained blood was not determined India ink injections of the umbilical vein demonstrated the cord matrix vessels to be in communication with this vein. The presence of blood vessels in the mesodermal stroma of the cord was recently reported in chinchilla by Tibbitts and Hillemann ('59) and in the spotted hyena by Morton ('57) Most ungulates and cetaceans are known to possess a rich supply of small vessels and capillaries in the cord (Flexner '54)

The cord is covered by a simple squamous epithelium continuous with that of the amnion.

No indication of an allantoic entodermal epithelium was identified in the cord substance

Near the placental disc the vitelline artery and vein together depart at an acute angle to the umbilical cord and continue to the disc as elements of the vitelline stalk. The yolk stalk is short at term and mesometrially oriented having rotated from the original antimesometrial position From this point of separation the umbilical cord vessels continue as elements of the allantoic stalk to the center of the disc face. The allantoic stalk proper is about 35 mm long and 3–4 mm in diameter the vitelline stalk proper is about 15 mm long and 2–3 mm in diameter The amnion is reflected over and fused with the umbilical cord as well as over both the allantoic and vitelline stalks.

Collagenic fibers are generously distributed throughout all of the 5 vessels of the cord but the veins appear to have proportionately more than the arteries. The

matrix (Wharton's jelly) contains collagenic fibers and their parental connective tissue cells (fig 6) In cross-section the cord matrix appears as a set of wavy concentric laminations. The collagenic fibers are denser around the three cord vessels than around the two cord veins but their greatest concentration occurs within the somatic mesodermal layer of the investing amnion.

Reticular fibers occur as heavy and fine branching threads, variously spaced within the tunica media (fig. 8) of the umbilical arteries and vein, as well as that of the vitelline artery and vein. These fibers tend to course along with the smooth muscle cells in the media. Reticular fibers do not occur in the cord matrix.

Elastic fibers are limited to the cord vessels, which in cross-section present concentric rings of such fibers tending to be evenly spaced within the vessel wall (fig 11). Each ring is very irregular with numerous curves, kinks and folds in fixed material. Each of the umbilical arteries has from 5 to 7 of these rings, the umbilical vein only 4 the vitelline artery from 4 to 5 smaller rings, and the vitelline vein from 3 to 4 small rings The outermost elastic fiber ring on each vessel contact the cord matrix. Although the two umbilical arteries and the vitelline artery have each the characteristic elastica interna lining the vessel lumen no such ring occurs in either the umbilical vein or vitelline vein. Elastic fibers do not occur in the cord matrix.

The amnion

No early material was available to determine whether or not amniogenesis in nutria occurs by cavitation as in the guinea pig, agouti, porcupine and chinchilla.

The amniotic ectoderm is a simple low cuboidal to squamous epithelium, the nuclei of whose cells are ovoid, stain darkly and occupy a central position in the cell.

No evidence was seen for any vascularization of the amnion near the placental disc, nor for its vascularization by vitelline vessels in the angle where the yolk stalk departs from the allantoic stalk nor in any other region of the amnion

Collagenic connective tissue fibers are common within the somatic mesodermal layer of the amnion.

SUMMARY AND CONCLUSIONS

1 The matured placenta of nutria *Myocastor coypus* (Molina) in both gross and fine morphology as well as in general topographical relations, is strikingly similar to that of the chinchilla and of the porcupine The allantoic placenta at term is discoid and attached mesometrially by a delicate and tenuous pedicel only owing to an all but complete undercutting

2 An average near-term nutria placenta is 34 4 mm long, 27 8 mm wide 18.9 mm thick, and weighs 14 5 gm

3 The chorioallantois is complexly lobate and labyrinthine. Trophoblast epithelium and allantoic capillary endothelium together separate fetal from maternal blood this placenta therefore is hemochorial.

4 Each lobe consists of a peripheral trophospongium an intermediate labyrinth and a central zone A large lobed subplacenta, without a cavity constantly persists to term occupying a central area in the disc but extending to its mesometrial aspect.

5 Uterine arteries and veins pass through an attenuated pedicel to supply the lobes but not the subplacenta. These arteries break up among (outside) the lobes and pass directly to the central zone where they open and release blood which bathes the hemochorial labyrinth as the blood passes peripherally to the trophospongium. Here it is collected along with that from the porous giant cell cortex in maternal channels en route to the pedicel No endovascular plasmodial cells were identified.

6. Two umbilical arteries and one umbilical vein reach the fetal aspect of the placenta and penetrate the disc The two arteries after forming an anastomosis ramify among the lobes penetrating each at multiple sites, and then reduce to arterioles in the trophospongium Here they give off multiple fine anastomosing and radially dispersed endothelial tubes (allantoic capillaries) which are co[illegible]red with trophoblast these vessels carry fetal blood to the central zone where the[illegible] coalescence

forms multiple tributaries to the umbilical venous system The larger veins unite among the lobes to form at last the single umbilical vein. Fetal blood courses parallel to but in a direction opposite to that of the maternal blood.

7 A few giant cells lie in the junctional zone next to the decidua basalis and in the highly channeled central zone of the disc.

8 No entodermal elements of an allantoic vesicle were found.

9 One half of one lobe of the nutria chorioallantois is the structural and functional equivalent of the entire placenta of the hamster

10 The yolk sac (completely inverted) is solely visceral, folded highly vascular and served by one vitelline vein and one vitelline artery the latter bifurcates to form a sinus terminalis on the fetal aspect of the chorioallantoic disc. There is a persistent remnant of the non-vascular bilaminar omphalopleure in the junctional zone and Reichert's membrane persists in the cortical zone of giant cells Possible remnants of yolk sac entodermal diverticula appear in the earlier chorioallantoic disc.

11 Both the presence and pattern of distribution of elastic, collagenic, and re[illegible]lar connective tissue fibers in the cord [illegible] in the placentae were demonstrated [illegible]th appropriate stains

LITERATURE CITED

Adams, F W and H H. Hillemann 1950 Morphogenesis of the vitelline and allantoic placentae of the golden hamster (*Cricetus auratus*) Anat. Rec 106 363–383.

——— 1953 Vascular pattern in the allantoic and vitelline placentae of the golden hamster (*Cricetus auratus* Waterhouse) Proc. Ore. Acad. Sci 3 63–63.

Amoroso, E C. 1952 Placentation. In Marshall's Physiology of Reproduction, vol. 2. Longmans, Green, New York, pp. 127–397

Becher H. 1920 Die Entwicklung des Mesoplacentariums und die Placenta bei Aguti (*Dasyprocta azarae* Schl.). Zeitschrift für *Anatomie* und *Entwicklungsgeschichte*, *61* 337–364

——— 1921 Der feinere Bau der reifen Placenta von Aguti (*Dasyprocta azarae* Schl.) Ibid., *61* 439–454

D vies, J E. C. Amoroso and E. W Dempsey 1959 The subplacenta of the guinea pig. Anat. Rec., 133 266. (Abstract No. 129)

Duval M. 1892 Le placenta des rongeurs. Alcan, Paris, p. 640

Flexner L. B (ed.) 1954 Gestation. Trans. First Conf., Josiah Macy J Fdn., New York, p. 238.

Hard, W L. 1946 A histochemical and quantitative study of phosphatase in the placenta and fetal membranes of the guinea pig. Am. J Anat., *78*: 47–77

Hillemann H H., A. L Gaynor and H P Stanley 1958 The genital systems of nutria (*Myocastor coypus*) Anat. Rec., *130* 515–531

Morton, W R. M 1957 *Placentation in the* spotted hyena (*Crocuta crocuta* Erxleben) J Anat., *91* 374–382

Mossman, H. W 1926 The rabbit placenta and the problem of placental transmission. Am. J Anat. 37 433–497

——— 1937 Comparative morphogenesis of the fetal membranes and the accessory uterine structures. Carnegie Inst. Wash. Pub. 479 Contrib. to Embryol., 26: 129–246.

——— 1953 The genital system and the fetal membranes as criteria for mammalian phylogeny and taxonomy J Mammal., *34* 289–298.

Perrotta, C. A. 1956 The fetal membranes of the new world porcupine *Erethizon dorsatum*. Anat. Rec. *124* 345–346. (Abstract No. 178)

——— 1959 Fetal membranes of the Canadian porcupine, *Erethizon dorsatum* Am. J Anat *104* 35–59

Sansom, G. S., and J P Hill 1931 Observations on the structure and mode of implantation of the blastocyst of *Cavia* Trans. Zool. Soc. London, *21* 295–351

Scholander P F 1957 The wonderful net. Sci. Am., 196 96–107

Stanley H. P and H. H. Hillemann 1959 Histology of the reproductive organs of nutria *Myocastor coypus* (Molina) J Morph., *106* 277–300.

Strahl, H. 1905 Eine Placenta mit einem Mesoplacentarium. Anatomischer Anzeiger 26 524–528

Tibbitts, F D and H. H. Hillemann 1959 The development and histology of the *Chinchilla* placentae. J Morph., 105 317–366.

PLATES

PLATE 1

EXPLANATION OF FIGURES

5 Placenta from animal 39 mesometrial aspect. 2 ×

6 Profuse collagenic fibers in substance of umbilical cord; part of umbilical artery is seen to the left. 100 ×

7 Placenta of figure 5 in section. Mesometrial area bove fetal surface below About 1 ×

8 Reticular fibers (Foot' method) distributed in circular pattern within substance of *umbilical artery in cord. Reticular fibers are seen as wavy vertical" lines in photograph;* vessel was injected with India ink. Taken from femal 37 loculus 4R. 100 ×

9 This is one of 12 such epithelial nests in section from an early placenta (from animal 29) These are presumed to be remnants of entodermal diverticula of the visceral yolk sac caught within the early labyrinthine area. 100 ×

10 Cast of placenta from animal 47 loculus 6L. Umbilical arteries injected with red vinylite 2 ×

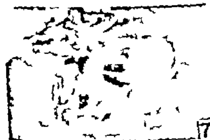
11 Several rings of elastic fibers (Macallum-Verhoeff method) within the substance of the umbilical artery in the cord. F male 47 locul 6. 150 ×

12 Reticular fibers (heavy black lines) in the subplacenta. Macallum modification of Verhoeff's stain. Animal 47 loculus 3 100 ×

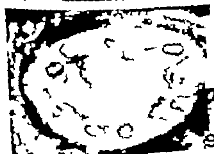

5


6


8


7


10


9


12

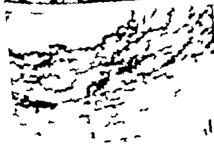

11

PLATE 2

EXPLANATION OF FIGURES

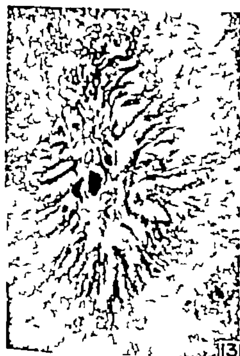
13 Mature placenta from animal 47 loculus 3, injected with India ink through the terine artery Ink ppeared in central zone (4 black spots in figure) demonstrating the maternal supply first to the central zone The umbilical vein was injected with red gelatin The green filter darkened this red color and the material may be seen backed into the central reaches of the labyrinth where the allantoic capillaries coalesce to form tributaries of the umbilical vein. The red gel tin is distributed peripherally and radially" in relation to the central zone. 40 ×

14 Cast of placenta from animal 47 loculus 1R. Umbilical vein injected with yellow vinylite uterine vein injected with blue vinylite. 2 ×

15 Section of placenta (loculus 4) from animal 47 This placenta was injected with India ink via the umbilical artery The India ink heavily permeated the subplacenta. Subplacenta has solely an allantoic vascular supply and drainage 50 ×

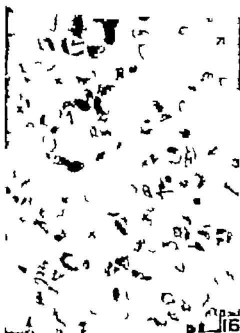
16 Section through labyrinthine zone at right angles to the trophoblastic and endothelial tubes. Endothelial tubes with nuclei are marked with half-arrows, trophoblast nuclei with full arrows, and maternal corpuscles enclosed within the trophoblast tubes are indicated by an x 485 ×

17 Section of mature placenta injected with India ink through the umbilical artery demonstrating the umbilical arterial supply from the trophospongium to the labyrinth. Arrow indicates direction of fetal blood flow Section very lightly counter-stained. From animal 47 loculus 4. 40 ×


13


14


15


16


17

PLATE 3

EXPLANATION OF FIGURES

18 Section through larger mature placenta than that of figure 19 The large subplacenta is again central in position and generally encompassed by lobes everywhere except on its central mesometrial aspect (left) Margin of fetal aspect of placenta is to the right note section through umbilical cord adjacent. 3 ×

19 Section through mature placenta previously perfused through the umbilical artery with India ink. The subdivided subplacenta occupies the central area, and placental lobes are present above and below Mesometrial margin left, margin of fetal aspect of placenta right. 3 ×

20 Photograph of tenuous pedicel of term placenta. Light gray area (bottom of picture) is the lining surface of the uterine wall (marked "x) t the mesometrial site f the placenta Uterine veins pass through the middle stem; uterine arteries pass through those stems disposed to the right and left of the middle stem. Placental disc here removed, but it was attached in the crotch bov and between the right and left arms noted in the photo at site marked with arrow Placenta from animal 15. Antimesometrial bov mesometrial below 1 ×

21 Reticular fibers (black) in trophospongium (top) in labyrinth (middle) and in central zone (below) Taken from female 47 loculus 3L 60 ×

22 Cast of vitelline arterial supply to yolk sac, injected with red vinylite; taken from female 47 loculus 7L 2


18


19


x
20


21


22

Electron Microscopy of the Implantation Site in the Rabbit[1]

JORGEN FALCK LARSEN[2,3]
Department of Anatomy Washington University School of Medicine St. Louis Missouri

The implantation process is a problem of interest to the biologist for several reasons. One of these is the nature of the interaction between the maternal and the fetal organisms, another is the phenomenon of erosion of the maternal tissue by the fetal organism, and a third is the consequences of these processes in immunological terms. Moreover the implantation process deserves the interest of the clinician as many cases of sterility or early abortions may result from defects in the implantation process.

Very little is known about the nature and cause of the changes in the uterine epithelium before the attachment of the blastocyst nor about the mechanism of invasion of the uterine tissues by the trophoblast. The invasion of the trophoblast has been explained in different ways, summaries of which have been given by Alden (48) and Blandau (49). Most authors agree that the trophoblast has the ability to resorb the degenerated uterine epithelium, but the real problem involved is the cause of this degeneration. Mossman ('37) who investigated implantation in the chipmunk, found that the regions of epithelial degeneration always overlie areas of subepithelial edema in which the blood supply may be reduced. After the epithelium has started to degenerate the trophoblast may absorb it, though Mossman did not find evidence for this.

Blandau (49) found in the guinea pig that there was considerable destruction of the epithelium before there was any evidence of edema or of a decidual reaction in the subepithelial tissues. He concludes therefore that the trophoblast appears to be responsible for the destruction of the epithelium, possible by producing a lytic substance. Evidence for a cytolytic and possibly even a phagocytic activity on the part of the trophoblast is presented in the guinea pig (Sanson and Hill '31) the monkey (Heuser and Streeter 41) and the bat (Wimsatt and Wislocki, 44). The descriptions are based, however on observations made by light microscopy. Electron microscopic evidence of a phagocytic activity by the paraplacental trophoblast in later stages of pregnancy has been found in the "brown border" of the cat (Dempsey and Wislocki, '56) and in the paraplacental chorion of the rabbit (Falck Larsen and Davies, '61). The trophoblast of the chorio-allantoic placenta has not been found however to be phagocytic but shows pinocytotic activity in the rat (Dempsey and Wislocki, '53 and '55) in the cat (Dempsey and Wislocki, '56) and in the human placenta (Boyd and Hughes '54 Wislocki and Dempsey '55) while Enders ('60) found no evidence for pinocytosis in the placenta of the armadillo.

To our knowledge, electron microscopy of the implantation site has not been described before in detail in any form. Enders ('60) has done a preliminary study in the armadillo but the investigation did not reveal the nature of the interaction between the trophoblast and the epithelium.

Previous observations on the implantation site in the rabbit

Descriptions of the implantation site in the rabbit observed by conventional light microscopy have been given by Duval (1889) Chipman ('03) Mossman ('26)

---

[1] This investigation was aided in part by grant No. [illegible] and No. [illegible], National Institutes of Health and by the Mary [illegible] Foundation.

[2] [illegible] Foreign Scientist Research Fellow. Grant No. [illegible].

[3] A supplementary grant for travel and [illegible] expenses supplied by the Danish State ([illegible] Videnskabsfond).

inclusions indicative of phagocytosis are seen. The cytoplasms of the two tissues rather merge as the trophoblastic nuclei displace the uterine nuclei. The fate of the latter has not been established.

The penetration of the basement membrane of the uterine epithelium (figs 7 to 13)

The basement membrane of the uterine epithelium appears to present a definite barrier to the invasion of the trophoblast for some time estimated to be approximately half a day It is intact in most cases until the last part of the 9th day of pregnancy In any event penetration is never seen before the uterine nuclei have disappeared. The penetration does not occur preferentially near the maternal vessels but seems to take place more rapidly in the immediate vicinity of a vessel. The penetrating trophoblast takes the form of a number of club-shaped processes (figs. 7 8) These processes have a granular cytoplasm and some of them contain elongated narrow mitochondria. For the first time inclusions are seen in the cytoplasm of the syncytial trophoblast, appearing as round [illegible]icles of medium electron density some-[illegible] larger than the mitochondria. In some of the trophoblastic processes the *plasma membrane seems to be broken and* through the defect delicate fibrils project out in the connective tissue (figs. 9 11)

The invasion of the perivascular connective tissue presents a different appearance (figs. 10 to 13) The trophoblastic processes here are longer and slender giving the impression that they are advancing at a faster rate. They often form a complex reticular pattern superficially resembling the appearance of the infoldings of the plasma membrane of the uterine symplasma in the earlier stages. Their true nature becomes apparent when examined in high-power electron micrographs. Apart from their elongated form the processes have the same ultrastructural characteristics as the club-shaped processes in the free connective tissue including the granular cytoplasm and the electron dense inclusions. Mitochondria, however are rarely seen in these long processes. By the 10th day the trophoblast has broken through the basement membrane over most of the implantation site. The processes in the perivascular connective tissue now have taken on the club-shaped form resembling the processes in the free connective tissue.

In places where the trophoblast has not yet replaced the epithelium massive concentrations of mitochondria can be observed in the cytoplasm of the syncytial trophoblast (fig. 13)

The perivascular cells (fig 10)

The maternal vessels are surrounded by cells probably of fibroblastic origin. Two forms are common. One is a more or less cuboidal type of approximately the same size as the cytotrophoblastic cell but containing large amounts of fine granular substance. This material is PAS positive in corresponding stained sections and since it is removable by pre-treatment with saliva, probably represents glycogen. These cells are probably the first decidual cells. The other type has a more ovoid shape with large dilated endoplasmic channels containing moderately electron dense material. This type is perhaps another stage of the first type. The perivascular cells have not been particularly studied and their fate is so far unknown.

The formation of the trophoblastic lacunae (fig 14)

Late on the 9th day numerous vacuoles appear in the cytoplasm of the syncytial trophoblast. These are the forerunners of larger cavities approximately 30–40 μ in diameter and by their confluence are later transformed into the lacunae of the definitive placenta. The lacunae are later filled with maternal blood following the penetration of the maternal vessel by the trophoblast. Inclusions still are seen only in the trophoblastic processes invading the connective tissue

The invasion of the maternal vessels by the trophoblast (figs 15 16)

Direct invasion of the wall of the maternal vessels was observed at the 10th day of pregnancy The penetration of the basement membrane of the endothelium probably occurs rapidly as it has been possible to find only one example in the great num-

br of sections examined As soon as the trophoblast has invaded the vessel it acquires the ultrastructural characteristics of the syncytium in the rest of the pregnancy The cytoplasm becomes vacuolated with an abundance of endoplasmic reticulum and mitochondria and also contains fat droplets and other inclusions The surface of the syncytial trophoblast which now serves as the lining of the maternal blood spaces is provided with microvilli typical of an actively absorbing surface

The fetal connective tissue and the fetal vessels (fig 17)

From the 11th day the fetal connective tissue is observed following the advancing line of the cytotrophoblast. It contains fetal vessels with large nucleated red blood cells Large cells with big nuclei are seen between the vessels and are probably phagocytic as they contain small ring shaped bodies of marked electron density these bodies also can be seen in the intercellular substance They are between 1 ?0 and 1 μ in diameter have a double contour and a clear center often divided by one or two septa.

From this stage the cellular trophoblast often is missing between the fetal vessels and the syncytial trophoblast which now are separated in many places only by a narrow rim of fetal connective tissue

DISCUSSION

In the early literature on the rabbit placenta much discussion was devoted to the cellular or syncytial nature of the attaching trophoblast. In all sections from the early stages the attaching trophoblast has been found to be syncytial when examined in the electron microscope No mitotic figures have been observed in the syncytial trophoblast but mitoses were numerous in the cellular trophoblast at all stages. The present investigation however contributes nothing to the solution of the problem of the origin of the syncytium

Böving ('58 '59) has surveyed the problems involved in implantation in general and in particular the attachment of the blastocyst to the antimesometrial uterine mucosa in the rabbit. In the author's opinion the term "implantation should be reserved for the process which is followed by the formation of the chorio-allantoic placenta on the mesometrial side In preliminary observations of the ultrastructural event at the antimesometrial side a similar cytoplasmic fusion of the trophoblast and the uterine epithelium has been found This formation of the temporary yolk-sac placenta in the rabbit will be described in a subsequent paper

Graf v Spee (1883) described pseudopodia like processes of the trophoblast penetrating the zona pellucida in the guinea pig Blandau ('49) confirmed this observation and found that in the guinea pig the zona pellucida was partly retained until the implantation had begun The zona pellucida has not been found in sections later than the 6th day of pregnancy in the present investigation

In the light of the present observations the interaction between the trophoblast and the uterine epithelium cannot be considered as a phagocytic or lytic process but is rather a fusion of two syncytia. This is an unusual process which to the author's knowledge is not described before in mammalian tissue The fusion of the cytoplasm of cells from two different organisms is seen in one other situation namely at the moment of fertilization

The disappearance of the membrane between the syncytial trophoblast and the uterine symplasma may perhaps be attributed to inadequate fixation It is not very likely however as the phenomenon has been observed in all sections taken from animals in different stages of pregnancy and fixed and embedded in different ways All other membranes in the sections were well preserved and there were fields where nuclei of the syncytial trophoblast and of the uterine symplasma were found packed closely together with no intervening homogeneous border This fusion presents a rare immunological situation which may underlie certain clinical cases of defective implantation. The fetal nuclei exist for some time within the maternal cytoplasm, and maternal nuclei also in direct contact with the fetal cytoplasm. It would be interesting to know what substances are exchanged in this situatio

Considering the important and numerous differences existing between the placentae of the different species it would be premature to claim that this process of syncytial fusion represents the nature of the interaction between the trophoblast and the uterine epithelium in all animals. The symplasmic changes of the uterine epithelium are found however in the implantation process in many forms. It is interesting that a study of the light microscopic pictures of the implantation site in the monkey (Heuser and Streeter 41) reveals several places where no line can be seen between the trophoblast and the uterine symplasma. Moreover the implantation site seen in the micrographs of the 7 days old human embryo (Hertig and Rock, 45) resemble very much the implantation site in the rabbit. Small and large nuclei are found in a homogeneous cytoplasm. This does not prove that it is a fusion process like the one observed in the rabbit but it is a possibility that should be elucidated by the use of the electron microscope. Examination of the human placenta might be difficult at this stage, namely in the first week after the conception but it should be possible to investigate the problem in the monkey

The fate of the uterine epithelium is still not clear The cytoplasm seems to become part of the cytoplasm of the trophoblast and the nuclei to be dissolved. But it is remarkable that this process does not leave any trace in the form of inclusions in the cytoplasm of the syncytial trophoblast Inclusions are not seen in the syncytium before it invades the maternal connective tissue.

The club-shaped processes by which the penetration of the basement membrane of the epithelium takes place have not been described before. They can be seen even in high-power light microscopy in very thin sections. The appearance of these processes presents a dynamic picture of the rupture of the basement membrane of the uterine epithelium and of their subsequent unrestricted movement into the subepithelial tissues.

The nature of the electron dense ring shaped bodies in the fetal mesenchyme is not known. They are seen also in placentae from later stages of pregnancy Dempsey and Amoroso ('61) have observed similar bodies in the fetal mesenchyme of the placenta of the cat and they believe that they may represent bile pigment from decomposed erythrocytes phagocytosed in the paraplacental region. This could be true in the rabbit placenta as a similar phagocytic process is observed in the paraplacental chorion of the rabbit (Falck Larsen and Davies, '61)

SUMMARY

The ultrastructure of the implantation site in the rabbit was studied from the 7th to 11th day of pregnancy The trophoblast is syncytial at the time of attachment The cytoplasm of the syncytial trophoblast and the uterine epithelium which is transformed into a symplasma seem to fuse and fetal and maternal nuclei exist in a common cytoplasm for some time. The basement membrane of the uterine epithelium resists the invasion by the trophoblast approximately half a day When the nuclei of the uterine epithelium disappear the basement membrane is penetrated by club-shaped trophoblastic processes. Vacuoles are formed in the syncytial trophoblast they merge into lacunae which become filled with maternal blood when the trophoblast invades the maternal vessels late on the 10th day of pregnancy Fetal connective tissue and fetal vessels are found in the placenta from the 11th day following the invasion by the trophoblast.

ACKNOWLEDGMENTS

I am indebted to Dr E. W Dempsey for making available to me the facilities of his department and for his many helpful suggestions during this investigation Dr Jack Davies has given me valuable help in overcoming a great number of theoretical and technical problems. I am indebted to Dr Keith C. Richardson for sharing his great knowledgment on embedding and staining procedures.

Finally I want to thank Mrs. Susan Philpott and Mr Paul Meyers for excellent technical assistance

LITERATURE CITED

Alden, R. H 1948 Implantation of the rat egg III. Origin and development of the primary trophoblastic giant cells. Am. J An t., 83: 143–181

Amoroso, E. C. 1952 Placentation. Marshall's Physiology of Reproduction, 3rd ed., edited by A. S. Parkes, Longmans, Green, New York, 2: 127-311.

Boyd, J. D., and A. F Hughes 1954 Observations on the human chorionic villi using the electron microscope. J Anat., 88 356-362.

Böving, Bent G. 1958 Implantation. Ann. New York Acad. Sc., 75 700-725.

——— 1959 The biology of trophoblast. Ibid., 80, 21-43.

Blandau, R. J 1949 Observations on the implantation of the guinea pig ovum. Anat. Rec 103 19-36.

Chipman, W 1903 Observations on the placenta of the rabbit with special reference to the presence of glycogen, fat and iron. Lab. Reports of the Royal College of Physicians Edinburgh, 8 227

Dempsey E. W and E. C. Amoroso 1961 Personal communication.

Dempsey E. W and G. B Wislocki 1953 Electron microscopy of the rat placenta. Anat. Rec., 117 581-582.

——— 1955 Electron microscopy of the placenta of the rat. Ibid 123 33-64

——— 1956 Electron microscopic observations on the placenta of the cat. J Biophys. Biochem. Cytol 2 743-754

Duval, M 1889 Le placenta des rongeurs le placenta du lapin. J anat. et physiol., 25 309-342.

Enders, A E. 1960 Electron microscopic observations on the villous haemochorial placenta of the 9 banded armadillo. J Anat 94 205-213.

Falck Larsen, J 1961 Electron microscopy of the uterine mucosa in the rabbit. To be published.

Falck Larsen, J and J Davies 1961 Observations on the paraplacental chorion in the rabbit. Under Preparation.

Hertig, A. T and J Rock 1945 Two human ova of the pre villous stage Contrib Embryol., 29 127-156.

Heuser C. H., and G. L. Streeter 1941 Development of the macaque embryo. Ibid 29 127-156.

Moore R. C., V Mumaw and M. D Schoenberg 1960 Optical microscopy of ultrathin sections. J Ultrastruct. Research, 4 113-115.

Mossman, H W 1926 The rabbit placenta and the problem of placental transmission. Am. J Anat 37 433-497

——— 1937 Comparative morphogenesis of the fetal membranes and accessory uterine structures. Contrib. Embryol 26 129-246.

Richardson, K. C., L. Jarett and E. H. Finke 1960 Embedding in epoxy resins for ultrathin sectioning in electron microscopy Stain. Technol 35 313-323.

Sansom, G. S., and J P Hill 1931 Observations on the structure and mode of implantation of the blastocyst of cavia. Trans. Zool. Soc. Lond., 21 295-354.

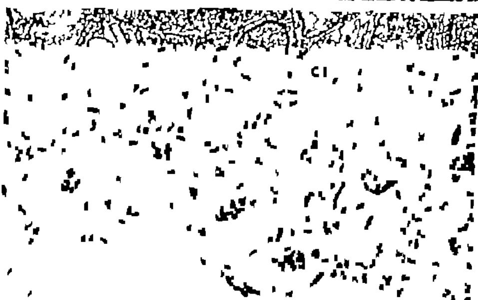
v.Spee F Graf 1883 Die Implantation des Meerschweincheneies in die Uteruswand. Ztschr Morph. Antropol., 3 130.

White, P R. 1954 The cultivation of animal and plant cells. Ronald Press Co., New York.

Wimsatt, W F and G. B Wislocki 1944 Implantation in the bat. Am. J Anat., 80 361-436.

Wislocki, G. B., and E. W Dempsey 1955 Electron microscopy of the human placenta. Anat. Rec., 123, 133-168.





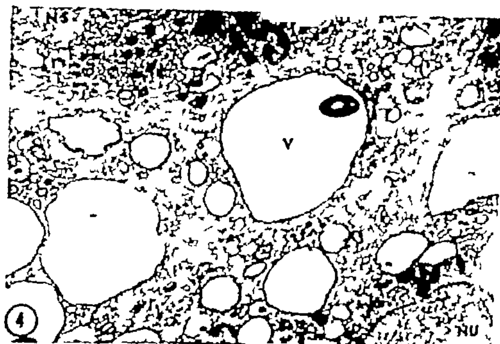
With the exception of figure 1 all photographs are electron micrograph.

1 Phase micrograph of the border of the implantation site at the 9th day of pregnancy. CT Cytotrophoblast. ST Syncytial trophoblast. US Uterine symplasma. MV Maternal vessel. UL Uterine lumen. C Maternal connective tissue. The arrow indicates the line of junction between the trophoblast and the uterine epithelium. × 400.

2 The trophoblast immediately outside the implantation site. CT Cytotrophoblast. ST Syncytial trophoblast. M Mitosis in the cellular trophoblast. The short arrows indicate desmosomes between *cytotrophoblastic cells*; *the long arrows indicate desmosomes be*tween the cytotrophoblast and the syncytial trophoblast. UL Uterine lumen. The star indicates the space between the cytotrophoblast and the syncytial trophoblast. × 2,000.



3 The junction between the trophoblast and the uterine epithelium t the 8th day f pregnancy CT Cytotrophoblast. ST Syncytial trophoblast. NT Nucleus of the syncytial trophoblast. The fusion between the cytoplasm of the trophoblastic syncytium and the uterine symplasma is seen between the two straight arrows. NU Nucleus of the terine symplasma. UL Uterine lumen. The curved arrow indicates cell membrane in the terine symplasma. × 3,500.





4 *The junctional zone between the trophoblast and the uterine epithelium pregnancy NS Nucleus of the syncytial trophoblast. NU Nucleus of* plasma. V Vacuole within the homogeneous substance between the two tissues. × 5,000.

5 The basal part of uterine epithelium fused with the syncytial trophob[illegible] *of the uterine symplasma NS Nucleus of the syncytial trophoblast.* an endothelial cell of maternal vessel. *Note the convoluted basal of the epithelium and the associated basement membrane. × 3,000.*





6 The degenerating uterine epithelium. LG Former lumen of the uterine gland. US Uterine symplasma. NG Nucleus of cell in the gland not involved in the formation of the symplasma. NU Nucleus of the uterine symplasma. The large arrow indicates an area with round vacuoles; the smaller arrows indicate areas with crescentic vacuoles. Note that the membrane separating the epithelium from the connective tissue is convoluted in places where the uterine cells have been transformed into a syncytium, whereas it is straight under the single cell. MV Maternal vessel. × 2,000.

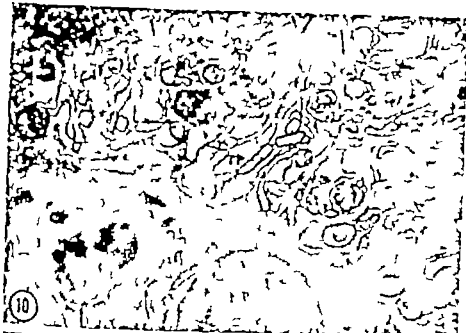
7 A trophoblastic process penetrating the basement membrane at the end of the 9th day of pregnancy. ST Cytoplasm of the syncytial trophoblast. MC Maternal connective tissue. TP Trophoblastic process. I Inclusion in the trophoblastic process. The basement membrane of the uterine epithelium, which now is replaced by the trophoblast, is broken at the place indicated by the arrow. × 10,000





4 The junctional zone between the trophoblast and the uterine epithelium at the 9th day of pregnancy. NS Nucleus of the syncytial trophoblast. NU Nucleus of the uterine symplasma. V Vacuole within the homogeneous substance between the cytoplasm of the two tissues. × 5,000.

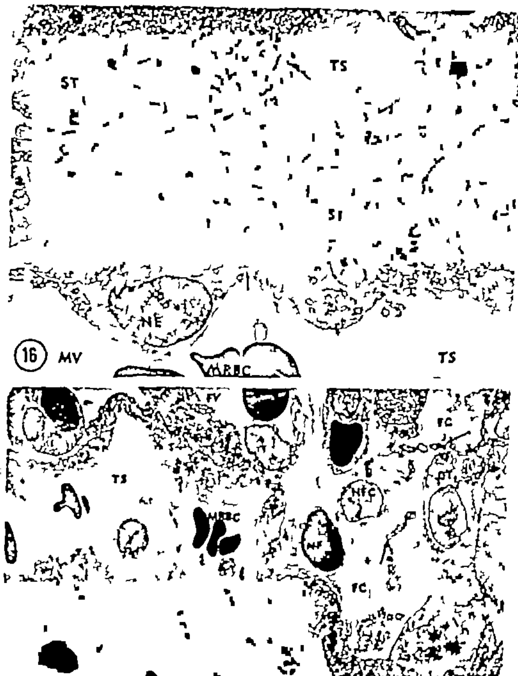
5 The basal part of uterine epithelium fused with the syncytial trophoblast. NU Nucleus of the uterine symplasma. NS Nucleus of the syncytial trophoblast. NE Nucleus of an endothelial cell of maternal vessel. Note the convoluted basal plasma membrane of the epithelium and the associated basement membrane. × 3,000.





10 The trophoblastic processes (TP) near perivascular cell. ST Syncytial trophoblast. CP Cytoplasm of perivascular cell. NP Nucleus of perivascular cell. The arrows indicate the places where the trophoblastic processes penetrate the basement membrane. × 6,000.

11 Tenth day of pregnancy. NT Nucleus of the syncytial trophoblast. TP Trophoblastic processes. NE Nucleus of maternal endothelial cell. The arrows indicat fibrils projecting out from the trophoblastic processes × 5,000



16 Blood space in the placenta from the 11th day of pregnancy T the left the pace l lined by maternal endothelium and to the right of the arrow by trophoblast TS Trophoblastic space ST Syncytial trophoblast. F Fat droplet NT Nucleus of the yncytial trophoblast. NP Nucleus of perivascular cell. MV M ternal vessel MRBC Mate nal red blood cell × 2,.00

17 Placenta at the 14th day FC Fetal connective tissue containing hain of lectron dense round bodies (at the arrows) NFC Nucleus of fetal connective tissue cell. NF Nucleus of a fetal red blood cell. CT Cytotrophoblast. FV Fetal vessel. NT Nucleus of the syncytial trophoblast. TS Trophoblastic space MRBC Maternal red blood cells. × 1,000.

Index